Electric Vehicles Integration in the Electric Power System with Intermittent Energy Sources - The Charge/Discharge infrastructure

Marra, Francesco; Larsen, Esben; Træholt, Chresten

Publication date:
2013

Document Version
Publisher's PDF, also known as Version of record

Technical University of Denmark

Francesco Marra

Electric Vehicles Integration in the Electric Power System with Intermittent Energy Sources - The Charge/Discharge infrastructure

PhD Thesis, March 2013

DTU Electrical Engineering
Department of Electrical Engineering

Francesco Marra

Electric Vehicles Integration in the Electric Power System with Intermittent Energy Sources - The Charge/Discharge infrastructure

PhD Thesis, March 2013

Electric Vehicles Integration in the Electric Power System with Intermittent Energy Sources - the Charge/Discharge infrastructure, PhD Thesis, March 2013

Author:
Francesco Marra

Supervisors:
Assoc. Prof. Chresten Træholt and Assoc. Prof. Esben Larsen

Department of Electrical Engineering
Center for Electric Power and Energy (CEE)
Technical University of Denmark
Elektrovej Byg. 325
DK-2800, Kgs. Lyngby
Denmark

www.cee.dtu.dk
Tel: (+45) 45 25 35 00
Fax: (+45) 45 88 61 11
E-mail: cee@elektro.dtu.dk

Release date:	March, 2013
Class:	public
Edition:	1
Comments:	This thesis is presented by Francesco Marra to the Department of Electrical Engineering in partial fulfilment of the requirements for the degree of Doctor of Philosophy.

ABSTRACT

The replacement of conventional fuelled vehicles with electric vehicles (EVs) is going to increase in the coming years, following the trend seen for renewable energy sources (RES), as photovoltaic (PV) and wind power. In this scenario, the electric power systems in Europe are going to accommodate increased levels of non-dispatchable and fluctuating energy sources, as well as additional power demand due to EV charging. If the charging of EVs can be intelligently managed, several advantages can be offered to the power system. How useful coordinated EV charging can be, in combination with RES, is answered in this research work. Two real cases are addressed:

- the EV load coordination for power fluctuations due to wind power, in the Danish power system;
- the EV load coordination for the power fluctuations due to Photovoltaic (PV) in low voltage grids, in several European countries.

The research work starts with the definition of EV requirements for enabling a bi-directional power exchange with the grid. A set of monitoring and control requirements are defined to achieve EV coordination. The validation of the defined requirements is performed with a full-scale EV test bed made of real EV components such as a lithium-ion battery pack, a battery management system and charging/discharging units.
The second part of the research exploits the use of EV load coordination to facilitate the integration of wind power in the Danish power system. A proof of concept of regulating power reserves is realized, using the target power requests from the Danish Transmission System Operator (ENERGINET.DK), valid as the control signal for the EVs. The EV coordination is realized under the control framework of a Virtual Power Plant. The tests performed show that an EV can respond according to the time plan and the power levels needed. Furthermore, during EV coordination, a number of nonlinearities and battery ageing issues should be taken into account, to ensure a correct EV coordination and to preserve the EV battery lifetime.
The third part of this research exploits the use of EV load coordination as an energy storage solution to facilitate PV integration in LV distribution grids. In this context, the storage capabilities of EV charging stations are analyzed. Two concepts of stations are investigated: *public charging station*, to accommodate the parallel charging of EVs at public locations, and *private charging stations* at private homes. The coordination of EV load of public or private charging stations creates benefits in feeders with PV. A

method based on voltage sensitivity analysis is proposed to evaluate the influence of EV load coordination at different locations in the grid. Time-series simulations and a proof of concept prove the usefulness of coordinating the load from EV stations in LV feeders with PV.

As a general conclusion, it is observed how important the role of EV load coordination can be, in coping with the fluctuations of renewable power sources at different power system levels.

RESUMÉ

I de kommende år forventes det, at skiftet fra køretøjer drevet af konventionelle energikilder (ICE – Internal Combustion Engine) til elektriske køretøjer (elbiler) øges med voksende hastighed svarende til den sete udvikling mod udnyttelse af vedvarende energikilder som solceller og vindenergi. Elsystemet i Europa vil under dette scenarie inkludere øgede mængder af fluktuerende energikilder samtidigt med en øget efterspørgsel på elektricitet til opladning af elbiler. Projektets tese er at der kan opnås flere fordele hvis opladningen af elbiler kan styres intelligent. Målet med denne afhandling er at undersøge hvor brugbar koordineret opladning af elbiler kan være i kombination med energikilder med en uforudsigelig produktion. To cases er undersøgt:

- belastningskoordinering i det danske elsystem vha. elbiler med henblik på at udjævne fluktuationer opstået pga. vindenergi
- koordinering for at udjævne fluktuationer opstået på grund af solceller i lavspændingsnettet.

Forskningsarbejdet starter med definitionen af krav, der muliggør tovejs effektudveksling mellem elbiler og nettet. En række monitorerings- og kontrolforanstaltninger er defineret for at muliggøre en koordination vha. elbiler. Batteriets opladningstilstand (State of Charge - SOC) og effektudveksling med nettet skal monitoreres ved kontrolleret ladning af elbiler. Samtidigt er aktivering af opladnings- og afladningsmodes nødvendige kontrolforanstaltninger. Valideringen af de definerede foranstaltninger er udnyttet ved implementering af en fuldskala forsøgsopstilling som består af en lithium-ion batteripakke, et batteristyringssystem (BMS) og opladnings-/afladningsenheder.

I den anden del af afhandlingen er koordinering af opladningen af elbiler udnyttet til at facilitere integration af vindenergi i det danske elsystem. Et proof-of-concept for levering af regulerkraftreserver er realiseret ved at anvende de gældende krav givet af den danske transmissionssystemoperatør (ENERGINET.DK). Koordineringen vha. elbiler er realiseret under kontrolrammen for et virtuelt kraftværk som tidligere blev introduceret i det danske EDISON projekt. Testopstillingen reagerede under dette eksperiment i henhold til tidsplanen og ydede den nødvendige regulerende effekt. Ved denne type af anvendelser bør der defineres et optimalt anvendelsesvindue til sikring af unødig brug af ekstra batterilevetid.

I den tredje del af afhandlingen undersøges belastningskoordinering i form af elbiler som en energilagringsløsning for lavspændingsnet med en betydelig elproduktion fra solceller. I denne sammenhæng ses ladestationen som en energilagringslokation. To koncepter er undersøgt: *Offentlige ladestationer* til parallel opladning af elbiler i det offentlige rum, og *Private ladestationer* ved private hjem. Koordination af belastningen fra de elbiler tilsluttet offentlige og private ladningsstationer blev undersøgt for herved at levere spændingsstøtte. I begge tilfælde opnås gunstige resultater for lavspæningsnet. En metode baseret på spændingssensitivitetsanalyse er udviklet for at identificere effektiviteten af spændingsregulering med belastningskoordination vha. elbiler. Dynamiske simuleringer og et eksperimentelt proof-of-concept har vist effektiviteten ved at bruge elbiler som en lagringsløsning på lavspændingsradialer med solceller.

Overordnet konkluderes, at koordination af belastning fra elektriske køretøjer kan være en effektiv løsning til at håndtere fluktuationer ved vedvarende energikilder på forskellige spændingsniveauer i elsystemet.

PREFACE

This thesis was prepared at the Center for Electric Power and Energy (CEE, former CET), Department of Electrical Engineering of the Technical University of Denmark (DTU), in partial fulfilment of the requirements for the Ph. D. degree, in Denmark.
The Ph.D. project has been partly financed by the Danish EDISON project which has been formally completed in December 2011.

This research project is grateful to the support of many people. Herewith, I am heartily thankful to my supervisors Assoc. Prof. Chresten Træholt and Assoc. Prof. Esben Larsen, who have been genuinely helpful while offering invaluable support and guidance from the beginning of my research, till the end. Deepest thanks go to Prof. Jacob Østergaard, who inspired me to conducting research on electric vehicles and for the support through the years. A great thank you goes to Louise Busch-Jensen for the fundamental guidance and help at my arrival in Denmark, and for the friendship developed through the years.

Among my colleagues, I have been in close collaboration with Peter Bach Andersen, Anders Bro Pedersen, Dario Sacchetti, who have helped me with their Information and Communication Technology (ICT) background for setting up part of the laboratory demonstrations. I am thankful to Guang Ya Yang, Rodrigo Garcia-Valle and Morten Møller Jensen, for the relevant discussions and exchange of views in the field of electric power engineering.

A great thank you goes to Thorsten Bülo, Yehia Tarek Fawzy and Gerd Bettenwort for giving me the chance to spend a very fruitful research period at SMA Solar Technology, working on my Ph.D. project.

Last but not least, to my dear family: thank you for your understanding and your endless love through the duration of my studies.

TABLE OF CONTENT

LIST OF PUBLICATIONS

The following 8 papers have been written during this PhD project. The journal papers JP1, JL2, JP3 and the conference papers P4 – P8 contain the most relevant results in relation to the research performed.

[JP1] F. Marra, G. Y. Yang, C. Træholt, E. Larsen, B. Blazic, and W. Deprez, "Electric Vehicle Charging Facilities and Their Application in LV Feeders with Photovoltaic", *IEEE Transactions on Smart Grid*, accepted, Jul. 2013.

[JL2] F. Marra, G. Y. Yang, Y. T. Fawzy, C. Træholt, E. Larsen, R. Garcia-Valle, and M. Møller Jensen " Improvement of Local Voltage in Feeders with Photovoltaic using Electric Vehicles", *IEEE Trans. on Power Systems*, vol. PP, No. 99, Mar. 2013.

[JP3] F. Marra, G. Y. Yang, C. Træholt, E. Larsen, J. Østergaard, " A Decentralized Storage Strategy in Residential Feeders with Photovoltaic", *IEEE Trans. on Smart Grid*, under review.

[P4] F. Marra, D. Sacchetti, C. Træholt, and E. Larsen, "Electric Vehicle Requirements for Operation in Smart Grids", *in Proc. of IEEE Innovative Smart Grid Technology Europe (ISGT2011)*, Manchester, Dec. 2011.

[P5] F. Marra, D. Sacchetti, A. B. Pedersen, P. B. Andersen, C. Træholt, and E. Larsen, "Implementation of an Electric Vehicle Test Bed Controlled by a Virtual Power Plant for Contributing to Regulating Power Reserves", *in Proc. of IEEE Power and Energy Society – General Meeting (PES-GM 2012)*, San Diego, Jul. 2012.

[P6] F. Marra, C. Træholt, E. Larsen and Q. Wu, "Average Behavior of Battery-Electric Vehicles for Distributed Energy Studies", *in Proc. of IEEE Innovative Smart Grid Technology Europe (ISGT2010)*, Goteborg, Oct. 2010.

[P7] F. Marra, G. Y. Yang, C. Træholt, E. Larsen, C. Nygaard Rasmussen and S. You, "Demand Profile Study of Battery Electric Vehicle under Different Charging Options", *in Proc. of IEEE Power and Energy Society - General Meeting (PES-GM 2012)*, San Diego, Jul. 2012.

[P8] F. Marra, Y. T. Fawzy, T. Buelo and B. Blazic, “Energy Storage Options for Voltage Support in Grids with High Penetration of Photovoltaic”, *in Proc. of IEEE Innovative Smart Grid Technology Europe (ISGT2012),* Berlin, Oct. 2012.

LIST OF FIGURES

LIST OF TABLES

SYMBOLS AND ABBREVIATIONS

	Unit	Definition
SOC	-	Battery State of Charge (%)
E_n	kWh	Nominal energy
V_n	V	Nominal battery cell voltage
C_n	Ah	Nominal battery capacity
C	Ah	Remaining battery capacity
P_c	kW	Charging power
P_d	kW	Discharging power
P_{AC}	kW	Power exchanged with the AC grid
P_{DC}	kW	Power exchanged with the battery
η_{CH}	-	Efficiency grid-to-battery during charging
η_{DISC}	-	Efficiency battery-to-grid during discharging
η_{RT}	-	Round-trip efficiency, grid-to-battery and battery-to-grid
Target value	MW	Regulating power reserves' target value from TSO
EV regulation	kW	EV power regulation for ancillary services
Measured power	kW	Measured power under regulating power reserves
Voc_{eq}	V	EV battery pack's open circuit voltage
V_{pack}	V	EV battery pack voltage
R_{eq}	Ω	Equivalent resistance of EV battery pack
i	A	Charge/discharge DC current
i_c	A	Charge/discharge AC current

V_c	V	Grid voltage
P_{RES}	kW	Active power injected by renewable energy sources
Q_{RES}	kVAr	Reactive power consumed by renewable energy sources
P_L	kW	Active power to load
Q_L	kW	Reactive power to load
P_{EV}	kW	Active power due to EV charging
P	kW	Nodal power exchanged on the grid
U_G	V	Grid voltage
ΔV	V	Voltage magnitude variation
P_S	kW	Storage power for voltage support
P_{PV}	kW	Active power injected by PV system
P_{PVmax}	kW	Maximum active power injected by PV system
V_{PCC}	V	Grid voltage at the point of common coupling of PV
RES	-	Renewable energy sources
RE	-	Renewable energy
WT	-	Wind turbine
TSO	-	Transmission System Operator
DSO	-	Distribution System Operator
TS	-	Transmission System
DS	-	Distribution System
C-rate	-	Charging/discharging current normalized to the nominal battery capacity, known also as C-rate
DOD	%	Depth of discharge, the dual of State of charge (SOC)
T	ºC	Battery pack temperature

1 INTRODUCTION

In 2008, the European Commission published the climate and energy package “20 20” in “2020”, with the objective of reducing the greenhouse gas (GHG) emissions and increasing the production from renewable energy sources (RES) [1]. The electrification of the transport sector is considered an important element in pursuing the first of the objectives [2], [3] in harmony with the realization of the latter [4].

The phenomenon of climate change, the rise of fuel prices, the prospected scarcity of oil, as well as the technological innovations on battery technology, have convinced several car manufacturers worldwide [5], in investing in new vehicle models powered by batteries, recognized as electric vehicles (EVs).

EVs contribute to lower the GHG emissions as they produce no exhaust as opposed to internal combustion engine (ICE) vehicles [2]. However, the emissions levels by EVs vary depending on how the electricity is produced. If the generation is based on coal power plants, the air benefits of using EVs are only local, because the emissions are shifted to the location of the production plant [2]. If the electricity is produced by less carbon-intensive energy sources, such as wind power and photovoltaic (PV), GHG emissions are significantly lower [2]. However, it is found that even with coal-generated electricity, GHG emissions are lower for EVs than ICE vehicles [2].

National and local authorities in different countries [6] have started to provide support to the introduction of EVs, granting them special treatments in comparison to conventional cars, with measures like tax incentives, reduced tariffs in parking lots, free access to restricted traffic areas, the use of bus lanes etc. [6].

One major difference between EVs and ICE vehicles is the EV’s ability to be *refuelled* using the electrical grid.

For ICE cars, the invention of the refuelling method dates back to the early 1900 [7]. The first refuelling was carried out by a pharmacy that used to sell gasoline tanks, thus the process was entirely manual and taking a few seconds. For EVs, the need of a longer charging time and the absence of public charging infrastructures have posed limitations to the sector through the years [8]. Today, EV charging is largely performed using onboard vehicle’s chargers; the charging time needed to recharge an empty battery can be of several hours [8]. Fast charging technology has been developed to decrease the

charging time, though it is only possible on few vehicle models; fast charging allows charging a fully depleted 24 kWh battery up to 80% of its capacity in 30 minutes, using a specialized fast charging station [9]. However, the rate of charging is still slow compared to refilling a fuel tank. Furthermore, fast charging can impact negatively on the battery lifetime if used on a daily basis [9].

With regard to vehicle costs, consumers worldwide tend to focus on initial costs, rather than on operating costs, when making purchasing decisions [2], [8]. The purchase cost of an EV is about 30-40% higher than an ICE vehicle [5].

The running costs of an EV can be quite different from the ones of an ICE car [6]. The cost of charging depends on the electricity price, which may vary according to the country [2]. Currently, in European countries as well as in the U.S., the cost per km driven by an EV is about one-fifth of the cost per km driven with an ICE city car[1] [11], [12].

With regard to EV integration in electric grids, the electric demand due to EV charging is still negligible today [4], [13]. With a widespread adoption of EVs, the additional electric demand can have proportions that affect the operation of the electric power system, in a positive or negative manner [4], [13]. In fact, if the charging of EVs is unconstrained [13], the additional demand during peak electricity hours can challenge the operation of the power system and underutilize the energy produced by RES [4], [13]. As a consequence, the unconstrained charging can lead to extra investments in generation and transmission capacity, to increased wear on distribution components and to power quality issues [9], [13].

On the contrary, if the charging of EVs is supported by more intelligent charging schemes that take into account the actual production of RES, both the environmental value and the value created for the electric energy sector may result increased [4], [9], [13].

1.1 Wind Energy in the electric power system

The global wind energy market has grown for several years, **Figure 1-1**. The market slowdown that began in 2008 has seen a slight recovery in 2011 [14]. In particular, Europe remained on track to achieve its “20-20” targets. The cumulative global capacity of wind power at the end 2011 is about 238 GW [14].

The main drivers of this growth are the newly installed wind farms in Asia, with China and India as the leading countries. While the Chinese market has seen a slowdown in growth, it still accounts for about 43% of the global market [14].

[1] According to the British acceptation, a *city car* is equivalent to a B-segment car in Europe [10].

The future growth of the market depends on the uncertainty on future incentives for wind power, on taxation changes, as well as on power system issues, on the technical and economic challenges for the offshore development in Europe [14].

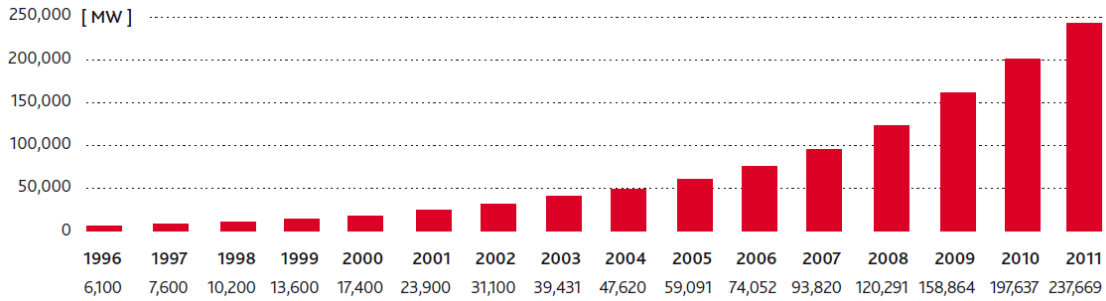

Figure 1-1: Global cumulative installed Wind power capacity 1996-2011 [14].

The cumulative installed wind power capacity of **Figure 1-1** represents the available wind power production under ideal wind conditions of nominal wind speed; however, it hides the challenges of its integration in power systems.

As of 2011, the energy penetration of wind power in Europe has reached 26% in Denmark, 16% in Spain and Portugal, 9% in Ireland and 7% in Germany [14].

The transmission system operator (TSO) in Denmark has started to face system operation challenges due to the production characteristics of this alternative energy source. In **Figure 1-2** (a), the aggregated wind power production and demand during a 3-week period in the 2008's Danish scenario, with 20% wind energy penetration, is depicted. During some hours, the wind power production matches the demand. In contrast, in **Figure 1-2** (b), a future scenario with 50% wind energy penetration is depicted: wind power production exceeds the demand in several days. In both scenarios, it is also observable that relying on wind power alone may lead to several days with almost no power production.

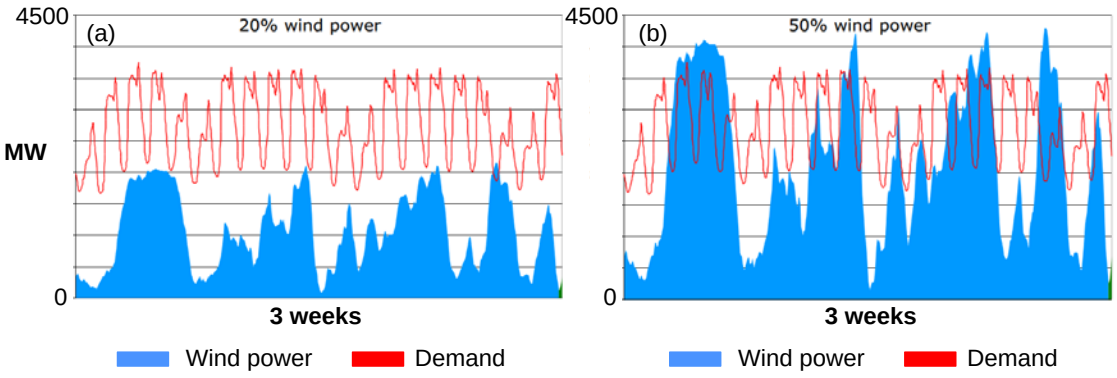

Figure 1-2: Wind power production and demand profiles for a 3-week period in Denmark. (a) The 2008 scenario (b) Future scenario with 50% wind penetration [15].

Wind power is a non-dispatchable source, as its availability cannot be controlled, and a highly fluctuating source, as wind speed variations occur at all time-scales, seconds, minutes, hours and seasons [16]. To cope with these characteristics, wind power forecasting methods with horizons of few minutes ahead are being proposed that all try to minimize the uncertainty of wind speed [16]. It has been calculated that an error in the wind speed forecast of 1 m/s in Denmark can result in a wind power prediction error of up 450 MW [17]. To ensure a secure operation of the power system, a number of services are used to maintain the balance between production and consumption; these are regarded as ancillary services [18]. In the Western Danish power system, the services include: primary reserve, secondary reserve (LFC), manual reserve, short-circuit power, reactive power reserves and voltage control [18]. In a power system with increasing wind power capacity installed, like the Danish power system, the need of ancillary services increases, requiring additional conventional power plants for their provision. Measures that limit the need of additional power plants are being considered and these are based on the reinforcement of grid interconnections with neighbouring countries [19], on energy storage solutions [20] including EVs, and on flexible demand options [21].

The use of EVs as a large-scale solution to facilitate the integration of wind power in the power system is a motivation of this research project.

1.2 Photovoltaic (PV) in the electric power system

As observed for wind energy, also the photovoltaic (PV) market has seen an unprecedented growth in the last decade [22].

In 2011, the market has reached a cumulative installed capacity of about 40 GW worldwide, which produces 50 TWh of electric energy annually [22]. Most investments in the PV sector are still inhomogeneous among the different countries; this is not only due to the conditions of solar exposition of the countries but also due to different national regulations and incentive's programs [22].

The success of PV is mainly linked to the rapid growth of the European market. With 24 GW of installed PV capacity at the end of 2011, Germany currently dominates the PV market worldwide, followed by Italy, with an installed PV capacity of 12 GW [22].
Other markets such as Japan and the United States have almost reached the "GW dimension" while the market in China and India is still in expansion [22].

From an energy point of view, the PV energy source is alternative to traditional fossil fuels; likewise wind energy, it is characterized by similar drawbacks concerning the power production: the day-night cycles and the clouds passage are some of the natural phenomena which make PV a non-dispatchable and fluctuating energy source, as wind power [4]. Because its large-scale integration into the power system generates similar

ancillary services needs to wind power integration, these are not repeated for the PV case.

Unlike wind turbines, PV systems are well suited in LV distribution grids, in urban or rural areas, at public places or at private houses. This is mainly thanks to their static operation and to a lower visual and noise impact compared to wind turbines.

If we consider the German scenario as of 2011, a total of 13 GW of installed PV capacity is in LV grids [23]. From a power system point of view, PV has a good correlation between generation and demand in LV grids, as PV power is generated during the day when the demand is relatively high compared to overnight [4]. In this case, possible benefits from PV may include reduced transmission and distribution losses, and the loading alleviation of LV grid components [4], [24].

If the demand is low, the power production from dispersed PV generation can cause situations of power flow inversion in LV grids, which can lead to significant voltage magnitude variations [23], [43] and consequent deterioration of voltage quality [25].

Some areas in Germany and in other European countries have started to experience such problems due to the high PV capacity installed [23]. Possible solutions addressed are the curtailment of the power feed-in by PV systems, grid reinforcement measures, and reactive power based options [23].

The use of EVs as a storage solution to support the grid voltage in feeders with PV is another motivation for this research project.

1.3 Research objectives

The three-year Ph.D. project “Electric Vehicles Integration in the Electric Power System with Intermittent Energy Sources – the Charge/Discharge Infrastructure” was initiated by the Center for Electric Technology (now Center for Electric Power and Energy) at DTU, in connection with the Danish EDISON project (2009-2011).
The research of solutions that allow an active participation of EVs in power systems with renewable energy sources is the main goal of the project. The project objectives address the definition of requirements and control strategies for EV load coordination, in combination with RES.

The project considers the real needs of a power system with high penetration of Wind power and the case of LV grids with high penetration of PV, both characterizing different countries and regions in Europe.

In relation to the two scenarios, solutions using coordinated EV charging/discharging are proposed to cope with the following needs:

1. Provision of ancillary services in a power system with high penetration of wind power.
2. Local voltage regulation in LV grids with high penetration of PV.

Both scenarios are addressed looking at the capabilities of an EV to operate according to two coordination targets:

EV Coordination 1

According to the project framework depicted in **Figure 1-3**, *coordination 1* addresses the need of system reserves due to the fluctuations in wind power production; solutions for enabling bi-directional power operation of EVs in response to the requests from the Danish TSO are implemented.

The definition of EV requirements, the proposal of a possible EV control architecture, the identification of EV components' constraints during EV coordination periods, are covered. A proof of concept of secondary reserves and regulating power provision, using EV load coordination, is implemented, highlighting some limitations.

EV Coordination 2

According to *coordination 2*, in LV grids with high penetration of residential PV, solutions that mitigate voltage magnitude variations are proposed using coordinated EV load as storage, **Figure 1-3**. The solutions consider the presence of private and public charging stations in future urban or rural areas and realistic charging power levels. A typical residential network with roof-mounted PV is simulated and a proof of concept on the use of EVs for voltage support is implemented.

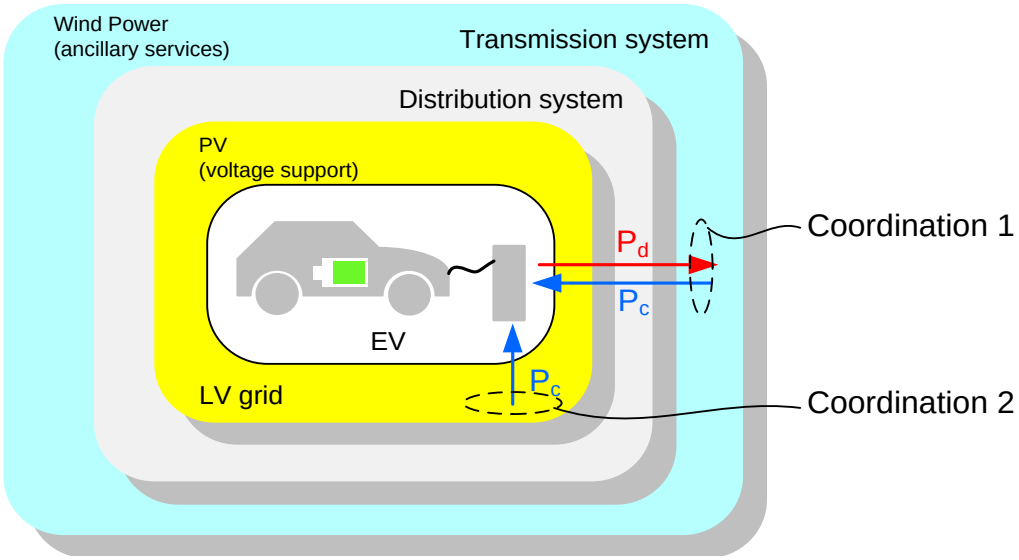

Figure 1-3: Project framework.

The key questions to be answered in this project are:

- What is the potential for EVs to interact in a power system with wind power and what are the requirements to enable EV load coordination?

  The requirements to enable an active EV participation with the power system are defined. The interaction between the EVs and the grid should involve a safe bi-directional EV battery operation. An experimental EV setup is built using full-scale EV components to assess the EV system response under an EV coordination concept.

- What EV control architecture is required to enable the provision of ancillary services? Are there any constraints related to EV load coordination?

  An EV's control architecture is developed to enable the EVs for the provision of ancillary services within a centralized coordination concept of a Virtual Power Plant. A proof of concept of EV coordination is provided to demonstrate the interaction between the vehicle and the power system, **Figure 1-3**.

- What is the potential of EV load coordination in LV grid feeders with high penetration of PV? Can EV load coordination facilitate PV integration?

  Considering the simplified LV distribution feeder of **Figure 1-4**, the goal is to propose methodologies for the coordination of EV load, to provide voltage regulation in a feeder, during periods of high PV generation and low consumption.

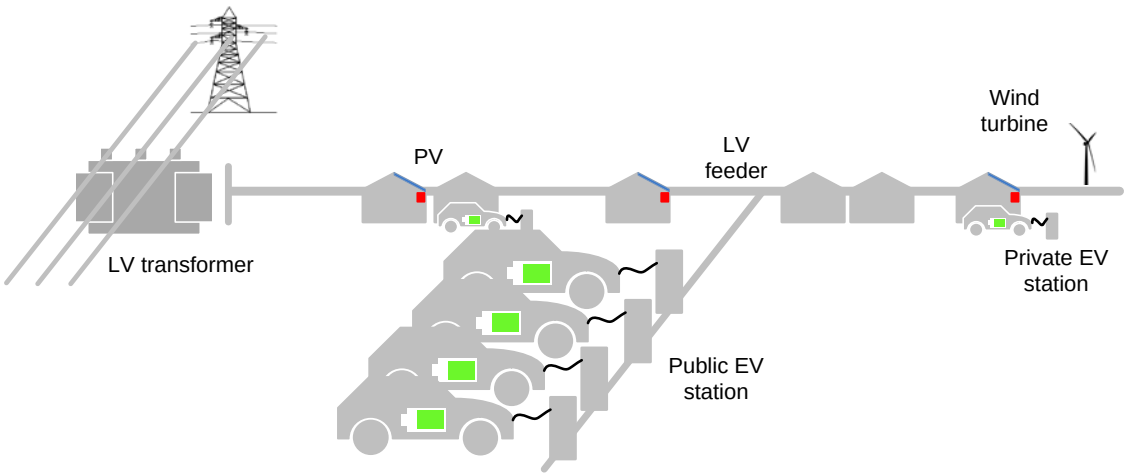

Figure 1-4: EV charging infrastructures in a LV distribution grid.

Because voltage variations are one of the most urgent issues to be solved in LV feeders with PV [23], different control concepts involving private and public charging are proposed as storage solutions for voltage support.

1.4 Outline and contributions

The present report is organized in the following chapters:

Chapter 2: in ***State of the art of EV and Interaction with RES***, a literature review on the prospective interaction of EVs with renewable energy sources, Wind Power and PV is presented. An overview of the state for EV technology, EV coordination technology and battery technology is also presented.

Chapter 3: in ***EV Requirements for Ancillary Services***, the hardware and control requirements to achieve EV coordination are defined and described. An EV test bed, implemented with full-scale EV components, is used for testing the bi-directional power capabilities and controllability of an EV.

Chapter 4: in ***EV Coordination for Ancillary Services***, a control architecture to enable the EV provision of ancillary services is proposed. A proof of concept of secondary reserves and regulating power from EVs is shown, using 5-minutes interval power requests from the Danish TSO. The EV coordination is realized under the control framework of a Virtual Power Plant. The optimal usage of the EV battery is analyzed and recommendations are given dealing with nonlinearity aspects and ageing factors arising during EV load coordination.

Chapter 5: in ***EV Coordination for Local Grid Support***, the EV load coordination is investigated for the integration of PV in LV distribution grids. A novel approach is proposed to provide voltage regulation in feeders with PV, using EV load coordination. The control of the electric demand from public and private EV stations is investigated. A LV grid model with high PV penetration is used as case study. A proof of concept of voltage support using EV load coordination is implemented. This chapter contains the main academic contribution of this thesis.

2
CURRENT EV TECHNOLOGY AND INTERACTION WITH RES

This chapter reviews the existing literature looking at the role of electric vehicles (EVs) in the power system with renewable energy sources (RES), wind power and Photovoltaic (PV). The previous research on the potential use of coordinated EV load for the provision of ancillary services and energy storage is reviewed. Ultimately, an overview on state-of-the-art of EV and battery technology and on the developed EV coordination concepts is provided.

2.1 EV interaction with RES

In different countries in Europe, the increasing wind power and PV installed capacity has set high requirements on power balance control as well as on power quality.
Large off-shore wind farms concentrate a high power capacity at a single location. Due to the wind speed variations, the magnitude of the power fluctuations can reach very high values. As an example, in **Figure 2-1**, the 10-minute average wind power profile from the 160 MW wind farm Horns Rev, is depicted. Over the 11-day period, the normalized wind power production varies from zero to almost 100% production [26]. Wind power fluctuations are visible at different time-scales, short (intra-hour) and long (several hours) [26]. Also PV has in common that the active power production is variable over time; this aspect makes wind power and PV non-dispatchable energy sources [27]. The Transmission System Operator (TSO) has the challenging task to ensure the balance between consumption and production, at all times, including at intra-hour time scales.

To facilitate the integration of RES in the power system, the research has focused on the potential contribution of EVs. The topic has been developed within the paradigm of *smart grid* and it is centred on the EV's potential of creating mutual benefits to both the electric power system with RES and future EV users. With the term *smart grid* is meant the operation of the power system using communication and control technology, power electronics technologies and storage technologies to balance production and consumption at all levels [28].

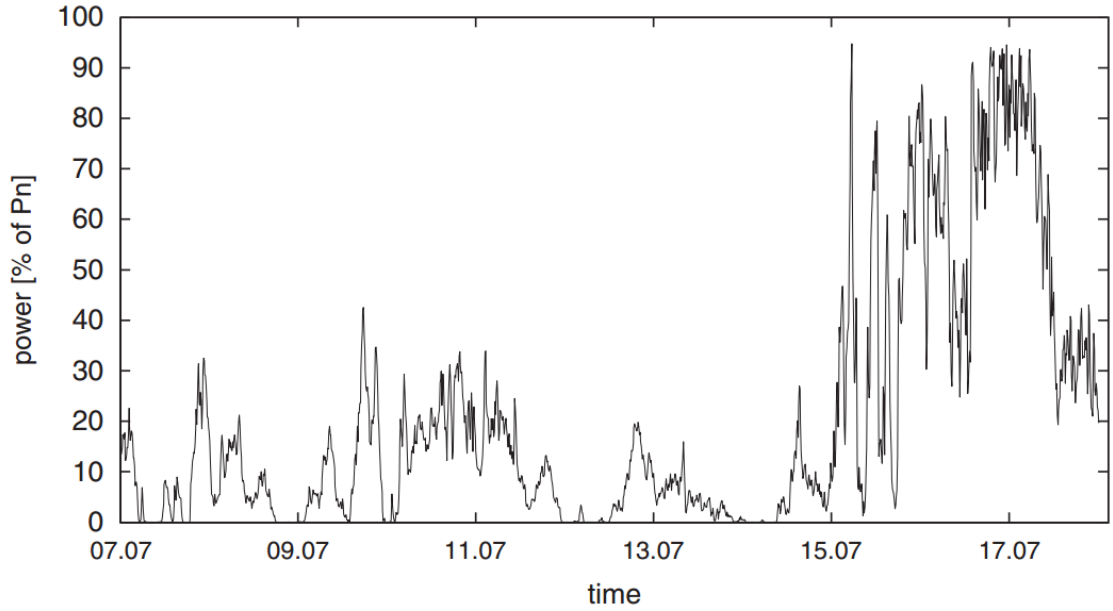

Figure 2-1: Wind power generated over an 11-day episode. Power values consist in 10 min averages, normalized by wind farm nominal capacity of 160 MW [26].

Within this vision, an EV can act as a controllable load or as a storage, charging or discharging part of its battery capacity back to the grid, according to the Vehicle to Grid (V2G) concept introduced by Kempton *et al.*, in 1997 [29].
If the charging of EVs is uncoordinated, their impact on the grid has proven to be equivalent to a large electric load, leading to higher power system's peak-load and to distribution grid congestion issues [30]. To avoid such scenario, the research has looked at what role EV coordinated charging can have, in combination with RES production. In particular, solutions using EVs for the provision of ancillary services for wind power integration and energy storage for PV integration have been addressed.

2.1.1 EV interaction with Wind energy

The use of EVs in power systems with wind power is reported to be best suited for the provision of ancillary services [31]. The studies by Kempton *et al.* [31], [32] suggest that, in the short term, EVs should be coordinated for high value services, such as ancillary services, which can potentially lower the running cost to EV owners, despite a higher initial cost compared to ICE cars. Pillai and Bak-Jensen [33] looks at the technical benefits of ancillary services' provision by EVs in the Western Danish power system, which is regarded as a wind power dominated power system. In particular, the provision of secondary reserves, Load Frequency Control (LFC), is assessed, via simulation models. The authors demonstrate how the power mismatch caused by the variability of wind power can be managed by EVs, thus relieving the use of conventional power plants. A similar idea is developed by Galus *et al.* [34], where large amounts of clustered EVs and household appliances are used to provide secondary reserves, LFC, in the power system. From the simulation results, it is observable also

how the vehicle's batteries are subject to wide energy excursion, passing from empty to full state of charge. The Danish EDISON project report by Hay *et al.* [35] looks at the opportunity of using EVs for regulating power [18]: it is envisioned that to limit the excessive use of automatic reserves [18], and in order to re-establish the availability of these, the use of regulating power shall be increased in Denmark. According to the authors, the use of EVs to provide regulating power in Denmark is one of the solutions for substituting the reduced reserve power from conventional power plants in the future. Other studies on EVs for wind power integration look at micro-grid applications. In [36] and [37], Lopes *et al.* present how EV load coordination can be used to stabilize the system frequency in a micro-grid with wind power, by applying a droop control strategy. It is found that the penetration level of wind power can be further increased in presence of coordinated EV load.

In the different studies, EVs and power systems are generally regarded as ideal controllable loads in a simulation environment; however, the possible constraints such as EV control requirements and EV components response during periods of coordination are not addressed.

2.1.2 EV interaction with Solar energy

The literature on the use of solar energy with EVs is much more diversified than the studies on wind energy and EVs. Electric energy from PV can be produced at medium voltage as well as at low voltage level in the power system; the latter option generates further motivations to closely integrate PV production with EVs [4]. As observed in the review by Bessa *et al.* [38], the use of EVs in distribution grids with PV is seen by several studies as an energy storage option, rather than a controllable load; the peak solar irradiation during daytime can be used to store the energy in the vehicle batteries for later use. Some contributions aim at maximizing the charging of EVs during solar irradiation hours, according to a "green" charge concept [38]. Another application is addressed by Birnie [39], namely the case where daytime charging of EVs is performed in parking lots that are located e.g. at workplaces; the EV can be fully recharged during working time, realizing a solar-to-vehicle (S2V) strategy. The study performed shows also that the energy produced from each single parking space could generate enough energy to fulfil the transportation need of the EV user, to and from workplace.

Low voltage grids with high penetration of PV have one major problem to cope with, which is related to voltage magnitude variations along the feeders. These variations are particularly evident during periods of high generation and low load conditions [40]-[43]. Such events may occur on a daily basis in residential areas with high concentration of roof-top PV. Several options for voltage rise mitigation have been investigated and the most important include: grid reinforcement [41], coordinated active power curtailment [42], reactive power control strategies [43]-[47], and stationary storage [48].

According to the literature, how to use coordinated EV load in feeders with high PV penetration has not been investigated.

2.2 Electric Vehicle coordination

The provision of ancillary services from EVs is a compelling option if this is provided by a large fleet of vehicles [49]. As noticed by Kempton *et al.* [49] in 2001, a single EV cannot directly bid in the electricity market nor establishing transactions with electrical utilities due to its limited power capacity. The solution suggested by the authors is an aggregator technology that serves as a *middleman* between the vehicle, the utility companies and the electricity market, according to a framework similar to the one depicted in **Figure 2-2**. Other types of aggregator frameworks are described in [10], [50].

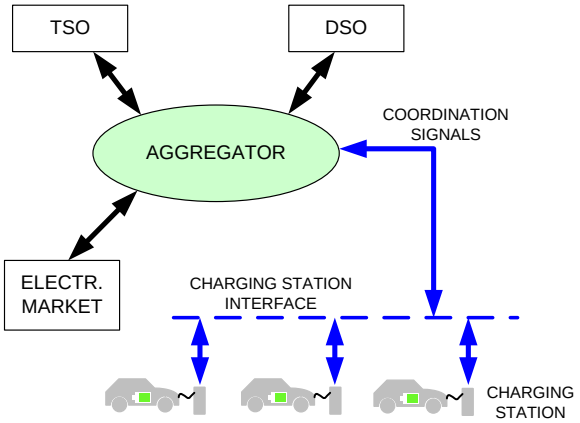

Figure 2-2: Simplified EV coordination framework.

In all cases an EV aggregator generates the coordination signals for its EV fleet, in consideration of the information exchanged with the TSO, the DSO and the electricity market. Fell *et al.* [51] defined that an EV aggregator is needed to coordinate the grid-connected operation of multiple EVs to meet product or service commitments to the TSO, while also achieving targeted charging schedules to satisfy the driving needs. The aggregator will need to sign up a sufficient number of EVs to provide the product or service and meet the regulation requirements by the TSO. An EV aggregator is also defined by Brooks and Cage [52]; its priority looks at the driving needs of the EV users. The authors propose a method in which the users communicate their driving needs to the aggregator and the aggregator processes this information. With the availability of all driving profiles, the aggregator creates a "virtual power plant" where the number of vehicles expected to be plugged, as well as the aggregated power and energy levels, can be better estimated on an hourly basis. Bessa *et al.* [53] develop an optimization approach to support the aggregator in the participation of the day-ahead (spot market) and secondary reserves sessions. The authors conduct a 2-year simulation of the Iberian market deriving the following conclusions: 1) an aggregator agent with optimized bidding can decrease the charging costs compared to uncoordinated charging; 2) if the payment of a reserve capacity is available, then the EV participation in the regulation reserves is economically convenient; 3) without the reserve capacity payment, optimized bidding still pay off, however forecasting the EV load and estimating

uncertainties becomes an important problem to solve. Lopes *et al.* [54] describe an architecture where the EVs are aggregated under a micro-grid and multi-micro-grid concept. Also in this case, the aggregator acts as an intermediary between the EV users and the electricity market and it can be responsible for providing frequency control. A different concept of aggregator is presented by Galus and Andersson [55]; the aggregator is not a company but an abstract computational entity monitoring a control area; it acts as an intelligent interface between the EVs and the electrical utility. In the Danish EDISON project [56], the conceptual role of the EV aggregator is designed considering the needs of the Danish power system, with high penetration of wind power. The role of the EDISON aggregator (EDISON Virtual Power Plant) is to coordinate the provision of ancillary services from EVs, in relation to the needs of the TSO, acting as an intermediary with the electricity market, **Figure 2-2**.

In general, EV coordination can be realized if EVs are able to respond to coordination signals. The EV requirements to respond to ancillary services and the technical constraints that arise during EV coordination periods are addressed in this research project.

2.3 EV charging demand and user behaviour

The coordination of EV load during a day, month or year, should count on the EV availability for charging. The EV user driving behaviour [57] and his willingness to plug the EV into the grid are important factors to enable the provision of power system services from EVs [57].

The project report by Christensen [58] analyzes the EV driving behaviour of private households in Denmark, considering two data sets: the National Travel Survey data[2] and the data from 350 cars in 2002-2003, AKTA data[3], respectively. In the analysis, it is assumed for an EV, a 24 kWh battery capacity and an average range of 150 km. It is observed that charging at residential premises is largely realized using single phase grid connection, requiring about 7-8 hours for a full recharge; while, charging at public places, e.g. at shopping centres, large parking lots and other public areas, can be realized with three-phase charging using 16 A or 32 A. An interesting finding in the analysis is that the share of vehicles not driving during the day is about 26% on weekdays, and 36% during weekends. In both cases, the vehicles are normally parked at home [58]. If the EVs are all plugged into the grid, a significant EV capacity is available for coordination [58]. Finally, it is found that night charging seems very likely by private owners and it has high potential for the ancillary services provision overnight [58]. Bessa *et al.* [53] look at the importance of forecasting the EV load, in relation to the daily driving needs of EV users and to the charging flexibility offered. The EV load

[2] National Travel Survey: for the interested reader, reference to the data can be found in [58]
[3] AKTA data: for the interested reader, reference to the data can be found in [58]

is classified as "inflexible" for those users not participating in coordinated charging and flexible for those able to respond to coordination signals. With regard to private and public charging for PV integration, it is found that high energy storage potential is available from EVs, during daytime [58], [59], [60]. According to Dallinger *et al.* [59] and Weiller *et al.* [60], the time interval between 10:00 AM and 15:00 PM shows a lower driving activity compared to the early morning interval 7:00 AM to 9:00 AM, which may correspond to a higher probability of EV connected to the grid. Weiller [60] estimates the EV load profiles for different charging power scenarios, using the large American household travel survey[4] (US DOT 2003) data set. In particular, for the public charging scenario, the EV load profile is mainly present in the 8-hour interval 10:00 AM to 18:00 PM, with peaks of EV demand between 12:00 AM and 14:00 PM in weekend and weekdays, at private or public stations. The identified interval corresponds indeed to the hours of PV generation.

2.4 Electric Vehicle technology

The coordination of EV load relies on the existing EV technology. A thorough description of the actual vehicle architectures is provided by Chen *et al.* [61]. A common feature is that all plug-in vehicle concepts use the grid to recharge the battery to the full charge state. Two vehicle classes can be distinguished: plug-in hybrid EV (PHEV), with different categories, and battery EVs (BEV), **Figure 2-3**:

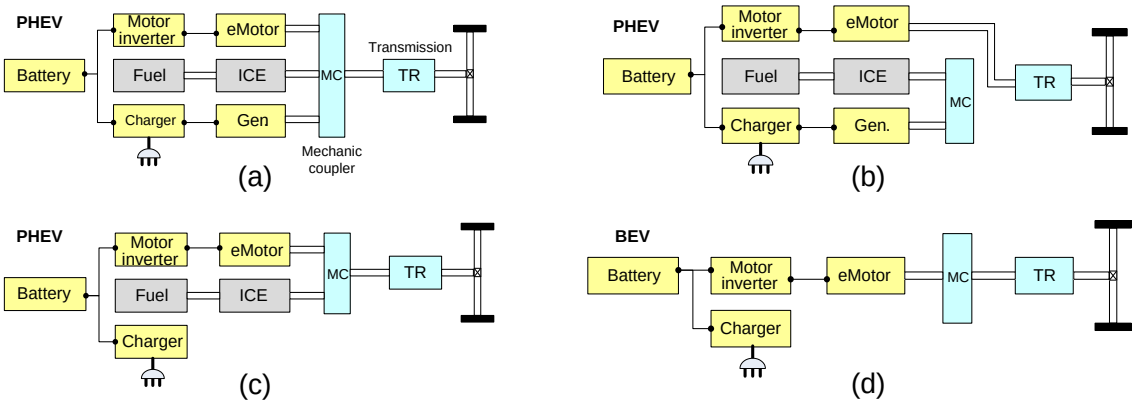

Figure 2-3: Plug-in vehicle architectures.

A general definition for the four depicted categories is as follows:

- Battery electric vehicle (BEV) – A BEV is an electric vehicle that is powered solely by electricity stored in onboard batteries [61], **Figure 2-3** (d). A BEV does not feature a combustion engine and is charged by plugging into the electricity grid or, on a limited number of models, swapping the battery pack. In the BEV class, the

[4] US DOT 2003: for the interested reader, reference to the data can be found in [60]

drive system is realized using an electric motor (eMotor) and a motor inverter. The coupling to the wheels is realized via a mechanic coupler (MC) and a transmission shaft (TR). Part of the energy drawn from the battery during driving can be recovered by regenerative breaking. The only source of energy is the battery pack which is designed to fulfil a certain range.

- Plug-in hybrid electric vehicle (PHEV) – A PHEV is a combined electric and internal combustion engine (ICE) vehicle capable to charge using the grid and to operate over a short distance in electric-only mode and it can feature regenerative breaking. The battery in a PHEV has a smaller size than a BEV battery, thus a conventional engine and fuel tank are employed to extend the range [61]. The three categories of series-parallel hybrid, serried hybrid and parallel hybrid belong to the PHEV class and these are depicted in **Figure 2-3** (a), (b) and (c), respectively.

The energy content of the some of the PHEVs and BEVs currently on the market (or close to be launched) is shown in **Table 2-1**, [62].

Table 2-1: Battery energy for different PHEVs and BEVs

	PHEV			**BEV**		
Model	VolvoV70	VW Golf Variant	Chevrolet Volt	Renault Fluence	Ford Focus E.	Nissan Leaf
Energy (kWh)	11.3	13	16	22	23	24

On average, the energy content of a BEV is higher than a PHEV. However, a common aspect of both classes is the use of a point of connection in the low-voltage (LV) distribution grid to realize the charging purpose. For the scope of this project, both classes presented will be simply regarded as “EV”.

The charging power levels used for charging are defined in Standard IEC 61851-1 [63]. The standard defines different charging options, single-phase or three-phase, to which correspond different power levels, **Table 2-2**.

The standardization activity has focused on EV requirements for conductive charging with AC and DC supply. The *quick* charging power levels of 11, 22 and 43 kW will be accommodated gradually in three phases: the 22 kW will be deployed first; the second phase will involve the 43 kW charging power, a third phase will involve DC charging, which entails next generation batteries requiring at least 50 kW (400Vdc - 125A) charging power. With DC charging, a fully depleted 24 kWh battery pack can be

charged up to 80% state-of-charge (SOC) in about 30 minutes. Thanks to the shorter charging time, DC charging is commonly known as *fast* charging [64].

Table 2-2: Most common EV charging options and charging power levels

AC current	AC voltage	Grid connection	Power
10 A[5]	230 V	single phase	2.3 kW
16 A	230 V	single phase	3.7 kW
32 A	230 V	single phase	7.4 kW
16 A	400 V	three-phase	11 kW
32 A	400 V	three-phase	22 kW
63 A	400 V	three-phase	43 kW
DC current	DC voltage	Grid connection	Power
125 A	400 V	three-phase	50 kW

The charging power levels presented are referred to unidirectional charging power. However, through the V2G technology, it is possible to realize a bi-directional power exchange between the EV and the grid [65].

2.4.1 Vehicle-to-Grid (V2G) technology

Research on V2G was firstly introduced in 1997 by Kempton and Letendre [29] after filing the first patent on this technology on behalf of the University of Delaware. According to this technology, the vehicle shares with the grid part of the energy stored in the battery pack. It follows that the power components used need to be bi-directional. From a grid perspective, the concept enhances the old vision which considers the vehicles as a mere electric load and presents the scenarios in which they can act as small generating units.

The power level available from a single V2G-capable EV may vary depending on the features of the power electronics equipment in the vehicle. Kempton and Dhanju [66] compute the potential available power from V2G in several countries, assuming an electric power capacity of 15 kW per vehicle. For example, in Portugal, 5.8 millions of vehicles would lead to 87 GW, for an average load of 5 GW; Germany, with 44.6 million of vehicles has a potential of 670 GW, for an average load of 58 GW. Of course, these calculations refer to ideal scenarios.

Lately, Brooks and Thesen [67] attribute to V2G a conceptual meaning, rather than a particular technology. The authors mention that the V2G concept does not necessarily entail a power flow from battery to grid, since also those vehicles with unidirectional charging capability may provide grid services. Quinn *et al.* [68] have a different opinion: V2G is a technology which shall be recognized as the EV ability to provide

[5] The charging current of 10 A is often used to perform domestic charging in different EU countries.

electric power from the battery towards the grid. In this thesis, V2G is considered as a technology, according to [68]. In the review on V2G studies by Richardson [4], a conclusion is that the marginal benefit of V2G technology, in comparison to the overall benefits of EVs, appears to be relatively small.

2.4.2 EV batteries

The key component in the EV interaction with RES is the battery. With regard to battery technology, market expectances indicate lithium-ion (Li-ion) as the favourite technology in the EV sector [69]. A research report by Frost & Sullivan [69] foresees that about the 80% of newly registered EVs in 2015 will be powered by Li-ion battery technology, **Figure 2-4**. As a consequence, a significant increase in the cost of lithium as a raw material is envisioned around 2020.

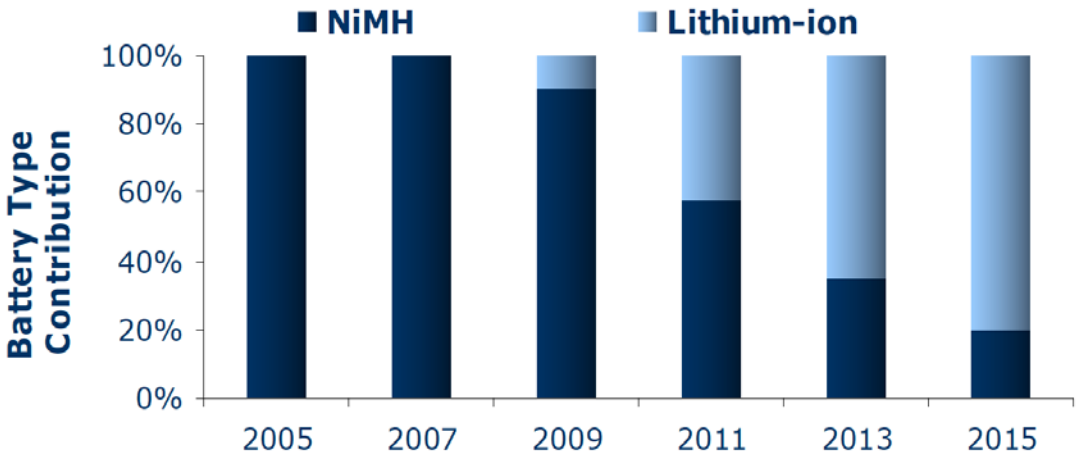

Figure 2-4: Share of lithium technology in the EV market [69].

The actual EV development is strongly dependent on the advances of Li-ion battery technology. Compared to other battery technologies, Li-ion batteries have shown to offer a greater energy-to-weight ratio, no memory effect and low self-discharge when not in use [70]. These are fundamental aspects for the establishment of Li-ion batteries as the leading solution in automotive applications. For the same reasons highlighted, Li-ion technology is considered as the battery technology in this thesis.

In general, every Li-ion battery technology is characterized by a nominal cell voltage, nominal capacity (in Ah), nominal energy (in Wh), maximum charging/discharging current (C-rate), minimum and maximum cell voltage, internal resistance, operating temperature range, power density, energy density and weight [70].

The main aspects which still pose some limitations to a breakthrough on the market of EVs are related to battery cost and lifetime. As of today, the cost of a Li-ion EV battery is about 500 $/kWh (384 €/kWh) [71], which thus amounts to a significant part of the vehicle cost. The battery lifetime is regarded as the number of cycles that brings the battery to the 80% of its nominal capacity (Ah), after a complete charge, according to [72]. The retained capacity, which is the usable battery capacity after a full charge

cycle, is a non-linear time-variant parameter, which varies depending on climatic and use conditions. From an electrical point of view, the variation is due to the alteration of the internal equivalent battery impedance over time [73]-[78].

For this reason, the alteration of the internal impedance of the battery is often used as an indicator of the ageing process and expected remaining lifetime. For any type of Li-ion battery, four major factors can be considered as influencing the ageing process: number of cycles (N), operating and storage temperature (T), the charge or discharge rate, C-rate (1C is the rate required to charge in 1-hour a fully discharged battery), depth of discharge (DOD) [70]-[78]. A description of these factors is provided in **Table 2-3**. The use of the EV battery for driving and for the provision of ancillary services entails in both cases a battery ageing process.

Table 2-3: Factors influencing EV battery lifetime

Number of cycles (CN)	Energy and lifetime are affected by the number of cycles. This variable is the counter of complete charge/discharge cycles of a battery-EV. If the vehicle is used in Vehicle-to-Grid mode, the number of cycles' counter will take into account the discharging phase.
Temperature (T)	The temperature strongly affects the battery performances and lifetime. Low temperature conditions, -20°C to -10°C are very common at northern latitudes. The usable energy is considerably reduced at low temperature, and at the same time the charging process is not effective, as it is for temperatures of 20-25°C. Operating under higher temperature conditions, 45°C or above, has shown to negatively affect the battery lifetime.
Depth of discharge (DOD)	The DOD level affects considerably the battery lifetime and energy fade. It is shown by manufacturers' datasheets that the use of 100% DOD instead than 60% DOD, results in faster battery degradation and shorter cycle life. Therefore, battery-EV manufacturers limit the usable energy window to a percentage which is a trade-off between vehicle range and battery lifetime.
Charge/discharge rate (C)	The current rates used for charging/discharging the battery strongly affects the lifetime and the energy fade of the battery. The design of a PHEV and EV is made considering an average current of around C/2 in a normal driving cycle and a peak current in the measure of 1C to 2C during high speed or accelerations [57]. If the use of the battery-EV is often characterized by high current rates during driving, the battery lifetime decreases. The same consideration is valid for a frequent use of the V2G mode, when the battery-EV delivers energy back to the grid. On the same extent, during charging, the battery lifetime will decrease if fast-charging ($> 2C$) instead of slow charging ($\leq 0.5C$) is used.

2.5 Summary and discussions

In this chapter, the previous work on the EV interaction with renewable energy sources is reviewed.

According to the reviewed research studies, with gradually increasing penetration levels of wind power and PV in different countries, the use of coordinated EV load can serve as an option to facilitate RES integration. In this way, EVs are not just an additional uncoordinated electric load, but they can function as controllable loads.

With regard to wind power integration in the power system, the research has highlighted that the electric load originated by EV charging can be coordinated for providing ancillary services. To achieve such scenario, the coordination of EV fleets is needed and this can be achieved by deploying an EV aggregator. The EV aggregator, e.g. a Virtual Power Plant, should elaborate the regulation requests from the TSO and translate these in charging/discharging requests which are feasible by the individual EVs.

Wind power-dominated power systems have received particular attention in relation to the need of ancillary services by EVs. Simulation studies show that EVs are suitable for the provision of secondary reserves, due to a short response time, in comparison with the reserve technical requirement. At the same time, the potential use of EV load coordination has been also simulated in micro-grid contexts with embedded generation, thus demonstrating their versatile operation.

However, the practical implementation issues of ancillary services provision from EVs, the EV control requirements and the constraints arising during EV coordination, need to be further addressed.

Ultimately, the use of EVs in grids with PV is reviewed. These studies have a more limited scope than the ones looking at wind energy integration. In particular, they look at the storage capability of EVs during daytime in grids with PV. The charging of EVs using local PV production at parking areas or workplaces has received particular attention.

With regard to the needs of LV feeders with high penetration of PV, voltage magnitude variations due to the decentralized PV power production are still an issue to be solved. However, the use of coordinated EV load for the provision of voltage support in feeders with PV is not addressed in the literature yet.

3
EV REQUIREMENTS FOR ANCILLARY SERVICES

The requirements to enable the provision of ancillary services from EVs within a centralized Virtual Power Plant coordination framework are defined and implemented in this chapter. The ancillary services we refer to are *secondary reserves (LFC)* and *regulating power*, and these are utilized by the TSO in the Western Danish power system [98]. Following a TSO request, the reserve by EVs should be fully activated within 15 minutes [98]. Considering the aforementioned TSO condition, a sampling time of 1 second is chosen as the time interval to update all variables involved in EV coordination for the two ancillary services examined.

In Section 3.1, an overview on the EV coordination control concepts is presented. In Section 3.2, the EV coordination using a VPP is defined. In Section 3.3, the EV capabilities for grid interaction are defined. Technical and market issues of V2G technology are discussed. In Section 3.4, the infrastructure involved in the EV coordination using a VPP is described. In Section 3.5, the EV requirements for the provision of ancillary services within a VPP framework are defined. Finally, in Section 3.6, the implementation of the requirements is performed with a full-scale EV test bed. Summary and discussion follow in Section 3.7. Detailed information on the test performed is documented in paper [P4].

3.1 Coordinated control concepts

The generic coordination strategies for distributed energy resources (DERs), including EVs, can be divided into the following two categories:

1) ***Centralized control***, where a centralized coordinator dictates *when* EV charging or discharging should take place and *what* power level to aggregate. Decisions could be made in relation to power system needs, such as ancillary services, or they could target EV user preferences, e.g. a desired time window for charging, a desired final state of charge, or a minimum charging cost [79].

2) ***Distributed control,*** where the individual EVs determine their own charging or discharging patterns. Decisions on charging can be made on the basis of e.g. time of the day or electricity price. A critical aspect is that the synchronized charging activation of

a large fleet of EVs, due to a common control signal, e.g. the electricity price, might lead to grid congestion issues [79].

The two coordination concepts have been described with respect to EV coordination, though the same concepts are applicable to any type of DERs [80]. The coordination of EVs can be realized with a Virtual Power Plant technology, whose possible architecture derives from the generic coordination concepts described.

3.2 EV coordination with Virtual Power Plant

The generic aggregator concept is based on the coordinated use of decentralized power generation by distributed energy resources (DERs) [80]. A Virtual Power Plant is an aggregator with the goal of combining the power production of several DER units, as if produced by a single large production facility, enabling them in market participation. In relation to this, the term “virtual” is used. By joining the VPP, the DER owners can share overhead costs and delegate the trading responsibility to a trader representing the VPP on the market [80]. The research on VPP technology aim at technical aggregation solutions for the growing variety of DERs, e.g. wind turbines, PV systems and EVs [81].

A VPP is also characterized by its role in the society; it can operate on the power market to generate profit for its DER members or it can be used to provide power system services. Based on the role, the VPP can be classified as commercial or technical power plant. These two types of VPPs were described and tested in the European FENIX project [82].

The three most important VPP architecture concepts derive directly from the coordinated control concept of Section 3.1. In relation to EV coordination, these can be described as follow:

A. Centralized Control VPP

   In the centralized VPP, all control functions lie within the VPP and all the information about the market or power system needs are decoupled from the single EVs, **Figure 3-1** (a). A characteristic of this design is that the VPP is given a direct way of utilizing the EVs to meet the power system needs. Monitoring and control of the vehicles is realized from the VPP to the single EVs [80].

B. Distributed Control VPP

   The distributed control VPP, **Figure 3-1** (b), is composed of a hierarchical architecture, with VPPs on local levels. A local VPP aggregates and coordinates a limited number of EVs and delegate some decisions to a higher level VPP. The responsibility to communicate and coordinate each EV is split among different VPPs [80].

C. Fully Distributed Control

   The third concept is the Fully Distributed Control **Figure 3-1** (c). In this design each EV can act as an independent and intelligent agent that participates and reacts based

on the service requested by a service provider. Monitoring of vehicle data may be not communicated to the service provider. EV control decisions are taken locally, instead of centrally, as it happens in the previous two architectures [80].

The technical comparison of the VPP architectures, in relation to EV coordination, is not covered in this thesis.

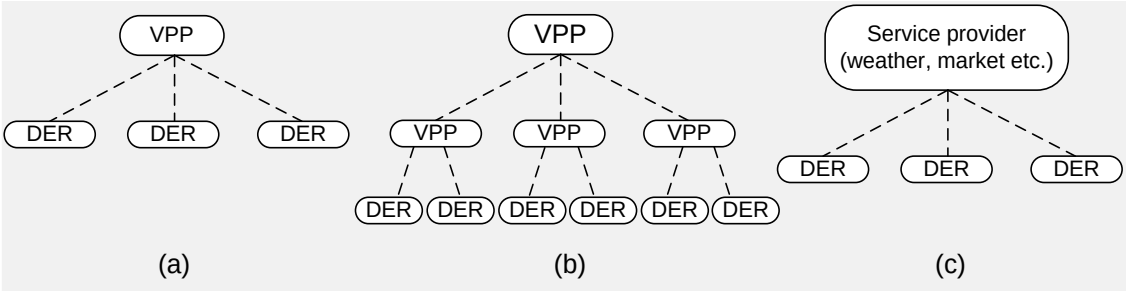

Figure 3-1: VPP architecture concepts. (a) Centralized; (b) Distributed; (c) Fully distributed.

3.2.1 The EDISON VPP

In the Danish EDISON project [56], the aggregation platform of a VPP is designed to fit to the requirements for the provision of ancillary services by EVs. The role of the EDISON VPP is mixed commercial-technical role, and the concept architecture is **centralized** [83]. In this research project, this architecture concept is used as reference for the definition of the EV requirements for the provision of ancillary services.

The EDISON VPP acts as a standalone market player. The VPP has the responsibility to buy the electric energy to satisfy the driving needs of the EV users, as well as to bid on the ancillary service market to support the power system using its EV fleet. The VPP has a modular architecture for the management of different tasks [83]. An EV module contains the following functions:

Table 3-1: EV module functions [83]

Functions	Description
Schedule generation	the generation of a schedule compatible to an EV, based on charging/discharging requests
Feedback	the feedback or power response of an EVs during charging/discharging
Transaction	the metering of the electricity consumed or service provided by the single EV
Charging prediction	the prediction of the EV availability for charging or discharging

Other modules compose the VPP software architecture and these are involved in the communication with external entities such as the TSO, the electricity market, the DSO. More details can be found in [83].

3.3 Grid interaction of EVs

By definition, EVs are capable of interacting with the power system, as they are able to charge using the electrical grid.

The grid interaction functions of EVs can be enabled at different stages in the EV technology development and smart grid development. Merging together industries of different backgrounds, such as vehicle manufacturers with battery companies, or DSO with TSO, appears a major challenge to solve [84].

It is envisioned that different *generations* of EV interaction with the power system will be enabled at different stages [84].

As indicated in **Table 3-2**, a *first generation* of EV interaction involves minimal control functions, under the known "grid-to-vehicle" (G2V) unidirectional power technology. Today, all EVs belong to this class, except for a limited number of models [84].

Table 3-2: Most common grid-interaction concepts of EVs

EV generation	Power flow	Communication characteristics	Grid interaction functions
First generation	Unidirectional G2V	Maps or EV status info over mobile phone network	Manual setting of charge window
Second generation	Unidirectional G2V	Electricity price, plus all previous features	Intelligent charging considering price, local consumption of RES, plus all previous features
Third generation	Bi-directional G2V, V2L,V2H, V2G	All previous features	House load relief, electricity peak relief, local consumption of RES, using net metering, plus all previous features
Fourth generation	Bi-directional G2V, V2L,V2H, V2G	External aggregator for EV coordination	Ancillary services (regulating power reserves), distribution grid services, plus all previous features

With the first generation of vehicles, the power flow is solely unidirectional, for the purpose of charging. Mobile phone applications for EV users will serve as a search tool for charging stations in the range of the EV or similar applications. The EV user may have the possibility to manually program the time window for charging to his best convenience.

A *second generation* of EV interaction entails optimized charging schemes that shall minimize the cost of charging seen by the EV user, using charging mechanisms that consider the existing electricity tariffs.

A *third generation* of EV interaction involves V2G technology, i.e. the capability of bi-directional power exchange of EVs. According to [84], the first real use of V2G will be deployed in vehicle-to-load (V2L) applications. In this case, the EV would be acting as a generator for an isolated load. An extended concept of V2L is vehicle-to-home (V2H), where the vehicle acts as a power supply for the house. Furthermore, vehicle-to-grid (V2G) is expected to be enabled for this generation of vehicles. EV aggregators will not come with this phase. Therefore, the V2G technology will be mainly used to minimize the payback time of the vehicle using energy arbitrage i.e. charging during low-cost off-peak electricity hours and release of the energy back to the grid at higher rates, e.g. around peak hours.

A *fourth generation* of EV interaction introduces higher level coordination schemes for EVs, offering an extensive use of the V2G technology [31], [32]. At this stage, EV aggregator technologies are assumed to be active on the market and EVs are enabled to provide ancillary services.

A fourth generation of EV interaction is addressed in this research project for the provision of ancillary services.

3.3.1 V2G technical and market issues

In 2002, Brooks [85] evaluated the feasibility and practicality of a fourth-generation EV interaction using V2G technology, for providing regulation services to the power system. This was possible thanks to the involvement of the company ACPropulsion (ACP), which was the only manufacturer producing V2G-capable power electronics worldwide. The test was performed using a Volkswagen Beetle converted to electric, with an 18 kWh lead-acid battery pack and a power converter capable of charging and discharging. The vehicle was remotely controlled using wireless communication, while an aggregator technology was used to send the control signals to the vehicle, in relation to the TSO needs.

The experience by Brooks has proven the technical feasibility of the concept, showing the potential benefits. However, there are still some impediments and barriers to the V2G transition: battery degradation, impact on distribution grids, energy losses, the resistance of the automotive sector and customer acceptance are the main ones [86].

The biggest challenge for V2G is the battery technology, its high initial cost and battery ageing. A carmaker designs the EV battery system to last at least a given mileage or a given time, with warranty coverage of several years. With V2G, other variables may affect the battery lifetime and these are out of control for a car manufacturer [86].

In contrast, in the research by Brooks, it is concluded that the economic value of the service offered by the vehicle is able to beat the battery wear cost, as the cost of the battery is between 20 to 60% of the annual gross value created [85]. However, this estimation was done considering a commercial lead-acid battery, whose market price today is about one-fifth of a Li-ion battery [87], and a particular type of service. Considering that EVs will be mostly powered by Li-ion technology in the coming 5-10 years [69], the conclusions in [85] are not applicable in the current scenario; these might become valid only once Li-ion batteries have a comparable market price to Lead-Acid batteries, which is about 88 $/kWh (68 €/kWh).

3.3.2 Driving behaviour and EV availability for coordination

The coordination of EV load for the provision of power system services should take into account:

- The EV fleet availability
- The proportion of EVs plugged and able to offer the services
- The proportion of the EVs allocated for the services

The EV fleet availability indicates the proportion of vehicles parked and plugged to grid. For the participation of EVs in power system services, the plug-in operation of the EV is a fundamental aspect that requires motivating the EV users for the service provision. It shall be noted that not all the plugged EVs are available for the services, but depending on the energy status of their batteries, these may or not participate in the service provision. Finally, the proportion of EVs allocated for the service should be considered; this indicates the number of EVs in the fleet that have been registered for the service provision, after an agreement with the EV users.

The EV load coordination is also closely related to the vehicles' driving patterns; the prediction of these is an important aspect for the VPP, to quantify the daily fleet capacity available for power system services. A fundamental assumption in this project is that the electric power consumption from EV charging is going to gradually increase in the years [87]. The probability of an EV charging at home is estimated for the 24-hour period in [87]; a maximum availability (normalized to 1) during night hours and an average availability of 0.7 during daylight, i.e. between 10AM and 6PM, is observed. These findings confirm that the domestic EV load coordination during the day and overnight is a realistic scenario. A similar outcome is obtained in [58]. Regarding public charging, in [59], [60] is found that the time interval between 10AM and 15PM shows a lower driving activity. During this period, the EVs may be parked at commercial places or at workplace, thus giving opportunities for EV load coordination.

3.4 Coordination infrastructure

The ancillary services provision for a *fourth-generation* EV interaction is defined, using the existing aggregator technology of the EDISON project, named EDISON Virtual Power Plant (VPP), [56]. The VPP has been specifically designed for EV coordination, thus its framework is used to define the EV requirements for power system ancillary services. The VPP – EV coordination infrastructure is composed of two main layers, as depicted in **Figure 3-2**:

- centralized coordination layer: VPP
- local functions at the grid interface: EV charging station

The *centralized* EV coordination is the upper layer of coordination, realized by the EDISON VPP. To combine the needs of the power system and those of the EV users, the EV coordinator generates a power schedule for the single vehicles. Under the same coordination scheme, all EVs are expected to respond according to the received schedules.

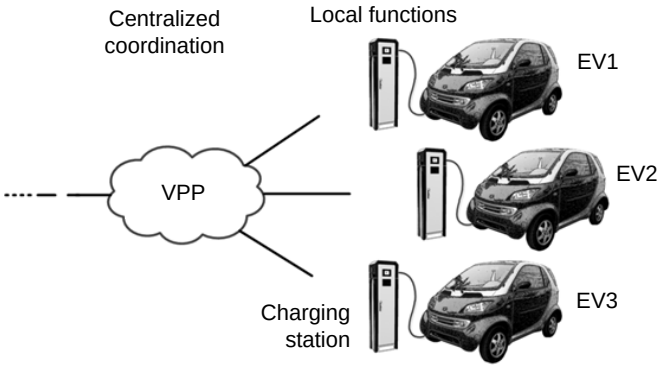

Figure 3-2: EV coordination infrastructure.

The *local* functions are realized at the charging station where the EV is connected. These include all those functions that are not feasible by centralized higher level coordination, without a significant increase of data flow. Local functions shall ensure that all electric variables, such as voltage, current, power during charging/discharging periods are within the allowed range. This is possible by equipping the charging station with *smart metering devices* that allow the control of protection devices, such as circuit breakers within the station [91]. The specific metering solution implemented to monitor the electric variables during EV load coordination is described in the following sections.

3.5 EV technical requirements for Ancillary Services

The ancillary services considered in this project are secondary reserves (LFC) and regulating power used by the Danish TSO [98]. A more detailed description of the services is given in the next chapter; other types of services are not treated.

An important issue is that both services should be fully activated within 15 minutes, from the TSO request. The definition of *real-time* in the context of EV load coordination, is given considering the aforementioned TSO condition, by choosing a sampling time of 1 second for all variables involved in the EV coordination operations.

3.5.1 EV technical requirements

The provision of ancillary services in the framework EV – VPP can be achieved considering that EVs have an accessible hardware and software architecture that satisfy the *EV module functions* in the VPP architecture, as defined in **Table 3-1** [P4].
For the provision of ancillary services, the EV module functions of **feedback** and **charging prediction** should be established and maintained during EV coordination periods [83]. This is possible with the monitoring and control of the EV system's variables indicated in **Figure 3-3**.

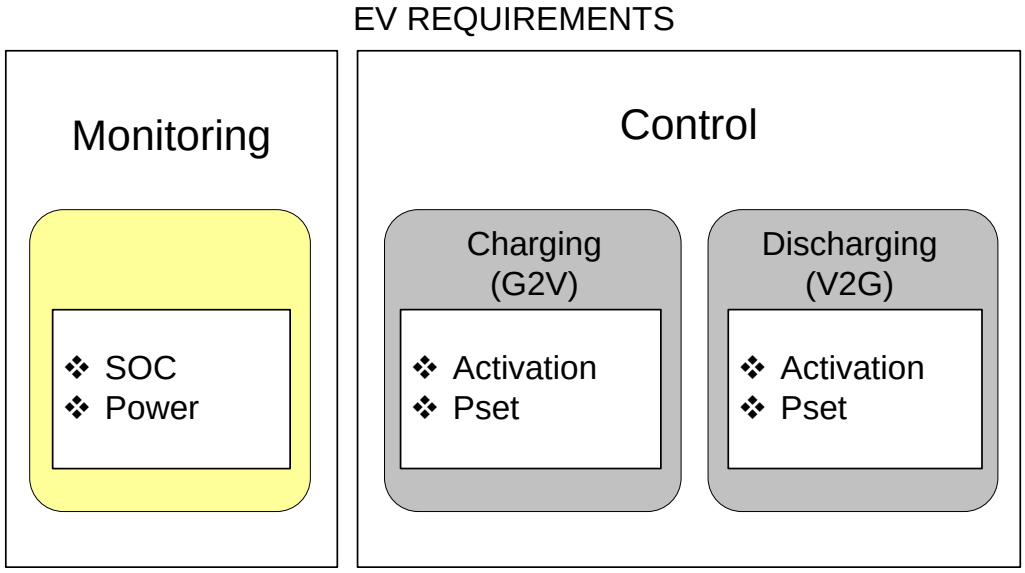

Figure 3-3: EV requirements for ancillary services.

- The function of **charging prediction, Table 3-1,** can be satisfied with the monitoring of the **SOC** information of the vehicle battery.
- The **feedback** function, **Table 3-1**, can be satisfied with the monitoring of the charging/discharging **power** P_{AC} exchanged between the EV and the grid.

The knowledge of the vehicle's SOC is important to the VPP to assess the vehicle availability for providing a service. As an example, if the vehicle battery is already at a fully charged state, or at empty state, the VPP may consider it unavailable for regulation.

On the other hand, the knowledge of the EV power response is important to the VPP to ensure that the provision of the service is taking place, according to the generated schedule.

With regard to control requirements, the **activation** of the charging and discharging should be realized. Optionally, a variable power level can be used for charging or discharging (P_{set}) the vehicle battery. This option is of lower importance in the provision of ancillary services from EVs, therefore it is not implemented.

The monitoring and control requirements can be implemented for a unidirectional EV as well as for a V2G-capable EV if both vehicles are able to share the required information with the VPP and if both are controllable.

In **Figure 3-4** (a), the monitoring and control requirements are shown for an EV capable of unidirectional power. The power set-point P_{set} sent to the vehicle is depicted in "grey", to indicate an optional requirement. In **Figure 3-4** (b), the monitoring and control requirements for an EV capable of V2G are depicted. Compared to the previous case, the power monitored can be positive or negative and the battery SOC increases or decreases accordingly during coordination periods. Furthermore, the charging and discharging equipment in the vehicle should respond to activation/deactivation commands.

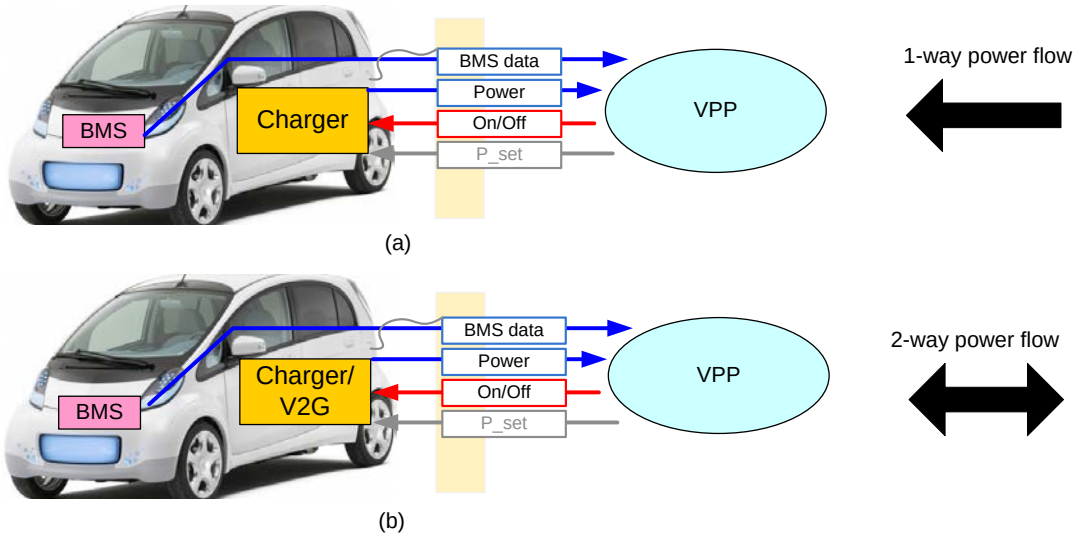

Figure 3-4: EV coordination data flow. (a) Coordination with unidirectional EV. (b) Coordination with bi-directional EV.

In principle, if the charging process of an external DC charger can be controlled by the VPP, also the DC charging concept can be used for the provision of ancillary services. So far, this appears an improbable option, since DC charging has as first priority a very short charging time, about 15-30 minutes [9].

The monitoring and control requirements of a fourth-generation type of EV interaction, corresponding to **Figure 3-4** (b), are implemented and tested on full-scale EV test bed.

3.5.2 Monitoring of internal vehicle data

As defined in [89], the basic task of a Battery Management System (BMS) is to ensure an optimal energy management of the EV battery during driving and during charging/discharging operations. The BMS should also avoid a battery misuse during its operation; this is achieved by monitoring and controlling the EV battery pack during plug-in periods or during driving. The BMS operates within the Vehicle Management System (VMS) architecture depicted in **Figure 3-5**. Monitoring and control functions are also implemented for the vehicle charger, the motor inverter and the motor.

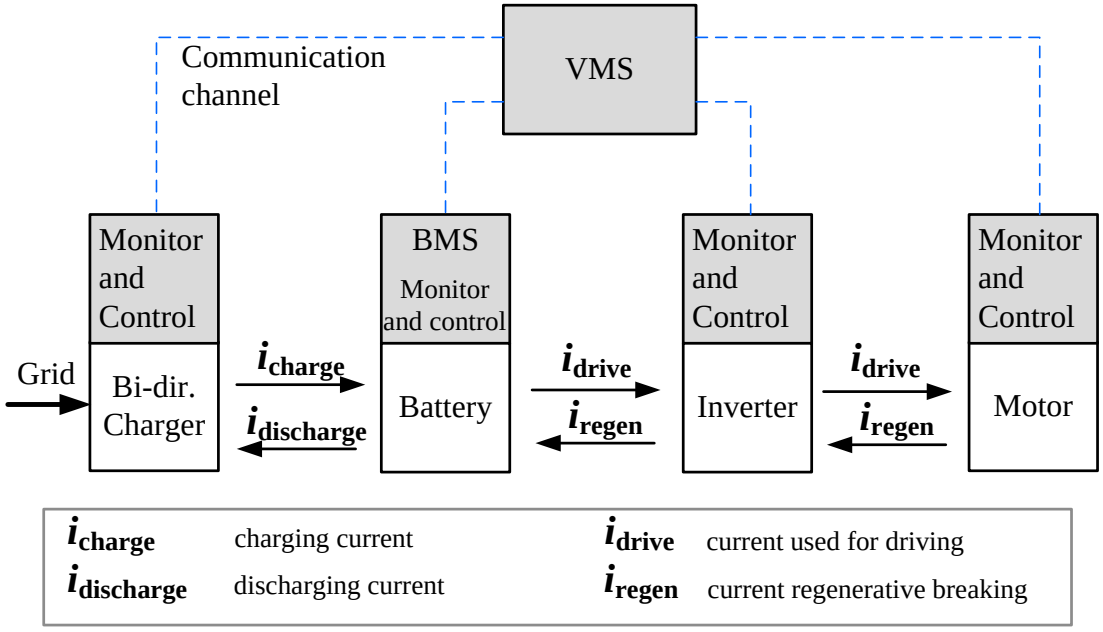

Figure 3-5: BMS within the VMS architecture.

n. b.: the monitoring and control functions in **Figure 3-5** should not be confused with the monitoring and control requirements defined for the provision of ancillary services. The functions of **Figure 3-5** are targeted to the correct operation of the vehicle components using a standard VMS.

For the purpose of ancillary services provision, not all information monitored by the BMS is necessary, but at least the battery SOC should be monitored. It shall be noted that the monitoring of the power on the DC side of the battery P_{DC} is not required for the provision of ancillary services, though the monitoring of this variable is important to quantify the power losses during the bi-directional power exchange between the EV and the grid.

Based on actual EVs, it is a hard task establishing the connection with the BMS; this is due mainly to data protection policies applied by carmakers, which prevent disclosing the communication protocol of their devices.

The knowledge of the nominal battery energy E_n is also needed from an EV aggregator. The value of E_n can be recorded by the VPP upon the registration of the vehicle in the aggregator fleet, without the need of communication between the VPP and the EV.
The nominal energy of the battery (kWh) can be expressed as follows:

$$E_n = V_n \cdot C_n \quad \textbf{(3.1)}$$

where C_n (Ah) is the nominal capacity of the battery pack, while V_n (V) is the nominal voltage of the battery pack. Both values are available on the EV battery user manual. The actual capacity of the battery C (Ah) indicates the capacity stored in the battery at the generic time t; while C_n is a fixed parameter, the actual capacity C varies as a consequence of the battery charging or discharging.

The SOC of the vehicle battery [90] is calculated as the ratio of the actual battery capacity C to the nominal capacity C_n. The SOC can be expressed as follows:

$$SOC = \frac{C}{C_n} \quad \textbf{(3.2)}$$

3.5.3 Monitoring of the power

The second monitored variable is the power exchanged between the EV and the grid. This could be measured within the EV charging station, using electricity meters with communication capability.
As presented by Samarakoon [91], smart meters are being introduced in many power systems worldwide to provide real time power consumption information to consumers and energy suppliers. A smart meter usually features different categories of functions. The *metering* category includes the measurement of phase voltage, current, active and reactive power, power factor, frequency and energy level. A second category may contain several *power quality indicators*, voltage THD, current THD, voltage and current unbalance factor, etc. An input/output (I/O) slot is optionally available on some models that allow receiving or sending signals for the activation of a relay.
An important feature of a smart meter is its communication capability. In fact, all monitored data can be available on a standard communication port, e.g. RS485, or Ethernet.
For an EV aggregator, the presence of smart meters in private or public charging stations allows the monitoring of the EV power used during the coordination periods. For the monitoring of the power P_{AC} in this project, a smart meter with Ethernet communication option is used; more details on the meter can be found in [92].

Alternatively, when a local metering option is not available within the station, the power P_{AC} can be measured approximated by monitoring the power P_{DC} via the BMS. It is important that the power information is communicated to the VPP, to keep track of the power and energy status of every single EV during coordination periods.

With regard to the power levels to use under EV coordination, the AC power levels of **Table 2-2** are considered. The available charging options are referred to the AC side of the EV chargers. It is expected that all on-board chargers will fall in one of these options [P4]. Currently, the vast majority of today's EV chargers are capable of single-phase charging with current levels of 16 or 32 A, according to [63].

3.5.4 Control of the charging/discharging operation

Monitoring the vehicle data is not enough alone to achieve EV coordination. The following EV control requirements are needed:

- Activation/deactivation of the charging mode
- Activation/deactivation of the discharging mode (V2G)
- Regulation of the power set point, P_{set} (optional)

The implementation of the first two control requirements is essential to realize EV coordination for a fourth-generation EV interaction. The third control requirement is an optional feature, for which the benefits and limitations have not been quantified.

3.6 Implementation of requirements

The defined requirements are implemented on an EV test bed, composed of full-scale EV components, **Figure 3-6**. The EV test bed is designed to test the provision of ancillary services and local grid support; its control architecture is compatible with the centralized VPP architecture of **Figure 3-1** (a).

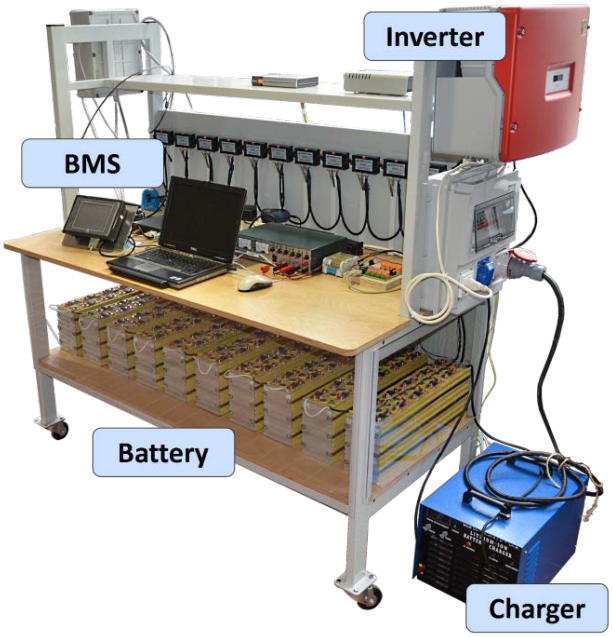

Figure 3-6: EV test bed.

3.6.1 EV test bed

The aim of the EV test bed is to reproduce and analyze the EV operation during charging or discharging; the EV test bed is capable of charging and discharging and it is designed to prioritize open access to the battery real time information and to control the charging and discharging modes. The main electrical features of the EV test bed are described in **Appendix A**. The hardware architecture is composed of two separate components for the charging and V2G operation, since the development of a bi-directional charger was out of the scope of the project.

The battery pack is designed with a nominal voltage of 363 V, which is well in the range of actual commercial EVs [93]-[95]. The battery is composed of 110 series-connected cells, based on lithium-iron-phosphate (LFP) technology. The datasheet of the battery cell is attached in **Appendix B**. A BMS is connected to the battery pack [P4] and is composed of 11 *voltage acquisition modules*, each of which acquires the voltage of 10 battery cells. A *current acquisition module* is used to measure the current flowing in or out of the battery pack. Using the voltage and current information, the BMS is able to estimate the SOC of the battery pack. A simplified diagram of the BMS is attached in **Appendix C**.

The nominal capacity and energy of the battery pack have fixed values and these are recorded once in the BMS data memory and read by the VPP.

The battery charger uses a charging power in the range of 0 to 3.7 kW, efficiency of 88% and power factor (PF) of 0.9 at the rated power. The discharging mode is implemented with a separate power converter unit which can operate in the power interval of 0 to 4 kW, with efficiency of 95% and unit PF. An onboard computer is used to interface with all hardware components previously described.

3.6.2 Test of EV charging/discharging

The implemented monitoring and control requirements are tested using the EV test bed and the charging/discharging schedule shown in **Table 3-3**, with time stamps in the format hh:mm:ss. It shall be noted that this is not a schedule based on a real TSO request of regulation, but it is generated by the VPP to test the correct bi-directional operation of the EV [P4].

A charging/discharging power of 2.3 kW, with current level of 10 A is chosen, considering that this power level is widely utilized for charging at residential installations. The control requirement is tested setting a power level of ± 2.3 kW for the charging and discharging operation. To verify that the defined requirements are met, the power P_{AC} and the SOC are measured. All measurements are performed with a sampling time of 1 second that is feasible with the available BMS and smart meter.

The power P_{AC} is measured at the point of connection of the EV with the grid, using the aforementioned smart meter. In addition to the monitoring requirements, the current I_{DC} flowing into the battery and the terminal voltage of the battery pack V_{DC} are measured

during the test to estimate the power P_{DC} and the efficiency values during charging and discharging.

Table 3-3: Test schedule for the EV test bed

Event nr.	Time stamp	Description of event
1	15:28:56	Activation of charging operation
2	-	Charging power level set at 2.3 kW
3	15:43:56	Deactivation of charging operation
4	15:43:59	Activation of discharging operation
5	-	Discharging power set at 2.3 kW
6	15:58:56	Deactivation of discharging operation
7	15:58:59	Activation of charging operation
8	-	Charging power level set at 2.3 kW

The test results are shown in **Figure 3-7** (a)-(b).

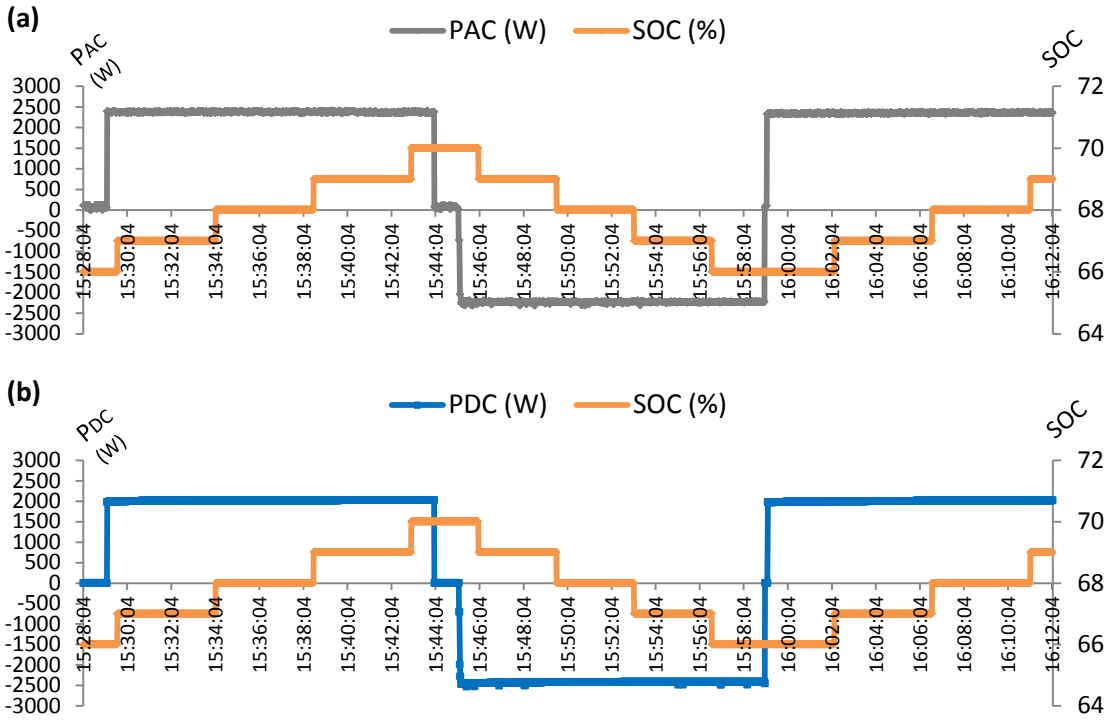

Figure 3-7: Tests of monitoring and control requirements. (a) Measurement of P_{AC} (positive sign if charging) and SOC. (b) Measurement of P_{DC} and SOC.

In **Figure 3-7** (a) the power profile measured on the grid side, P_{AC}, and the SOC profile are depicted. The monitoring functions are implemented via communication with the

smart meter and the vehicle BMS, respectively. The time axis is in the same format of the schedule, i.e. hh:mm:ss. The initial condition of the SOC is 66%; this is measured with resolution of 1%.
It is observable that the charging profile, with duration 15 minutes, brings the SOC to a level of 70%. The activation of the discharging operation takes about 1 minute; this is due to the synchronization time with the grid frequency and the monitoring of the grid voltage, by the discharging unit.
A steady power profile, P_{AC}, of ± 2.3 kW is observable during both charging and discharging. This highlights that both the charging and discharging units respond to the generated schedule. A negative sign convention is used to indicate the power during discharging operation.

In **Figure 3-7** (b), the power P_{DC} is shown based on the measurements of I_{DC} and V_{DC} available from the BMS. To calculate P_{DC} based on the BMS data, the following expression is used:

$$P_{DC} = V_{DC} \cdot I_{DC} \qquad \textbf{(3.3)}$$

where the current I_{DC} is taken with a positive sign during charging, while with a negative sign during discharging.
In (3.4) and (3.5) the power exchanged on the grid side is expressed as a function of the charging and discharging efficiency values, η_{CH} and η_{DISC} respectively.

Charging: $$P_{AC} = P_{DC} / \eta_{CH} \qquad \textbf{(3.4)}$$

Discharging: $$P_{AC} = P_{DC} \cdot \eta_{DISC} \qquad \textbf{(3.5)}$$

This efficiency is estimated based on the information of P_{DC} and P_{AC} depicted in **Figure 3-7** (a)-(b). During charging, an efficiency grid-to-battery of about 87% is measured, while during discharging the efficiency battery-to-grid is about 95%, because a different component for discharging is used. In relation to the two efficiency values obtained for charging/discharging, a round-trip efficiency η_{RT} of 82% is calculated, according to the following expression:

$$\eta_{RT} = \eta_{CH} \cdot \eta_{DISC} \qquad \textbf{(3.6)}$$

For comparison, the use of a bi-directional charger, as a single component, with same charging efficiency as the EV test bed's one, would have led to a round-trip efficiency of about 76%. Thus, with the present hardware architecture, featuring two separate components for charging and discharging, the market choice of a more efficient V2G unit has allowed obtaining a better round-trip efficiency.

It shall be noted that the calculated round-trip efficiency does not take into account the power losses which occur in the battery pack during charging or discharging. These

have a smaller contribution at this power level and can be quantified knowing the battery parameters. Each battery cell's impedance amounts to 10 mΩ, as identified in [P7]; therefore, considering the battery pack composed of 110 series-connected cells, the equivalent impedance R_{eq} of 1.1 Ω is calculated. The battery losses P_{BAT} are obtained as follows:

$$P_{BAT} = R_{eq} \cdot i^2 \qquad \textbf{(3.7)}$$

where

i is the current flowing in or out of the battery

With a charging power P_{AC} of 2.3 kW, considering the charger efficiency of 87%, a power of about 2 kW is available at the battery terminals during charging. Assuming for the battery pack voltage its nominal value of 363 V, the losses in the battery amount to 33 W, which corresponds to 1.43 % of P_{AC}. The result is an approximation of the battery losses, because the calculation is done assuming a constant value for both R_{eq} and the battery pack voltage.

3.7 Summary and discussions

In this chapter, the requirements to enable the provision of ancillary services from EVs are defined and implemented for a V2G-capable EV, under the coordination of a centralized EV aggregator, the VPP.

The EV load coordination is possible with the *monitoring* and *control* of the individual EVs, relying on a communication link between the VPP and the EVs. The VPP should gather vehicle's information that is fundamental to identify its status during the provision of the service. The monitored EV data allow the EV aggregator to assess the EV availability for charging or discharging, to perform charging prediction and to receive a feedback in relation to the power response.

For the provision of the ancillary services of secondary reserves and regulating power, the following basic requirements have been defined [P4]:

- **Battery SOC monitoring**
  The VPP must be able to access the SOC information, in order to determine the vehicle status, thus its availability for charging or discharging, and to estimate the available energy capacity from its EV fleet.
- **Power monitoring**
  The VPP requires a feedback from its EV fleet, to evaluate the power response of the coordinated vehicles during the periods of services provision.

- **Charging/discharging control**
  The EV must be prepared to receive the coordination signals from a VPP, in accordance to the services required. Thus the battery and charging/discharging units should respond accordingly.

Optionally, a variable power set-point can be implemented to regulate the charging or discharging power used; however, the advantages derived by variable charging power are of minor interest in the provision of ancillary services.

The implementation of the EV requirements is performed on a full-scale EV test bed. We observed that accessing the vehicle information, like the SOC, is not of easy implementation on current EV models. The data protection conditions posed by vehicle manufacturers are so that it is not possible to log EV battery data, which is a precondition to enable a centralized VPP in the provision of ancillary services.

In order to access the BMS data of an EV battery, vehicle manufacturers should agree on sharing the proprietary communication protocol used. To overcome this barrier, in this project, the BMS communication protocol has been obtained directly by a BMS manufacturer, on request. Accessing the BMS allows the acquisition of additional data such as battery current, battery pack voltage, cell voltages, cells temperature, and power P_{DC} that are potentially usable for other purposes than ancillary services.

With the communication with VPP established, it has been possible to measure the SOC and the charging/discharging power using a smart meter, both with a time resolution of 1 second. Considering that the TSO regulation requests for secondary reserve and regulating power come every 5 minutes, the measurement's time resolution is compatible with the provision of the services.

The test of bi-directional power operation has also revealed an aspect which has not been addressed in depth in past research [31]-[37], i.e. the round-trip efficiency of the charging/discharging process. Based on the measurements performed, the round-trip efficiency is about 82%, in relation to the EV test bed components. This value is obtained because a bi-directional EV architecture with two separate components for charging and discharging is used. For comparison, the use of a bi-directional charger with efficiency of 87% would have shown an overall round-trip efficiency of about 76%. By choosing a specialized inverter for the discharging (V2G) operation, a higher efficiency is obtained. As long as EVs are not of fourth-generation, i.e. incapable of V2G, a recommendation is that the V2G functionality can be technically realized in the form of a hardware extension to the original EV setup, with the integration of a new inverter to the battery system. Yet, the safety issues that arise when dealing with this option should be considered.

4 EV COORDINATION FOR ANCILLARY SERVICES

In this chapter, the EV load coordination for the provision of ancillary services, secondary reserve – LFC and regulating power, in the Western Danish power system is implemented, **Figure 4-1**. The EV system response and possible limitations are analyzed. In Section 4.1, Section 4.2 and Section 4.3, the ancillary services addressed are introduced, limited to secondary reserves (LFC) and regulating power. In Section 4.4 and Section 4.5, the control architecture of an EV within a VPP framework is presented. In Section 4.6, a proof of concept of EV provision of ancillary services is provided. In Section 4.7, the EV charger and battery management under EV coordination is studied, highlighting possible limitations. Finally, summary and discussion are presented in Section 4.8. The findings of Chapter 4 are contained in [P5], [P6] and [P7].

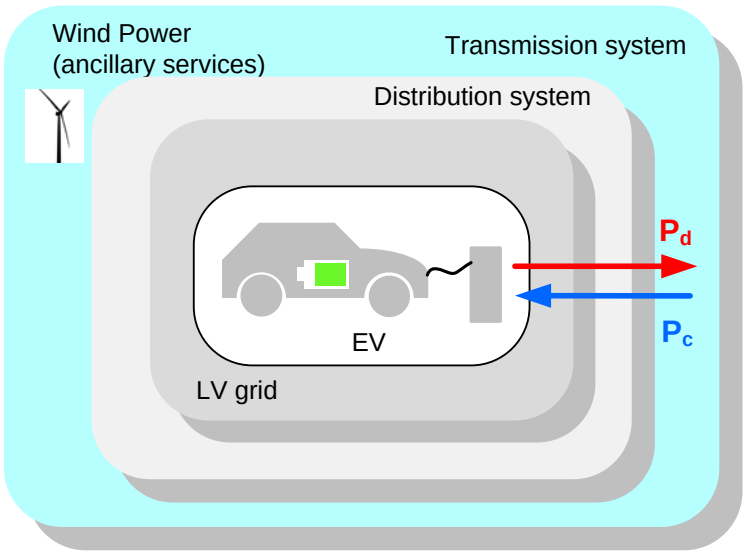

Figure 4-1: EV coordination for ancillary services.

4.1 Ancillary Services for Wind Power integration

The wind *energy penetration*[6] in Denmark has reached a level of 26% in 2011 [97]. The uncertainty in wind power prediction challenges the power system operation by the

[6] Wind energy penetration is defined as the ratio of the amount of energy obtained from wind generation to the total energy consumed in the power system, normally on an annual basis [96].

TSO. An increasing need of ancillary services is expected and EVs are seen as option for their provision. To better understand how EVs can offer ancillary services to facilitate wind power integration, it is worthwhile analyzing the actual electricity market situation.

4.1.1 The Nordic Power Market

The electricity market we refer to is the Nordic Power Market, where Norway, Sweden, Finland and Denmark are the participating countries. The power market offers different timeframes for different services and these are depicted in **Figure 4-2**.

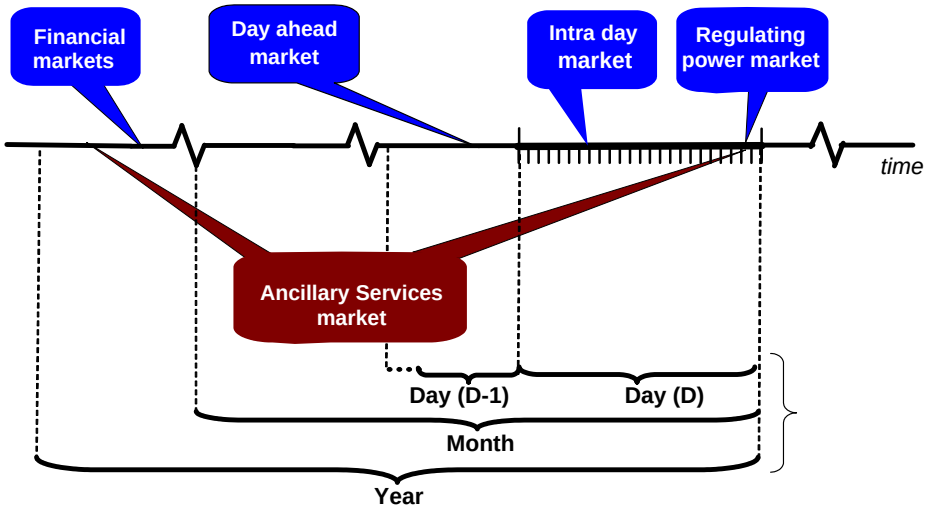

Figure 4-2: Timeframes for different services in the Nordic Power Market [80].

The financial markets deal with those kinds of contracts that are agreed months or years before they get executed. The day-ahead market, also called Elspot market, provides to the market participants a place where hourly power contracts are traded daily for physical delivery in the next 24-hour period. The intra-day market Elbas plays as an alternative of balancing market and provides continuous power trading up to one hour prior to delivery. However, power deviations that occur in the hour of operation need to be balanced. For this reason, several types of reserves are used to ensure stability in the power system. The reserves can be automatic or manual and the TSO requirements are initially managed via automatic reserves. To anticipate an excessive use of automatic reserves and in order to re-establish the availability of these, regulating power is used [35].

The provision of ancillary services using EV load coordination is limited in this project to the provision of:

- Secondary Reserves, LFC[7] (DK1)
- Regulating power

[7] The provision of secondary reserve LFC is used in the Western Danish power system (DK1)

4.2 Secondary Reserves – LFC

In a wind power dominated power system, like the Western Danish power system, when a major operational disturbance occurs, LFC is the reserve used to indirectly restore the system frequency to 50 Hz, following the stabilization of the frequency by means of primary regulation [98].

Secondary reserves serve two purposes:

1) releasing the primary reserve which has been activated, i.e. restore the frequency to 50 Hz;
2) restoring any imbalances on the interconnections to follow the agreed plan.

Secondary reserves regulation is automatic and it is provided by production or consumption units which, by means of control equipment, respond to signals received from the TSO. The reserves consist of upward and downward regulation which is requested in the form of symmetrical power [98].

The Danish TSO buys the secondary reserves on a monthly basis. The European network of TSOs (ENTSO-E) recommends a secondary reserve of approx. +/- 90 MW [99], but the individual TSOs in Europe can increase their reserves to levels far in excess of 90 MW. Thus, this reserve is not required to be of a certain size. The Danish TSO requirements are determined on the basis of ENTSO-E RG Continental Europe's recommendations and take into account the uncertainty of wind forecasting.

4.2.1 Technical conditions

The technical conditions that apply for the provision of secondary reserves are issued by the TSO [98] and listed in **Table 4-1**:

Table 4-1: Technical TSO conditions for the provision of secondary reserves

	Technical conditions
1	The reserve is primarily supplied by units in operation.
2	It must be possible to supply the reserve requested within 15 minutes. Alternatively, the reserve can be supplied by a combination of units in operation and fast-start units.
3	The reserve to be supplied within any coming five-minute period must be provided by units in operation.
4	It must be possible to maintain regulation continuously.
5	The regulation signal is sent online as an output value from the TSO.

The service requires also that each individual production or consumption unit shall be connected via communication media to the control centre of the TSO. For each individual unit, the control centre must generally have online access to:

- Status reports on the production or consumption unit in/out
- Online measurements of production and consumption (MW)
- Currently possible reserve up (MW)
- Current max gradient up (MW/min)
- Current time constant for upward regulation (sec.)
- Currently possible reserve down (MW)
- Current max gradient down (MW/min)
- Current time constant for downward regulation (sec.)

The aforementioned features are applicable to an EV fleet which is coordinated via an EV aggregator, e.g. a VPP. However, due to the unavailability of a large number of vehicles, these features are not treated further.

4.3 Regulating Power Reserves

In the Nordic Power Market, regulating power is a manual reserve [35]. Regulating power is used to deal with forecast imbalances and to release automatic reserves in the event of power stations or transmission lines outages [98]. Regulating power is realized with increased or decreased generation/consumption and it must be possible to fully activate the reserve within 15 minutes [35], likewise secondary reserves.

In Denmark, the participation in the regulating power market requires the following technical conditions:

- A minimum bid size of 10 MW
- Real-time measurement of the power exchanged with the grid

As the minimum bid cannot be met by individual EVs, an aggregation technology such as a VPP is needed also in the case of regulating power provision.

4.4 The EV aggregator

The aggregation technology used for the provision of ancillary services is based on the existing EDISON Virtual Power Plant (VPP), acting as the EVs aggregator. More details on the software implementation of the VPP and the communication technology used can be found in [83].

As depicted in **Figure 4-3**, the Edison VPP operates in a multi-entity platform interfacing with other players. The main goal is to encourage the single EV users to actively participate in ancillary services provision, to support the integration of wind power in Denmark. There are other entities to which the VPP is interfaced with: a

Transaction Interface with a billing provider, to allow the billing of the energy during charging or discharging; a Transmission System Operator (TSO) interface, where a Balance Responsible Party is involved to create and submit mandatory power schedules for the correct operation of the power system; an Electricity Market interface and a Distribution System Operator (DSO) interface avoid grid congestion issues [83].

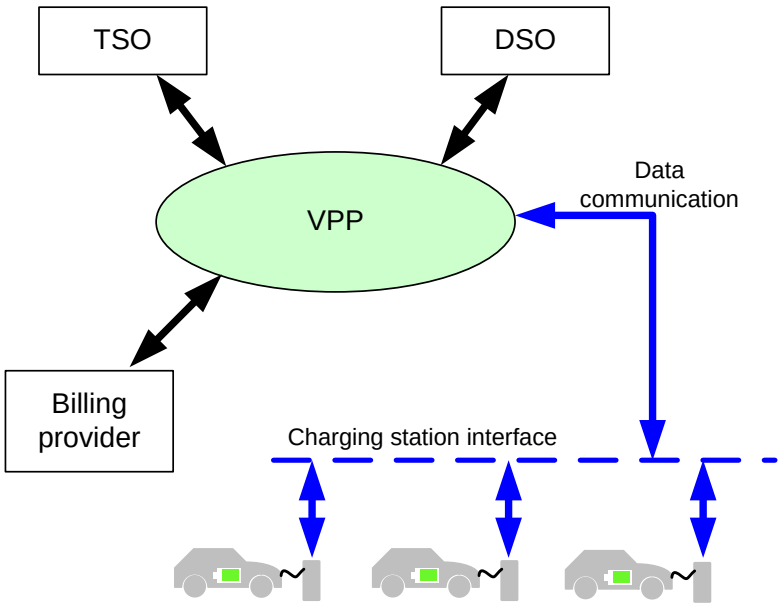

Figure 4-3: EV coordination for ancillary services using centralized VPP.

The major challenge of the services provision is that activating charging or discharging of an EV fleet is not equivalent to activating a single centralized power unit in the power system; in the case of EVs, *connectivity*[8] should be ensured to every single EV. Finally, the EV provision of LFC and regulating power should comply with the technical conditions.

4.5 Establishing connectivity with a VPP

The connectivity of each vehicle with the VPP is possible if the monitoring and control requirements defined in Chapter 3 are established.

The control architecture of **Figure 4-4** is implemented to allow the coordination of the EV test bed by the EDISON VPP [P5].

The communication with the EV is based on the IEC 61850 standard [100]. In the attempt to promote the use of existing web standards in power system communication, the IEC 61850 standard was mapped to HTTP/REST by Pedersen *et al.* [101]. The VPP is used to generate and send power requests to the EVs, according to the specific

[8] Connectivity is intended as the ability to make and maintain a connection between the vehicles and the VPP.

regulation needs of the TSO. The provision of the services is simply based on positive or negative power requests with an associated time stamp, corresponding to the upward and downward regulation.

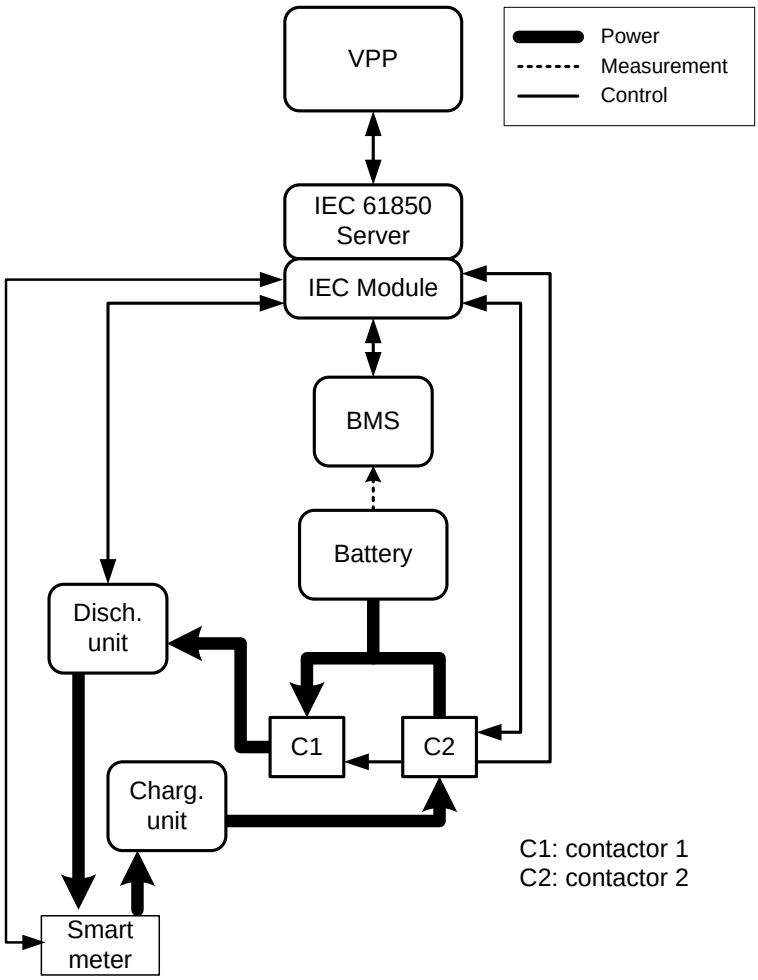

Figure 4-4: EV test bed communication and control architecture.

The IEC 61850 *Server*, which was developed by Pedersen *et al.* [101], is composed of a modular plug-in architecture that facilitates the adaptation and installation of new devices. A device specific plug-in, **Figure 4-5**, is implemented for an EV for the extraction of the SOC information. The module is mapped according to a "tree" structure made of: logical device, logical nodes, data class and attributes.

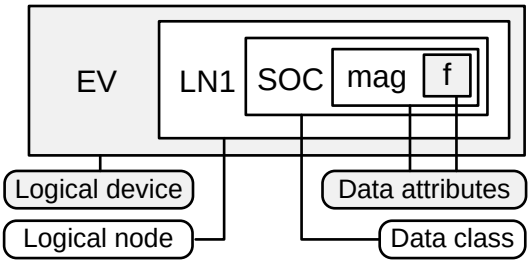

Figure 4-5: Mapping of the SOC information in the IEC Module.

4.5.1 Charging/Discharging

As indicated in **Figure 4-6**, there is no direct link, between the software plug-in (IEC Module) and the charger. The charger is set to a fixed power level and it is coupled or decoupled from the battery by means of a DC contactor, which is controlled via serial interface RS232.

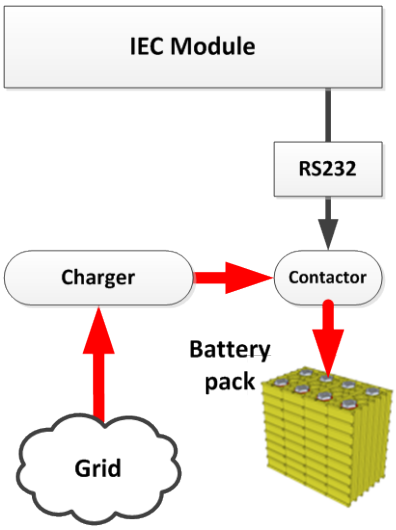

Figure 4-6: Charging communication.

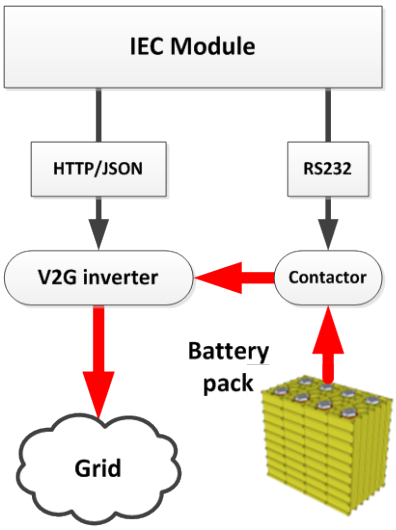

Figure 4-7: Discharging communication.

The coupling of the discharging unit is achieved by means of an identical DC contactor as implemented for the charger. Under discharging operation, the generated power level is controllable and this is managed through an attached communication hub. The same hub implements an HTTP/JSON web interface. A more detailed illustration of the communication used for the activation of the discharging mode is depicted in **Figure 4-7**.

4.5.2 Battery Status Information

The SOC of the battery is monitored through the BMS, according to the simplified scheme of **Figure 4-8**; a more detailed picture of the BMS is provided in **Annex** C. With the IEC Module – BMS established, all real-time battery data can be made available to the VPP. The list of variables includes:

- Total battery pack voltage (V)
- Total Current (A)
- SOC (%)
- Battery pack temperature (ºC)
- Remaining energy (kWh)
- Single cell voltages (V)

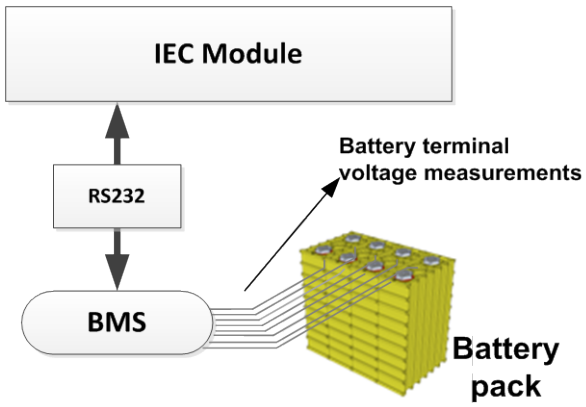

Figure 4-8: BMS-to-battery communication.

The extraction of such data is only possible if the BMS manufacturer is willing to share the communication protocol used. It is therefore thanks to the knowledge of the BMS communication protocol that the monitoring and control requirements can be met.

4.6 Ancillary Services with EV – Proof of Concept

The EV participation in secondary reserves (LFC) is tested using the EV test bed under VPP coordination [P5]. The secondary reserve required on the 1st of January 2009 in Western Denmark is used as a test scenario [102]. The upward/downward power request for the single EV is generated by the VPP, in relation to the reserve needs.

The target value of LFC is provided by the TSO in 5-minute average MW values as shown in **Figure 4-9** (a) in blue. The target power value is derived by the sum of all regulation requests sent out by the TSO to a list of providers in the same 5-minute interval. The target anyway does not reflect the exact need of the system but rather the value used to drag the reserve providers in the right direction. Nevertheless, the target value is a very good approximation of the real-time need of regulation reserves [P5].

A new regulation request is generated by the VPP every 5-minute, and received by the EV. The reserve provision is tested in the 3-hour time interval 16h30 to 19h30. The EV regulation (in KW) is shaped as ±2.3 kW power with time stamps, indicating the activation/deactivation time of the charging and discharging mode, red profile in **Figure 4-9** (a). It shall be noted that only due to graphical reasons, the target value may seem zero in few cases, in the 3-hour regulation interval; in reality the TSO target is not zero (a few hundreds of kW, positive or negative), thus the EV regulation signal is present also in those 5-minute intervals.

The efficiency during charging and discharging is taken into account, in such a way that the power P_{AC} matches exactly ±2.3 kW at the point connection of the EV with the grid.

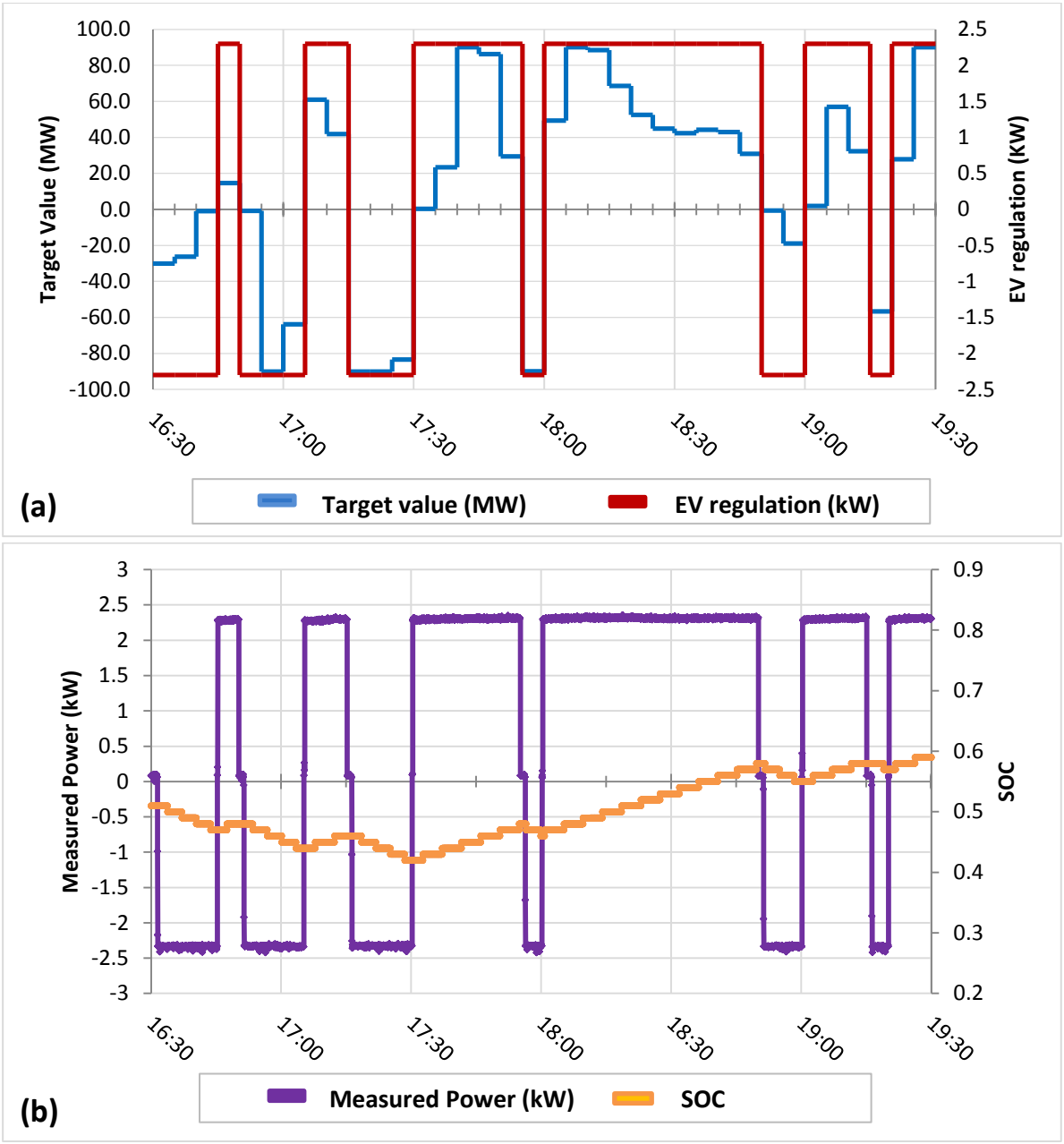

Figure 4-9: Secondary reserves provision results with EVs (a) Target value from the Danish TSO (blue); EV power regulation (red). (b) EV power exchanged (violet); EV battery SOC (orange).

Since each EV has a small capacity compared to the LFC total reserve of ± 90 MW, we assume that the VPP is able to meet the TSO target by aggregating a large fleet of EVs.

Based on the TSO request, the EV system response is depicted in **Figure 4-9** (b). The exchanged power P_{AC} at the point of connection of the EV is measured with a sampling time of 1 second. The EV power response matches the *EV regulation request* (in kW) by the VPP. The activation delay of the charging process (G2V) is negligible. The activation delay of the discharging (V2G) process is about 1 minute. This is due to the

time used by the V2G unit to synchronize itself with the grid voltage. In relation to the maximum response time required by the TSO for the services provision (15 minutes), the discharging activation delay has a negligible impact.

The battery SOC profile shows the energy variation of the EV battery during the coordination period. The EV coordination for secondary reserves in the 3-hour period starts with an initial SOC of about 50% (0.5 in **Figure 3-7**) and ends with a final SOC of about 60%.

As previously mentioned, the provision of *regulating power* is not performed, as from an EV perspective, the only difference with LFC is that the minimum bid on the market is of ±10 MW, which also in this case can be achieved with the aggregation of a large EV fleet.

4.6.1 EV response and Quality of Service

The EV system response to the technical conditions posed by the TSO, with regard to LFC (and potentially Regulating Power) is reported in **Table 4-2**:

Table 4-2: EV system response to the secondary reserves provision (LFC)

	Technical conditions	EV system response
1	The reserve is primarily supplied by units in operation.	✓ The EV is activated automatically upon charging or discharging activation request by the VPP
2	It must be possible to supply the reserve requested within 15 minutes. Alternatively, the reserve can be supplied by a combination of units in operation and fast-start units.	✓ The EV regulation request is met within 15 minutes by the single EV. The EV acts as fast-start unit considering the time response to charging or discharging.
3	The reserve to be supplied within any coming 5-minute period must be provided by units in operation.	✓ The EV is able to continuously provide the service and to respond to the schedule within any coming five-minutes.
4	It must be possible to maintain regulation continuously.	✓ The EV can provide continuously the regulation as far as the maximum and minimum SOC level is not reached.
5	The regulation signal is sent online as an output value from the TSO.	✓ The EV is able to receive the coordination signal from the VPP, which is based on the real need of the TSO.

It is also possible to do an assessment on the *quality of service* [103], or QoS, during the EV provision of secondary reserves or regulating power. By definition, the network

QoS refers to the ability of a network to handle his traffic such as that it meets the service needs of certain applications [103]. Different applications have different requirements regarding the handling of their traffic in the network. The requirements are usually expressed using the following QoS-related parameters: bandwidth, latency, jitter and loss. In relation to the secondary reserves provision using EV load coordination, it has not been observed any communication latency or loss of data, in the communication link VPP to EV and vice versa, which had an impact on the test results. These findings may result optimistic compared to a future scenario, where an EV aggregator should communicate with a large fleet of EVs. In that case, the QoS can be exploited in a more comprehensive way.

4.7 EV management under EV coordination

Under EV coordination, the EV load profile from each EV is according to the power request received by the VPP, as shown in the proof of concept results of **Figure 4-9**. However, the combined system *EV battery – EV charger* is a more complex element than a simple electric load, as it involves a number of nonlinearities and ageing aspects, due to the electrochemical nature of the battery. The EV coordination should be performed considering the existing battery technology limitations.

When plugged into the grid, the EV can be described with the block diagram of **Figure 4-10**; a battery model, with equivalent controlled voltage source Voc_{eq} (function of the SOC) and equivalent resistance R_{eq}, represents the EV battery with terminal voltage V_{pack}; the battery is charged with current i and it is directly connected to a battery charger. The variables V_c and i_c indicate the grid voltage and current, respectively. The operation of the battery and charger are modelled in the following paragraphs.

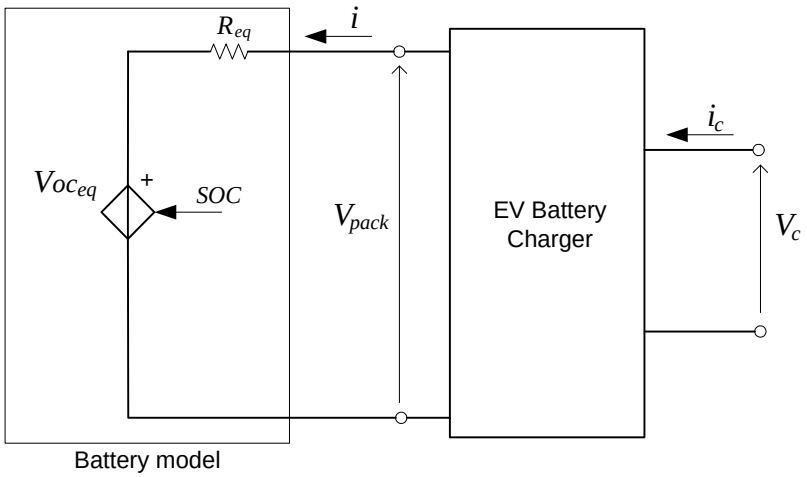

Figure 4-10: Simplified EV block diagram.

4.7.1 EV Battery

There are several ways to model a battery [P7]: ad-hoc methods have been developed for different battery technologies such as Li-ion, Lead Acid, Nickel Metal Hydride as well as for different types of Li-ion batteries. The modelling method can be more or less complex and can utilize sophisticated laboratory tools for the estimation of the battery parameters. In this project, the battery is modelled using the methodology presented by Tremblay *et al.* in [104]-[105], since short term (milliseconds) dynamics are not relevant to the initial project goals. The methodology is used for the estimation of the EV test bed's battery parameters, considering the charging/discharging curves of the battery datasheet, provided by the manufacturer. Validation of the manufacturer's curves is performed for a single Li-ion battery cell, under controlled charging/discharging conditions, using a fixed current *i* of ±20A (0.5 C). The charging and discharging voltage profiles of the battery cell are depicted in **Figure 4-11** in blue and violet, respectively. With reference to **Figure 4-10**, V_{pack} is estimated by scaling up the cell voltage profiles, depending on the number of series-connected cells in the battery pack.

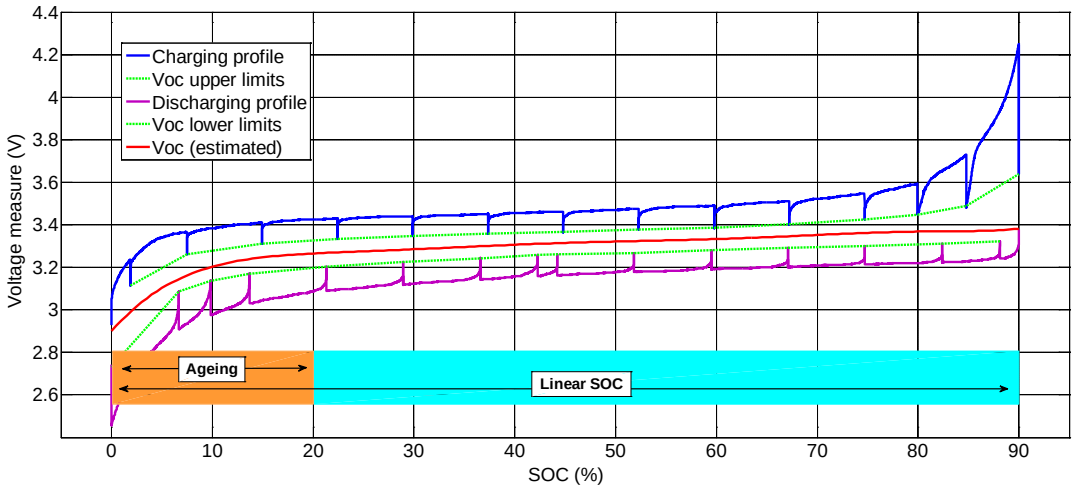

Figure 4-11: Battery cell voltage profiles during charging.

The battery cell voltage can be expressed as follows:

$$V_{oc}(Q) = V_0 - \frac{K \cdot Q_{nom}}{Q_{nom} - Q} + A \cdot e^{(-B \cdot Q)} \qquad \textbf{(4.1)}$$

where the parameters, V_0, A, B and K are estimated according to [104] and explained in [P7].

From an EV perspective, the feasibility of EV coordination involves the coexistence of two important conditions:

- A linear SOC window
- Allowed charging/discharging power levels

The SOC behaviour is studied taking into consideration the charging/discharging tests performed for a Li-ion battery cell. The cell's voltage curves are obtained applying constant current of 20 A. The same test is done for the EV battery pack, showing similar results.

In the SOC interval of 0 to 90%, it is observed a linear SOC increase or decrease, depending on the power flow. The region highlighted with orange colour indicates a SOC area that, if crossed, results in quicker ageing process of the battery, according to the analysis in [P6].

During charging, it is possible to distinguish a constant current (CC) zone and a constant voltage (CV) zone; the latter is not depicted in **Figure 4-11**. The battery voltage increases continuously during CC charging, until the cell voltage reaches 4.2 V. Such value corresponds to the maximum voltage level for this type of battery, see **Appendix** B, and this occurs with a SOC level of about 90% according to:

$$SOC = \frac{C}{C_n} \qquad \textbf{(4.2)}$$

At about 90% SOC, the CC charging process should switch to CV mode. Under CV charging, the power P_{AC} and the current i_c are not controllable anymore, thus the SOC increment becomes non-linear. The only controlled variable under CV charging is the battery pack voltage which is maintained at a constant value until the SOC level of 100% is reached. In the light of this finding, the CV charging region cannot be used for ancillary services provision.

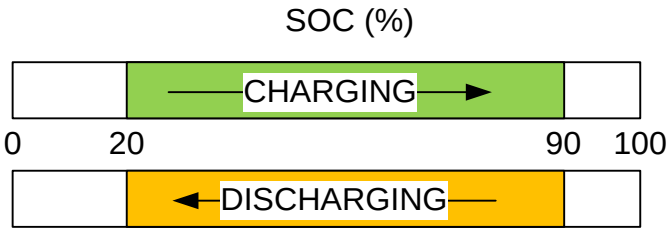

Figure 4-12: Optimal SOC region for EV coordination.

A preferable SOC window is depicted in **Figure 4-12**. Based on the results of simulations and tests, a SOC window between 20% and 90% shall be used for the task of EV coordination. The choice of the minimum SOC of 20% is based on ageing considerations for Li-ion batteries made in [P7].

4.7.2 EV Charger

An EV battery charger can be modelled as a controllable electric load, if we look at the resulting load profile on the grid side. The charger load profile is analyzed considering the most common charging options available for conventional EV chargers. A charger can operate according to the following modes:

- Constant Power - Constant Voltage mode (CP-CV)

❖ Constant Current - Constant Voltage mode (CC-CV)

The two operation modes lead to different EV demand profiles, though the initial charging power is equally set for both. A CP-CV charger ensures that the power level P_{AC} set for charging is kept constant during the charging cycle. On the contrary, a CC-CV charger ensures that the battery is charged with constant current *i* (DC side) and this leads to an increasing power P_{AC} on the grid side, during the charging cycle. In fact, since the current is kept constant during charging, the battery pack voltage increases as depicted in **Figure 4-11**; for this reason, the power P_{AC} increases with similar trend as for the voltage. This behaviour causes an unexpected nonlinearity during EV charging coordination.

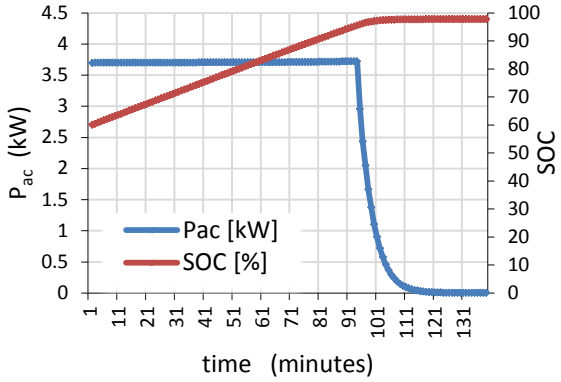

Figure 4-13: EV demand with CP-CV charger.

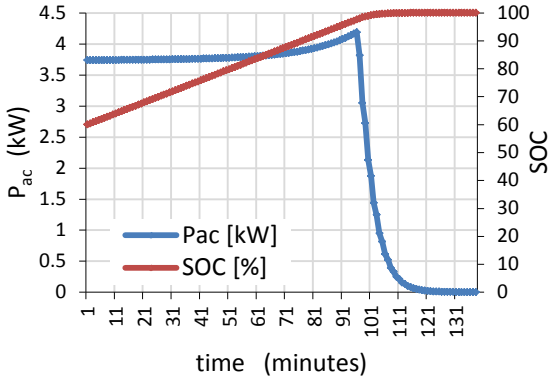

Figure 4-14: EV demand with CC-CV charger.

The modelling and simulation of the EV charging systems is performed in [P7]. In the simulation, a charging power P_{AC} of 3.7 kW is chosen as the charging power level.
The simulated demand profile of a CP-CV charger is depicted in **Figure 4-13**. The demand profile of a CC-CV charger is depicted in **Figure 4-14**. In both cases, the initial SOC level is 60%. As the simulations results show, the difference in the demand profiles is quite evident and the same would be under EV coordination.
A test for validating the demand profile of an EV charger with CC-CV operation is performed using the battery pack of the EV test bed. The initial charging power is set to 3.7 kW with initial estimated SOC of 60%. The test results are depicted in **Figure 4-15**.

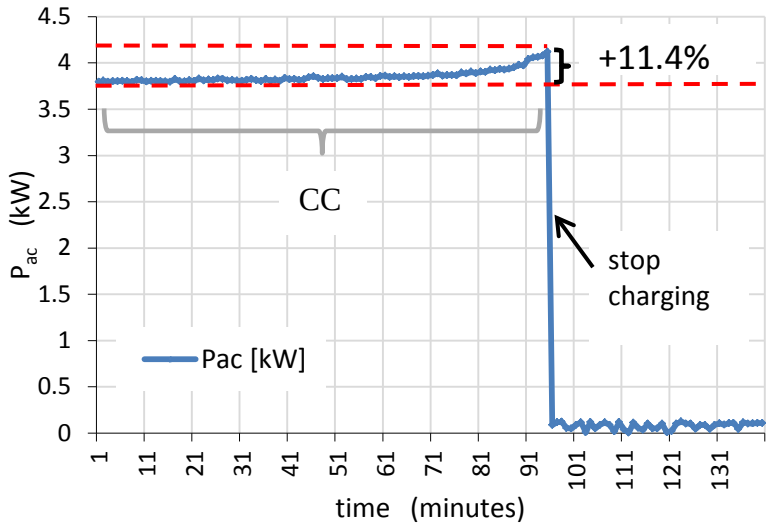

Figure 4-15: EV demand using a charger with CC-CV operation.

The power level increases continuously during charging. At the end of the CC region, at about 90% SOC, the test results show a power increase ΔP_{AC} of 11.4% compared to the initial charging power of 3.7 kW. While this aspect could be negligible for low charging power levels (e.g. 2.3 or 3.7 kW), it can become an issue for the three-phase charging power levels of 11, 22 and 43 kW.

It is also worthwhile noticing that in the simulation results depicted, the charger is modelled with unit efficiency. Simulations are also conducted considering a charging efficiency of 88%, which represents the charger's efficiency of the EV test bed. In this case, assuming identical initial SOC of 60%, the time needed to charge the battery up to 90% SOC, is 14% longer than with unit efficiency. The efficiency is another important aspect to consider by the VPP, in order to generate a correct schedule that meets the EV user driving needs.

4.7.3 Ageing considerations

During the 3-hour coordination interval of **Figure 4-9**, the SOC profile varies from 50% (initial condition) to 60%, passing by 40%. The relative SOC variation is therefore 30%, corresponding to a displaced energy of 4.35 kWh of the EV test bed battery pack.
Assuming the same schedule applied to the EV for 9-hour time interval on a daily basis, the total displaced battery energy would correspond to the nominal energy of the battery, i.e. 14.5 kWh, which is equivalent to a full charging/discharging cycle for the EV battery; the provision of this service on a daily basis would drastically decrease the calendar battery lifetime. Anyway, it should be considered that such finding is strictly related to a number of pre-conditions:

- the charging power used for charging or discharging
- the EV battery size and the energy window used for the service provision
- the number of cycles performed for the service provision

Presently, there are not enough elements to perform a cost-benefit analysis for EV users participating in ancillary services due to unclear pre-conditions and due to the absence of compensation schemes justifying the benefits. Such analysis would require also an assumption on the number of EVs providing such services. For these reasons, the ageing process of the EV battery, due to the ancillary services provision, is not treated further in this project.

4.8 Summary and discussions

This chapter has looked into the EV ability for the provision of the ancillary services of secondary reserves (LFC) and regulating power, highlighting possible limitations.
An EV control architecture for the provision of the ancillary services has been defined and implemented to match with a VPP centralized control framework. Two separate components for charging and discharging (V2G) have been integrated, both controllable via the VPP. The proposed V2G architecture is alternative to the one used by Brooks [85]. Furthermore, it has proven the efficacy of using two separate units instead of a bi-directional EV charger, which is currently not available on the market.
A precondition to allow the ancillary services provision is that monitoring and control of those vehicle's components involved in the charging and discharging process should be ensured. A proof of concept of secondary reserves (LFC) and regulating power for the Western Danish power system has been implemented using the EV test bed coordinated by a VPP. The technical TSO conditions, valid for secondary reserves provision, can be met by an EV:

- ✓ The reserve can be supplied by the EVs in operation or by newly activated EVs.
- ✓ An EV can supply part of the reserve requested within 15 minutes, showing fast response behaviour as opposed to the service response's requirement.
- ✓ The EV is able to provide the reserve within any coming 5-minute period.
- ✓ It is possible to maintain the regulation continuously, as long as the SOC of the vehicle's battery is in its allowed range.

These findings support the research outcomes of [31], [33] and [34] that investigated on the provision of secondary reserves by EVs, using EV simulation models. It should be noted that the maximum aggregated power target of the Danish TSO for secondary reserves amounts to ± 90 MW and a minimum bid of 10 MW is applied for regulating power. Thus, the target power can only be met by a large fleet of EVs. Although we demonstrated EV load coordination with a single EV, the regulation response of a large EV fleet could not be addressed. With regard to the quality of service (QoS), the EV coordination period has not revealed data loss or communication delays that were critical to the provision of the services.

With regard to the battery management under EV coordination, the following aspects are important for preserving the battery lifetime and to avoid nonlinearities during the coordination periods:

- the SOC level should not go below 20% during EV coordination, in order to preserve the battery lifetime [P6].
- the SOC must stay within a linear region, below 90% SOC, for a Li-ion type of battery. Outside the linear SOC region, the charging power is not controllable anymore, thus EV coordination cannot take place [P7].

The EV charger behaviour during the coordination period is another important aspect to consider. By modeling, simulating and testing EV charging, two main operation modes are identified for an EV charger: constant power and constant current operation. With the two options, a major difference is identified on demand profile seen on the grid side. With the first type of charger, the AC charging power is kept constant during charging, until the maximum battery voltage is reached. With the second type of charger, the DC charging current is kept constant during charging until the maximum battery voltage is reached; in the latter case, the AC charging power increases according to the battery voltage, leading to an additional unexpected electric load, up to 11.4% for the test conducted. This aspect is not modelled in [31], [33], [34] and [36]. Thus, the EV aggregator, such as a VPP, may receive an EV power response (in kW) which is different by the given power set point for the provision of ancillary services. Furthermore, it is recommended that this aspect is taken into account by charging station planners, to ensure that cables and grid protections within the station are properly sized to withstand the different charger options. Though, with the low charging power options of 2.3 kW or 3.7 kW, the power increase can have a minor impact on the station equipment and on the aggregator side, with the three-phase charging options of 11, 22, and 43 kW, the additional EV load cannot be neglected.

The EV charging/discharging efficiency is another aspect, which is currently neglected by the aggregation concepts presented in [49]-[56]. From a centralized VPP perspective, the charging efficiency influences the charging time required to displace a certain amount of energy into the EV battery; the charging schedule by the VPP should thus be adjusted accordingly, to meet the EV user driving needs.

5
EV COORDINATION FOR LOCAL GRID SUPPORT

With high penetration of PV in LV grids, voltage variations along the feeders may become a challenge to cope with. If no measures are taken, grid reinforcement or power curtailment will be some of the options available. This chapter investigates on how EV load can be coordinated to provide voltage support in feeders during high PV production hours. Unlike the EV operation for ancillary services, the coordination of EV load targets an improved integration of PV in LV grids, **Figure 5-1**. Situations of undervoltage due to EV load are not treated; it is implied that, in absence of PV production in the feeder, during peak consumption hours and during overnight, the EV load is coordinated in such a way not to generate undervoltage situations.

In Section 5.1, the problem of voltage rise is defined. In sections 5.2, 5.3 and 5.4, two different concepts of EV coordination for local grid support are defined. In Section 5.6, a case study for voltage support using EV load is presented and results are shown in Section 5.7; in Section 5.8, a proof of concept of voltage support at private location with PV is presented. Summary and discussion follow in Section 5.9. The main results of this chapter are contained in papers [JP1], [JL2], [JP3] and [P8].

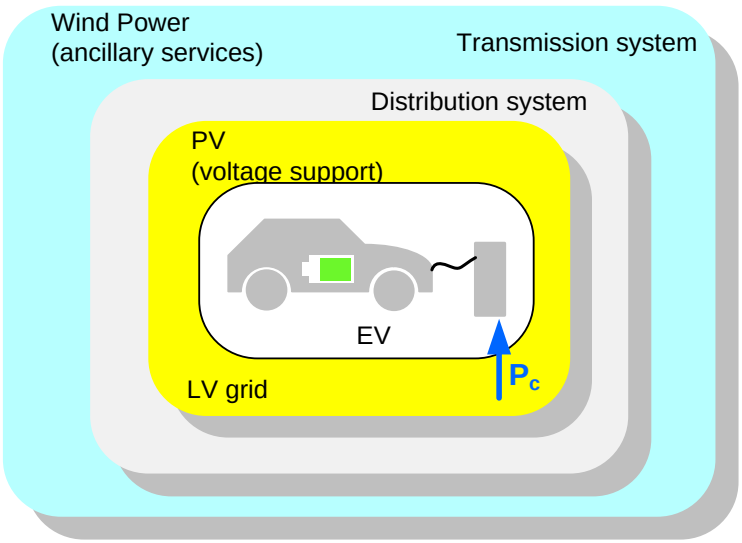

Figure 5-1: EV coordination for local grid support.

5.1 LV grid constraints in presence of RES

In a typical distribution grid, the purpose of the LV grid is to provide connection from the medium voltage (MV) grid to the supply points for the individual customers. This should be realized ensuring that the grid components such as the distribution transformer, lines and cables operate within their allowed range. At the same time, the voltage profiles at the different buses should meet the power quality requirements, as stated by the power quality standard EN 50160 [106].

With the increase of PV penetration in LV grids, one of the options available in LV grids is the control of EV load to improve the feeder operation, avoiding investments on grid reinforcements (upgrade of lines, cables, transformers, etc.).
In a LV grid with high penetration of PV, a number of electrical grid constraints should be taken into consideration. In relation to the project goals, a classification of grid constraints is given in **Figure 5-2**. From a customer's viewpoint, the improvements in a feeder operation with RES can be seen in terms of reliability, voltage quality or price. Other improvements dealing with loading of cables or transformers are secondary to the consumer.

A major voltage quality improvement which is expected in the near future is aiming at the reduction of long-term voltage-magnitude variations due decentralized PV generation [25], [43]-[47], [107]. On a theoretical basis, both under-voltages and over-voltages might be mitigated by keeping the correct local balance between production and consumption and this can be facilitated using EV load coordination.

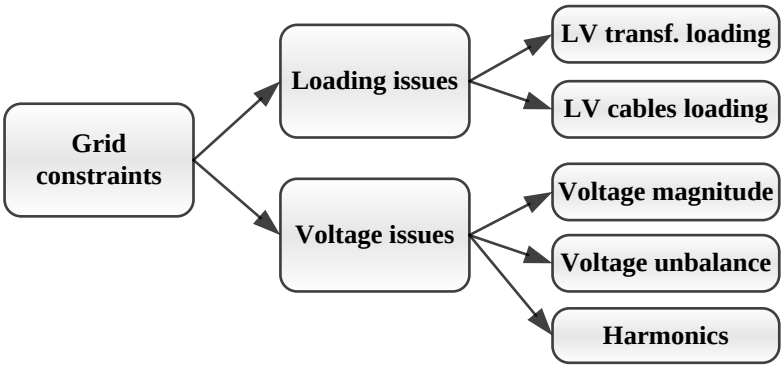

Figure 5-2: Classification of grid constraints.

5.1.1 LV grids with high RES penetration

Under high generation and low load conditions, one of the goals is to limit the risk that the feeder's voltages exceed the allowed limits at the different buses. In **Figure 5-3**, a simplified feeder model is used to explain the approach followed to address the problem.

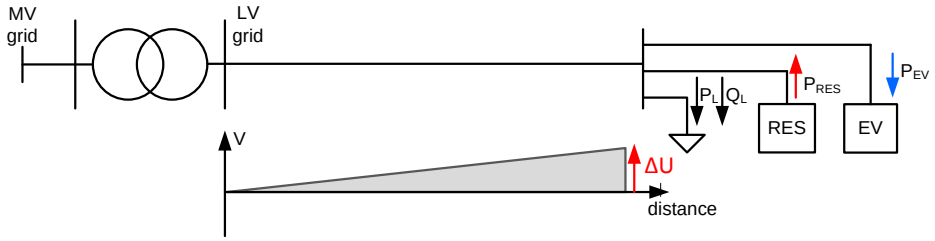

Figure 5-3: Voltage rise in a LV feeder with high RES generation.

where

P_{RES} is the active power injected from PV or wind turbines
P_L, Q_L is the load in the feeder
P_{EV} is the load due to EV charging or generally EV station load

In grids with high PV penetration, it can occur that the generation becomes larger than the load for several hours during the day that may lead overvoltage problems. In **Figure 5-4**, the voltage profile (RMS value) on bus 7 of the LV feeder studied in [P8] and the normalized PV power, are depicted for one-week period, respectively. The LV feeder presents a PV penetration level of 23%. The definition of PV penetration used refers to the ratio between the PV installed capacity and the capacity of the first feeder's line section capacity:

$$PV_{penetration}(\%) = \frac{\text{PV installed capacity (kVA)}}{\text{Feeder capacity (kVA)}} \qquad \textbf{(5.1)}$$

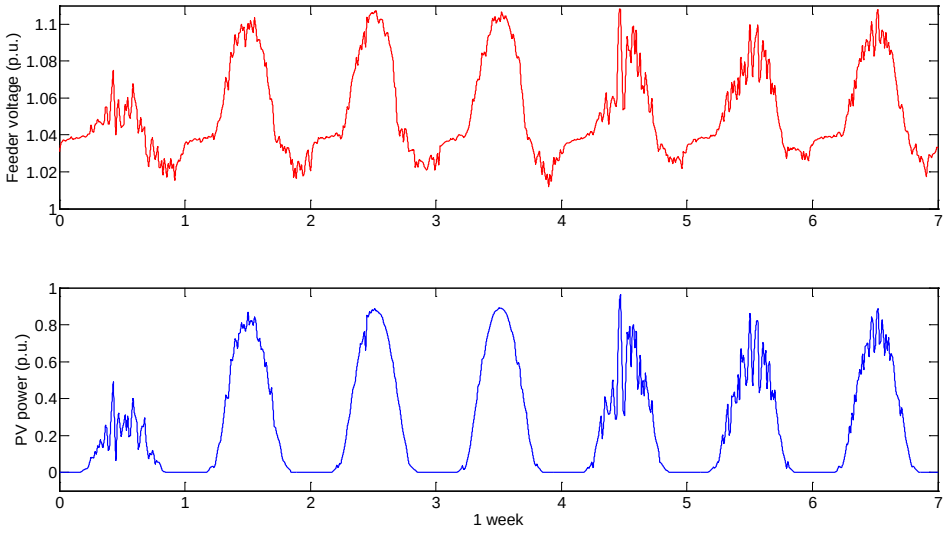

Figure 5-4: Voltage profile at a feeder bus due to PV.

The voltage profile reaches and exceeds the value of 1.1 p.u., which is the maximum allowed by the Standard EN 50160 [106]. A correlation in the shape of the voltage profile and the PV power profile in the feeder is observable.

For the same LV grid feeder, assuming identical penetration level of wind power instead of PV, the voltage magnitude variations of **Figure 5-5** are obtained.

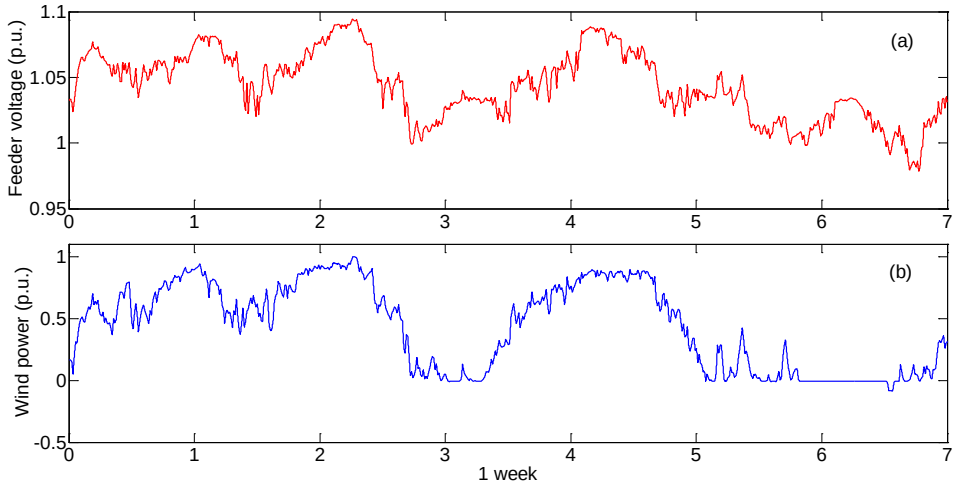

Figure 5-5: Voltage rise a feeder bus due to wind power.

With wind power in the feeder, the voltage profiles do not show anymore a daily periodic behaviour. The wind power generation profile is measured on the Risø's Gaia wind turbine, described in **Appendix D**.

Utilities in different European countries are currently revising the planning rules to accommodate increased RES penetration, ensuring voltage quality. As described in [41], some of the technical options include:

- Upgrade of the network circuit thermal capacity
- Upgrade of the upstream transformer capacity
- Rerouting the power path to reduce circuit length
- Upgrade with MV/LV transformer capable of automatic voltage control
- Construction of new substations
- Changes to the network topology
- Upgrade of the network's rated voltage level
- Installation of supplemental reactive power compensation

The aforementioned options can be classified as grid reinforcement. Lately, also automatic active power curtailment is being considered as an option available to the distribution system operators (DSOs), in the case that voltage variations due to RES exceed the allowed limits [42], [44]. However, the latter option requires a communication infrastructure linked to every single generation unit and it may be not convenient to the owners, unless compensation is given following a curtailment.
Reactive power methods for LV grids have been also extensively investigated [43], [45]-[47]. The effectiveness of reactive power methods for voltage rise mitigation has been demonstrated, showing some limitations. Considering the case of PV, most PV

units already installed in LV grids operate with unit power factor; in addition, the high R/X ratio of LV cables makes challenging the effectiveness of these methods. To have visible effects on voltage rise mitigation in a feeder, reactive power contribution should be provided by all PV units [47]. As an alternative, active power solutions can be used. In this chapter, EV load coordination with the function of voltage support is investigated.

5.1.2 Study assumptions

To perform voltage regulation, we consider the availability of EV load from public or private charging stations during PV generation hours. In accordance to several studies [108]-[113], we assume that a stationary *energy storage system* (ESS) is part of a public EV charging station. Thus, we assume that the same ESS can be operated to control the voltage in the feeder [JP1], [JL2] in cooperation with the electric load due to EV charging. We also consider that, relying on the load due to EV charging alone may not guarantee voltage support [57]-[60], thus the ESS is sized for a worst case scenario, with no EV charging load in the station. Also, we assume that EVs are plugged to the grid when parked at home [JP3], or when parked at commercial places or at workplaces, during PV generation hours [57]-[60]. The ESS charging load for voltage support in the feeder is not predetermined but a decision variable.

5.2 Voltage Support from EV charging stations

The voltage variation on a feeder node can be described as follows:

$$\Delta U \approx \frac{R \cdot P + X \cdot Q}{U_G} \qquad \textbf{(5.2)}$$

$$P = P_{RES} - P_L \qquad Q = Q_{RES} - Q_L \qquad \textbf{(5.3)}$$

where

P	is the nodal active power exchanged
Q	is the nodal reactive power exchanged
U_g	is the substation bus voltage
P_{RES}, Q_{RES}	are the active and reactive power of the RE unit
P_L, Q_L	are the active and reactive power of a generic load
R, X	are the cable resistance and reactance

A situation of voltage rise can occur during high generation and low load conditions, i.e. when $P_L < P_{RES}$. The storage function that an EV charging station can offer is described by the expression:

$$P = P_{RES} - P_L - P_S \qquad \textbf{(5.4)}$$

where

P_S	is the storage charging/discharging power

The storage component P_S can be realized with EV charging, or with the ESS in the station, or with a combination of both [JP1]. The main difference between the EV load and the ESS load is that the first is proportional to the number of vehicles charging simultaneously, while the latter is able dynamically adjustable according to the needs.

5.2.1 Energy storage from EV stations

The choice of the ESS technology within an EV station can include a wide range of options. With regard to EV public stations, battery technologies are often considered, thus this technology is assumed for the ESS [108]-[113]. As the main goal is to provide voltage regulation in LV feeders, the performances comparison of different battery chemistries, such as energy-to-weight ratio, self-discharge rate and battery charge/discharge efficiency is out of the scope of this work. The ESS, as well as an EV battery, can be modeled with the equations **5.5** and **5.6**, where P_d is the discharging power and P_c is the charging power of the battery, respectively; E is the energy stored in the battery at time t; Δt is the duration time of each interval. The two coefficients indicated with η are the discharge and charge efficiency, respectively.

$$E(t+\Delta t) = E(t) - \Delta t \cdot P_d / \eta_{DISC} \quad \textbf{(5.5)}$$

$$E(t+\Delta t) = E(t) + \Delta t \cdot P_c \cdot \eta_{CH} \quad \textbf{(5.6)}$$

For simplicity, P_d and P_c will be regarded as P_S, in the rest of the chapter. The operation of the battery system should also take into account power and energy constraints. The maximum power limits during charging/discharging can be described by:

$$P_S^{\min} \le P_S(t) \le P_S^{\max} \quad \textbf{(5.7)}$$

The same power limits are important for sizing the power electronics for the ESS. The energy and SOC limits of a battery system can be described as follows:

$$E_S^{\min} \le E_S(t) \le E_S^{\max} \quad \textbf{(5.8)}$$

$$SOC_{\min} \le SOC(t) \le SOC_{\max} \quad \textbf{(5.9)}$$

where $E_S^{\min}$ and $E_S^{\min}$ are the minimum and maximum energy levels of the ESS; $SOC_{\min}$ and $SOC_{\max}$ are the minimum and maximum SOC levels of the ESS. E_S in **5.8** is considered as the actual usable energy window of the ESS battery, regardless of the optimal energy management of a particular battery's chemistry.

5.2.2 EV station's storage concepts

To provide voltage support using EV load coordination, two concepts of energy storage are proposed that can lead to different business cases if implemented. With reference to **Figure 5-6**, the two concepts can be defined as:

1. Storage by public EV station: it can be realized within a public EV charging station, using an ESS, coordinated EV charging, or with a combination of both [JP1].
2. Storage by private charging: it can be realized at private households with PV and EV charging, [JL2], [JP3].

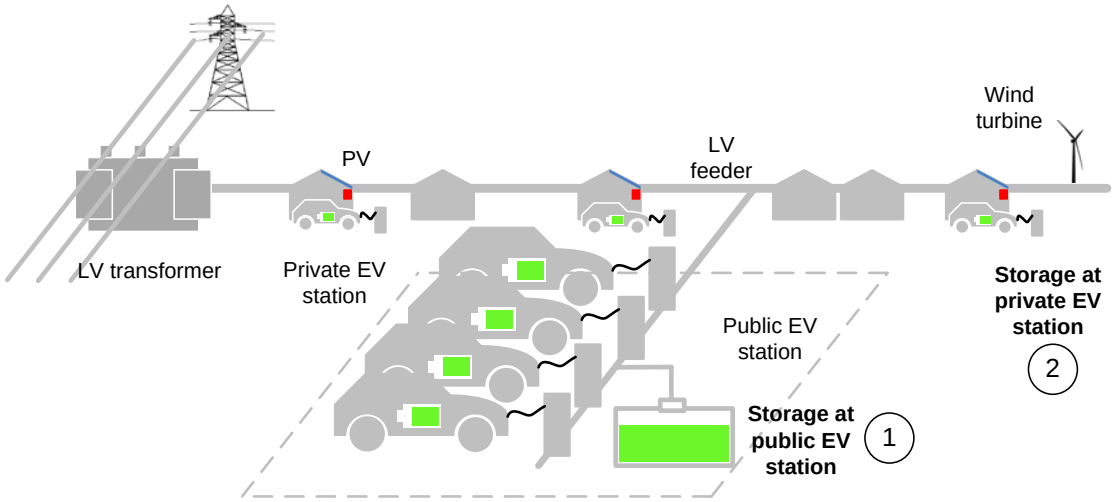

Figure 5-6: EV charging infrastructures in LV distribution grids.

The concept of *public storage* is achievable within a public EV charging station, where the station's owner can increase his revenue based on the additional service offered, e.g. ancillary services or voltage regulation in feeders with PV. The implementation of public charging stations in distribution feeders can facilitate the aggregation and control of EV load compared to the case of dispersed charging of EVs. Based on the initial assumptions, the electric load of the station is composed of two components: the ESS load and the load due to EV charging. If the latter is available and enough for voltage support, the ESS is automatically relieved of this task.
The concept of *private storage* can be implemented in feeders with residential roof-mounted PV and EVs. The households with PV units and EVs can increase their local consumption rate, by charging the EV during PV generation hours. According to this concept, a dual benefit can be created for the owner, which is based on voltage support, thanks to EV charging and increased local consumption.

5.3 Public EV charging stations

A public charging infrastructure is made of one or more charging stations installed at public locations to accommodate EV charging. A public charging station in Europe is designed according to the AC conductive charging standard, IEC 61851 [63].

Two design options of EV public stations are defined in [112]-[113], and in particular the AC-distribution and the DC-distribution charging station. In **Figure 5-7** the AC-distribution station is depicted.

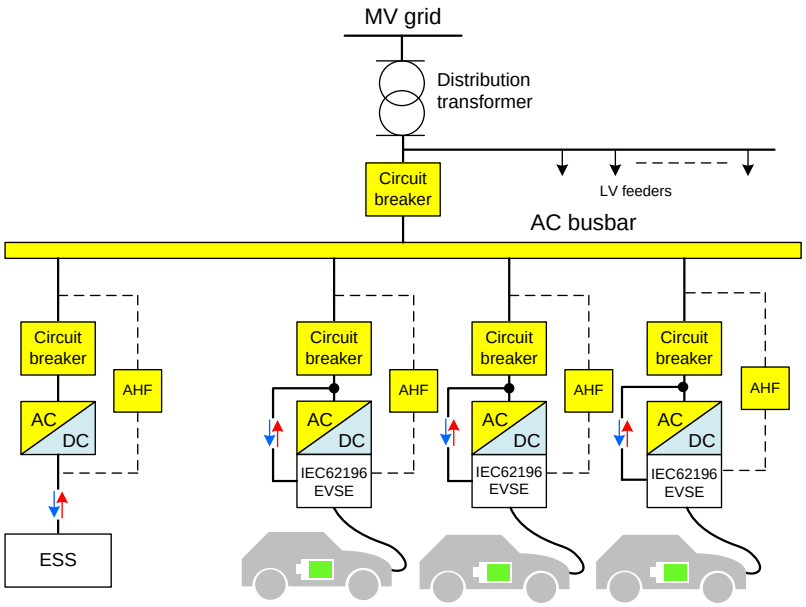

Figure 5-7: AC-distribution EV public station.

With this station option, external DC chargers can be optionally installed to increase the station flexibility offering the DC charging option.

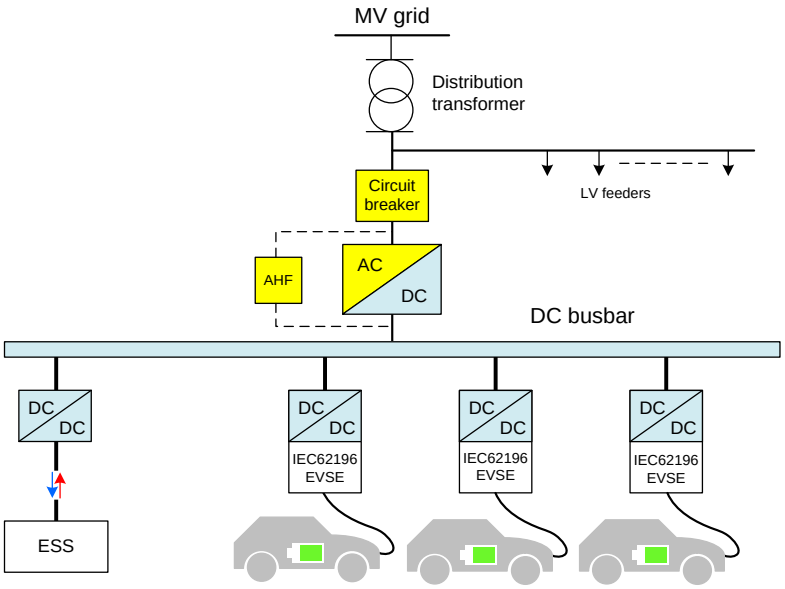

Figure 5-8: DC-distribution EV public station.

The station incorporates a certain number of charging stations (Electric Vehicle Supply Equipment - EVSE) using standard plugs for charging according to IEC 62196 [114]. The station protection is realized by means of circuit breakers, while active harmonic filter (AHF) can be employed for mitigating harmonics problems. With the DC-distribution station's architecture, **Figure 5-8**, a DC busbar is employed to transfer the

power to the different charging spots. Both stations embed an ESS, whose primary purpose is to handle the transient conditions due to EV parallel charging.

5.4 Private EV charging stations

Private EV charging stations are designed in compliance with charging power options of Standard IEC 61851 [63]. Voltage support from EV stations at private homes with PV represents a storage opportunity in LV grids with high penetration of PV. This is the second storage concept investigated in this chapter.

If we consider the case of LV grids with roof-mounted PV, e.g. in Germany, Italy and Spain, the storage function required for voltage regulation can utilize the electric load by private EV charging at the different house locations with PV. The probability of an EV charging at home is estimated for the 24-hour period in [87]; a maximum availability (normalized to 1) during night hours and an average availability of 0.7 during daylight, i.e. between 10AM and 6PM, is observed. If an EV is available at all houses with a roof-mounted PV system, a storage-based strategy can be adopted to support the voltage profiles during PV generation hours, though this is only an assumption today.

In the case of three-phase roof-mounted PV systems in LV feeders, which is expected in Europe in the next years, three-phase EV chargers are a better option to use with the function of storage. Though, most EV chargers are single-phase, the need of a shorter charging time will likely push for the adoption of three-phase EV chargers.

5.5 Control of EV stations for voltage support

The two concepts of private and public stations use EV load coordination to provide voltage regulation in the feeder. The control of public and private EV stations is performed according to the following two strategies:

- Control of public EV station [JP1], [JL2]. The EV load within a public EV station is controlled according to: $P_s = f(U)$, where U is the critical bus voltage in the feeder.
- Control of private EV station [JL2], [JP3]. The EV load within a private EV station is controlled according to $P_s = f(P_{PV})$, where P_{PV} is the PV power production of the PV system. Also for a private EV stations, the strategy could be the same as for a public station, but in order to guarantee an equal storage contribution from the different PV owners at the different feeder locations, the strategy $P_s = f(P_{PV})$ is implemented.

For public EV stations, the main questions to address are:

- What is the required ESS size within a public EV station, to provide voltage regulation in the feeder? How the ESS size changes depending on the EV station location in the feeder?

For private EV stations, the location of each station corresponds to the location of the different houses with PV. The main question to address is:

- What is the required storage power and energy, in order to provide voltage regulation in the feeder, using EV private charging?

5.5.1 Problem formulation

A common technique used to analyse the impact of active power injection from RES on voltage profiles in a feeder is voltage sensitivity analysis [115].

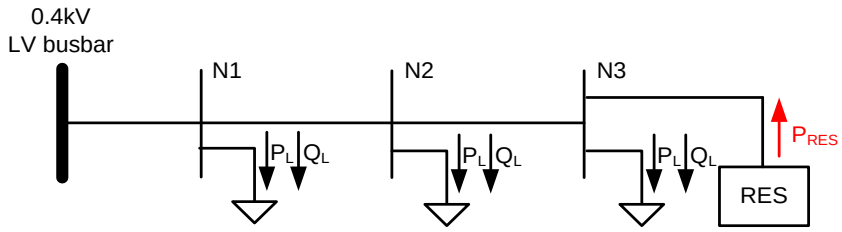

Figure 5-9: LV test feeder.

Voltage sensitivity analysis reveals the critical locations for active power injection in a LV feeder, as well as the most effective locations for voltage support.
The voltage sensitivity matrix *S* for a LV feeder can be derived by solving nonlinear load flow equations using the Newton–Raphson algorithm. If we consider the 3-node test feeder of **Figure 5-9**, with grid parameters in **Table 5-1**, two voltage sensitivity matrices can be obtained, **Table 5-2** and **Table 5-3**, for active and reactive power respectively. The nodes are indicated with N1, N2 and N3.

Table 5-1: LV feeder parameters

Parameter	Type/value
Cable type	NA2XRY 0.6/1kV, Cu
Cable cross section	4x95 mm^2
Cable length / segment	200 m
Cable impedance / segment	0.064 + j0.0138 Ω

Table 5-2: dU/dP sensitivity matrix

dU/dP (p.u./MW)	N1	N2	N3
N1	0.389	0.387	0.385
N2	0.387	0.766	0.763
N3	0.385	0.763	1.142

Table 5-3: dU/dQ sensitivity matrix

dU/dQ (p.u./MVAr)	N1	N2	N3
N1	0.148	0.148	0.148
N2	0.148	0.230	0.230
N3	0.148	0.230	0.312

The diagonal coefficients of both matrices represent the voltage sensitivities to active and reactive power injection, *dU/dP* and *dU/dQ*, respectively. As LV cables are predominantly resistive [116], the matrices' coefficients show that a certain amount of injected active power has a larger impact on voltage than the equivalent amount of reactive power. Furthermore, the voltage sensitivity coefficients increase linearly with the distance from the transformer. At the feeder's head, the voltage sensitivity to active power is the minimum one; at the feeder end, active power has a much larger contribution on voltage variation, than reactive power. The non-diagonal elements are the mutual coefficients of voltage sensitivity due to power exchange on different nodes. With the voltage sensitivity method it is possible to calculate the voltage variations due to active power injection at a generic feeder location.
For a generic LV feeder with *N* buses, by considering the two possible states of, with or without an EV station at each node, the search space contains 2^N combinations. Considering only active power for voltage support, the voltage on the generic bus *N* can be lowered below U_{max} with the following expression:

$$U_N \approx U_G + \sum_{k=1}^{N} \frac{\partial U_N}{\partial P_k}(P_{PV,k} - P_{L,k} - P_{S,k}) \qquad \textbf{(5.10)}$$

where U_G is the base grid voltage, P_{PV} is the active power injected from PV, P_L is the load, P_S is the storage power required for voltage support, dU_N/dP_k is the sensitivity coefficient. It shall be noted that the reactive power component of loads in LV grids is assumed with minor influence, therefore neglected. A similar equation to **5.10** can be solved in case of the application of reactive power methods for voltage support. To identify the minimum ESS size for the public and private storage concepts, the problem to solve can be formulated as follows:

Objective function:

$$f = \min \sum_{k=1}^{N} P_{S,k} \qquad \textbf{(5.11)}$$

Subject to:

$$\begin{aligned} &a) \quad u \le U_{\max} \\ &b) \quad P_S^{\min} \le P_{S,k} \le P_S^{\max} \end{aligned} \qquad \textbf{(5.12)}$$

where

f is the objective function of the problem, which minimizes the storage power $P_{S,k}$ needed at bus k, to lower all bus voltages below the maximum allowed voltage magnitude;

k identifies the bus vector of the feeder, with k = [1,..,N];

- Constraint a) indentifies the first problem's constraint, which imposes all bus voltages below the maximum allowed voltage magnitude $U_{\max}$;
- Constraint b) identifies the second problem's constraint, which imposes the ESS power in a power range $0 \le P_{S,k} \le P_S^{\max}$.

The solution to this problem should identify a minimum power size $P_{S,k}$ of the ESS, which is a real number, i.e. $P_S \in R$. Furthermore, the solution identifies an optimal configuration of ESS position in the feeder.

Such problem is a typical mixed-integer linear programming problem [117], whose canonical formulation is as follows.

Objective function:

$$\min_x c^T x \qquad \textbf{(5.13)}$$

Subject to:

$$\begin{aligned} &Ax \le b \\ &x_j \in R \ \forall j \in D \end{aligned} \qquad \textbf{(5.14)}$$

where D is the set of indices of the integer variables in *x*.

With the sole linear programming (LP) method, it is possible to solve a constrained optimization problem in which the objective function and the constraints are linear. The method seeks a solution that minimizes the inner product of *c* and *x* within the feasible region. In a LP problem, the elements of *x* can take any real value. Instead, in a mixed-integer linear programming problem, which is shown above, some of the elements of *x* are constrained to be integer.

In the papers [P8] and [JP1], the problem described by **5.11** and **5.12** is solved with the following two methods:

1) An iterative method [P8], which is described in the next section;

2) A Mixed-Integer Linear Programming (MILP) method [JP1] which is described in Section 5.5.3.

In the paper [JP3], the problem is solved with LP, as the location of an EV in the feeder is fixed and corresponds to the location of a house with PV system.

5.5.2 Search-algorithm

The iterative method presented [P8] is illustrated in the flow chart of **Figure 5-10**. The method is developed during the Ph.D. research period at SMA Solar Technology, Germany.

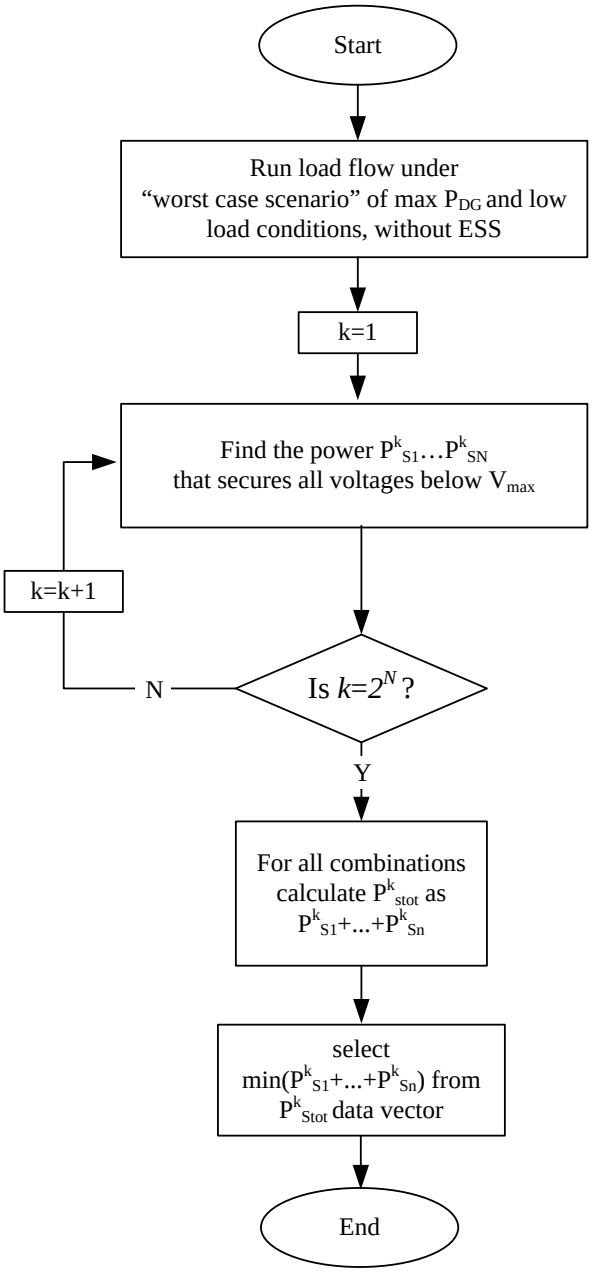

Figure 5-10: Search-algorithm flow diagram.

The solution algorithm can be described with the following steps:

1. Perform a preliminary sensitivity analysis for the LV grid to identify the voltage sensitivity coefficients to active power injection;
2. Run load flow under a "worst case" scenario of maximum generation from PV and no load at the different buses in the feeder;
3. Set a combination of storage in the feeder, and identify the storage size to have all feeder voltages below a predefined U_{max};
4. Check if all combinations of storage locations have been tried out, otherwise go back to step 3;

5. For all storage configurations in the feeder, select the one with minimum storage size required, i.e. minimum power and energy levels.

In summary, the applied method gives as output a result table with all storage power combinations P_{S1},…, P_{SN} combinations, where N is the number of buses in the analyzed feeder. Among all the combinations, the one with minimum power level for lowering the voltage below U_{max} is identified as the optimal storage configuration. This is done by calculating first an aggregated value of power P_{Stot} as the sum of all storage results for a given combination. With the selection of the minimum power solution, the best location of public EV station is automatically identified.
As previously mentioned, the method proposed permits to identify the best location to provide voltage regulation minimizing the storage size, i.e. the charging power. It shall be noted that the method aims at determining the *relative differences* in charging power, in relation to the different locations, and not at quantifying the storage energy required. The latter is addressed with measurement-based time-series simulations.
One of the limitations of the iterative method is its application to feeders with a high number of nodes. In this case, the number of iterations increases significantly, therefore the same problem has been solved with mixed-integer linear programming.

5.5.3 MILP method

The problem presented is solved with Mixed Integer Linear Programming. The overall formulation of the MILP problem is as follows:

Objective function:

$$f = \min \sum_{k=1}^{N} P_{S,k} \qquad \textbf{(5.15)}$$

Constraint 1)

$$U_N \approx U_G + \sum_{k=1}^{N} \frac{\partial U_N}{\partial P_k}(P_{PV,k} - P_{L,k} - P_{S,k}) \le U_{\max} \qquad \textbf{(5.16)}$$

Constraint 2)

$$\begin{cases} 0 \le P_{S,k} \le \delta_k P_S^{\max} \\ with \quad \delta \in \{0,1\}, \ \text{integer variable} \end{cases} \qquad \textbf{(5.17)}$$

where

f is the objective function which identifies the minimum ESS charging power and the optimal location;

N is the number of buses in the feeder;

U_N is the voltage magnitude at bus *N*;

U_G is the base grid voltage magnitude (p.u.);

$P_{PV,k}$ is the active power feed-in by PV at bus *k*;

$P_{S,k}$ is the ESS power at bus *k;*

$P_{L,k}$ is the load at bus *k;*

$\partial U_N/\partial P_k$ is the voltage sensitivity coefficient to the active power exchanged (p.u./MW).

$U_{\max}$ is the maximum allowed voltage magnitude at all buses in the feeder.

δ_k is the integer variable which defines the installation status of storage at bus *k*;

5.5.4 Methods comparison

The first method presented is a search-algorithm in the form: "*try all possible combinations and pick the best one*".

The solution of the problem with this method requires 2^N iterations, where N is the number of buses in the feeder. Thus, if for every bus in the network there is a number of possible storage sizes, e.g. *k*, then the order of this problem becomes 2^{N*k}.

This means that the search-algorithm is only applicable to problems with a small number of buses (about 10) and limited number of possible storage sizes; otherwise, the problem may become intractable with regard to computational time.

The Mixed-Integer Linear Programming method overcomes the limitation presented by the search-algorithm. The MILP method is faster in terms of computational time and it is applicable to larger grid feeders containing a high number of buses.

Furthermore, the MILP results more precise than the search-algorithm in the identification of the optimal power size. In fact, while the iterative method searches for the optimal size among a limited number of possible storage sizes, e.g. 0, 0.5, 1, 1.5 kW etc., the MILP finds the optimal solution in the range $0 \le P_{S,k} \le P_S^{\max}$, without the need of a power step size.

5.6 Case study

The defined concepts of public and private EV station are investigated for a real LV grid with high penetration of PV, though the study can be extended to contexts of micro-grids with wind power production. The two presented methods are implemented for a Belgian LV feeder affected by voltage rise issues due to high PV penetration. The grid layout is depicted in **Figure 5-11**, [JP1]. The proposed methods are not meant to quantify the exact storage size needed for voltage support, but rather to enlighten the relative differences in storage size assuming the ESS placed at different locations in the feeder.

To more precisely quantify the power and energy requirements of the ESS at the different feeder locations, time-series simulations using real load/generation profiles are performed. With simulations, the performance comparison of voltage regulation by public and private EV stations is addressed according to the scenarios depicted in **Figure 5-11** and **Figure 5-12**.

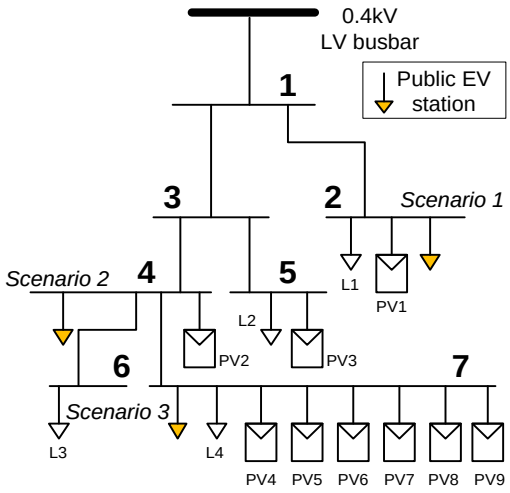

Figure 5-11: Voltage regulation via public EV station.

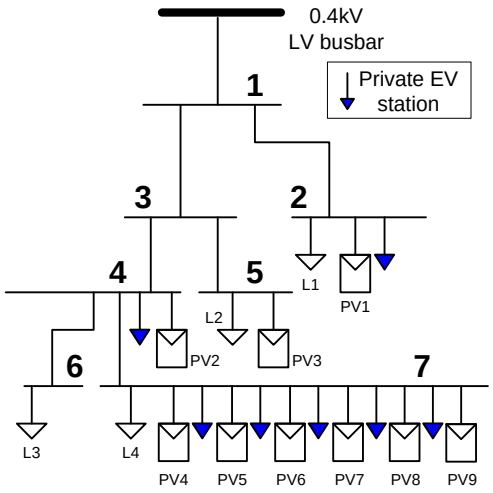

Figure 5-12: Voltage regulation via private EV stations.

In **Figure 5-11**, three different scenarios of public EV station are depicted:

- Sc. 1: Public EV station closer to the distribution transformer (Scenario 1)
- Sc. 2: EV station at an intermediate location in the feeder (Scenario 2)
- Sc. 3: EV station at the end of the feeder (Scenario 3)

In **Figure 5-12**, the case of private EV station is addressed considering a private EV station at each household with PV.

5.6.1 Method Implementation

The storage power results obtained with the application of the MILP method are depicted in **Figure 5-13**; very similar results are obtained with the search-algorithm approach, thus these are not depicted.
The method is implemented upon the assumptions of:

- maximum allowed voltage magnitude of 1.1 p.u
- maximum PV generation and no load at the different buses

Details on the feeder characteristics, as well as on load and generation, are indicated in [JP1] and [JP3]. In the diagram, the results obtained with the MILP method are compared with the load flows in PowerFactory, considering the ESS at the different nodes. The storage placement at node 7 results as the optimal solution for voltage support as it requires a lower charging power compared to other locations.

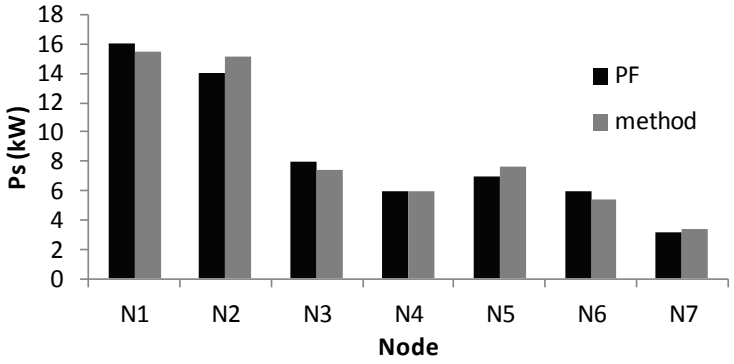

Figure 5-13: Storage power results for the different feeder locations.

5.7 Simulation results

The performances of voltage regulation are evaluated under the three public station scenarios of **Figure 5-11** and private charging scenario of **Figure 5-12**, with the support of time series simulations. The main goal is to keep the bus voltages in the feeder below 1.1 p.u., as required by the standard EN 50160 [106]. Simulations are conducted using 15-minute average load and generation profiles for 1-week summer period in Belgium, which represents a worst case scenario for the voltages in the feeder [47]. The daily power and energy levels required for a public station's ESS are depicted in **Figure 5-14** and **Figure 5-15**. The identified levels refer to the day in summer, with the highest storage requirement. The main finding is that with 1-year time-series simulations the results obtained with the proposed methods are confirmed. A public EV station located at the end of the feeder offers voltage regulation with a lower charging power and energy effort, compared to other locations. The discharging phase of the ESS is assumed to take place after sun set, during evening or overnight.

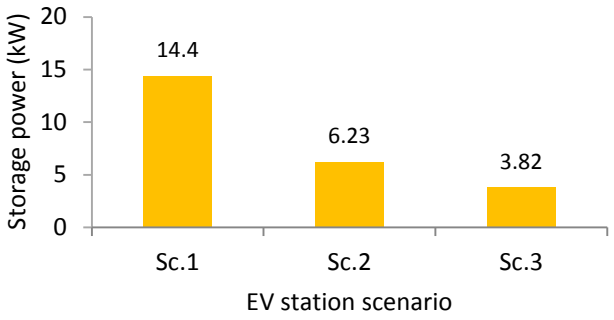

Figure 5-14: Storage power for voltage support for the different scenarios.

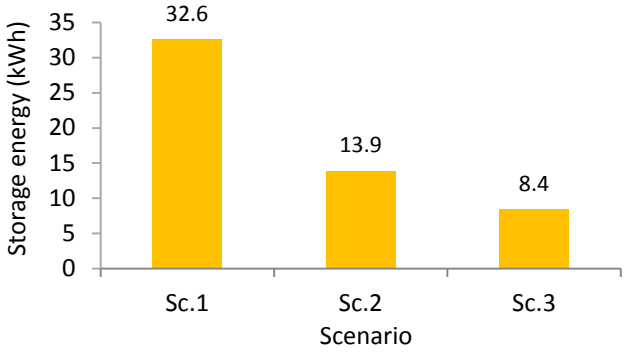

Figure 5-15: Storage energy for voltage support for the different scenarios.

For the three scenarios of EV public station, the voltage profiles (phase-to-ground in p.u.) of the most critical bus in the feeder, bus 7, are depicted in **Figure 5-16**. The effect on voltage profiles with the three storage scenarios is equivalent.

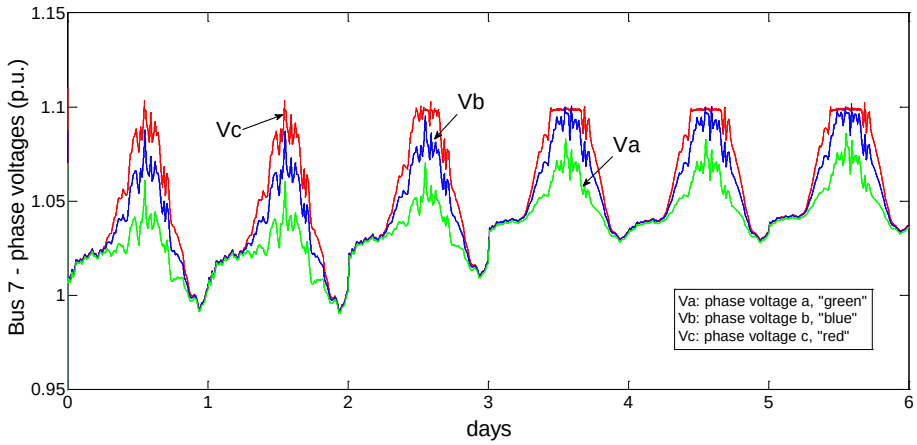

Figure 5-16: Voltage profiles with the three public EV station scenarios.

In presence of parallel EV charging, the ESS within the station can be relieved of the task of voltage support, thus prolonging its expected lifetime. In **Table 5-4**, the number of EVs required to absorb the power levels of **Figure 5-14** is depicted.

Table 5-4: Number of EVs required for voltage support

EV Charging option	EV Charging power (kW)	Sc.1 #EVs	Sc.2 #EVs	Sc.3 #EVs
AC - 16A/230V	3.7	4	2	2
AC - 32A/230V	7.4	2	1	1
AC - 16A/400V	11	2	1	1
AC - 32A/400V	22	1	1	1
DC	50	1	1	1

With regard to the private EV station concept, the results of storage power and energy are depicted in **Figure 5-17** and **Figure 5-18** (in blue), and put in relation to the results obtained for the EV public stations. These results are obtained in [P8], considering an ESS at each house with PV. The control strategy used for private storage is thoroughly described in [JP3].

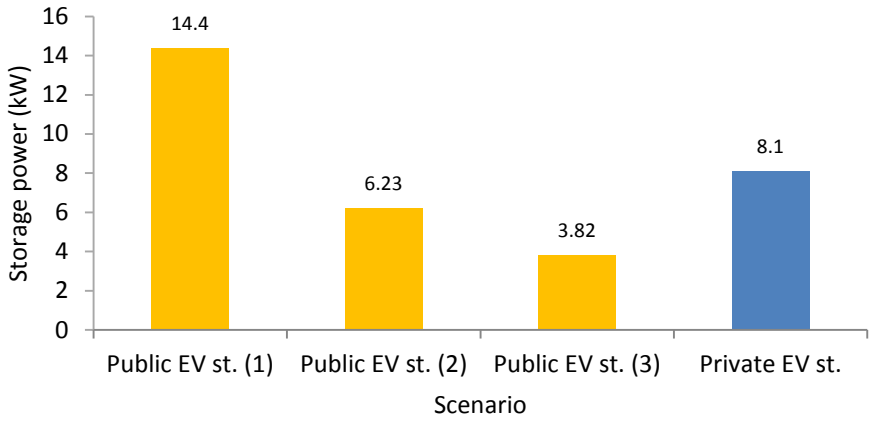

Figure 5-17: Storage power for private EV stations.

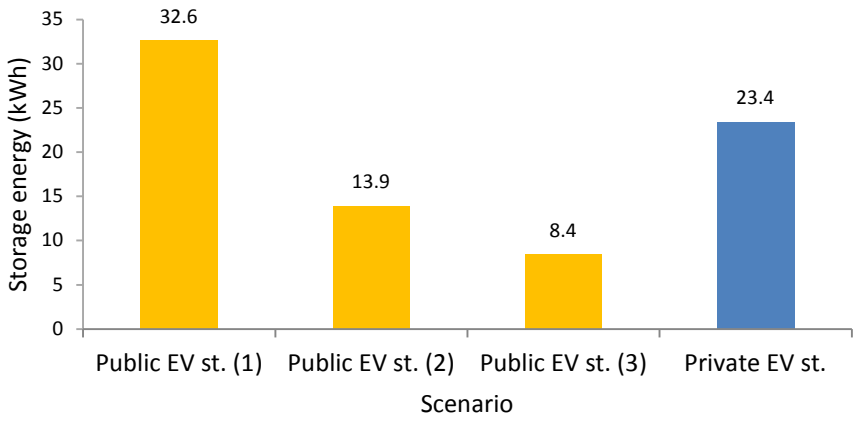

Figure 5-18: Storage energy for private EV stations.

The storage power and energy levels depicted for private EV stations represent the aggregated storage, i.e. the storage contribution at every private household with PV.

5.7.1 Discussion

A relatively small storage contribution from each PV owner would be enough to secure the voltages within the limits in the feeder. This can be realized with EV load coordination at private houses with PV. On the other hand, a single public EV charging facility would be enough to provide voltage support in the feeder. In [JP3], a 1-year simulation is performed, showing the need of voltage support for 98 days, mostly distributed in spring and summer. If a grid reinforcement approach is considered, the replacement of two feeder cables with total length of 500 m and cross section of 150 mm^2 is required to obtain the voltages at all buses below 1.1 p.u. Based on current market prices, the implementation of the solution of Sc. 3 with a 4 kW battery-inverter (500 €/kW) and a 10 kWh Li-ion battery (700 €/kWh) would cost about 10,000 €. With the grid reinforcement option, considering 130,000 €/km (roughly the Danish rate) for the new cable and the installation cost, the initial investment is about 7 times higher than with the storage option. Nevertheless, the running costs of the ESS, the power losses during charging/discharging and the battery life degradation due to voltage support are not considered.

5.8 Voltage Support using EV load – Proof of Concept

To validate the concept of voltage support using EV load coordination, a test setup is implemented at Center for Electric Power and Energy (CEE) laboratory, PowerLabDK.
The main goal is to realize a proof of concept of the proposed voltage support strategy using coordinated EV charging. Considering the availability of the EV test bed, and due to logistic reasons, a proof of concept of private EV storage for voltage support is implemented and presented, [JL2]

5.8.1 Proof of concept assumptions

To create the realistic conditions of voltage rise problems, similar to the simulation case, the only option available is to reproduce the scenario of a household with roof-mounted PV and private EV charging, at a remote location in a LV feeder. Unlike the simulation case study, where 42 kW of PV capacity are installed in a LV feeder with 33 households, the laboratory facility is equipped with one three-phase PV system with peak power capacity of 6 kW. According to the original configuration, the PV generator is directly connected to the main grid; however, with such configuration it is not possible to observe any significant voltage rise at the PCC.
To create situations of voltage rise at the PCC of the PV generator, a relatively long LV cable with small cross section is used. The criterion used for dimensioning the cable characteristics is described in the following subsection.

5.8.2 Test setup

The setup is depicted in **Figure 5-19** and is composed of:

- 100 m, 1.5 mm^2, 5-wires copper cable, with impedance of 13.3 Ω/km;
- three-phase PV plant with typical Danish installed power of 6 kW;
- three-phase EV battery charger with charging power of 3.7 kW;
- 14 kWh Li-ion battery with battery management system (BMS).

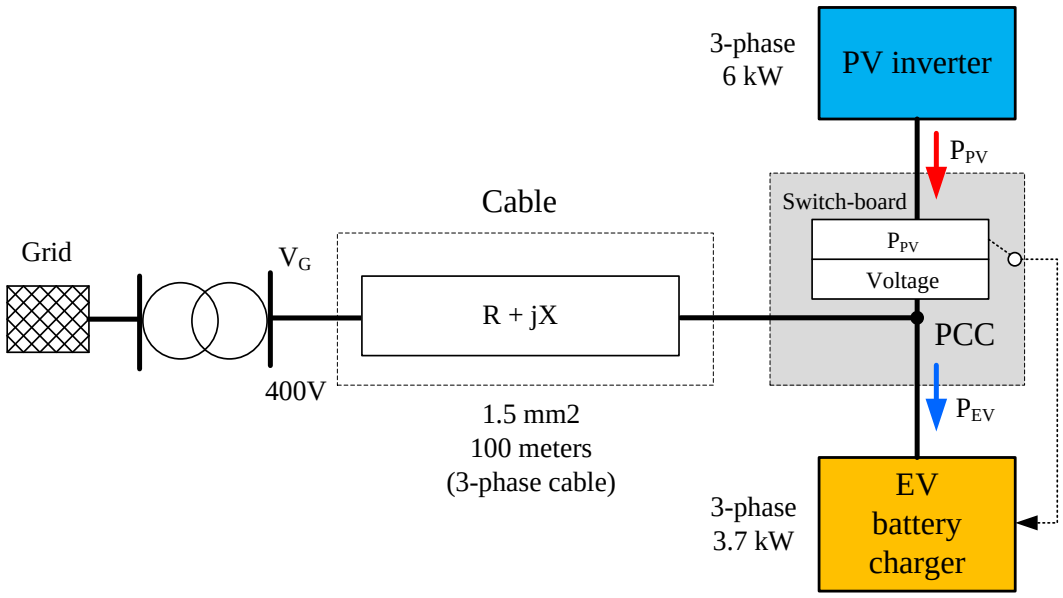

Figure 5-19: Simplified single-line diagram of the experimental setup.

The cable is dimensioned to reproduce voltage magnitude variations comparable to the ones observed with the Belgian LV feeder. With a 6 kW PV system and base grid voltage of 1.04 p.u., a 5-wires cable with 100 m length and 1.5 mm^2 cross section is used.

5.8.3 Control strategy

The EV charging is controlled and activated according to two possible control strategies:

1) the voltage at the PCC is greater than a predefined maximum voltage U_{max};
2) the feed-in active power at time *t*, $P_{PV}(t)$ is greater than a predefined value P_{PVmax}.

With the first strategy, one limitation is that only those customers with EV at the end of the feeder are more likely to be involved in voltage support due to larger voltage variations at the end of the feeder than at intermediate points. To activate also the customers near the transformer, a strategy using the power $P_{PV}(t)$ is adopted as the criterion for the activation of EV charging. Therefore, the second strategy is

implemented and tested. Recalling that voltage regulation is possible with the the expression:

$$U_{PCC} = U_G + \frac{R \cdot P + X \cdot Q}{U_G} + j\frac{X \cdot P - R \cdot Q}{U_G} \quad \textbf{(5.18)}$$

where:

U_{PCC} is the phase voltage magnitude at the PCC;
U_G is the grid voltage;
P and Q are the exchanged nodal powers, with $P = P_{PV} - P_{EV}$;
R and X are the cable parameters.

the EV charging is activated with the following criterion as resulting from the :

$$P_{PV} > 0.7 \cdot P_{PVmax}$$

A similar criterion is applied in Germany, according to the Renewable Energy Act, EEG 2012, and has come into force on January 1st, 2012 [JP3]. When EV charging is activated, a fixed electric load of 3.7 kW is used. This is because the EV load profile does not follow the variations of the PV generation profile, as this is not the task of an EV charger.
The proof of concept is realized with a three-phase PV and EV charger, therefore the expression **5.18** applies. However, the same voltage support concept is applicable to a single-phase system with PV and EV, connected to the same phase. In this case, the expressions used for the calculation of the voltage variation changes, as well as the effect on voltage at the PCC.

5.8.4 Test results

The results of the tests performed are shown for a 24-hour period with 1-minute resolution in **Figure 5-20** (a)-(b); the power and voltage measurements during the most meaningful time interval are indicated in **Table 5-5**.

Table 5-5: Voltage measurement at PCC

Time	PPV (kW)	PEV (kW)	V1 (V)	V2 (V)	V3 (V)
14.50	4.13	0	246.2	247.5	247.2
15.00	4.21	3.7	240	241.4	241
15.10	4.45	3.7	240.8	242	242
15.20	3.97	3.7	238.8	239.8	240.3
15.30	3.90	3.7	238.9	240.1	240.6
15.40	3.87	3.7	239.8	241.4	240.9
15.50	3.91	3.7	238.9	241.1	240.5
16.00	3.83	3.7	238.6	239.7	240.2
16.10	3.60	3.7	236.8	238.2	237.8
16.20	3.49	0	243.6	244.9	245.2

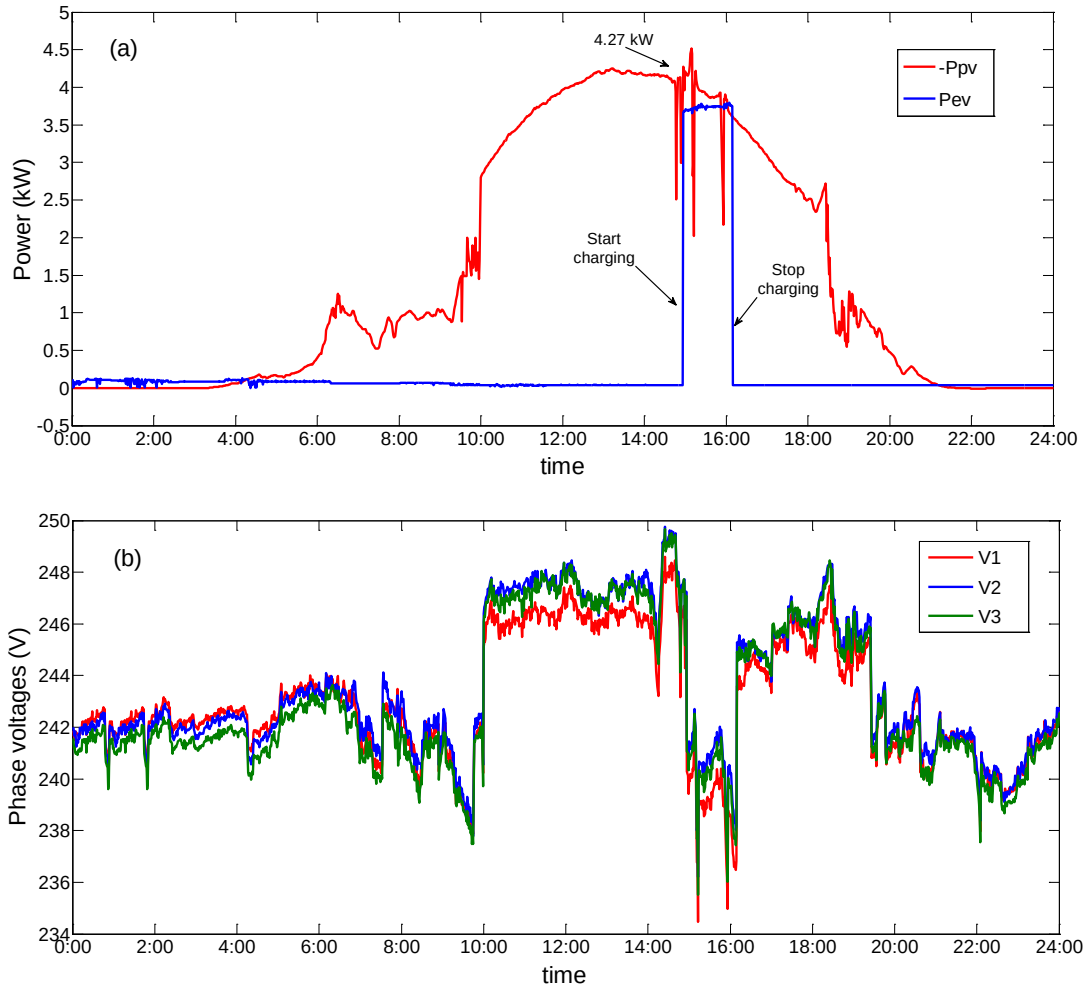

Figure 5-20: Test results. (a) PV power profile and EV load profile. (b) Phase-to-ground voltages at PCC.

In **Figure 5-20** (a) the PV power profile (P_{PV}) and the EV charging profile P_{EV} are depicted. The measurements are taken on the 4th of July 2012, at PowerLabDK, Kongens Lyngby, Denmark. The phase voltage profiles in **Figure 5-20** (b) show that EV charging contributes to lower the voltages at the PCC of about 6.1 V, thus avoiding that the voltage limit of 1.1 p.u. is exceeded.

5.9 Summary and discussions

A major finding in this chapter is that the coordination of electric demand of EV charging stations has beneficial effects in LV grids with PV generation.
The EV load coordination for voltage support in feeders with PV has been investigated with two main infrastructure concepts: public EV charging and private EV charging.

A public EV charging station, where the parallel charging of EVs takes place, is likely to come equipped with a stationary ESS in the next years [108]-[112]. The station load is then a combination of the EV load due to charging and to the ESS load. The combined ESS and EV load profiles can offer the storage power needed to keep the voltage magnitude in the feeder within the allowed range. This scenario is alternative to power curtailment, grid reinforcement and reactive power methods that have been already addressed as possible options by previous research [41]-[47]. In order to guarantee enough charging load for voltage support in the feeder, the station ESS shall be sized considering a worst case scenario of maximum PV generation and no load conditions in the feeder. The location and size of a public station can play an important role for voltage support in a feeder with PV. A novel method, based on voltage sensitivity analysis is developed to identify favourable feeder's location for the ESS operation. The method is applied to a residential LV feeder with roof-mounted PV systems, showing that a certain location could be more convenient than others, in terms of required storage size. The method is applicable to any distribution grid or feeder. In order to obtain satisfactory results, an accurate LV grid model should be available.

The scenario of EV charging at private houses with PV is also considered. The availability of EVs at houses with PV and the coordination of EV charging during PV generation hours is a likely scenario in the next years [58]-[60]. Private charging can mitigate voltage rise problems in the feeder, thanks to an increase of the local consumption rate during PV generation hours. A proof of concept of voltage support for private EV charging at a location with roof-mounted PV has shown the validity of the proposed concept, assuming certain penetration levels of EVs in the feeder. Though, a limitation on using private EV charging is that there is no guarantee that there will be enough charging load for the required voltage support.

With time-series simulation of a residential LV feeder with PV, we observed the need of voltage support for 98 days a year [JL2], [JP3]. The use of time-series simulations based on load and generation profiles has proven to be a fundamental tool to quantify the energy storage requirements for voltage support, under the two EV charging station concepts. A comparison between the storage power requirements for a public EV charging station at the different buses, versus the reactive power requirements is shown in [JL2]; due to the high R/X ratio of LV cables, the required amount of reactive power for voltage support results 3 times higher [JL2]. By using EV load coordination for voltage support in feeders with PV, grid reinforcement and curtailment of the active power feed-in by PVs can be postponed.

6 CONCLUSIONS

Electric vehicles (EVs) and renewable energy sources (RES) are expected to gradually replace internal combustion engine (ICE) cars and conventional power plants, in the coming years [4], [9]. This thesis has explored possible ways of using EVs, to facilitate the integration of wind power and photovoltaic (PV) at different levels in the power systems.

We demonstrated the use of EV load coordination for wind power integration, considering the transmission system operator (TSO) needs of ancillary services, secondary reserves and regulating power, in the Danish power system. We defined measurement and control requirements that allow the services provision from EVs, according to a centralized coordinated control concept of a Virtual Power Plant (VPP). We have taken into account the technical TSO conditions that apply for the provision of secondary reserves and regulating power. Through a full-scale proof of concept, we have shown that an EV can serve as a controllable load with response time compatible with the TSO regulation requests. We have also highlighted technical limitations of EV components, such as the battery and the charger, that occur during periods of EV load coordination. Simulation and tests of ancillary services provision using EVs have identified potential nonlinearities in the EV load profile and battery ageing aspects, which should be considered when using EVs to support the power system for wind power integration.

With regard to PV in power systems, we studied the potential use of EV load coordination in low voltage (LV) residential grids with voltage rise problems due to PV generation. We found that the coordinated EV load can be used as a storage solution to mitigate voltage rise problems in feeders with PV. We proposed the use of public and private charging station concepts to support the voltage in LV feeders with PV. A method, based on voltage sensitivity analysis, has been proposed to determine the storage size requirements for voltage support by public or private EV stations. The method application on a real LV residential feeder with PV has highlighted that the sizing and placement of public EV stations are crucial aspects in their potential contribution for voltage support. With regard to private charging for voltage support, we proposed a decentralized storage strategy for private PV owners with EV. We verified, through simulations and a proof of concept, that the application of the proposed strategy

in real feeders with PV can offer the dual benefit of increasing the local consumption and supporting the voltage in the feeder. The qualitative results obtained are applicable to other grids and can be considered for the planning of EV charging stations. Overall, the EV load coordination for voltage support from public and private stations can be an alternative to the adoption of more costly grid reinforcement options.

The findings of this project meet some of the present and future targets of transmission and distribution system operators, facilitating the integration of wind power and PV at different levels in the power system using EVs. The knowledge gained and the technical solutions developed in this Ph.D. project can be utilized in research projects and demonstrations, looking at the interaction between RES and EVs.

6.1 Future work

The results obtained in this project have also uncovered topics that give motivation for further research.

- The quantification of benefits and costs related to EV coordination for ancillary services and local grid support are not addressed. Such analysis can bring to light which of the different concepts are the most immediately applicable, considering the needs of the different European countries, as well as the needs of regions and areas.

- In relation to the provision of ancillary services using EVs, the ageing of the battery has not been addressed, due to a lack of realistic use scenarios of EVs for ancillary services.

- The provision of ancillary services using EV load coordination takes place in the LV grids. The impact on voltage profiles due coordinated EV charging has not been investigated. Fleet of EVs are equivalent to electric loads when charging and to PV units when discharging back to the grid, thus leading potentially to similar voltage magnitude variations caused by PV systems. The grid impact to accommodate bi-directional charging can be addressed, considering realistic charging power levels and grid layouts.

- With regard to communication technologies for EV coordination, the centralized aggregation of EVs for providing a service in the amount of several MW requires thousands of vehicles and a stable low-latency communication with all of them. This has not been tested yet and unlikely will be tested in the coming 5 years, due to low density of EVs. The use of real-time simulators (e.g. RTDS, real time digital simulator) where communication links can be emulated together

with EVs could help addressing the quality of service for coordinating large fleets of EVs.

- For the evaluation of the communication latency involved in centralized EV coordination by a VPP, field tests can be implemented in LV feeders with several EV stations accommodating EV charging. Situations of simultaneous charging or discharging of EVs can lead to issues like voltage unbalance and overloading of grid components. These issues can be further explored with the implementation of field tests.

- For the provision of local grid support using EV load, the combination of active power solutions using the load of EV charging stations with other options such as reactive power options from PV inverters, electric space heating, electric boilers have not been addressed. Furthermore, voltage support using EV load coordination, in cooperation with tap-changer transformer strategies can be addressed. The stochastic behaviour of EV charging can be addressed in relation to the use of EV load for voltage support.

REFERENCES

[1] European Commission, “20 20 by 2020 Europe's climate change opportunity”, COM (2008) 30 final, Brussels, 2008.

[2] T. H. Ortmeyer, and P. Pillay, “Trends in Transportation Sector Technology Energy Use and Greenhouse Gas Emissions”, *Proceedings of the IEEE*, vol. 89, no. 12, pp. 1837-1847, Dec. 2001.

[3] L. D. D. Harwey, “Global climate-oriented transportation scenarios”, *Energy Policy*, vol. 54, pp. 87-103, 2013.

[4] D. B. Richardson, “Electric Vehicles and the electric grid: A review of modeling approaches, impacts and renewable energy integration”, *Renewable and Sustain. Ener. Reviews*, Elsevier, vol. 19, pp. 247-254, Dec. 2012.

[5] International Energy Agency, IEA, “Hybrid and Electric Vehicles – The Electric Drive Captures the Imagination”, Annual Report 2011, Mar. 2012, [Online]. Available: www.ieahev.org.

[6] P. Crist, “Electric Vehicles Revisited: Costs, Subsidies and Prospects”, Discussion Paper No. 2012-O3, International Transport Forum, Paris, Apr. 2012. [Online]. Available: http://www.bec.mise.gov.it/site/bec/home/contributi/approfondimenti.html.

[7] J. A. Jackle, and K. A. Sculle, “The Gas Station in America”, the Johns Hopkins University Press, 1994.

[8] S. Carley, J. Graham, R. M. Krause, B. W. Lane, “Intent to purchase a plug-in electric vehicle: a survey of early impressions in large US cities”, *Transportation Research Part D: Transport and Environment*, vol. 18, pp. 39-45, Sep. 2012.

[9] A. Boulanger, “Vehicle Electrification: Status and Issues”, *Proc. of the IEEE*, vol. 99, no. 6, pp. 1116-1138, Jun. 2011.

[10] Commission of the European Communities, “Regulation (EEC) No 4064/89 Merger Procedure”, Mar. 1999. [Online]. Available: www.ec.europa.eu.

[11] U.S. Energy Information Administration, “Electric power monthly”, Feb. 2013. [Online]. Available: www.eia.gov/electricity/monthly.

[12] Europe’s Energy Portal, Mar. 2013. [Online]. Available: www.energy.eu.

[13] J. A. P. Lopes, F. J. Soares, P. M. R. Almeida, “Integration of Electric Vehicles in the Electric Power System”, *Proc. of the IEEE*, vol. 99, no. 1, pp. 168-183, Jan. 2011.

[14] Global Wind Energy Council, “Global Wind Report”, 2011. [Online]. Available: http://gwec.net/wp-content/uploads/2012/06/Annual_report_2011_lowres.pdf.

[15] Energinet.dk, “Wind power production in Denmark”, [Online]. Available: www.energinet.dk.

[16] P. Pinson, H. Madsen, "Adaptive modelling and forecasting of offshore wind power fluctuations with Markov-switching autoregressive models", *J. of Forecasting*, vol. 31, no. 4, pp. 281-313, Jul. 2012.

[17] Energinet.dk, 2010. [Online]. Available: www.energinet.dk.

[18] Energinet.dk, "Energinet.dk's ancillary services strategy", Aug. 2011. [Online]. Available: www.energinet.dk.

[19] Energinet.dk, "Annual Report 2011", [Online]. Available: www.energinet.dk, 2011.

[20] D. Connolly, H. Lund, B. V. Mathiasen, E. Pican, M. Leahy, "The technical and economic implications of integrating fluctuating renewable energy using energy storage", *Renewable Energy*, vol. 43, pp. 47-60, Nov. 2011.

[21] A. J. Roscoe, G. Ault, "Supporting high penetration of renewable generation via implementation of real-time electricity pricing and demand response", *Renewable Power Generation, IET*, vol. 4, no. 4, pp. 369-382, Jul. 2010.

[22] European Photovoltaic Industry Association EPIA, Global Market Outlook for Photovoltaics until 2015, 2011.
[Online]. Available: http://www.heliosenergy.es/archivos/eng/articulos/art-2.pdf.

[23] T. Stetz, F. Marten, and M. Braun, "Improved Low Voltage Grid-Integration of Photovoltaic Systems in Germany", *IEEE Trans. on Sustain. Energy*, vol. PP, no. 99, Jun. 2012.

[24] International Energy Agency, "Overcoming PV grid issues in urban areas", IEA PVPS Task 10, Activity 3.3, 2009. [Online].
Available: http://www.iea-pvps-task10.org/IMG/pdf/rep10_06.pdf.

[25] M. H. J. Bollen "Understanding Power Quality Problems: Voltage Sags and Interruptions" Chapter 1: Overview of Power Quality and Power Quality Standards, *Wiley-IEEE Press*, 2000.

[26] P. Pinson, L. E. A. Christensen, H. Madsen, P. E. Sørensen, M. H. Donovan, L. E. Jensen, "Regime-switching modelling of the fluctuations of offshore wind generation", *J. of Wind Eng. and Industr. Aerodynamics*, vol. 96, no 12, pp. 2327-2347, Dec. 2008.

[27] R. A. Jabr, B. C. Pal, "Intermittent wind generation in optimal power flow dispatching", *J. of Generation, Transmission and Distribution, IET*, vol. 3, no. 1, pp. 66-74, Jan. 2009.

[28] M. H. J. Bollen, J. Zhong, F. Zavoda, J. Meyer, A. Mc Eachern, and F. Corcoles Lopez, "Power Quality aspects of Smart Grids", *Proc. of Int. Conf. on Renewable Energy and Power Quality (ICREPQ 2010)*, Mar. 2010.

[29] W. Kempton, S. E. Letendre, "Electric vehicles as a new power source for electric utilities", *Transportation Research Part D*, vol. 2, no. 3, pp. 157-175, 1997.

[30] K. Clement-Nyns, E. Haesen, J. Driesen, "The impact of Charging Plug-in Hybrid Electric Vehicles on a Residential Distribution Grid", *IEEE Trans. Pow. Syst.*, vol. 25, no. 1, pp. 371-380, Feb. 2010.

[31] W. Kempton, J. Tomic "Vehicle-to-grid power implementation: from stabilizing the grid to supporting large-scale renewable energy", *J. of Power Sources*, vol. 144, no. 1, pp. 280-294, Apr. 2005.

[32] W. Kempton, V. Udo, K. Huber, K. Komara, S. Letendre, S. D. Brunner, N. Pearre, "A test of vehicle-to-grid (V2G) for energy storage and frequency regulation in the PJM system", Technical Report, MAGIC Consortium, Jan., 2009.
Available at: http://www.magicconsortium.org/_Media/test-v2g-in-pjm-jan09.pdf.

[33] J. R. Pillai and B. Bak-Jensen, “Integration of Vehicle-to-grid in the Western Danish Power System”, *IEEE Trans. on Sustainable Energy*, vol. 2, no. 1, pp. 12-19, Jan. 2011.

[34] M. D. Galus, S. Koch, G. Andersson, “Provision of Load Frequency Control by PHEVs, Controllable Loads, and a Cogeneration Unit”, *IEEE Trans. on Ind. Electr*., vol. 58, no. 10, pp. 4568-4582, Oct. 2011.

[35] C. Hay, M. Togeby, N. C. Bang, C. Søndergren, L. H. Hansen, “Introducing electric vehicles into the current electricity markets”, Project Report, EDISON Deliverable D2.3, May 2010.

[36] J. A. P. Lopes, P. M. R. Almeida, and F. J. Soares, “Using Vehicle-to-Grid to Maximize the Integration of Intermittent Renewable Energy Resources in Islanded Electric Grids”, in *Proc. of Internat. Conf. on Clean Electrical Power*, Jun. 2009.

[37] J. A. P. Lopes, S. A. Polenz, C. L. Moreira, R. Cherkaoui, “Identification of control and management strategies for LV unbalanced microgrids with plugged-in electric vehicles”, *J. of Electric Pow. Syst. Research*, vol. 80, no. 1, pp. 898-906, Jan. 2010.

[38] R. J. Bessa, M. A. Matos, “Economic and technical management of an aggregation agent for electric vehicles: a literature survey”, *European Trans. Electr. Power*, vol. 22 pp. 334-350, Feb. 2011.

[39] D. Birnie, “Solar-to-vehicle (S2V) systems for powering commuters of the future”, *J. of Power Sources*, vol. 186, no. 2, pp.539-542, Jan. 2009.

[40] M. H. J. Bollen, F. Hassan, “Integration of Distributed Generation in the Power System”, Chapter 5: Voltage Magnitude Variations, First Edition, John Wiley & Sons Inc., 2011.

[41] K. Corfee, D. Korinek, W. Cassel, C. Hewicker, J. Zillmer, M. Pereira Morgado, H. Ziegler, N. Tong, D. Hawkins, and J. Cernadas, “Distributed generation in Europe – Physical infrastructure and Distributed Generation Connection, Memo, no. 1, 2011, online.

[42] N. Etherden, and M. H. J. Bollen, “Increasing the Hosting capacity of Distribution Networks by Curtailment of Renewable Energy Sources”, in *Proc. of IEEE Power Tech*., Trondheim, 2011.

[43] P. Carvalho, P. Correia, and L. Ferreira, “Distributed Reactive Power Generation Control for Voltage Rise Mitigation in Distribution Networks”, *IEEE Trans. Power Syst.*, vol. 23, no. 2, pp. 766-772, 2008.

[44] R. Tonkoski, L. A. C. Lopes, and T. El-Fowly, “Coordinated Active Power Curtailment of Grid Connected PV Inverters for Overvoltage Prevention”, *IEEE Trans. on Sust. Energy*, vol. 2, no. 2, pp. 139-147, 2011.

[45] T. Fawzy, D. Premm, B. Bletterie, and A. Gorsek, “Active contribution of PV inverters to voltage control – from a smart grid vision to full-scale implementation”, *J. of Elektrotechnik & Informationstechnik*, vol. 128, no. 4, pp.110-115, 2011.

[46] E. Demirok, P. Casado Gonzalez, K. H. B. Frederiksen, D. Sera, P. Rodriguez, and R. Teodorescu, “Local Reactive Power Control Methods for Overvoltage Prevention of Distributed Solar Inverters in Low-Voltage Grids”, *IEEE J. of Photov.*, vol. 1, no. 2, pp. 174-182, 2011.

[47] B. Blazic, I. Papic, B. Uljanic, B. Blatterie, C. Dierckxsens, K. De Brabandere, W. Deprez, T. Fawzy, “Integration of Photovoltaic Systems with Voltage Control Capabilities into LV Networks”, in *Proc. of 1st Int. Workshop on Integ. of Solar Power into Power Syst*., 2011.

[48] X. Liu, A. Aichhorn, L. Liu, H. Li, Coordinated Control of Distributed Energy Storage System with Tap Changer Transformers for Voltage Rise Mitigation under High Photovoltaic Penetration, *IEEE Trans. on Smart Grid*, vol. 3, no. 2, pp. 897-906, Jun. 2012.

[49] W. Kempton, J. Tomic, S. E. Letendre, A. Brooks, T. Lipman, "Vehicle to grid power: battery, hybrid, and fuel cell vehicles as resources for distributed electric power in California", Working Paper Series ECD-ITS-RR-01-03, Jun. 2001. [Online]. Available: http://escholarship.org/uc/item/5cc9g0jp.

[50] M. D. Galus, M. Zima, and G. Andersson, "On integration of plug-in hybrid electric vehicles into existing power system structures", *Energy Policy*, vol. 38, no. 11, pp. 6736–6745, Nov. 2010

[51] K. Fell, K. Huber, B. Zink, "Assessment of plug-in electric vehicle integration with ISO/RTO systems", Technical Report, Mar. 2010.
Available at: http://www.isorto.org/atf/cf/%7B5B4E85C6-7EAC-40A0-8DC3-003829518EBD%7D/IRC_Report_Assessment_of_Plugin_Electric_Vehicle_Integration_with_ISORTO_Systems_03232010.pdf.

[52] A. Brooks, T. Gage, "Integration of electric drive vehicles with the electric power grid - a new value stream", *18th Internat. Electric Vehicle Symposium and Exhibition*, Oct. 2001.

[53] R. J. Bessa, M. A. Matos, F. J. Soares, J. A. O. Lopes, "Optimized Bidding of a EV Aggregation Agent in the Electricity Market", *IEEE Trans. on Smart Grid*, vol. 3, no. 1, pp. 443-452, Mar. 2012.

[54] J. A. P. Lopes, F. J. Soares, P. M. R. Almeida. "Integration of electric vehicles in the electric power system", *Proceed. of the IEEE*, vol. 99, no. 1, pp. 168-183, Jan. 2011.

[55] M. D. Galus, G. Andersson. "Demand management of grid connected plug-in hybrid electric vehicles", in proc. of *IEEE Energy2030 Conf.*, Nov. 2008.

[56] D. Gantenbein, B. Jansen, D. Dykeman, P. B. Andersen, E. B. Hauksson, F. Marra, A. B. Pedersen, C. A. Andersen, J. Dall, "Distributed Integration Technology Development", Project Report, EDISON Deliverable D3.1, Apr. 2011, http://www.edison-net.dk/.

[57] R. Faria, P. Moura, J. Delgado, A. T. de Almeida, "A sustainability assessment of electric vehicles as a personal mobility system", *J. of Energy Conversion and Management*, vol. 61, pp. 19-30, 2012.

[58] L. Christensen, "Electric vehicles and the customers", Project Report, EDISON Deliverable D1.3, Nov. 2011, http://www.edison-net.dk/.

[59] D. Dallinger, D. Krampe, and M. Wietschel, "Vehicle-to-Grid Regulation Reserves Based on a Dynamic Simulation of Mobility Behavior", in IEEE Trans. on Smart Grid, vol. 2, no. 2, pp. 302-313, Jun. 2011.

[60] C. Weiller, "Plug-in Hybrid Electric Vehicle Impacts on Hourly Electricity Demand in the United States", J. of Energy Policy, vol. 39, pp. 3766-3778, Apr. 2011.

[61] K. Chen, A. Bouscayrol, A. Berthon, P. Delarue, D. Hissel, and R. Trigui, "Global modeling of different vehicles", *IEEE Vehicular Technology Magazine*, vol. 4, no. 2, pp. 80-89, Jun. 2009.

[62] F. Nemry, G. Leduc, and A. Muñoz, "Plug-in Hybryd and Battery-Electric Vehicles: State of the research and development and comparative analysis of energy and cost efficiency", JRC Technical Notes, European Commission, 2009.

[63] Standard IEC 61851-1.

[64] W. Mitchell, C. Bird-Borroni, L. Burns, "Reinventing the Automobile: Personal Urban Mobility for the 21st Century", MIT Press, 2010.

[65] T. B. Gage, "Development and Evaluation of a Plug-in HEV with Vehicle-to-Grid Power Flow", Final Report, 2003.

[66] W. Kempton, A. Dhanju, "Electric vehicles with V2G: storage for large-scale wind power", Windtech International, vol. 1, no. 2, Mar. 2006.

[67] A. Brooks, S. H. Thesen, "PG&E and Tesla Motors: vehicle to grid demonstration and evaluation program". 23rd Internat. Battery, Hybrid and Fuel Cell Electric Vehicle Symposium & Exhibition (EVS23), Dec. 2007.

[68] C. Quinn, D. Zimmerle, T. H. Bradley. "The effect of communication architecture on the availability, reliability, and economics of plug-in hybrid electric vehicle-to-grid ancillary services". *J. of Power Sources*, vol. 195, no. 5, pp. 1500-1509, Mar. 2010.

[69] Frost&Sullivan, "Global Electric Vehicles Lithium-ion Battery Second Life and Recycling Market Analysis", report M5B6-18, Nov. 2010.

[70] N. A. Chaturvedi, R. Klein, J. Christensen, J. Ahmed and A. Kojic, "Algorithms for Advanced Battery Management Systems", *IEEE Control Systems*, vol. 30, no. 2, pp. 49-68, Jun. 2010.

[71] J. Axsen, A. Burke, K. Kurani, "Batteries for Plug-in Hybrid Electric Vehicles (PHEVs): Goals and the State of Technology circa 2008", UCD-ITS-RR-08-14, May 2008. [Online]. Available: www.pubs.its.ucdavis.edu/download_pdf.

[72] M. A. Roscher, J. Assfalg, O. S. Bohlen, "Detection of Utilizable Capacity Deterioration in Battery Systems", *IEEE Trans. on Vehic. Tech.*, vol. 60, no. 1, pp. 98-103, Jan. 2011.

[73] D. V. Do, C. Forgez, L. El Kadri, Benkara, G. Friedrick, "Impedance Observer for a Li-Ion Battery Using Kalman Filter", *IEEE Trans. on Vehic. Tech.*, vol. 58, no. 8, pp. 3930-3937, Oct. 2009.

[74] A. Zenati, P. Desprez, H. Razik, S. Rael, "Impedance measurements combined with fuzzy logic methodology to assess the SOC and SOH of lithium-ion cells", *Proc. of IEEE Vehicle Power and Propulsion Conference (VPPC)*, Sept. 2010.

[75] W. Xuezhe, Z. Bing and X. Wei, "Internal Resistance Identification in Vehicle Power Lithium-ion Battery and Application in Lifetime Evaluation", *Proc. of International Conference on Measuring Technology and Mechatronics Automation*, pp. 388-392, Apr. 2009.

[76] T. Guena and P. Leblanc, "How Depth of Discharge Affects the Cycle Life of Lithium-Metal-Polymer Batteries", *Proc. of 28th Annual International Telecommunication Energy Conference, INTELEC*, Sept. 2006.

[77] D. Haifeng, W. Xuezhe and S. Zechang, "A New SOH Prediction Concept for the Power Lithium-ion Battery Used on HEVs", *Proc. of IEEE Vehicle Power and Propulsion Conference, VPPC*, pp. 1649-1653, Sept. 2009.

[78] A. F. Burke, "Batteries and Ultracapacitors for Electric, Hybrid, and Fuel Cell Vehicles", *Proc. of the IEEE*, vol. 95, no. 4, pp. 806-820, Apr. 2007.

[79] Z. Ma, D. S. Callaway, I. A. Hiksens, "Decentralized Charging Control of Large Populations of Plug-in Electric Vehicles", *IEEE Trans. on Control Syst. Techn.*, vol. 21, no. 1, pp. 67-78, Jan. 2013.

[80] S. You, "Generic Virtual Power Plant for Micro Combined Heat and Power Units", Ph.D. thesis, 2011.

[81] A. Timbus, M. Larsson, and C. Yuen, "Active Management of Distributed Energy Resources Using Standardized Communications and Modern Information Technologies", *IEEE Trans. on Ind. Electr.*, vol. 56, no. 10, pp. 4029-4037, Oct. 2009.

[82] A. van der Welle, C. Kolokathis, J. Jansen, C. Madina, A. Diaz, FENIX, "Financial and socio-economic impacts of embracing the FENIX concept", Final Report, FENIX Deliverable D3.3, Jan. 2010. [Online]. Available: www.fenix-project.com.

[83] P. B. Andersen, C. Træholt, F. Marra, B. Poulsen, C. Binding, D. Gantenbein, B, Jansen, O. Sundtroem, "Electric Vehicle Fleet Integration in the Danish EDISON Project", in proc. of *IEEE Power and Energy Soc. Gen. Meet.*, Jul. 2010.

[84] D. P. Tuttle and R. Baldick, "The Evolution of Plug-In Electric Vehicle-Grid Interactions", *IEEE Trans. on Smart Grid*, vol. 3, no. 1, pp. 500-505, Mar. 2012.

[85] A. N. Brooks, "Vehicle-to-grid demonstration project: Grid regulation ancillary service with a battery electric vehicle", Project, Report, pp. 1–12, prepared for the California Air Resources Board, 2002.

[86] M. Yilmaz, P. Krein, "Review of the Impact of Vehicle-to-Grid Technologies on Distribution Systems and Utility Interfaces", *IEEE Trans. on Pow. Electron.*, vol. PP, no. 99, Nov. 2012.

[87] Ultralife, "Li-ion vs. Lead Acid", [Online]. Available: www.ultralifecorporation.com. Mar. 2012.

[88] D. Wu, D. C. Aliprantis, K. Gkritza, "Electric Energy and Power Consumption by Light-Duty Plug-In Electric Vehicles", *IEEE Trans. on Power Syst.*, vol. 26, no. 2, pp. 738-746, May 2011.

[89] K. Cheng., B. P. Divakar, H. Wu, K. Ding, H. F. Ho, "Battery-Management System (BMS) and SOC Development for Electrrical Vehicles", *IEEE Trans. Vehic. Techn.*, vol. 60, no. 1, pp. 76-88, Jan. 2011.

[90] J. D. Dogger, B. Roossien, and F. Nieuwenhout, "Characterization of Li-Ion Batteries for Intelligent Management of Distributed Grid-Connected Storage", *IEEE Trans. on Energy Conversion*, vol. 26, no. 1, 2011.

[91] K. Samarakoon, J. Ekanayake, N. Jenkins, "Investigation of Domestic Load Control to Provide Primary Frequency Response Using Smart Meters", *IEEE Trans. on Smart Grid*, vol. 3, no. 1, pp. 282-292, Mar. 2012.

[92] Acuvim II Series, User Manual, Feb. 2012, online: www.accuenergy.com/download/.

[93] Nissan Motor Co., LTD, "EV / HEV Safety", [Online]. Available: www.nhtsa.gov.

[94] General Motors, "Chevrolet Volt, Quick Reference Sheet", [Online]. Available: www.evsafetytraining.org.

[95] Mitsubishi, "Traction Battery", [Online]. Available:http://www.mitsubishi-cars.co.uk/imiev/technology.aspx.

[96] G. C. Tarnowski, "Coordinated Frequency Control of Wind Turbines in Power Systems with High Wind Power Penetration", Ph.D. thesis, [Online]. Available:http://www.cee.dtu.dk/upload/centre/cet/projekter/11-15/gctarnowski_thesis.pdf.

[97] Danish Energy Agency, "Energy Statistics 2011", Dec. 2012. [Online]. Available: www.ens.dk.

[98] Energinet.dk, "Ancillary Services to be delivered in Denmark Tender conditions", Oct. 2012, www.energinet.dk.

[99] ENTSO-E, "10-Year Network Development Plan 2012", Jul. 2012.

[100] IEC 61850, Communication networks and systems for power utility automation, 2009.

[101] A. B. Pedersen, E. Bragi Hauksson, P. Bach Andersen, B. Poulsen, C. Træholt, and D. Gantenbein "Facilitating a generic communication interface to distributed energy resources", *Proc. of First IEEE Int. Conf. on Smart Grid Comm.*, 2010.

[102] Energinet.dk, "Load Frequency Control - Secondary Reserve data", January, 2009.

[103] Microsoft, "What is Network Quos?", Sep. 1999. [Online]. Available: www.technet.microsoft.com/en-us/library/bb742481.

[104] O. Tremblay and L. Dessaint, "Experimental Validation of a Battery Dynamic Model for EV Applications", World Electric Vehicle Journal, Vol. 3, AVERE, 2009.

[105] O. Tremblay, L.A. Dessaint, A. Dekkiche, "A Generic Battery Model for the Dynamic Simulation of Hybrid Electric Vehicles", *Proc. of IEEE Vehicle Power and Propulsion Conf.*, 2007.

[106] Standard EN 50160.

[107] M. H. J. Bollen, F. Hassan, "Integration of Distributed Generation in the Power System", Chapter 5, Voltage Magnitude Variations, J. Wiley & Sons, 2011.

[108] I. Safak Bayram, G. Michailidisy, M. Devetsikiotis, S. Bhattacharya, A. Chakrabortty, F. Granelli, "Local Energy Storage Sizing in Plug-in Hybrid Electric Vehicle Charging Stations Under Blocking Probability Constraints", in *Proc. of IEEE Smart Grid Comm*, pp. 78-83, 2011.

[109] S. L. Kristensen, A. Foosnæs, P. Nørgård, O. Gehrke, A. Schmitt, "Concept study on fast charging station design", Project Edison - WP4.5 report, online.

[110] P. Lombardi, M. Heuer, and Z. Styczynski, "Battery Switch Station as storage system in an autonomous power system: optimization issue", in *Proc. of IEEE Power and Energy Soc. General Meeting*, 2010.

[111] I. S. Bayram, G. Michailidis, M. Devetsikiotis, S. Bhattacharya, A. Chakrabortty, F. Granelli, "Local energy storage sizing in plug-in hybrid electric vehicle charging stations under blocking probability constraints", in *Proc. of IEEE Smart Grid Comm.*, pp. 78-83, 2011.

[112] F. Marra, "Central Station Design Options", EDISON WP4 Deliverable D4.1, http://www.edison-net.dk/.

[113] F. Marra, C. Træholt and E. Larsen, "Planning Future Electric Vehicle Central Charging Stations Connected to Low-Voltage Distribution Networks", in *Proc. of 3rd IEEE Int. Symp. on Pow. Electr. for Distr. Gen. Syst.*, pp. 636-641, Jun. 2012.

[114] Standard IEC 62196.

[115] R. Aghatehrani, R. Kavasseri, "Reactive Power Management of a DFIG Wind System in Microgrids Based on Voltage Sensitivity Analysis", *IEEE Trans. on Sust. Energy*, vol. 2, no. 4, pp. 451-458, Oct. 2011.

[116] Y. Du, J. Burnett, "Experimental Investigation into Harmonic Impedance of Low-Voltage Cables", in *IEE Proc. of Gen. Transm. and Distrib*., vol. 147, no. 6, pp. 322-328, 2000.

[117] P. C. Paive, H. M. Khodr, J. A. Dominiguez-Navarro, J. M. Musta, and A. J. Urdaneta, "Integral Planning of Primary-Secondary Distribution Systems Using Mixed Integer Linear Programming", *IEEE Trans. on Pow. Syst*., vol. 20, no. 2, pp. 1134-1243, May 2005.

APPENDIX

A
EV TEST BED

The EV test bed used for the various demonstrations and proof of concepts, during the Ph.D. project, is depicted below:

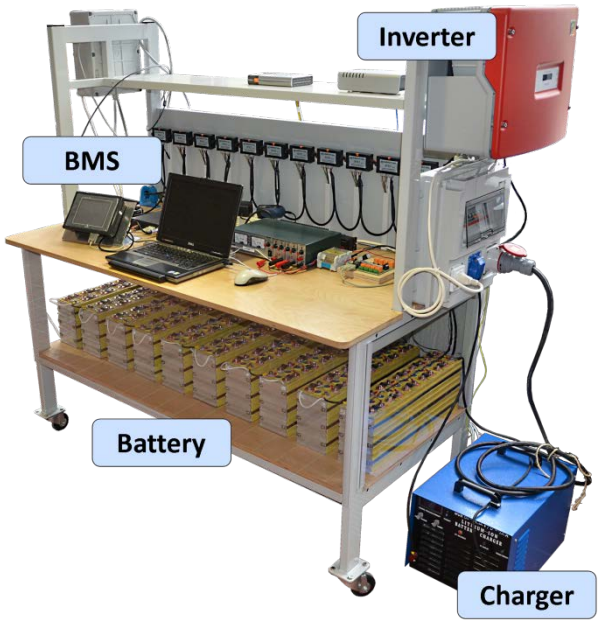

Figure A-**1:** EV test bed

Table A-**1:** EV test bed components and features

BATTERY PACK	Li-ion battery type Voltage: 363 V Battery capacity: 40 Ah Battery energy: 14.5 kWh
CHARGER unit	0 – 5.5 kW
V2G unit	0 – 3.8 kW
BMS	Voltage, current and temperature acquisition

B
LITHIUM BATTERY CELL

The electrical features of the battery cell type TS-LFP40AHA are indicated in this appendix. This battery cell depicted is used in the EV test bed battery pack.

Figure B-1: Battery cell, model TS-LFP40AHA

Table B-**2:** Li-ion battery cell specifications

Parameter	Value
Nominal voltage	3.3 V
Nominal capacity	40 Ah
Maximum charge voltage	4.25 V
Minimum discharge voltage	2.5 V
Charging current (recommended)	0.5 C
Max charging/discharging current	3 C
Internal impedance	10 mΩ

C
BATTERY MANAGEMENT SYSTEM

The BMS architecture of the EV test bed is depicted below. A series of 11 voltage acquisition modules acquires the voltage of the single cells. A hall current sensor measures the total DC current. The Main Controller aggregates and elaborates the data.

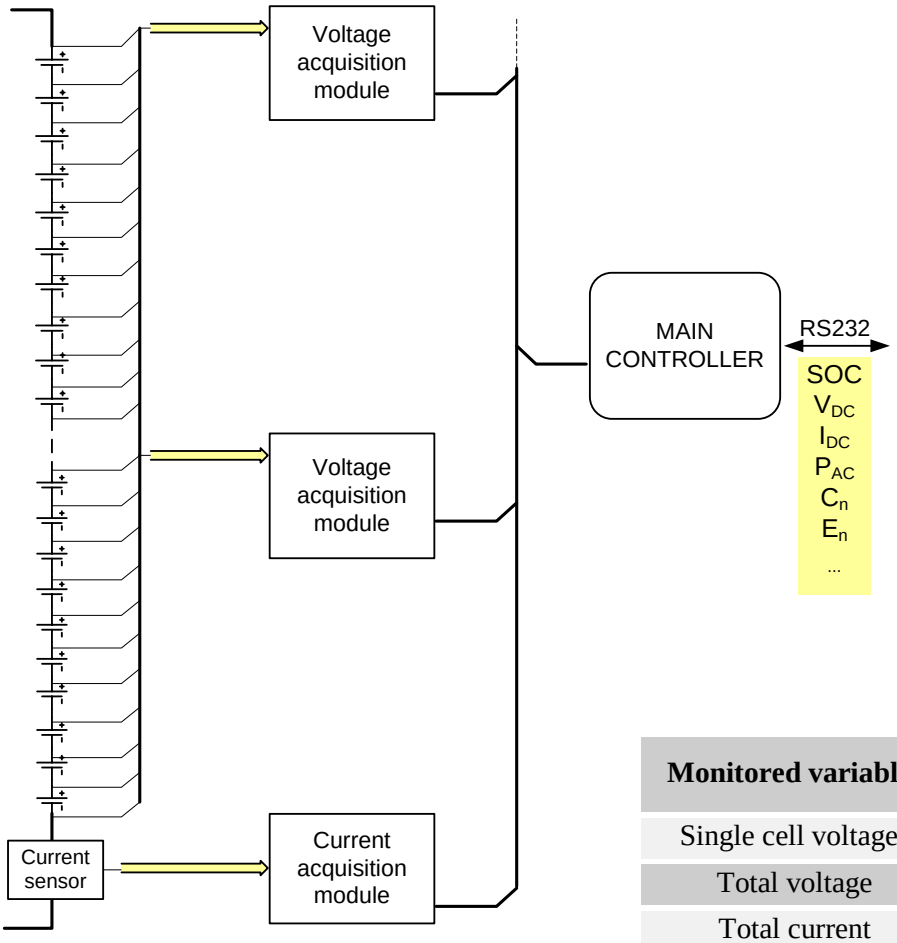

Figure C-1: Battery Management System architecture

Monitored variables	Unit
Single cell voltages	V
Total voltage	V
Total current	A
Single cells temperature	ºC
SOC (%)	-
Remaining energy	kWh
Power	kW

D
GAIA WIND TURBINE – RISØ DTU

The wind turbine profile used in Chapter 5 belongs to the GAIA Wind Turbine, located at Risø DTU, Roskilde, Denmark. The wind turbine and its power curve are depicted below:

Figure D-**2:** GAIA wind turbine

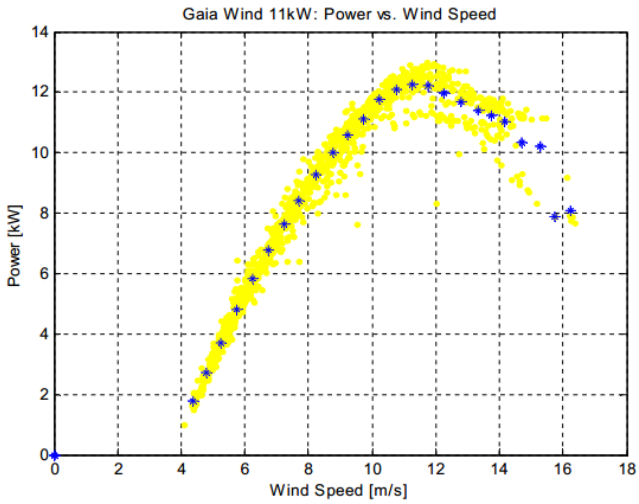

Figure D-**1:** Wind turbine power curve

Table D-**3:** Wind turbine specifications

Feature	Value
Rated power	11 kW
Hub height	18.2 m
Rotor diameter	13 m
Rotor speed	56 rpm
Nacelle weight	900 kg
Total weight	2400 kg
Grid connection	3-phase, 400VAC

ATTACHED PAPERS

EV Charging Facilities and Their Application in LV Feeders with Photovoltaics

F. Marra, G. Y. Yang, C. Træholt, E. Larsen, J. Østergaard, B. Blažič and W. Deprez

***Abstract*— Low-voltage (LV) grids with high penetration of photovoltaics (PVs) are often affected by voltage rise problems. Reactive power methods for voltage support have been thoroughly investigated, presenting several practical limitations. The energy storage systems (ESSs) of prospective public electric vehicle (EV) stations are considered to be a viable alternative to this problem. This paper proposes a method for the identification of the feeder location that leads to minimum ESS size for providing voltage regulation. The ultimate goal is to validate the method results via dynamic simulations and to quantify the power and energy for the ESS, operating virtually at different locations in the feeder. A real Belgian LV grid with measurement-based generation-load profiles is used as case study. The results show the effectiveness of using public EV charging facilities with ESS for providing the additional function of voltage regulation.**

***Index Terms*— Electric vehicle station, energy storage, low voltage grids, voltage regulation, voltage support**

I. Introduction

THE necessity of meeting the environmental targets [1] and the advances of technology on renewable energies are leading to a growing share of photovoltaic (PV) installations in European LV distribution grids [2].

High penetration of PV presents concerns to voltage quality in LV feeders [3]-[4]. Situations of high generation and low load conditions may lead to an inversion of power flow, with consequent voltage rise events [5]. This is an urgent problem to be solved in order to increase the penetration levels.

Utilities in different European countries are currently revising the planning rules to accommodate increased distributed generation and still securing voltage quality [6]. As described in [7]-[8], some of the technical options include:

- Upgrade of the network circuit thermal capacity
- Upgrade of the upstream transformer capacity
- Rerouting the power path to reduce circuit length
- Construction of new substations
- Changes to the network topology
- Installation of supplemental reactive power compensation.

All these options are classified as grid reinforcement. Lately, also automatic active power curtailment is being considered as an option available to the distribution system operators (DSOs), in the case that voltage variations due to intermittent generation exceed the allowed limits [9]-[10].

Reactive power methods for LV grids have been also extensively investigated [11]-[18]. The effectiveness of reactive power compensation for voltage rise mitigation has been demonstrated with field test, however, some of the limitations are due to the fact that most of the PV units already installed in LV grids operate with unity power factor; in addition, the high R/X ratio of LV cables poses a limit to a massive reactive power consumption from PV units, due to consequential increasing grid's losses [11], [18].

This paper proposes the use of energy storage systems (ESS) available at public EV charging facilities, for providing voltage regulation as an additional function. A stationary ESS within a public EV charging station is generally required for securing power quality during charge's switching events [19]-[23]. The same ESS can then be used to store renewable energy during periods of high generation and low load, and redispatch it during evening or overnight. If this process can be intelligently controlled, the station can provide a valuable service in LV feeders with PV, thus avoiding the need of grid reinforcement or active power curtailment.

This paper sets forth a method for the identification of optimal locations for an ESS operation in feeders with high penetration of PV. The storage power and energy required for the ESS are investigated with dynamic simulations using a Belgian LV residential grid as a case study and real generation-load profiles.

II. System Modeling

A. Feeder Model

Distribution feeders are commonly operated in a radial fashion. When PV generators are connected at a bus in the feeder, the voltage profile at the point of common coupling (PCC) is likely to increase according to the following expression:

F. Marra, G. Y. Yang, C. Træholt, E. Larsen and J. Østergaard are with the Electrical Engineering Department, Technical University of Denmark (DTU), Kgs. Lyngby DK-2800, Denmark (e-mail: {fm, gyy, ctr, ela,joe}@elektro.dtu.dk).

B. Blažič is with the Electrical Engineering Department, University of University of Ljubljana, Slovenia. Ljubljana, Slovenia (e-mail: Bostjan.Blazic@fe.uni-lj).

W. Deprez is with Infrax, Hasselt BE-3500, Belgium (e-mail: wim.deprez@infrax.be).

$$\vec{U}_{PCC} \approx U_G + \frac{R \cdot P + X \cdot Q}{U_G} + j\frac{X \cdot P - R \cdot Q}{U_G} \quad (1)$$

$$P = P_{PV} - P_L \quad (2) \qquad Q = Q_{PV} - Q_L \quad (3)$$

where

- P is the nodal active power exchanged;
- Q is the nodal reactive power exchanged;
- U_g is the substation voltage magnitude, assuming that the phase angle is zero;
- P_{PV}, Q_{PV} are the active and reactive power of the DG unit;
- P_L, Q_L are the active and reactive power of a generic load;
- R, X are the equivalent resistance and reactance of the cable;

Reactive power methods can be used to mitigate voltage rise issues. However, a limitation of reactive power methods is that in most of LV residential grids, the majority of already installed PV inverters work with unity power factor, thus they are not capable of reactive power (Q) control. In addition, due to the predominantly resistive nature of LV cables, to make the Q strategies effective in radial feeders, almost all PV generators shall contribute under the same Q scheme, leading in this case, to increased Q consumption and losses [11], [18].

B. Active Power Control from Public EV Stations

The approach used to cope with voltage regulation relies on active power control using a battery-ESS within a public EV charging station, Fig. 1. An EV public station equipped with ESS, e.g. a battery switch station or a parallel charging station, can provide the storage component needed for voltage regulation, based on the following expression:

$$P = P_{PV} - P_S - P_L \quad (4)$$

where P_S is the storage power required to keep the bus voltages in the feeder within the limits.

In the Danish EDISON project [24], two main architectures of public station were defined, namely the AC-busbar and DC-busbar station, Fig. (a) and (b) respectively, both equipping an ESS that can provide active power support. Together with the ESS, the load profile due to EV charging can play an important role in terms of energy storage. The driving behavior of normal drivers during weekdays was analyzed in [25]. The time interval between 10:00 AM and 15:00 PM shows a lower driving activity. This information could be linked to the analysis in [26], where the daily vehicle load profiles were estimated for different charging scenarios, based on the large American household travel survey (US DOT 2003). In particular, for the public charging scenario, called commercial charging in [26], the EV load profile is mainly identified in the 8-hours time interval from 10:00 AM to 18:00 PM, with peaks of EV demand between 12:00 AM and 14:00 PM in weekend and weekdays, see Fig. 2. The identified interval corresponds also to the hours of maximum PV generation. Due to the uncertainty of the EV charging behavior, the EV demand alone may not be able to accomplish the task of voltage regulation in LV feeders however it has the potential to complement the ESS operation in pursuing such a task. In this paper, voltage regulation is achieved via the ESS control, while the stochastic EV charging behavior is neglected.

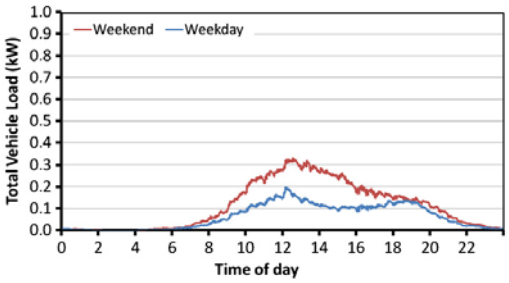

Fig. 2. Average EV load profiles for public charging [26].

C. Energy Storage System (ESS)

A wide range of technical solutions for ESS applications are described in [25]. Since most of the studies on EV charging facilities considered battery-ESS technology [19]-[23], the

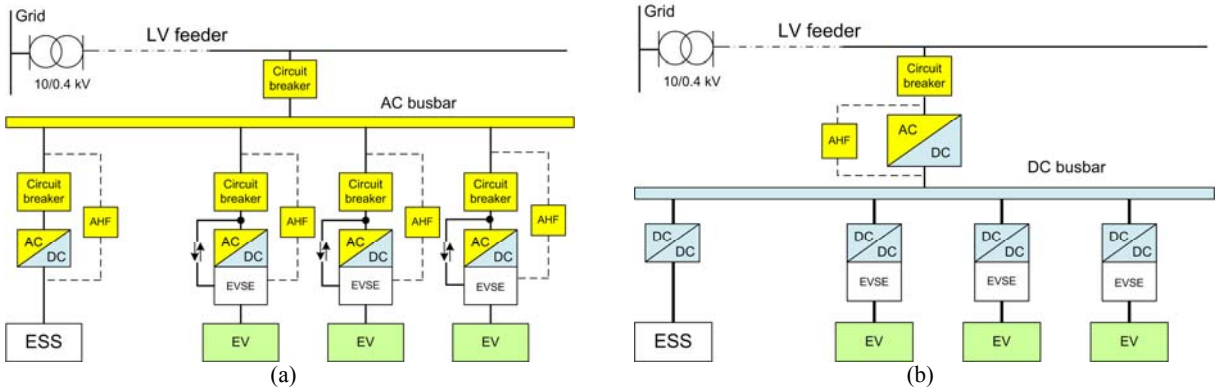

Fig. 1. EV (public) charging station architectures. (a) AC-distribution EV station. (b) DC-distribution EV station.

same ESS technology is assumed in this study. As the main goal is to provide voltage support in LV feeders, the performance comparison of different battery chemistries, such as energy-to-weight ratio, self-discharge rate and charge/discharge efficiency are considered out of the scope of this work. The ESS is modeled with the charge/discharge equations as expressed in (5) and (6) [28], where P_d is the discharging power and P_c is the charging power of the ESS battery, respectively; E is the energy stored in the battery at time t; Δt is the duration time of each interval. The two coefficients η_d and η_c are the discharge and charge efficiencies respectively.

$$E(t+\Delta t) = E(t) - \Delta t \cdot P_d / \eta_d \quad (5)$$

$$E(t+\Delta t) = E(t) + \Delta t \cdot P_c \cdot \eta_c \quad (6)$$

The operation of the battery system should also take into account power and energy constraints. The maximum power limits during charging/discharging can be described by (7) and (8) respectively:

$$0 \le P_d(t) \le P_d^{\max} \quad (7)$$

$$0 \le P_c(t) \le P_c^{\max} \quad (8)$$

The same power limits are important for sizing the power converter of the ESS. In this paper, we will refer to P_S to indicate the power flow in or out of the storage, including both phases of charge and discharge. The energy limits of an ESS system can be described as follows:

$$E_{\min} \le E(t) \le E_{\max} \quad (9)$$

where E_{min} and E_{max} are the minimum and maximum energy levels of the storage, defining the usable energy window. The energy limits, or state of charge limits (SOC), can be set according to the storage application and to the battery technology, however, in this paper, (9) is considered as the actual usable energy window of the ESS, regardless of the optimal energy management of a particular type of battery.

III. Problem Formulation

The optimization model for the identification of the optimal location for ESS operation L^* can be written as follows:

$$L^* = \min \sum P_{S,k} \quad (10)$$

$$\text{subject to} \quad \begin{matrix} u \le U_{\max} \\ 0 \le P_{S,k} \le P_{S,k}^{\max} \end{matrix} \quad (11)$$

where $P_{S,k}$ and $P_{S,k}^{\max}$ are the storage size and the maximum limit respectively, u is the column vector that contains all bus voltages in the feeder, U_{max} is the maximum voltage magnitude allowed. Objective function (10) minimizes the storage power needed for voltage support on bus k. Constraints (11) represent the operative constraint that bounds the voltage magnitude at all feeder's buses below the maximum allowed and the maximum storage size, respectively. Furthermore, the voltage constraint includes all network equations, which incorporate the characteristics of loads and PV generation.

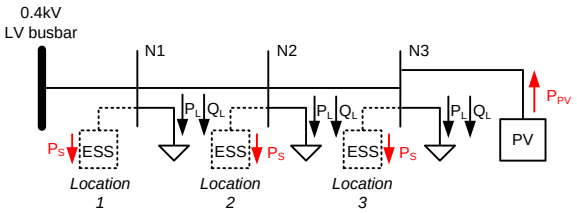

Fig. 3. Single-line diagram of a LV feeder with different ESS locations.

The problem is solved with a mixed integer linear programming approach (MILP). In order to obtain a MILP model that sufficiently approximates the problem of interest (10)-(11), both the objective function and all of the problem constraints should be expressed by linear relationships.

It is presumed that the installation status of the ESS in the feeder is configurable. The active, reactive power characteristics of all loads and PV units are assumed to be known.

A. Objective Function

According to (10), the optimization problem searches for the location with minimum storage size required in the whole feeder. Considering the example feeder of Fig. 3, the proposed method searches the location that minimizes the storage power required to keep the voltages at all buses within U_{max}. An EV station placed at a feeder's bus can provide the storage component P_S to lower the voltage rise.

B. Bus Voltage Constraints

The bus voltage constraints require the calculation of the voltage sensitivity coefficients for the LV grid feeder under study. Considering bus N as one of the feeder's buses, the expression for the bus voltage U_N is as follows:

$$U_N = U_g + \sum_{k=1}^{N} \frac{\partial U_N}{\partial P_k}(P_{PV,k} - P_{L,k} - P_{S,k}) \quad (12)$$

where

U_g is the base grid voltage (p.u.);

P_{PV} is the active power injected from PVs on bus k

P_{Sk} is the storage power on bus k to lower the voltage below U_{max}

$\partial U_N/\partial P_k$ is the voltage sensitivity coefficient (p.u./MW).

With (12), the overall formulation for the MILP problem is as follows:

Objective function: $L^* = \min \sum P_{S,k}$ (13)

$$\text{Constr. 1)} \quad \begin{cases} U_g + \sum_{k=1}^{N} \frac{\partial U_N}{\partial P_k}(P_{PV,k} - P_{L,k} - P_{S,k}) \le U_{\max} \end{cases} \quad (14)$$

$$\text{Constr. 2)} \quad \begin{cases} 0 \le P_{S,k} \le \delta_k P_{S,k}^{\max}, \\ with \quad \delta \in \{0,1\}, \ \text{integer variable} \end{cases} \quad (15)$$

where

δ_k is the integer variable which defines the installation status of storage at bus k;

U_g is the voltage magnitude at the substation busbar;

U_{max} is the maximum allowed voltage at bus k which is the same for all buses, therefore simply indicated with U_{max}.

With a number of N buses in a feeder, by considering the two possible states of, with or without an EV station at each bus, the search space shall contain 2^N combinations. In summary, among all combinations of ESS location in the feeder, the one leading to minimum active power level to keep all bus' voltages below U_{max} is identified as the optimal one. This method, however, is not meant to quantify the exact storage size needed for voltage support, but rather to enlighten the relative differences in storage size of the ESS as a function of the different possible locations.

IV. Method Implementation

The method has been tested on a real LV grid feeder with residential PV. The feeder cables are type NA2XRY with characteristics indicated in Fig. 4. The feeder is part of a larger LV grid composed of 9 feeders in total; additional information on the whole grid can be found in [18]. The feeder is predominantly residential, as it supplies 33 households and it counts of 9 roof-mounted PVs with total capacity installed of 42.6 kW; the feeder is composed of 7 buses in total, where 4 out of 7 host PV generation on bus 2, 4, 5 and 7, respectively. The PV capacity installed on each bus is indicated in Table I.

A. Definitions

The definition of PV penetration used in this paper refers to the one given in [17] and it is expressed as follows:

$$\text{PV}_{\text{penetration}} = \frac{\text{PV installed capacity}}{\text{feeder capacity}} \quad (16)$$

The PV penetration in a feeder is the ratio of the amount of total PV capacity installed in the feeder to the nominal feeder capacity. In this case study, the feeder capacity is considered the capacity of the cable connecting the feeder to the substation's busbar, which in this case is 185 kVA.

B. Voltage Sensitivity Analysis

For the LV feeder, voltage sensitivity analysis is performed to obtain all the sensitivity (∂U/∂P) coefficients [29]. Bus 7 in the feeder is found the most sensitive location in relation to voltage variation, with a ∂U/∂P of 1.505 p.u./MW, corresponding to a voltage rise of 3.5 V for a three-phase power injection of 10 kW. The ∂U/∂P sensitivity matrix for the feeder under analysis is indicated in Table II. It shall be noted that the coefficients are calculated with load flow conditions of maximum PV generation (42.6 kW in total) and no load. The coefficients' values are function of the load and generation in the feeder, however their variation compared to the values of Table II is small enough that can be neglected for the scope of this paper.

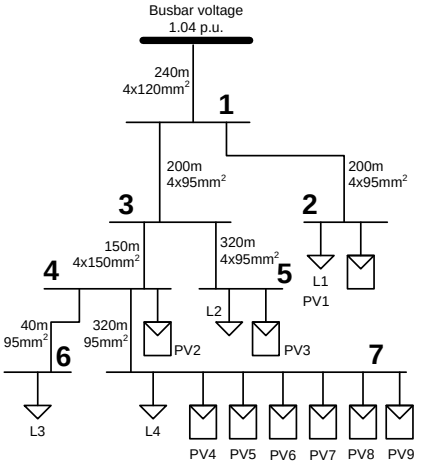

Fig. 4. Single-line diagram of the Belgian LV grid feeder.

TABLE I
PV Installed Capacity on Different Buses

Feeder buses	Bus 2	Bus 4	Bus 5	Bus 7
PV power (kW)	5.7	5	5	26.9

TABLE II
Feeder Voltage Sensitivity Matrix

dV/dP p.u./MW	1	2	3	4	5	6	7
1	0.37	0.36	0.37	0.35	0.35	0.34	0.34
2	0.37	0.72	0.36	0.71	0.71	0.69	0.72
3	0.36	0.36	0.76	0.35	0.35	0.34	0.35
4	0.36	0.72	0.36	0.91	0.91	0.88	0.88
5	0.36	0.72	0.36	0.89	1.35	0.71	0.69
6	0.36	0.71	0.36	0.91	0.89	0.98	0.98
7	0.36	0.71	0.35	0.89	0.68	0.88	1.51

C. Assumptions on Load and Generation Conditions

The assumptions taken for the method implementation are as follows:

- The base grid voltage, i.e. the transformer secondary voltage, is assumed of 1.04 p.u. This value is indeed used for the LV grid of the case study and it is also largely adopted in other countries in Europe [18], [30].

- The households' demand is assumed with PF of 0.95. Without additional information, the load in the different buses is assumed equally distributed among the phases and for the method application it is assumed to be null, to reproduce a worst case scenario.
- The PV generation units at the different buses are based on single-phase inverter technology and operate with unity PF. The active power injected on each bus by PVs is indicated in Table I. The power injection can be unbalanced among the three phases. The worst case scenario considers the load flow for the phase with highest generation.

An EV station with ESS can be located at any bus and the maximum charging power is limited to $P_c \leq 20$ kW which is chosen as an intermediate value compared to the maximum PV generation level of 42.6 kW.

D. *Best Location Identification*

With a maximum voltage U_{max} set to 1.1 p.u., the voltages at all buses do not exceed this value. For this reason, the method is repeated with U_{max} of 1.09 p.u. Under these circumstances, the voltage limit is exceeded and bus 7 is identified as the location that minimizes the storage effort by the ESS. To verify the validity of the MILP method implemented, unbalanced load flow is performed in PowerFactory (PF) [31], considering U_{max} of 1.09 p.u. The ESS value that lowers the bus voltages below 1.09 p.u. is identified in PF with the ESS at the 7 possible locations with the same load-generation conditions as for the method. Such verification led to the results diagram of Fig. 5 that confirms bus 7 as the best location for voltage support in the feeder. The small discrepancies in the results are due to the small variations of the ∂U/∂P coefficients when performing the load flows in PF, for the different ESS locations.

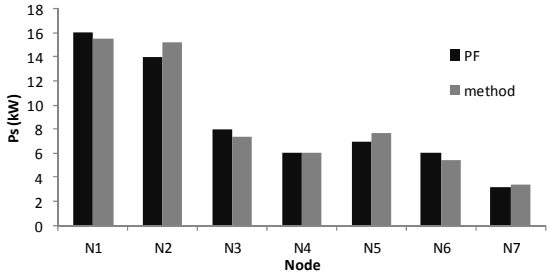

Fig. 5. ESS power effort for the different feeder locations.

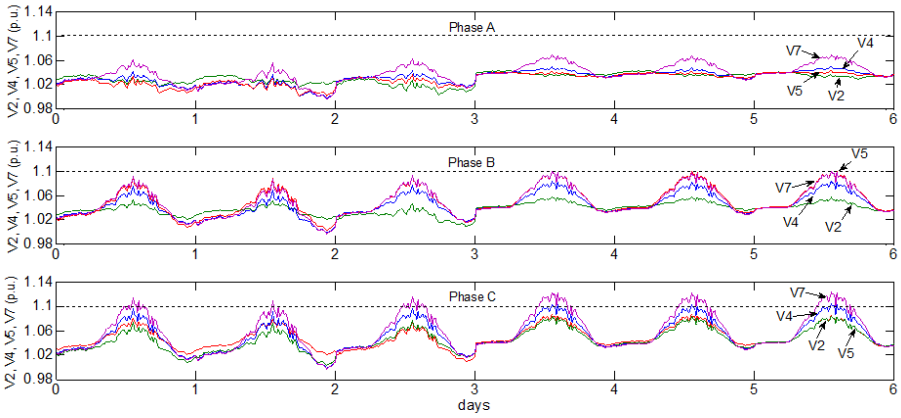

Fig. 6. Phase voltages on feeder 11 with PV without voltage support.

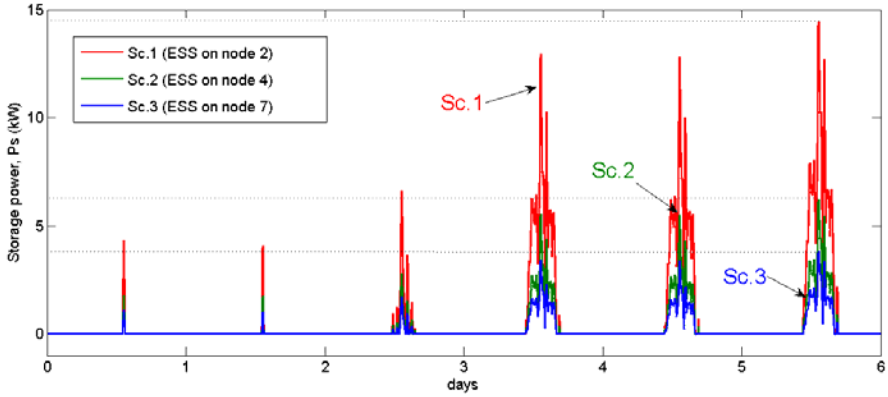

Fig. 7. Dynamic simulation results: storage power with Sc.1, Sc.2, Sc.3.

V. Dynamic Simulation

The method allowed the identification of the most favorable location to provide voltage regulation using active power solutions. To quantify the power and energy levels needed for an ESS at different locations, a dynamic simulation model is implemented. At the scope, 15-minutes average measurements for loads and PV generation in the feeder are used in the dynamic grid model. The phase voltages *A*, *B* and *C* on buses 2, 4, 5, and 7, are depicted in Fig. 6, for a 6-days time interval in Belgium, without storage. The profiles show voltage rise problems, with the maximum voltage of 1.1 p.u. exceeded on bus 7. During voltage rise above 1.1 p.u. it is observed that the generation/minimum load ratio is about 5.4. With dynamic simulation, voltage unbalance is also observable and this is due to the single-phase power injection from the PV units.

A. Dynamic Simulation Scenarios

Three different scenarios are considered as possible locations for an EV station with ESS and these correspond with ESS located at bus 2 (Sc.1), bus 4 (Sc.2), and bus 7 (Sc.3). With the chosen scenarios the following situations are reproduced: Sc.1) EV station closer to the transformer; Sc.2) EV station at mid-feeder; Sc.3) EV station at the most remote location. Based on the method results, the charging/discharging power limit for the ESS is considered: $P_c \leq 20$kW.

The storage power results are depicted in Fig. 7. Dynamic simulations confirm the results of the method proposed. Under dynamic conditions and using real load profiles for the grid, the minimum storage power for providing voltage support is achieved with an ESS located on bus 7. The same consideration is valid with regard to the energy levels required. The energy of the ESS is obtained by integration of the daily power profiles of Fig. 7. The 6th day in the simulated interval has the highest storage energy demand, due to a longer interval of high generation and low load conditions. For this reason, the storage power and energy results for Sc.1, Sc.2 and Sc. 3 are depicted in Fig. 8 and Fig. 9, considering only the 6th day. The control strategy used to control the ESS is $P_S(U)$ for all scenarios where U is the most critical bus voltage in the feeder, corresponding to the phase voltages on bus 7, in this particular case. For all scenarios, it is assumed that the ESS is discharged to the initial state during evening or overnight, with $P_d \leq 20$kW, however the discharging phase is not treated further. The ESS application for voltage regulation should take into account the power and energy levels obtained under dynamic simulations, as well as the storage technology.

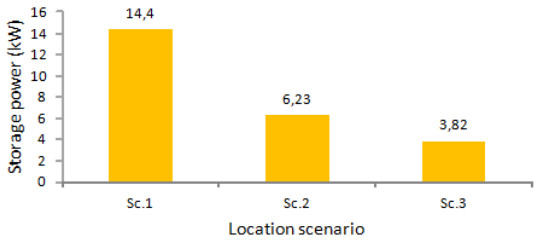

Fig. 8. ESS power needed for voltage support.

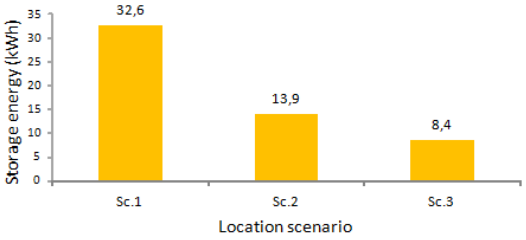

Fig. 9. ESS energy needed for voltage support.

In case of battery storage, the ESS should be over sized compared to the energy results, in order to achieve a feasible state-of-charge (SOC) window that ensures to the battery the desired lifetime [32].

B. Voltage Control Performances

For the 6-days simulated period, the phase-to-ground voltages on bus 7 are depicted in Fig. 10, for the three scenarios. It is evident that the effect on the phase voltages, Va, Vb, Vc, generated by the ESS at the three different location scenarios (Sc.1 to Sc. 3) is equivalent, though the storage power efforts are different.

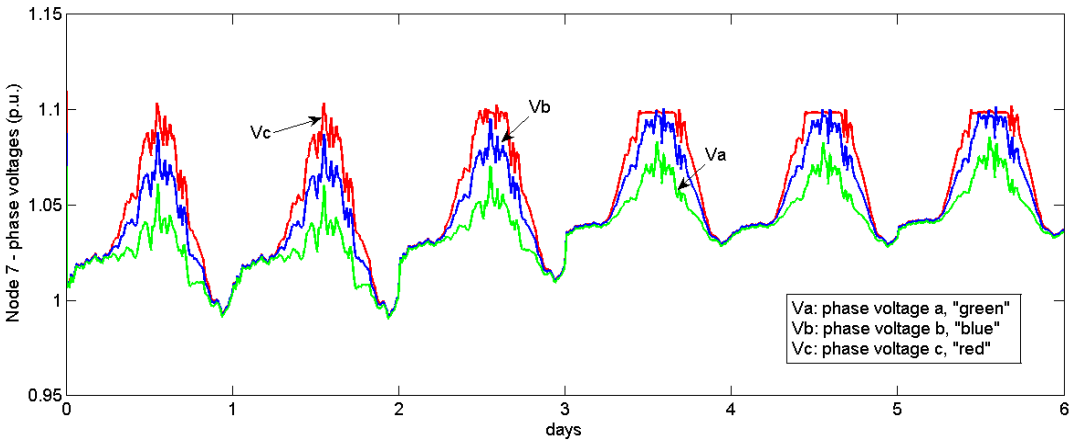

Fig. 10. Phase-to-ground voltage profiles on bus 7 for the three ESS scenarios.

C. Advantages and Limitations

The method shows that the preferred location for voltage support corresponds to a well defined configuration of storage in the feeder and this is verified under dynamic simulations. Based on the knowledge of the feeder layout and components characteristics, it is possible to identify the location leading to minimum storage size, considering the sensitivity coefficients for the different buses in the feeder. The method has been implemented for a 7-buses feeder with 23% of PV penetration; however the same method is scalable to larger grid's feeders with higher number of nodes and different penetration levels. It is also applicable to LV feeders with small scale wind power generation, rather than PV. Although the study is based on a three-phase operated feeder, the method can also be applied to a single-phase operated system. One of the limitations found is that the precise quantification of power and energy features for the ESS may be difficult with the proposed method, due to the stochastic nature of unbalanced load and generation which in turn affects the voltage sensitivity. Therefore, dynamic simulations, using real load and generation profiles are needed.

VI. Conclusions

This paper has introduced the application of EV public charging facilities for voltage support in feeders with high penetration of PV. Determining the feeder's location requiring minimum ESS size for voltage support has been addressed. The novelty of this contribution consists in the proposed MILP model that identifies the location with minimum power effort from an ESS, taking into account typical operating constraints in the grid's feeder. The method results are in agreement with the two verification methodologies used: 1) the load flows performed with the simulation tool PowerFactory; 2) the dynamic simulations performed for the same LV feeder with real load and generation profiles. By means of dynamic simulations, the power and energy levels required for an ESS within an EV station have been quantified according to three different location scenarios. For the analyzed residential grid feeder, with 23% of PV penetration, the farthest location from the transformer is found the most critical location for active power injection, as well as the most effective location for voltage regulation via ESS. The method proposed is applicable to any grid feeder as it only requires the knowledge of the grid layout, of the components characteristics and of the operative constraints in the feeder.

The storage capabilities of public EV charging facilities are important aspects to consider when dealing with the integration of increasing penetration levels of PV in urban grids. If an EV station can offer such additional function, grid reinforcement can be avoided or post-poned.

References

[1] European Commission, "20 20 by 2020 Europe's climate change opportunity", COM (2008) 30 final, Brussels, 2008.

[2] H. A. Gil, G. Joos, "Models for Quantifying the Economic Benefits of Distributed Generation", *IEEE Trans. on Power Syst.*, vol. 23, no. 2, pp. 327-335, May 2008.

[3] B. Renders, L. Vandevelde, L. Degroote, K. Stockman, M.H.J. Bollen, "Distributed generation and the voltage profile on distribution feeders during voltage dips", *J. of Elec. Power Systems Res.*, vol. 80, no. 12, pp. 1452-1458, 2010.

[4] M.H.J. Bollen, "Understanding Power Quality Problems: Voltage Sags and Interruptions", *IEEE Press*, 2000.

[5] M. Delfanti, M. Merlo, M. Pozzi, V. Olivieri, M. Gallanti, "Power flows in the Italian distribution electric system with Dispersed Generation", *20th Int. Conf. and Exhib. on Electricity Distrib.*, Part 1, CIRED, 2009.

[6] Standard EN 50160, "Voltage Characteristics of electricity supplied by public distribution networks", Cenelec, 2010.

[7] H. Chen, J. Chen, and X. Duan, "Integrated Planning of Distributed Generation Sources and Networks in Distribution Systems", in *Proc. of the 41st Univers. Power Eng. Conf., UPEC*, 2006.

[8] K. Corfee, D. Korinek, W. Cassel, C. Hewicker, J. Zillmer, M. Pereira Morgado, H. Ziegler, N. Tong, D. Hawkins, and J. Cernadas, "Distributed generation in Europe – Physical infrastructure and Distributed Generation Connection, *Memo*, no. 1, 2011, online.

[9] N. Etherden, and M. H. J. Bollen, "Increasing the Hosting capacity of Distribution Networks by Curtailment of Renewable Energy Sources", in *Proc. of IEEE Power Tech.*, Trondheim, 2011.

[10] R. Tonkoski, L. A. C. Lopes, and T. El-Fowly, "Coordinated Active Power Curtailment of Grid Connected PV Inverters for Overvoltage Prevention", *IEEE Trans. on Sust. Energy*, vol. 2, no. 2, pp. 139-147, Apr. 2011.

[11] T. Fawzy, D. Premm, B. Bletterie, and A. Gorsek, "Active contribution of PV inverters to voltage control – from a smart grid vision to full-scale implementation", *J. of Elektrotechnik & Informationstechnik*, vol. 128, no. 4, pp.110-115, 2011.

[12] P. Carvalho, P. Correia, and L. Ferreira, "Distributed Reactive Power Generation Control for Voltage rise Mitigation in Distribution Networks", *IEEE Trans. on Power Syst.*, vol. 23, no. 2, pp. 766-772, Apr. 2008.

[13] T. G. Hazel, N. Hiscock, J. Hiscock, "Voltage Regulation at Sites with Distributed Generation", *IEEE Trans. on Ind. Appl.*, vol. 44, no. 2, pp. 445-454, Mar. 2008.

[14] M. E. Elkhatib, R. El-Shatshat, M. M. A. Salama, "Novel Coordinated Voltage Control for Smart Distribution Networks with DG", *IEEE Trans. on Smart Grids*, vol. 2, no. 4, pp. 598-605, Dec. 2011.

[15] E. Demirok, P. Casado Gonzalez, K. H. B. Frederiksen, D. Sera, P. Rodriguez, and R. Teodorescu, "Local Reactive Power Control Methods for Overvoltage Prevention of Distributed Solar Inverters in Low-Voltage Grids", *IEEE J. of Photov.*, vol. 1, no. 2, pp. 174-182, Oct. 2011.

[16] T. Vu Van, A. Woyte, F. Harris, L. De Ghesselle, G. Plamers, J. Neyens, F. Truyens, B. Blatterie, H. Brunner, K. De Brabadere, J. Reekers, M. Sporleder, B. Blazic, I. Papic, R. Engelen, J. Alenus, "The MetaPV Project: Photovoltaics for Active Distribution Systems", in *Proc. of 24th Europ. Photov. Solar Energy Conf.*, 2009.

[17] V. Mendez Quezada, J. Rivier Abbad, and T. Gómez San Román, "Assessment of Energy Distribution Losses for Increasing Penetration of Distributed Generation", *IEEE Trans. on Power Syst.*, vol. 21, no. 2, pp. 533-540, May 2006.

[18] B. Blazic, I. Papic, B. Uljanic, B. Blatterie, C. Dierckxsens, K. De Brabandere, W. Deprez, T. Fawzy, "Integration of Photovoltaic Systems with Voltage Control Capabilities into LV Networks", in *Proc. of 1st Int. Workshop on Integ. of Solar Power into Power Syst.*, 2011.

[19] I. Safak Bayram, G. Michailidisy, M. Devetsikiotis, S. Bhattacharya, A. Chakrabortty, F. Granelli, "Local Energy Storage Sizing in Plug-in Hybrid Electric Vehicle Charging Stations Under Blocking Probability Constraints", in *Proc. of IEEE Smart Grid Comm*, pp. 78-83, 2011.

[20] P. Lombardi, M. Heuer, and Z. Styczynski, "Battery Switch Station as storage system in an autonomous power system: optimization issue", in *Proc. of IEEE Power and Energy Soc. General Meeting*, 2010.

[21] I. S. Bayram, G. Michailidis, M. Devetsikiotis, S. Bhattacharya, A. Chakrabortty, F. Granelli, "Local energy storage sizing in plug-in hybrid electric vehicle charging stations under blocking probability constraints", in *Proc. of IEEE Smart Grid Comm.*, pp. 78-83, 2011.

[22] Y. Rffonneau, S. Bacha, F. Barruel, and S. Ploix, "Optimal Power Flow Management for Grid Connected PV Systems with Batteries", *IEEE Trans. on Sust. Energy*, vol. 2, no. 3, pp. 309-320, Jul. 2011.

[23] D. P. Tuttle and R. Baldick, "The Evolution of Plug-in Electric Vehicle-Grid Interactions", in *IEEE Trans. on Smart Grid*, vol. 3, no. 1, Mar. 2012.

[24] F. Marra, "Central Station Design Options", Project EDISON deliverable, D4.1, online.
[25] D. Dallinger, D. Krampe, and M. Wietschel, "Vehicle-to-Grid Regulation Reserves Based on a Dynamic Simulation of Mobility Behavior", in *IEEE Trans. on Smart Grid*, vol. 2, no. 2, pp. 302-313, Jun. 2011.
[26] C. Weiller, "Plug-in Hybrid Electric Vehicle Impacts on Hourly Electricity Demand in the United States", *J. of Energy Policy*, vol. 39, pp. 3766-3778, Apr. 2011.
[27] J. P. Barton, D. G. Infield, "Energy storage and its use with intermittent renewable energy", *IEEE Trans. on Energy Conv.*, vol. 19, no. 2, pp. 441-448, Jun. 2004.
[28] S. X. Chen, H. B. Gooi, M. Q. Wang, "Sizing of Energy Storage for Microgrids", *IEEE Trans. on Smart Grid*, vol. 3, no. 1, pp. 142-151, Mar. 2012.
[29] R. Aghatehrani, R. Kavasseri, "Reactive Power Management of a DFIG Wind System in Microgrids Based on Voltage Sensitivity Analysis", *IEEE Trans. on Sust. Energy*, vol. 2, no. 4, pp. 451-458, Oct. 2011.
[30] SEAS-NVE, "Design manual for 10 kV and 0.4 kV", Denmark, 2010.
[31] DIg Silent PowerFactory, user manual.
[32] F. Marra, C. Traeholt, E. Larsen, Q. Wu, "Average Behavior of Battery – Electric Vehicles for Distributed Energy System Studies", in *Proc. of IEEE Innovative Smart Grid Technology Europe (ISGT 2010)*, 2010.

VII. BIOGRAPHIES

Francesco Marra was born in Copertino, Italy, in 1984. He received the B.Sc and M.Sc degrees in Electronic and Mechatronic engineering from Polytechnic of Turin, Italy, in 2006 and 2008, respectively. Currently, he is with the Electrical Engineering department of the Technical University of Denmark, where he is pursuing the Ph.D. degree. His fields of interest include renewable energy integration and control systems.

Guang Ya Yang received the B.Sc., M.Sc. and Ph.D. in 2002, 2005 and 2008 respectively, all in electric power system field. Currently, he is research scientist with the Department of Electrical Engineering of the Technical University of Denmark. His fields of interest include power system operation and control, renewable energy integration and wide-area system monitoring and protection.

Chresten Træholt received the M.Sc. master in Electrical Engineering in 1987, Ph.D. in Materials Science in 1994, both degrees at the Technical University of Denmark. Since then, he has spent several years on electron microscopy and materials research at the Technical University Delft, the Netherlands as well as several years of experience with the superconductor cable industry. His current fields of interest include smart grids, renewable energy, PV, wind power, electric vehicles and superconductivity.

Jacob Østergaard is head of the Centre for Electric Technology and head of section for Electrical Energy Systems at DTU Electrical Engineering. He is also head of the experimental platform for electricity and energy, PowerLabDK. He is member of the Advisory Council of the EU Technology Platform SmartGrids. He is coordinator of the M.Sc. program in Wind Energy (electric). His research focuses on the development of future intelligent power system with increased share of decentralized and environmentally friendly electricity, including wind energy.

Boštjan Blažič received the B.Sc, M.Sc and PhD degrees, all in electrical engineering, from the University of Ljubljana, Slovenia, in 2000, 2003 and 2005, respectively. He is presently an assistant professor at the Faculty of Electrical Engineering, Ljubljana. His research interests encompass power quality, distributed generation, mathematical analysis and control of power converters.

Esben Larsen received the M.Sc. in Electrical Engineering from the Technical University of Denmark, in 1977. He is currently Associate Professor at DTU. His main areas of interest include: high voltage engineering, wind power, photovoltaic, geothermal, hydro power, micro combined heat and power. He has been manager of "Information and Knowledge Center of Electric Vehicles" at DTU, in 2000-2003.

Wim Deprez received his M.Sc. in Electro-mechanical Engineering and PhD in Electrical Engineering from the K.U. Leuven in 2002 and 2008, resp. Until July 2010, he was assigned as a Post-doctoral Researcher at the research group ELECTA, Dept. of Electrical Engineering (ESAT), K.U. Leuven. Currently, he is smart grid engineer at Infrax, a major Belgian DSO. His fields of interest include machines, RES and efficiency.

Improvement of Local Voltage in Feeders with Photovoltaic using Electric Vehicles

F. Marra, *Student Member, IEEE*, G. Y. Yang, *Member, IEEE*, Y. T. Fawzy, C. Træholt, E. Larsen, R. Garcia-Valle, *Senior Member, IEEE,* and M. Møller Jensen

***Abstract*— In low-voltage (LV) feeders with high penetration of photovoltaic (PV), a major issue to be solved is voltage rise due to the active power injection. If no measures are taken, this may lead to generation's interruptions and to the malfunctioning of domestic appliances due to non-standard voltage profiles. This paper proposes a storage strategy to alleviate voltage rise in feeders with PV, using coordinated electric vehicle (EV) load as the storage solution. The voltage support strategy is easy to implement practically and it is demonstrated on a test feeder emulating a household with roof-mounted PV and an EV. The results show the effectiveness of using coordinated EV load in feeders with PV to mitigate voltage rise problems.**

***Index Terms*— Electric vehicle load, photovoltaics, storage, voltage support**

I. Introduction

IT IS experienced that low-voltage (LV) grids with high share of photovoltaic (PV) present voltage quality problems, with special concern to voltage magnitude variations [1]. In the coming years, this type of generation is likely to be combined with a new unconventional electric load: the electric vehicle (EV) power consumption [2]. While several reactive power and power curtailment methods have been implemented for voltage rise mitigation, this paper proposes a method and a proof of concept for voltage support, using coordinated EV load as a storage solution. A fundamental assumption is that the electric power consumption due to residential EV charging is going to increase in the next years. In the study in [2], the probability of an EV to be parked at home was estimated. A maximum availability (normalized to 1) during night and an average availability of 0.7 during the PV generation hours, i.e. between 10AM and 6PM, is observed. With the findings of [2], the control of EV power consumption during PV generation hours becomes a realistic scenario. This research builds on the work presented in [3], where a method for voltage support, based on storage solutions is applied to a Belgian LV feeder model with 33 households and 9 roof-mounted PVs. The dynamic simulations performed, based on 1-year generation and load profiles enlightened the need of storage for voltage support during 98 days a year. A decentralized storage strategy can be realized to support the voltage requiring a charging power of 0.9 kW at each house with PV. Additionally, centralized storage options were investigated at different buses, showing that a single storage capable of 3 kW charging power, located at the feeder end, can perform the same task of the 9 decentralized storages. In Fig. 1, the charging requirements (P_S) for voltage support are

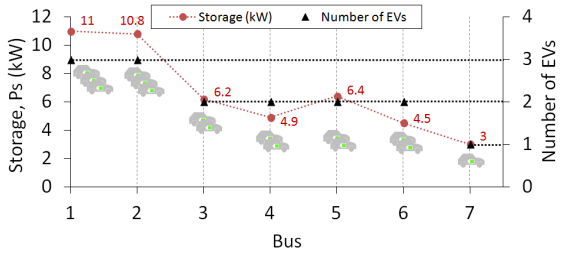

Fig. 1. EV load required for voltage support for a real LV feeder

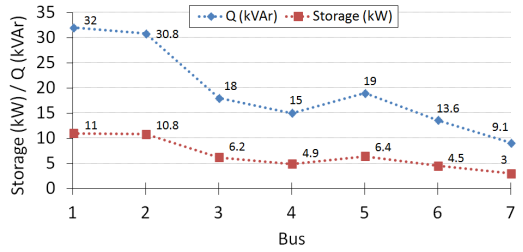

Fig. 2. Storage versus reactive power solutions

indicated. These are obtained with storage at the different buses, under maximum generation and low load conditions and related to the number of EVs needed to absorb a similar power level; a load of 3.7 kW is assumed as the EV charging power. For comparison, reactive power solutions at the different buses are investigated and compared to the centralized storage solutions, Fig. 2. Due to the high R/X ratio of LV cables, the required amount of reactive power for voltage support is about 3 times higher. Thus, with reactive power methods, greater grid losses may result in feeders with high PV penetration. The paper proposes a strategy for using the power consumption from domestic EV charging in feeders with PV, to alleviate voltage rise problems during high generation hours. A proof of concept is provided to validate the strategy.

II. The Test Setup

A household at a remote feeder location with roof-mounted PV and an EV is emulated with the test setup of Fig. 3.

F. Marra, G. Y. Yang, C. Træholt, E. Larsen and R. Garcia-Valle, are with the Department of Electrical Engineering, Center for Electric Power and Energy, Technical University of Denmark, Kgs. Lyngby DK-2800, Denmark (e-mail: {fm, gyy, ctr, ela, rgv}@elektro.dtu.dk).

M. Møller Jensen is with DONG Energy, Virum DK-2830, Denmark (email: momje@dongenergy.dk).

Y. T. Fawzy is with the ELENIA Institute, University of Braunschweig, Braunschweig DE-38106, Germany (e-mail: y.fawzy@tu-braunschweig.de).

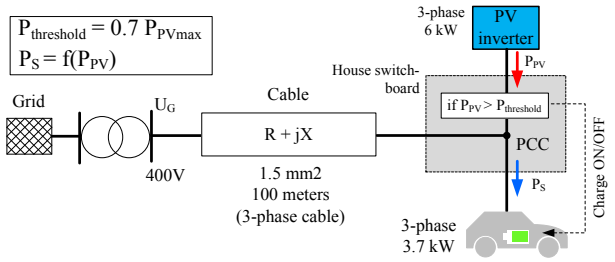

Fig. 3. Single-line diagram of the test setup.

The setup is composed of a 100 m, 1.5 mm^2, 5-wires copper cable, with impedance of 13.3 Ω/km to emulate a remote location in the feeder; a three-phase PV plant with P_{PVmax} of 6 kW; an EV with 3.7 kW three-phase charger and 14.5 kWh Li-ion battery pack. Voltage regulation at the point of common coupling (PCC) is achieved with active power control, by EV charging activation, according to the expression:

$$\vec{U}_{PCC} = \vec{U}_G + \frac{RP + XQ}{\vec{U}_G} + j\frac{XP - RQ}{\vec{U}_G} \qquad (1)$$

where: $\vec{U}_{PCC}$ is the voltage at the PCC; $\vec{U}_G$ is the grid voltage; P and Q are the exchanged active and reactive power, with $P = P_{PV} - P_S$, $Q = 0$; R and X are the cable parameters.

III. Control Strategy Implementation

The charging at the household with PV is locally activated by a house controller at 70% of PV installed power (P_{PVmax}), according to P_S=f(P_{PV}) [4]. All EVs at houses with PV start charging, regardless of the house location in the feeder. The test results are shown for a 24-hour period with 1-minute resolution, in Fig. 4 (a)-(b). The voltage and power measurements with time stamp are indicated in Table I for reference. The test results of Fig. 4 (b) show that EV charging contributes to lower the voltage magnitude of about 6.1 V at the PCC, thus increasing the margin from the upper voltage limit [5].

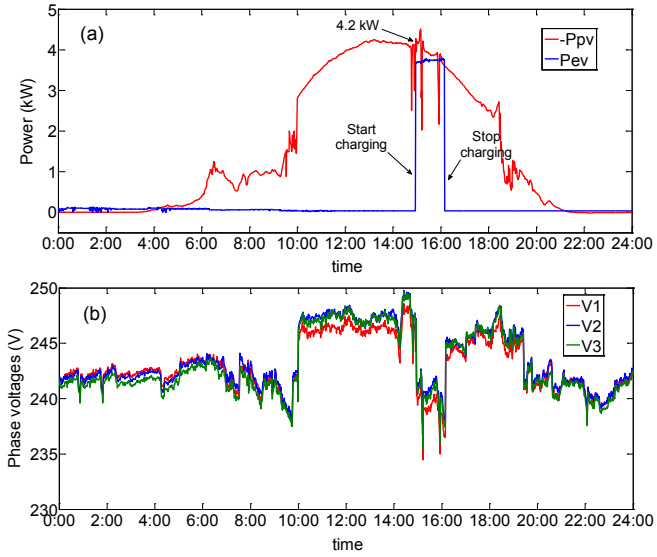

Fig. 4. Test. (a) PV and EV load profiles. (b) Phase voltages at PCC

TABLE I
Voltage Measurement at PCC

Time	Ppv	Ps (kW)	V1 (V)	V2 (V)	V3 (V)
14.50	4.13	0	246.2	247.5	247.2
15.00	4.21	3.7	240	241.4	241
15.10	4.45	3.7	240.8	242	242
15.20	3.97	3.7	238.8	239.8	240.3
15.30	3.90	3.7	238.9	240.1	240.6
15.40	3.87	3.7	239.8	241.4	240.9
15.50	3.91	3.7	238.9	241.1	240.5
16.00	3.83	3.7	238.6	239.7	240.2
16.10	3.60	3.7	236.8	238.2	237.8
16.20	3.49	0	243.6	244.9	245.2

IV. Discussions

Considering Fig. 1, the charging activation of 1 EV at a house with PV on bus 7, as well as the charging activation of 3 EVs on bus 1, would secure the voltages within the limits, while increasing local consumption. For the two cases, the EV penetration level, referred to the total number of households, is 3% and 9%, respectively. These findings are quite promising, considering the market expectation of newly registered EVs in the coming 5-10 years [6]. The implemented setup is a laboratory simplification of the real feeder in [3], using short distance and small cable cross-section to obtain comparable impedance values with the real feeder. The control strategy used P_s=f(P_{PV}) can be combined with other control strategies, such as P_s=f(U_{PCC}), depending on the severity of the voltage variations.

V. Conclusion

Voltage magnitude variations are more and more frequent in feeders with PV generation, resulting in a diffused deterioration of power quality; this paper has shown how EV load can be effectively used as a voltage support solution in those feeders. A relatively small EV penetration in residential grids with PV is enough for providing voltage support during high PV generation periods. If the EV load is then controlled according to the proposed strategy, there is the dual benefit of limiting grid reinforcement by increasing local consumption.

References

[1] P. Carvalho, P. Correia, and L. Ferreira, "Distributed Reactive Power Generation Control for Voltage Rise Mitigation in Distribution Networks", *IEEE Trans. on Power Syst.*, vol. 23, no. 2, pp. 766-772, May 2008.

[2] D. Wu, D. C. Aliprantis, K. Gkritza, "Electric Energy and Power Consumption by Light-Duty Plug-In Electric Vehicles", *IEEE Trans. on Pow. Syst.*, vol. 26, no. 2, pp. 738-746, May 2011.

[3] F. Marra, Y. T. Fawzy, T. Bülo and B. Blažič, "Energy Storage Options for Voltage Support in Low-Voltage Grids with High Penetration of Photovoltaic", in *Proc. of IEEE Innovative Smart Grid Europe (ISGT 2012)*, Oct. 2012.

[4] Renewable Energy Sources Act (EEG) 2012, www.bmu.de.

[5] EN 50160, "Voltage Characteristics of Electricity Supplied by Public Distribution Networks", CENELEC, Brussels, Belgium, 1999.

[6] T. Hazeldine, S. Kollamthodi, C. Brannigan, M. Morris and L. Deller, "Market outlook to 2022 for battery electric vehicles and plug-in hybrid electric vehicles", Jun. 2009, online.

A Decentralized Storage Strategy for Residential Feeders with Photovoltaics

Francesco Marra, *Member, IEEE*, Guangya Yang, *Member, IEEE*, Chresten Træholt, Jacob Østergaard and Esben Larsen

***Abstract*— This paper proposes a decentralized voltage support strategy for LV residential feeders with high roof-top PV capacity installed. The proposed strategy is capable of increasing the local consumption at private households with PV during high generation periods, by the use of locally controlled domestic energy storage systems (ESS). The traditional way of operating a domestic ESS to increase the local consumption rate does not take into account the need of voltage support in a feeder; the proposed storage concept improves the traditional one, by mitigating voltage rise due to PV in the feeder. The power sizing of the ESSs is performed with linear programming (LP) method, based on voltage sensitivity analysis. A Belgian residential LV feeder with private PV systems is used as a case study to demonstrate the effectiveness of the proposed strategy. Quantification of the required energy levels for the ESSs and estimation of LV grid losses is performed by means of time-series simulation using 1-year load and generation profiles.**

***Index Terms*— Energy storage, low voltage grid, photovoltaic systems, voltage control**

I. Introduction

WITH THE increasing penetration of photovoltaic (PV), there is a great potential of relieving the overall loading of LV distribution grids. Meanwhile, the LV grid operation encounters more and more uncertainties with regard to voltage quality [1], [2]. In several European countries, such as Germany, Spain, Belgium and others, several LV grids have reached high PV penetration levels with consequences on the quality of the supply voltage [3].

High generation and low load conditions are the pre-conditions of power flow inversion in a grid feeder; these situations are likely on a daily basis and may result in voltage rise problems at the different buses [4]. Therefore, solutions to increase the local consumption at private homes with roof-top PV, during periods of high solar irradiation are needed to preserve voltage quality. In Germany, the vast majority of PV plants, about 13 GW, are connected at the LV grid, causing voltage rise events during the year in different areas [5]. To avoid such events, from January 2012, a fixed limitation of the active power feed-in by each PV system is mandatory [5]. As of today, the limit is set to the 70% of the nominal peak-output power of the PV system; this corresponds to an inherent power curtailment of up to 30% when the peak-output power is being generated. Some alternative solutions to the active power curtailment may involve local consumption by domestic load shifting and energy storage [7], [8].

The state of the art on local consumption methods for private houses with PV has mainly focused on demand side management (DSM), in order to shape the domestic electric load during periods of high PV generation, thus minimizing the energy drawn from the mains [9]. Since the number of flexible domestic appliances is very limited and because these are not necessarily used on a daily basis (e.g. the washing machine), the local consumption rate can be significantly increased with the deployment of a stationary energy storage system (ESS). The conventional size of domestic ESSs for private households with PV is in the range of 5 kWh [9], [10], which allows obtaining a local consumption rate of about 55% on a twelve-month period [10]. The conventional way of performing local consumption consists on activating the charging of the ESS' battery as soon as the PV system's output power is greater than the domestic electric load, Fig. 1. However, this strategy does not guarantee voltage support during maximum PV generation hours (12:00 - 14:00 PM), as the morning hours of sunny days are generally used to fully charge the ESS battery [9].

In this paper, a novel decentralized storage strategy, for residential feeders with PV is proposed, prioritizing the charge of ESS batteries around peak generation hours, as shown in Fig. 1. Each ESS is activated at a certain power threshold, P_{th}, in Fig. 1, which is identified with linear programming method, using voltage sensitivity analysis. The combination of the proposed strategy with the conventional one is possible using day-ahead solar irradiation forecasts [11], however only the new proposed method is treated in this paper.

The application of decentralized storage from private houses with PV has the dual benefit of increasing the local consumption rate and providing voltage support in the feeder.

The strategy is implemented on a residential LV feeder with 23% PV penetration. The effectiveness of the decentralized ESS concept is evaluated with time-series simulations.

F. Marra, G. Y. Yang, C. Træholt, E. Larsen and J. Østergaard are with the Electrical Engineering Department, Technical University of Denmark (DTU), Kongens Lyngby DK-2800, Denmark (e-mail: {fm, gyy, ctr, joe, ela}@elektro.dtu.dk).

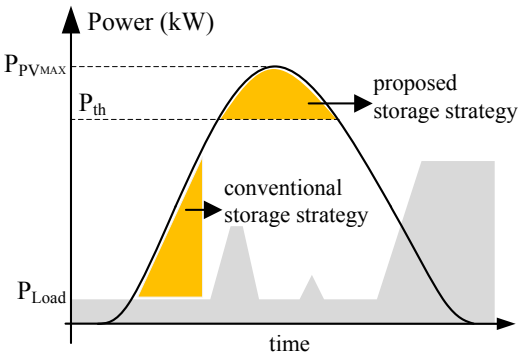

Fig. 1. Conventional storage strategy and proposed strategy compared.

II. LV Feeders With PV

LV distribution grids are designed and operated in a radial fashion [4]. The purpose of the LV grid is to provide connection from the medium-voltage (MV) grid to the supply points for the individual customers. Typically, a European LV grid consists of a secondary step-down transformer to step down the voltage from the MV level to a 0.4 kV line-to-line voltage. Voltage regulation is passive in most cases. Distribution feeders at the secondary side of the transformers are composed of lines or cable sections that distribute electric power to the different customers. When PV systems are connected at a feeder bus, as depicted in Fig. 2, the voltage magnitude at the PCC is likely to increase according to the following expression:

$$\vec{U}_{PCC} = \vec{U}_G + \frac{RP + XQ}{\vec{U}_G} + j\frac{XP - RQ}{\vec{U}_G} \quad (1)$$

$$P = P_{PV} - P_L \quad (2) \qquad Q = Q_{PV} - Q_L \quad (3)$$

where

- P is the nodal active power exchanged;
- Q is the nodal reactive power exchanged;
- $\vec{U}_G$ is the substation voltage magnitude, assuming that the phase angle is zero;
- P_{PV}, Q_{PV} are the active and reactive power feed-in of the PV system;
- P_L, Q_L are the active and reactive power absorbed by a generic load;
- R, X are the equivalent resistance and reactance of the cable;

To ensure a correct operation of domestic load appliances, the power quality Standard EN 50160 is considered, with regard to voltage magnitude variations [12]. It shall be ensured that during each period of one week, the 95% of 10-minute average values of the supply voltage shall be within the range +/-10% of U_n, where U_n is the nominal mean value [12].

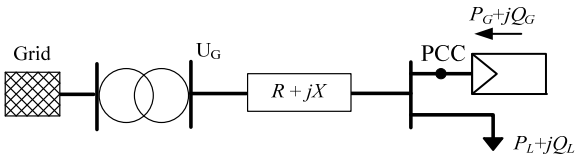

Fig. 2. Simplified single-line diagram of LV feeder with PV

III. Home Energy Management

The management of local consumption at houses with PV requires an electrical setup which comprises smart meters, smart sockets, for realizing the load-shift of different appliances, and a *main controller* to realize load management [13], [14]. The study in [10] analyzes the local consumption rate for a cluster of households with annual consumption of 4000 kWh and a 5 kW PV system. The local consumption rate amounts to about 25%. To reach higher levels of local consumption, the house shall be equipped with an ESS, whose operation is coordinated with the PV system. With a 5 kWh battery-ESS, the local consumption rate rises of about 30% showing a final local consumption rate of about 55% [10].

The typical AC system in a house with PV and ESS is depicted in Fig. 3 (a). The PV system is composed of a PV array and a PV inverter whose AC output power is monitored by the main controller via a real-time meter. The ESS is connected at the same PCC of the PV inverter and its input/output power is also real-time monitored [15]. A wide range of battery-ESS technologies can be utilized, such as lead-acid and Li-ion batteries. However, due to the better performances of Li-ion battery chemistries in terms of lifetime, energy-to-weight ratio, self-discharge rate and charge- discharge efficiency, this technology is adopted in this paper [16].

The ESS is modeled with the charge-discharge equations as expressed in (4) and (5), where P_d is the discharging power and P_c is the charging power of the ESS battery, respectively; E is the energy stored in the battery at time t; Δt is the duration time of each interval [17]. The two coefficients η_d and η_c are the discharge and charge efficiencies respectively.

$$E(t + \Delta t) = E(t) - \Delta t \cdot P_d / \eta_d \quad (4)$$

$$E(t + \Delta t) = E(t) + \Delta t \cdot P_c \cdot \eta_c \quad (5)$$

The operation of the battery system should also take into account power and energy constraints. The maximum power limits during charging-discharging can be described by (6) and (7) respectively:

$$0 \le P_c(t) \le P_c^{\max} \quad (6)$$

$$0 \le P_d(t) \le P_d^{\max} \quad (7)$$

The battery power limits are also considered for sizing the ESS power converter, however, for simplicity we refer to P_S to indicate the power flow in-out the ESS, thus including both the phases of charging and discharging. Positive values of P_S indicate the provision of voltage support. The energy limits of an ESS can be described as follows:

$$E_{\min} \le E(t) \le E_{\max} \quad (8)$$

$$SOC_{\min} \le SOC(t) \le SOC_{\max} \quad (9)$$

where

E_{min} and E_{max} are the minimum and maximum energy levels of the storage, defining the usable energy window;

SOC_{min} and SOC_{max} are the minimum and maximum SOC limits that shall be set in relation to the application.

In this paper, the size of the ESS is not predetermined, instead it is one of the decision variables, in order to comply with the voltage constraints in the feeder.

IV. Proposed Method

To lower the voltage profiles during voltage rise periods, the ESS at each household with PV shall be operated during the maximum generation interval, as illustrated in Fig. 1. The concept architecture to achieve voltage support by decentralized storage is depicted in Fig. 3. Every roof-mounted PV system is coupled with an ESS at the same PCC. The house *main controller* controls the activation of the ESS and appliances. If the PV power P_{PV} reaches a pre-defined threshold P_{th} (e.g. the 70% of the PV peak-power), the main controller sends a charging activation signal to the *ESS control*, corresponding to flag set to 1, in Fig. 3 (b). The flag is set to 0, otherwise. At the end of the PV generation period, i.e. after sun set, the main controller sets the flag to 2, so the ESS can be discharged back to the initial state. Depending on the flag setting, the *ESS control* generates an ESS activation signal corresponding to "*Charge on"*, "*Discharge on",* or *Idle*, as depicted in Fig. 3 (c). The ESS stores the incoming PV energy, by charging with a power level $P_S(t) = P_{PV}(t) - P_{th.}$. The charging process continues as long as $P_{PV}(t)$ is greater than the threshold. The ESS control can be also implemented introducing a power dead-band to avoid oscillations.

A safe usage of the ESS battery should be ensured at all times, during charging or discharging operation. This task is achieved by the *SOC control*, which is the inner control loop of the storage system. The charging of the ESS battery should be limited to a SOC window of 20-90 %, as determined in [18], for Li-ion battery types. Other types of batteries may be considered for the same concept, involving potentially a different usage window.

To provide voltage support in the feeder, the main problem to solve is the identification of the ESS maximum charging power under worst case conditions of maximum generation and no load. This problem is solved using linear programming (LP) method, based on voltage sensitivity analysis.

V. Problem Formulation

The main problem is to identify the power threshold for activating the ESSs in the feeder. The objective function in (10) shall minimize the ESS size while securing all bus voltages within the limit of 1.1 p.u. The method returns as output a value for α, between 0 and 1, same for all ESSs,

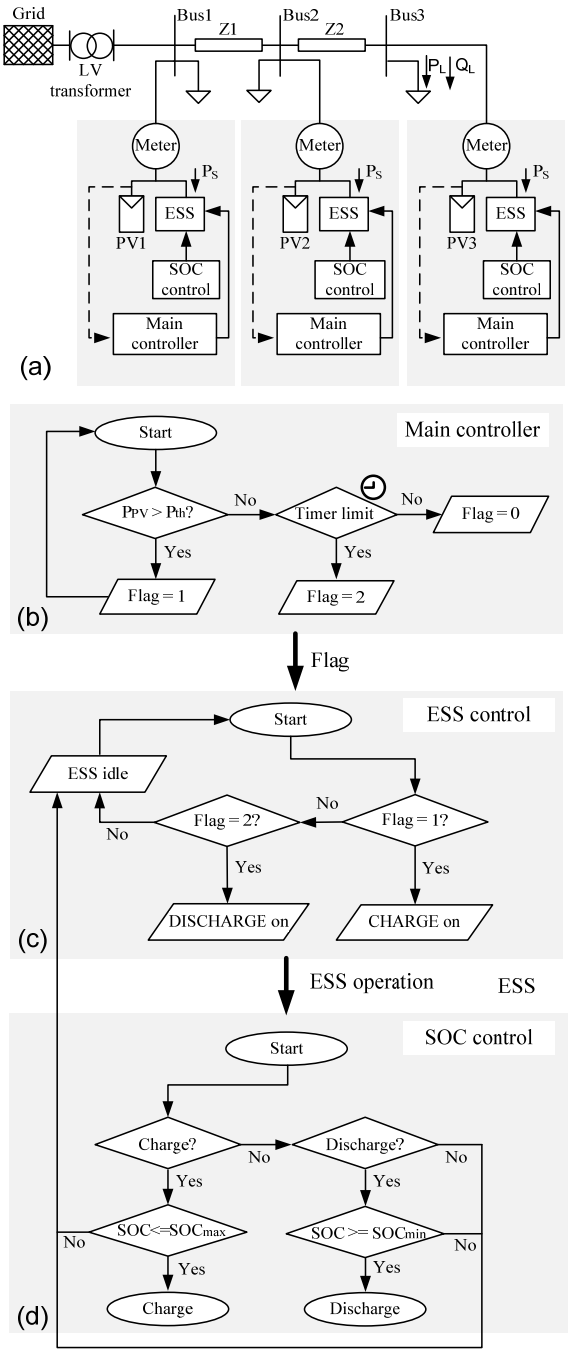

Fig. 3. Decentralized storage concept

which represents the maximum share of PV peak-output power used by the ESS for charging. For instance, the in-feed power limitation of 70% in Germany, is equivalent to adopting $\alpha = 0.3$. The overall formulation of the LP problem is as follows:

Objective function:

$$f = \min \sum_{k=1}^{N} \alpha_k P_{PV,k} \quad (10)$$

Constraints:

$$\text{subject to} \quad \begin{array}{ll} a) & u \le U_{\max} \\ b) & P_{S,k}^{\min} \le P_{S,k} \le P_{S,k}^{\max} \\ c) & \alpha_1 = \ldots = \alpha_N \end{array} \qquad (11)$$

where N is the number of PV plants in the feeder; $\alpha_k P_{PV,k}$ is the charging power of the k-ESS; $P_{S,k}^{\min}$ and $P_{S,k}^{\max}$ are the minimum and maximum ESS discharging and charging power, respectively; u is the column vector containing all bus voltages in the feeder; U_{max} is the maximum voltage magnitude allowed.

Constraints (11) are; a) the operative constraints that bound the voltage magnitude at all buses within the limits; b) the operative power range for each ESS; c) a global value for α respectively. It shall be noted that the voltage constraint a) in (11) includes the network equations that incorporate the characteristics of cables, load and generation. The expression in (12) describes the voltage constraint at the generic bus M. Reactive power contributions are neglected.

$$\left|\vec{U}_M\right| \approx \left|\vec{U}_g\right| + \sum_{i=1}^{M} \frac{\partial \left|\vec{U}_M\right|}{\partial P_i} (P_{PV,i} - P_{L,i} - P_{S,i}) \le \left|U\right|_{\max} \qquad (12)$$

where

$\left|\vec{U}_g\right|$ is the busbar grid voltage magnitude (p.u.);

$\left|\vec{U}_M\right|$ is the voltage magnitude at bus M (p.u.);

M is the number of buses in the feeder;

$P_{PV,i}$ is the active power feed-in by PV on bus i;

$P_{S,i}$ is the aggregated ESS charging power at bus i;

$\partial U_M/\partial P_i$ is the voltage sensitivity coefficient of bus M, to the active power exchanged (p.u./MW).

Due to the use of load flow equations, this method is not meant for precisely quantifying the ESS size for voltage support, but rather for providing an indication of the value of α needed for a certain PV penetration; this value is also dependent on the number of PV systems in the feeder. The quantification of the required ESS energy levels is estimated with time-series simulations using PowerFactory [19].

VI. Case Study

The Belgian residential LV feeder [20] is used as case study. The feeder comprises 7 buses, of which 4 out of 7 hosting PV systems, bus 2, 4, 5 and 7, respectively. It is composed of NA2XRY type LV cables and it is part of a larger LV grid which includes 9 feeders in total [20]. The feeder supplies 33 houses and it embeds 9 single-phase roof-mounted PVs located at different buses, with total PV capacity installed of 42.6 kW. The PV capacity per bus is indicated in Table I. On bus 2, 4, and 5 each PV system size corresponds to the value indicated in Table I, while for bus 7, 6 PV systems contribute as follows: 2 plants of 4.8 kW each; 2 plants of 4.25 kW each and finally 2 plants of 4.4 kW each, respectively. The definition of PV penetration used in this paper refers to the one given in [21]:

$$\text{PV}_{\text{penetration}} = \frac{\text{PV installed capacity}}{\text{feeder capacity}} \qquad (13)$$

The PV penetration in the feeder is the ratio between the total PV installed capacity to the nominal feeder capacity. The feeder capacity is intended as the capacity of the first line section of the feeder, corresponding to 185 kVA. It follows that a PV penetration of 23% is present in the feeder.

A. Method Implementation

The LP method proposed is configured for the grid feeder of Fig. 4. To reproduce a worst case scenario for voltage rise, the assumption of maximum generation and no load in the feeder is made. Under these conditions, the method identifies a value of α = 0.2, corresponding to an average ESS charging power of about 1 kW for each house with roof-mounted PV.

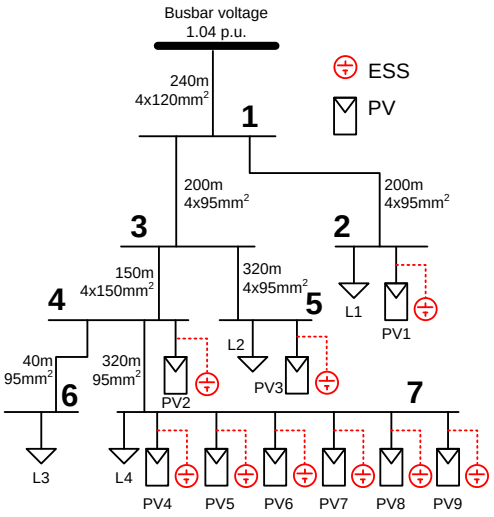

Fig. 4. Single-line diagram of the LV grid feeder.

TABLE I
PV IN THE FEEDER – 23% PENETRATION, ORIGINAL SCENARIO

Feeder buses	Bus 2	Bus 4	Bus 5	Bus 7
PV power (kW)	5.7	5	5	26.9

TABLE II
PV INSTALLED CAPACITY IN THE FEEDER – 50% PENETRATION

Feeder buses	Bus 2	Bus 4	Bus 5	Bus 7
PV power (kW)	12.3	10.8	10.8	58.1

A second scenario assuming 50% PV penetration is investigated using the LP method. The new PV installed capacity per bus is indicated in Table II. With this penetration level, the LP method identifies a value of α = 0.55, corresponding to a charging power for all ESSs of about 6 kW on average. It appears that, by doubling the PV penetration in the feeder, the ESS power requirement becomes 6 times higher. As a consequence, it is also expected that ESS's

energy window results quite different for the two scenarios; this is investigated via time-series simulations.

B. Load and Generation in the Feeder

The ESS operation is analyzed with time-series simulations using a 12-month 15-minutes average load and generation profiles. A previous study performed on the feeder, for a 6-day time interval, has shown voltage rise problems across the feeder buses [22].

The aggregated profiles of load and generation in the feeder, from the 1st of January till the 31st of December, are depicted in Fig. 5 and Fig. 6, respectively. The 12-month simulation performed show that voltage rise events at bus 7 are more critical, due to maximum voltage exceeded in 98 days.

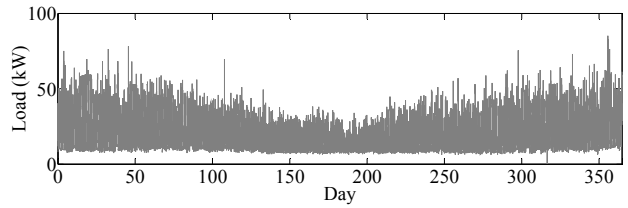

Fig. 5. Load in the LV feeder.

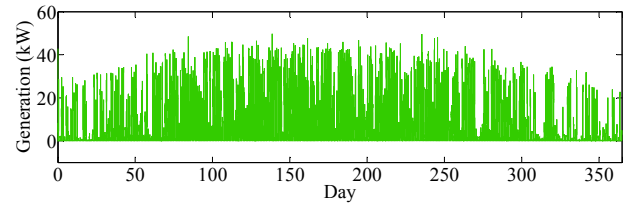

Fig. 6. PV generation in the LV feeder.

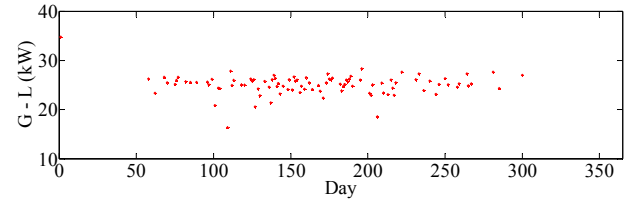

Fig. 7. "Generation - load" in the LV feeder.

In Fig. 7, the difference "PV generation (G) - load (L)" in those days with voltages above 1.1 p.u. is depicted. For graphical reasons, for each of these days, only one value of G-L is depicted, though this value may change during the entire period of over voltage. Some major findings are: 1) voltage rise events occur with a positive G-L difference that in this case corresponds to the active power range of 15 to 35 kW; 2) the highest concentration of days with voltage above the 1.1 p.u. is observed in spring and summer.

With regard to grid losses, the total energy losses in the feeder are calculated considering the losses on the single feeder cables; the profile of total power losses in the feeder during the 12-month period is depicted in Fig. 8. In this case it is observable that losses are lower in spring and summer and higher in winter and autumn.

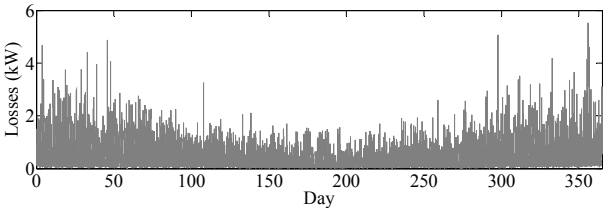

Fig. 8. Power losses in the LV feeder.

With regard to energy levels, the total energy consumption, energy production and energy losses are calculated and summarized in Table III.

TABLE III
ENERGY QUANTITIES IN THE LV FEEDER

	Energy consumption	Energy generation	Energy losses
Unit (MWh)	172	48	3.3

VII. DECENTRALIZED STORAGE

The LP method identified a value of $\alpha = 0.2$ for the base scenario with 23% PV penetration and a value of $\alpha = 0.55$ for 50% PV penetration. The following scenarios are investigated:

Case 1, which considers $\alpha = 0.2$, as obtained by the LP method application with 23% PV penetration; all residential ESSs are activated when $P_{PV}(t) > 80\%\ P_{PVmax}$.

Case 2, which considers $\alpha = 0.3$; all residential ESSs are activated with $P_{PV}(t) > 70\%\ P_{PVmax}$, as required by the Renewable Energy Sources Act, EEG 2012, in Germany [6].

Case 3, which considers $\alpha = 0.55$, as obtained by the LP method application with 50% PV penetration; all residential ESSs are activated with $P_{PV}(t) > 55\%\ P_{PVmax}$.

While α for Case 1 and Case 3 are applied as a result of the proposed method, the value of α for Case 2 is instead predetermined because it is based on an existing local consumption requirement [6].

A. Case 1

With $\alpha = 0.2$, the feed-in power by the PV system is at most the 80% of P_{PVmax}. The charging activity of the 9 ESSs is depicted in Fig. 9. The maximum charging power is about 1.1 kW, which is in line with the LP method's results. The phase voltage profiles *Va*, *Vb* and *Vc* of the most critical feeder location, bus 7, are depicted in Fig. 10. The profiles are apparently within the maximum voltage limit.

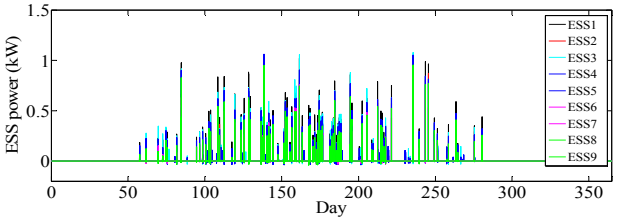

Fig. 9. ESS charging power for voltage support, $\alpha = 0.2$.

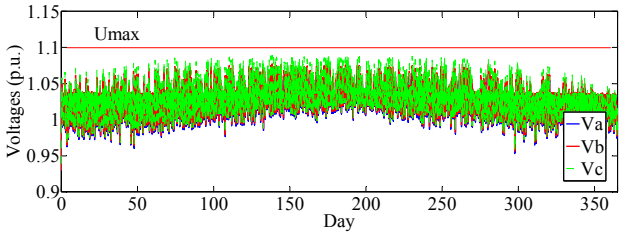

Fig. 10. Phase voltage profiles on bus 7, with $\alpha = 0.2$.

B. Case 2

With $\alpha = 0.3$, the feed-in power of the PV system is at most the 70% of P_{PVmax}. The charging activity of the residential ESSs is depicted in Fig. 11. In this case, the maximum charging power is about 1.7 kW and all ESS operate for 147 days. The phase voltage profiles *Va*, *Vb* and *Vc* of bus 7 are depicted in Fig. 12. Compared to the voltage profiles obtained for $\alpha = 0.2$, a wider margin from the limit of 1.1 p.u. is observable.

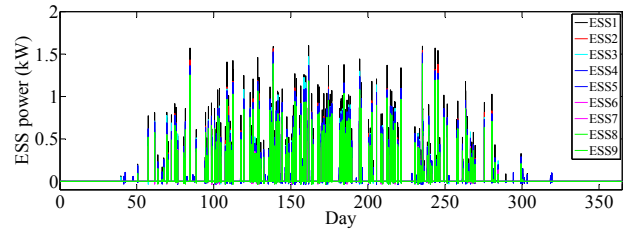

Fig. 11. ESS charging power for voltage support, $\alpha = 0.3$

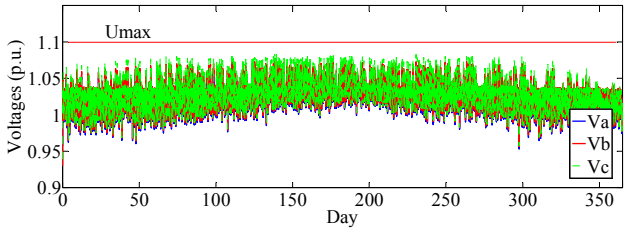

Fig. 12. Phase voltage profiles on bus 7, with $\alpha = 0.3$.

C. Case 3

With 50% PV penetration, the aggregated feed-in power by PV in the feeder is at most 92 kW. Such power amount leads to 231 days with voltage magnitude violations. While the method application found a value for α of 0.55, with simulations, a value of $\alpha = 0.5$ is required to comply with the voltage limit of 1.1 p.u.

The assumptions made to raise the PV penetration level from 23% to 50% have been the following:

- same number of PV systems than the original case, with augmented installed capacity per system;
- twice the number of PV systems than the original case, distributed according to the original configuration.

With 9 PV plants in the feeder, the maximum charging power of each ESS is on average 6 kW, as previously determined; while, with 18 PV plants the maximum charging power results of about 3 kW.

VIII. Energy Levels Quantification

The ESS energy levels are calculated based on the power profiles obtained for the three cases investigated. With 23% PV penetration and $\alpha = 0.2$, the required ESS energy is 1.1 kWh, Fig. 13. This value is obtained by integration over time of the ESS power profiles and selection of the day with highest storage energy content. Whereas, with $\alpha = 0.3$, the required ESS energy is of 3.8 kWh, Fig. 14.

With 50% PV penetration and $\alpha = 0.5$, the required ESS energy capacity with 9 ESSs in the feeder is 28 kWh per unit, whereas 14 kWh, with 18 ESSs.

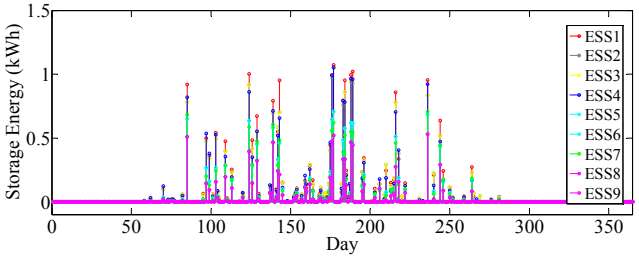

Fig. 13. ESS energy required for voltage support, with $\alpha = 0.2$.

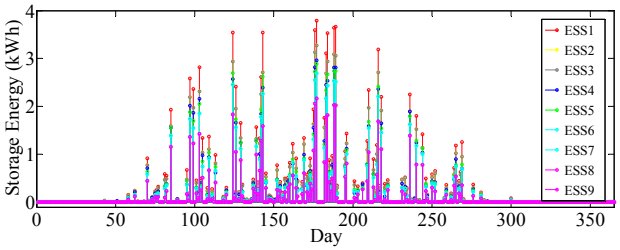

Fig. 14. ESS energy required for voltage support, with $\alpha = 0.3$

It shall be considered that the identified energy levels are referred to the operative energy window (in kWh) to achieve voltage support using decentralized ESSs. According to [18], to operate the ESS battery across a linear SOC region and to avoid deep discharge cycles, the battery should be oversized in relation to the operative energy window identified. For each ESS battery, a usable SOC window of 20% to 90% is imposed in this paper, complying with the recommendations made on the use of Li-ion batteries in [18]. Following, the nominal battery capacity E_N, the minimum and maximum energy constraints E_{min} and E_{max} are indicated in Table IV.

TABLE IV
ESS Operative Constraints

Case	No. PVs	E_N (kWh)	E_{min} (kWh)	E_{max} (kWh)	P_c^{max} (kW)	P_d^{max} (kW)
PV penetration: 23 %						
$\alpha = 0.2$	9	1.6	0.3	1.4	2	-2
$\alpha = 0.3$		5.4	1.1	4.9	2	-2
PV penetration: 50%						
$\alpha = 0.5$	9	40	8	36	6	-6
	18	20	4	18	3	-3

With 23% PV penetration, voltage support with α = 0.2 is possible with a nominal battery capacity of about 1.6 kWh. Instead, with α = 0.3, a battery capacity of 5.4 kWh should be used. While a smaller battery size represents a more affordable option for the user, the larger battery size gives the opportunity of a higher local consumption rate. It is also evident that the maximum charging and discharging power of the ESS is not a crucial issue for the provision of voltage support; in fact, the power level of ± 2kW is enough for both α-cases.

Drastic differences are observed in power and energy levels with 50% PV penetration. With either 9 ESSs or 18 ESSs in the feeder, the required ESS nominal capacity is not an economically feasible option for standard households.

A. ESS battery lifetime

The estimation of the battery lifetime L is limited to the sole voltage support operation of the ESS, regardless of the ESS activity in days without voltage problems. The number of cycles performed during the 12-month period for voltage support and the declared battery lifetime at 80% depth-of-discharge DOD (in number of cycles) are considered for the lifetime L estimation. Considering a Li-ion battery with 1500 cycles declared at 80% DOD [23], L is approximated as:

$$L = \frac{\text{No. cycles Voltage Support}}{\text{Declared No. cycles at 80\% DOD}} \qquad (14)$$

For the three different scenarios of α, the diagram of Fig. 15 is obtained.

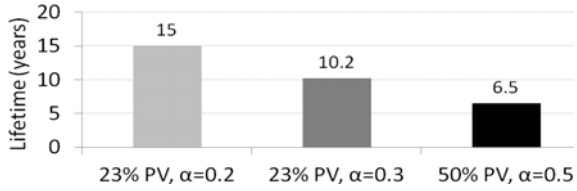

Fig. 15. ESS expected battery lifetime for the different scenarios.

It appears that, under the 23% PV penetration scenario, voltage support using decentralized storage has not significant impact on battery lifetime, considering that current batteries warranty is about 8 years [23]. A substantially shorter lifetime is obtained with the 50% PV penetration scenario and this is due to a highest number of cycles required for voltage support.

B. Energy losses in the feeder

A comparison of energy losses in the feeder with 23% PV penetration is performed for the three cases according to: 1) no storage; 2) storage with α = 0.2; 3) storage with α = 0.3. Results are indicated in Table V. With α = 0.2, the energy losses are reduced by 6.6% compared to the case without storage. If voltage support is activated with α = 0.3, the energy losses are reduced of about 7.3%.

TABLE V
ENERGY LOSSES IN THE LV FEEDER FOR DIFFERENT SCENARIOS

	No storage	DS α = 0.8	DS α = 0.7
Energy Losses (MWh)	3.3	3.080	3.057

IX. CONCLUSION

In this paper, a decentralized storage concept for feeders with high PV penetration has been set forth, which can be used as a storage planning tool.

The main contribution of the work is based on the qualitative results, which can be applied to real situations of LV residential feeders with high PV penetration. The deployment of private ESSs at private homes with PV appears a promising option for accommodating increased PV penetration levels. The novel storage strategy presented improves the traditional way of using ESSs at private homes with PV by the fact that battery charging is activated according to a computed power threshold, instead than "as soon as $P_{PV} > P_L$". The strategy allows also a reduction of the energy losses in the feeder, as opposed to the case with no storage.

For sizing the domestic ESSs, a method based on voltage sensitivity analysis has been proposed, which identifies the power thresholds for activating all ESSs in the feeder. By applying the method at a residential feeder model with 23% PV penetration, it is found that all ESSs shall be activated to limit the PV power feed-in to as low as 80% of the peak-output power of each plant. Instead, the application of the 70% limitation, as per EEG 2012, demands the over sizing of the ESS batteries. At the same time, a battery life of over 10 years is achievable in both cases.

Ultimately, by scaling up the PV penetration level to 50%, the method enlightens that the predetermined power limitation of 70% does not guarantee the required voltage support in the feeder. Instead a power limitation of 50% from each PV system is required. In this case, the ESS sizes result amplified of about 6 times than the original penetration level, which makes voltage support by private households uneconomical.

Though the novel storage strategy and the ESS sizing method proposed are applied to a specific case study, other distribution networks with different topologies and load patterns have been analyzed by the authors, obtaining similar qualitative results. Grid planners and distribution network operators can potentially benefit by the findings of the paper.

REFERENCES

[1] A. Bracale, P. Caramia, G. Carpinelli, A. Russo, and P. Verde, "Site and System Indices for Power-Quality Characterization of Distribution Networks with Distributed Generation", *IEEE Trans. Power Syst.*, vol. 26, no. 3, pp. 1304-1316, Jul. 2011.

[2] M.H.J. Bollen, "Understanding Power Quality Problems: Voltage Sags and Interruptions", *IEEE Press*, 2000.

[3] B. Renders, L. Vandevelde, L. Degroote, K. Stockman, M.H.J. Bollen, "Distributed generation and the voltage profile on distribution feeders during voltage dips", *J. of Elec. Power Syst. Res.*, vol. 80, no. 12, pp. 1452-1458, 2010.

[4] M. Delfanti, M. Merlo, M. Pozzi, V. Olivieri, M. Gallanti, "Power flows in the Italian distribution electric system with Dispersed Generation", *20th Int. Conf. and Exhib. on Electricity Distrib.*, Part 1, CIRED, 2009.

[5] T. Stetz, F. Marten, M. Braun, Improved Low Voltage Grid-Integration of Photovoltaic Systems in Germany, *IEEE Trans. on Sustain. Eng*, vol. PP, no. 99, 2012.

[6] Renewable Energy Sources Act (EEG) 2012, www.bmu.de.

[7] B. H. Bailey, J. R. Doty, R. Perez, R. Stewart, J. E. Donegan, Evaluation of a demand side management photovoltaic system, *IEEE Trans. on Energy Conv.*, vol. 8, no. 4, pp. 621-627, Dec. 1993.

[8] S. J. Chiang, K. T. Chang, C. Y. Yen, Residential photovoltaic energy storage system, *IEEE Trans. Ind. Electr.*, vol. 45, no. 3, pp. 385-394, Jun. 1998.

[9] M. Castillo-Cagigala, E. Caamaño-Martínb, E. Matallanasa, D. Masa-Boteb, A. Gutiérreza, F. Monasterio-Huelina, J. Jiménez-Leubea, "PV self-consumption optimization with storage and Active DSM for the residential sector", *J. of Solar Energy*, vol. 85, no. 9, pp. 2338-2348, Sep. 2011.

[10] J. Binder, C.O. Williams, T. Kelm, "Increasing PV Self-Consumption, Domestic Energy Autonomy and Grid Compatibility of PV Systems using Heat-Pumps, Thermal Storage and Battery Storage", in proc. of *27th Europ. Photov. Solar Energy Conf.*, Frankfurt, 2012.

[11] E. Lorenz, J. Hurka, D. Heinemann, H. G. Beyer, "Irradiance Forecasting for the Power Prediction of Grid-Connected Photovoltaic Systems", *IEEE J. of Selected Topics in Applied Earth Obs. and Remote Sensing*, vol. 2, no. 1, pp. 2-10, Mar. 2009.

[12] EN 50160, "Voltage Characteristics of Electricity Supplied by Public Distribution Networks", CENELEC, Brussels, Belgium, 1999.

[13] T. Ganu, D. P. Seetharam, V. Arya, R. Kunnath, J. Hazra, S. A. Husain, L. C. Da Silva, S. Kalyanaraman, "nPlug: A smart plug for alleviating peak loads", in proc. of the *Third Int. Conf. on Future Energy Syst.: Where Energy, Computing and Comm. Meet (e-Energy)*, May 2012.

[14] F. Shahnia, M. T. Wishart, A. Ghosh, G. Ledwich, F. Zare, "Smart demand side management of low-voltage distribution networks using multi-objective decision making", *IET Generat., Transm. and Distrib.*, vol. 6, no. 10, pp. 968 – 1000, Oct. 2012.

[15] X. Liu, A. Aichhorn, L. Liu, and H. Li, "Coordinated Control of Distributed Energy Storage System with Tap Changer Transformers for Voltage Rise Mitigation under High Photovoltaic Penetration", *IEEE Trans. on Smart Grid*, vol. 3, no 2, Jun. 2012.

[16] K. Chen, A. Bouscayrol, A. Berthon, P. Delarue, D. Hissel, and R. Trigui, "Global modeling of different vehicles", *IEEE Vehic. Techn. Magazine*, vol. 4, no. 2, pp. 80-89, Jun. 2009.

[17] S. X. Chen, H. B. Gooi, M. Q. Wang, "Sizing of Energy Storage for Microgrids", *IEEE Trans. on Smart Grid*, vol. 3, no. 1, pp. 142-151, Mar. 2012.

[18] F. Marra, G. Y. Yang, C. Træholt, E. Larsen, C. N. Rasmussen, and S. You, "Demand Profile Study of Battery Electric Vehicle under Different Charging Options", in proc. *IEEE Pow. and En. Soc. Gen. Meet.*, Jul. 2012.

[19] DIg Silent PowerFactory, user manual.

[20] F. Marra, Y. T. Fawzy, T. Bülo and B. Blažič, "Energy Storage Options for Voltage Support in Low-Voltage Grids with High Penetration of Photovoltaic", in proc. *IEEE Innov. Smart Grid Techn., ISGT 2012*, Oct. 2012.

[21] V. Mendez Quezada, J. Rivier Abbad, and T. Gómez San Román, "Assessment of Energy Distribution Losses for Increasing Penetration of Distributed Generation", *IEEE Trans. on Power Syst.*, vol. 21, no. 2, pp. 533-540, May 2006.

[22] B. Blazic, I. Papic, B. Uljanic, B. Blatterie, C. Dierckxsens, K. De Brabandere, W. Deprez, T. Fawzy, "Integration of Photovoltaic Systems with Voltage Control Capabilities into LV Networks", in *Proc. of 1st Int. Workshop on Integr. of Solar Pow. into Pow. Syst.*, 2011.

[23] LTC, GAIA Advanced Lithium Battery Systems, "Handling instructions for the lithium ion cell type HE 602030 NCA-55Ah/198Wh" [online]. Available: www.gaia-akku.com.

BIOGRAPHIES

Francesco Marra was born in Copertino, Italy, in 1984. He received the B.Sc and M.Sc degrees in Electronic and Mechatronic engineering from Polytechnic of Turin, Italy, in 2006 and 2008, respectively. Currently, he is with the Electrical Engineering department of the Technical University of Denmark, where he is pursuing the Ph.D. degree. His fields of interest include renewable energy integration and control systems.

Guang Ya Yang received the B.Sc., M.Sc. and Ph.D. in 2002, 2005 and 2008 respectively, all in electric power system field. Currently, he is research scientist with the Department of Electrical Engineering of the Technical University of Denmark. His fields of interest include power system operation and control, renewable energy integration and wide-area system monitoring and protection.

Chresten Træholt received the M.Sc. master in Electrical Engineering in 1987, Ph.D. in Materials Science in 1994, both degrees at the Technical University of Denmark. Since then, he has spent several years on electron microscopy and materials research at the Technical University Delft, the Netherlands as well as several years of experience with the superconductor cable industry. His current fields of interest include smart grids, renewable energy, PV, wind power, electric vehicles and superconductivity.

Jacob Østergaard is head of the Centre for Electric Technology and head of section for Electrical Energy Systems at DTU Electrical Engineering. He is also head of the experimental platform for electricity and energy, PowerLabDK. He is member of the Advisory Council of the EU Technology Platform SmartGrids. He is coordinator of the M.Sc. program in Wind Energy (electric). His research focuses on the development of future intelligent power system with increased share of decentralized and environmentally friendly electricity, including wind energy.

Esben Larsen received the M.Sc. in Electrical Engineering from the Technical University of Denmark, in 1977. He is currently Associate Professor at DTU. His main areas of interest include: high voltage engineering, wind power, photovoltaic, geothermal, hydro power, micro combined heat and power. He has been manager of "Information and Knowledge Center of Electric Vehicles" at DTU, in 2000-2003.

Electric Vehicle Requirements for Operation in Smart Grids

Francesco Marra, *Student Member, IEEE,* Dario Sacchetti, Chresten Træholt and Esben Larsen

***Abstract* — Several European projects on smart grids are considering Electric Vehicles (EVs) as active element in future power systems. Both battery-powered vehicles and plug-in hybrid vehicles are expected to interact with the grid, sharing their energy storage capacity. Different coordination concepts for EVs are being investigated, in which vehicles can be intelligently charged or discharged feeding power back to the grid in vehicle-to-grid mode (V2G). To respond to such needs, EVs are required to share their battery internal data as well as respond to external control signals. In this paper, the requirements for the interaction of EVs with the electrical grid are presented. The defined requirements have been implemented on an EV test bed, realized by using real EV components. Charging/V2G tests on the EV test bed have shown that the presented requirements are sufficient to ensure an intelligent coordination of EVs into the electricity grid.**

***Index Terms* – Electric vehicle, requirements, smart grids, virtual power plant**

I. Introduction

THE ongoing research on Smart Grids is playing a major role in the process of electrification of the transport sector.

In January 2008, the European Commission published the "20-20 by 2020" package [1]. This includes targets for reducing the EU's greenhouse gas emissions by 20%, with respect to 1990 levels, and increasing the share of final energy consumption from renewable sources to 20%. Both of these targets have to be achieved by 2020.

The electrification of transport, by means of plug-in EVs and plug-in Hybrid EVs (PHEVs) will most likely contribute in the coming years to achieve the CO2 target [2]. Battery-powered EVs are able to achieve zero-emissions during their driving cycles since all the energy needed is drawn out of the battery [3]. In the case of PHEVs, different classes of vehicles are available based on their system design. PHEVs combine both an electric system propelled by a battery and an internal combustion engine [4]. Also for these vehicles, the level of CO2 emission is much lower compared with the standard ICE cars. For simplicity, in this paper we will refer to EVs, including both plug-in hybrid and battery-powered vehicles.

Even though the replacement of conventional cars by EVs could give the opportunity for lowering CO2 emission levels, it is expected that a large-scale penetration of these new vehicles will increase the electricity consumption due to the charging process. Therefore, the need to manage the charging of EVs, so to optimize their interaction with the electrical grid, arises. If coordinated, EVs can provide multiple benefices, e.g. they can support the integration of renewable energy sources, thanks to their energy storage capability and they can participate in the provision of several power system services, including ancillary services [5]. But the intelligent operation of EVs into the grid will be possible provided the combination of:

- Grid-interactive EV architecture
- Open access to internal vehicle data

Several assessments on EV coordination have been carried out, based on the concept of a Virtual Power Plant (VPP) for the aggregation of EV fleets. In the Danish Edison project [6], a VPP is dedicated to the intelligent charging/V2G operation of EVs. The interaction of such vehicles with the grid requires accessible system architecture on the EV side, which enables the EV coordinators to communicate with the vehicles and get the relevant internal vehicle data. The EV coordinator is able to elaborate the EV data collected and thereby send the control signals to the vehicles, in the form of charging/V2G schedules [7].

The requirements to achieve intelligent coordination of EVs within a VPP framework are presented in this paper. The EV system architecture is described in the work, with emphasis on the hardware and software interfaces involved.

The implementation of such requirements is then performed at laboratory level, on an EV test bed, using real EV components. Tests and measurements of a charging/V2G schedule have been conducted on the EV test bed, showing the effectiveness of the defined requirements.

II. Related Work

In this section the conceptual framework developed in the Danish Edison project [5] is presented as a platform which conducts to the definition of EVs system requirements for intelligent coordination.

The reason for choosing the Edison VPP for the study is because this VPP has been specifically designed for EV coordination, rather than for others distributed energy

The authors are grateful to the financial support from the Danish project "Electric vehicles in a Distributed and Integrated market using Sustainable energy and Open Networks", EDISON, which is funded by the ForskEl program (ForskEL Project Number 081216).

Mr. F. Marra, Mr. D. Sacchetti, Mr. C. Træholt and Mr. E. Larsen are within the Centre for Electric Technology, Department of Electrical Engineering, Technical University of Denmark, 2800 Kgs. Lyngby, Denmark (e-mail: fm@elektro.dtu.dk).

resources (DERs).

In the Edison project, the interaction between the plug-in EVs and the electrical grid is considered using different hierarchical levels:

- Centralized EV coordination
- Local control at the EV interface

As depicted in Fig. 1, the control of EVs takes place at local level on the EV interface. The individual charging stations (CS) that receive the charging/V2G requests by the EV coordinator and send the control signals to the EVs.

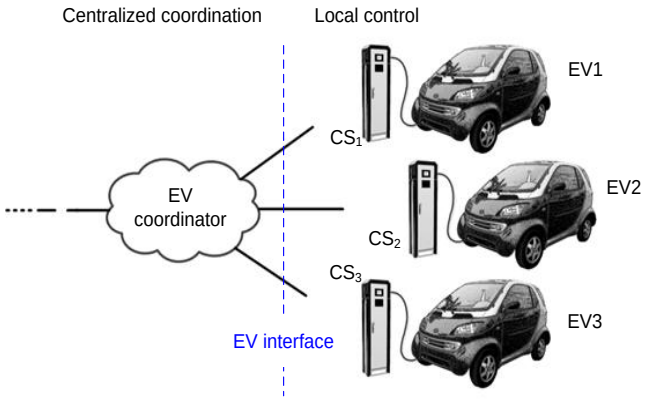

Fig. 1. EV coordination in the Edison project

The charging/discharging of vehicles is handled utilizing the necessary electrical circuitry and communication interfaces which lie on the EV interface. Such components could be partly included in the charging infrastructure, i.e. in the charging stations, as well as on board the vehicle.

At a higher hierarchical level, a centralized EV coordinator, the Edison VPP, aggregates and elaborates the actual status of the vehicles, thus it generates the schedule. As a result, the VPP sends the control signals to the plugged EVs so to coordinate their charging/V2G operation.

It is reminded that the Edison VPP operates in a multi-entities platform interfacing with other players, as depicted in the diagram of Fig. 2.

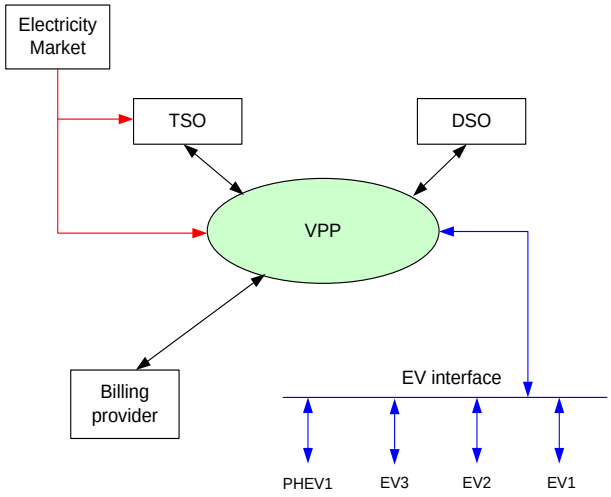

Fig. 2. Concept of EDISON Virtual Power Plant

In this context, each vehicle is encouraged to actively participate in supporting the power system where increasing amount of renewable energies is expected. Therefore the intelligent operation of EVs, within the illustrated framework, is expected to take place at the EV interface. The other interfaces in the framework are: a transaction interface with a Billing Provider to allow the billing of energy during charging or V2G operation; a Transmission System Operator (TSO) interface, where a Balance Responsible Party is involved to create and submit mandatory power schedules for the correct operation of the power system; an Electricity Market interface and a Distribution System Operator (DSO) interface to collect the grid status of every connected EV [5].

In this paper, the focus is dedicated to the requirements definition on the EV interface for the interaction between EVs and VPP.

III. Definition of Requirements

The coordination of EV fleets can be achieved given that vehicles have an accessible hardware and software architecture which can be monitored and controlled during plug-in periods.

The requirements for achieving the monitoring and control functions of EVs in a charging/V2G framework should therefore include the following:

- monitoring of internal vehicle data
- control of charging/V2G operation

A. Monitoring of internal vehicle data

The need for EV coordination involves the monitoring of several internal vehicle data. This requirement entails the real-time communication with the Battery Management System (BMS) of the vehicle. Accessing the info contained in the vehicle BMS is fundamental to the VPP in order to define the energy status of the vehicle and other relevant parameters. The following internal vehicle data, Fig. 3, are required for the EV status identification:

- Nominal battery energy, E_n
- Battery State-of-Charge, *SOC*
- Instant power during charging/V2G, *Power*

The nominal energy of the battery is an invariant parameter which is expressed in kWh as follows:

$$E_n = V_{BATT} \cdot C_n \quad (1)$$

where C_n (Ah) is the nominal capacity of the battery pack [8], while V_{BATT} (V) is the nominal voltage of the battery pack. The nominal energy is required by the VPP since it represents the absolute reference of energy of the vehicle.

The SOC of the vehicle battery, as defined in [9], is the measure of the charge left in the battery with respect to its nominal capacity. This can be expressed as follows:

$$SOC = \frac{C}{C_n} \quad (2)$$

where C (Ah) is the actual capacity contained in the battery at the time of measuring.

The third information needed to the VPP is the power used by the EV during charging/V2G operations. This could be achieved using either smart meters on a charging station or possibly BMS data.

In smart charging applications, the charging/discharging power should be measured in real-time and the information sent back to the VPP which keeps track of the energy exchanged between the EV and the grid. The power levels used are constrained by the charging infrastructure available, e.g. the size of the on-board EV chargers, the grid electrical cables, the transformer ratings etc. The EV coordination strategies are therefore aiming to avoid any grid reinforcement [10].

The fast-charging scenario of EVs is not considered in this paper, as it does not necessarily require any EV coordination. Fast-charging entails the installation of ad hoc charging infrastructures due to the high power demand as well as it requires an accurate charging management which cannot be influenced by higher level coordination [11].

Based on the existing electrical grid infrastructure, the most common power levels defined for EVs charging are listed in Table I.

TABLE I
CHARGING/DISCHARGING POWER LEVELS

AC current	AC voltage	Grid connection	Power
10 A	230 V	single phase	2.3 kW
16 A	230 V	single phase	3.7 kW
32 A	230 V	single phase	7.4 kW
16 A	400 V	three-phase	11 kW
32 A	400 V	three-phase	22 kW

The five listed charging options are referred to the AC side of the EV chargers. It is expected that all on-board chargers for EVs will fall in one of these use cases [12]. The same power levels could be used with vehicles entering the V2G mode, when provided with such a feature.

B. Control of Charging/V2G operation

Monitoring the internal vehicle data is not enough alone to achieve smart charging/discharging of EVs. In fact, the control requirement is also needed to achieve the following:

- Activation of the charging mode
- Activation of the V2G mode
- Control of power set point, *P_set*

EVs are controllable, provided that the EV charging/V2G components can receive a control signal sent by the EV coordinator, namely the Edison VPP, and respond accordingly. Control is needed to satisfy the activation of the operation mode, primarily. Secondly, the control requirement can provide the regulation of the power level used both during charging and V2G operation.

The defined requirements of monitoring and control are summarized in Fig. 3. In Fig. 3 (a) the BMS data and the measured power are represented as monitoring requirements of an on-board charger type of EV.

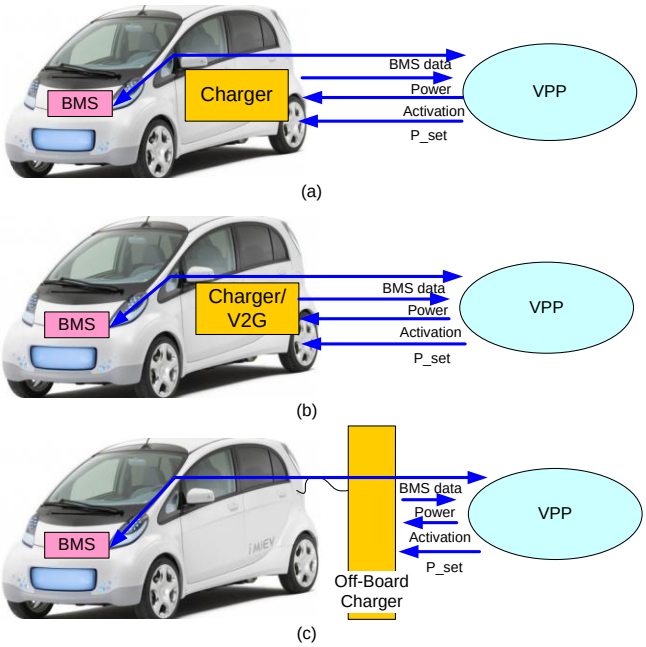

Fig. 3. Requirements for charging/V2G operation. (a) On-board charging concept. (b) On-board charging/V2G concept. (c) Off-board charging/V2G concept

The control requirements of the charging operation are depicted with an *activation* signal and *P_set* signal respectively. Both the control signals are sent by the VPP. Similarly, in Fig. 3 (b), an EV with bi-directional power components is represented. The required monitoring functions are the same as in the previous case. The only difference lies in the control requirements, where this time the activation and P_set control signals are used to control either the charging or the V2G operation. Finally, in Fig. 3 (c) the case of EV with off-board charger is represented. Some vehicles manufacturers, such as Nissan Leaf, have implemented the option of using an external charger [13], or DC charger, generally more powerful than the on-board one. The off-board charger is a future candidate for the last two power levels of Table I, corresponding to 11 kW and 22 kW respectively [14]. The defined requirements are also valid under the off-board charging case: each EV is required to send the BMS data and the charging/V2G power information to the VPP. The control requirement is still realized by the activation signal and the P_set signal sent by the VPP to the vehicle. Due to grid constraints, the P_set signal could have a significant role in the off-board charging concept [15].

IV. IMPLEMENTATION OF REQUIREMENTS

The defined requirements have been summarized in the diagram of Fig. 4, according to the definition performed in the previous section.

Monitoring and control requirements have been implemented on a real EV test bed, Fig. 5, considering the case of an EV capable of both charging and V2G, as depicted in Fig. 3 (b).

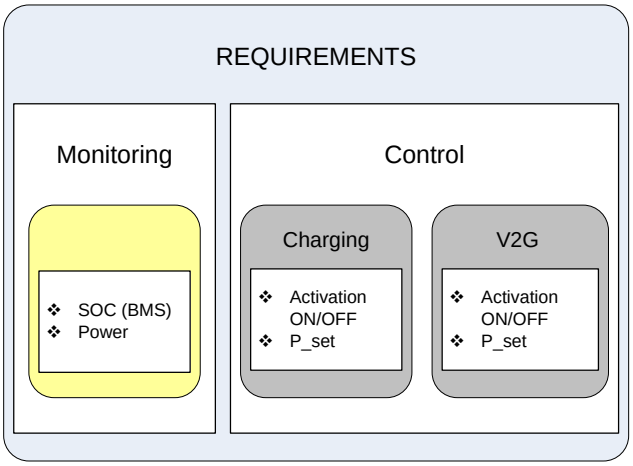

Fig. 4. Requirements for EV operation is Smart Grids

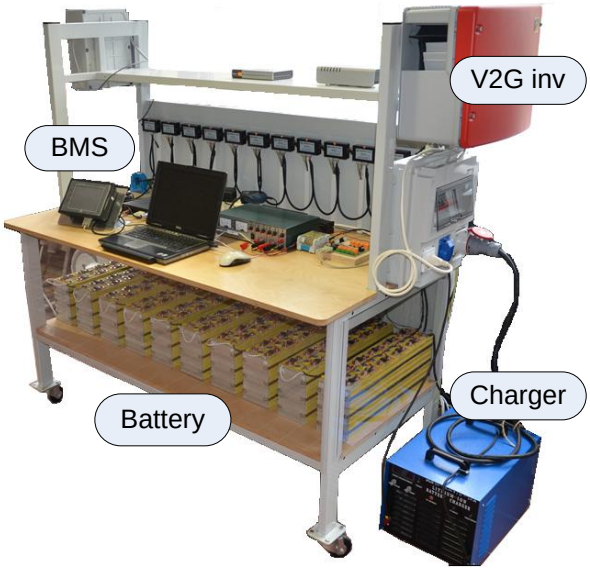

Fig. 5. EV test bed

A. *EV test bed*

The EV test bed is an experimental setup composed of real EV components; it is capable of charging and V2G operation and designed prioritizing open access to communication and control.

The EV test bed is composed by the following components:

- Battery pack: V_{BATT} = 363 V, C_n = 40 Ah, E_n = 14.5 kWh
- Charger: 0 - 5.5 kW
- V2G inverter: 0 - 4 kW
- BMS: battery pack voltage, total current, instant power, temperature, SOC, actual capacity C, nominal energy E_n, nominal capacity C_n
- On-board computer for communication between EV and VPP

The hardware architecture is composed by two separate components for charging and V2G operation, since the choice for a bidirectional operation came at a later stage in the design.

The battery pack was sized with nominal voltage of 363 V, considering the requirement for V2G operation and the common EVs design concepts. The battery is composed of 110 single cells, connected in series, lithium-iron-phosphate (LFP) technology based. A BMS is attached to the battery pack, Fig. 6, and is composed of 11 voltage acquisition modules each of whom acquires the voltage of 10 battery cells. A current acquisition module is used to acquire the current flowing in or out of the battery pack. Using the voltage and current information, the BMS is able to estimate the SOC of the battery pack. The nominal battery capacity and the nominal energy of the battery pack are invariant values that are stored in the BMS data memory and depend exclusively on the battery design.

The battery charger has a charging power of 0 to 5.5 kW, efficiency of about 0.88 and power factor (PF) of 0.9 at rated power. The V2G inverter has a power range of 0 to 4 kW, efficiency of about 0.95 and PF of 1. An onboard computer is used to interface with all hardware components described.

B. *Implementation of Monitoring*

As indicated in Fig. 4, the SOC and the real time Power are the two essential requirements for monitoring the EV status. To implement the monitoring requirements, a software interface which reads data from the BMS has been implemented, using a serial communication protocol. The diagram of Fig. 6 describes the architecture for reading the different BMS data on the EV test bed.

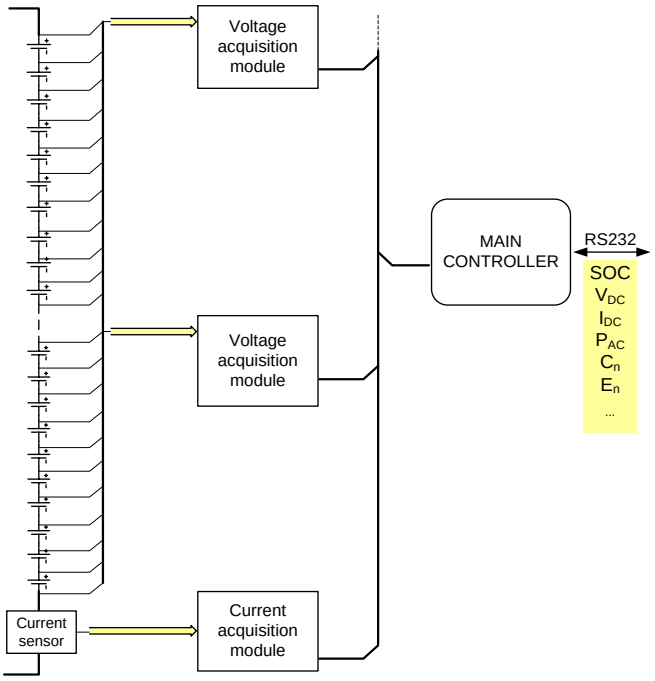

Fig. 6. Implementation of monitoring using the BMS on the EV test bed

Data acquired by the voltage and current acquisition modules is collected in the BMS controller, namely Main Controller, which computes the SOC level of the EV battery. The SOC, as well as the other real time data, are extracted using serial commands, over a serial port RS232 which is installed on the main controller.

C. Implementation of Control

Following the diagram of Fig. 4, the requirements for control can be split between the charging and the V2G operation. During charging or V2G operation, the EV test bed is required to respond to both the activation request and the P_set request sent by the VPP. Therefore the requirements for control are the same for both operation modes.

The activation requirement is implemented directly on the DC side of the power components, by using two DC contactors for the charger and the V2G inverter respectively. The diagram of Fig. 7 depicts the system architecture which realizes the control requirements. The onboard EV computer receives the charging/V2G schedule by the VPP, in the form of TCP/IP data packets, thus it converts the schedule into control signals for the contactors, through an I/O interface. The contactors are rated at 900V, 200A, and are connected on the positive terminal of the battery. The contactors are normally open, thus a voltage of 24V is applied on the contactor's coil by the I/O interface when an activation request is sent by the VPP.

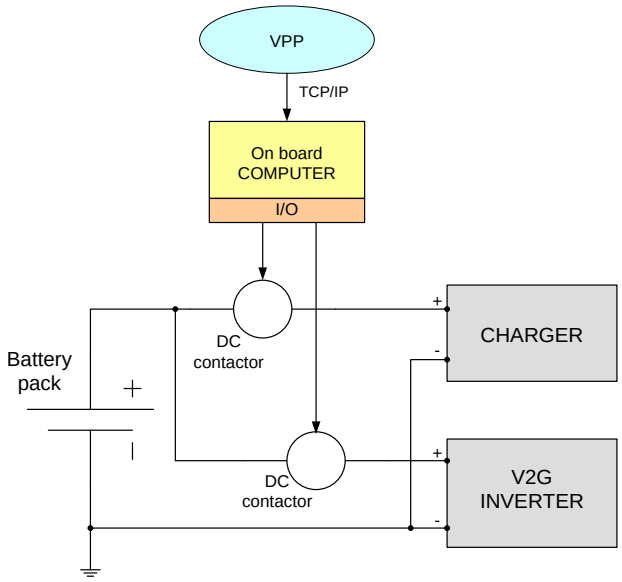

Fig. 7. Implementation of activation requirement

The power set point requirement, P_set, has been implemented for the V2G operation. A software interface using the communication standard RS485 was designed to communicate to the inverter the set point of the power level.

D. Coordination of Monitoring and Control

The implemented requirements of monitoring and control are not stand-alone functions taking place at different moments. A software interface, including both requirements, has been implemented to interface the monitoring and control functions with the VPP. The interface works as software plug-in which communicates with the BMS, the charger and the V2G inverter; it sends the collected data to the VPP for elaboration and it gets back the VPP requests for charging/V2G operation.

On top of the software plug-in, a server based on the communication Standard IEC 61850 was used to interface with the VPP [16].

V. Tests and Results

The implemented requirements of monitoring and control have been tested on the EV test bed, using a charging/V2G schedule generated by the Edison VPP, with power level of 2.3 kW, corresponding to the home charging case of Table I. The schedule is sent and received as a sequence of time stamps with format of hh:mm:ss as described below:

- Activation of charging operation, at 15:28:56; Charging power level set at 2.3 kW
- Deactivation of charging operation, at 15:43:56
- Activation of V2G operation, at 15:43:59; V2G power level set at 2.3 kW
- Deactivation of V2G operation, at 15:58:56
- Activation of charging operation, at 15:58:59; Charging power level set at 2.3 kW

The activation and deactivation apply to both charging and V2G operation. The control requirement has been tested setting a power level of 2.3 kW for the V2G operation. The charging power is instead fixed to 2.3 kW. To guarantee a safe change of operation from charging to V2G and vise versa, a time delay of 3 seconds is introduced via software between two consecutive commutations.

To verify that the defined requirements are met, the instant power and the SOC have been measured. All measurements were performed with a sample time of 1 second. The power on the grid side (P_{AC}) was measured on the grid connection point of the EV test bed. In addition to the essential monitoring requirements of SOC and Power, the current I_{DC} flowing into the battery and the terminal voltage of the battery pack V_{DC}, were measured during the test. The power on the battery side has been then calculated off-line and compared with P_{AC}. This allows estimating the efficiency during charging and V2G operation.

Test results are shown in Fig. 8 (a) and (b). In Fig. 8 (a) the power profile measured on the grid side, P_{AC}, and the SOC profile are depicted. The time axis is expressed in the same format as the schedule, e.g. hh:mm:ss. The initial condition of the SOC is 66% and the SOC resolution is 1%. It is observable that the charging profile, with duration 15 minutes, brings the SOC to a level of 70%. The activation of the V2G operation takes longer than the charging activation; this is due to the synchronization time with the grid frequency and check of the grid voltage, which occurs in the V2G inverter. This issue will be further addressed in a future work. A steady power profile, P_{AC}, of 2.3 kW is observable during both charging and discharging. This enlighten that both the charger and the V2G inverter correctly response to the power set point of 2.3 kW. A negative sign convention is used for representing the power during V2G operation.

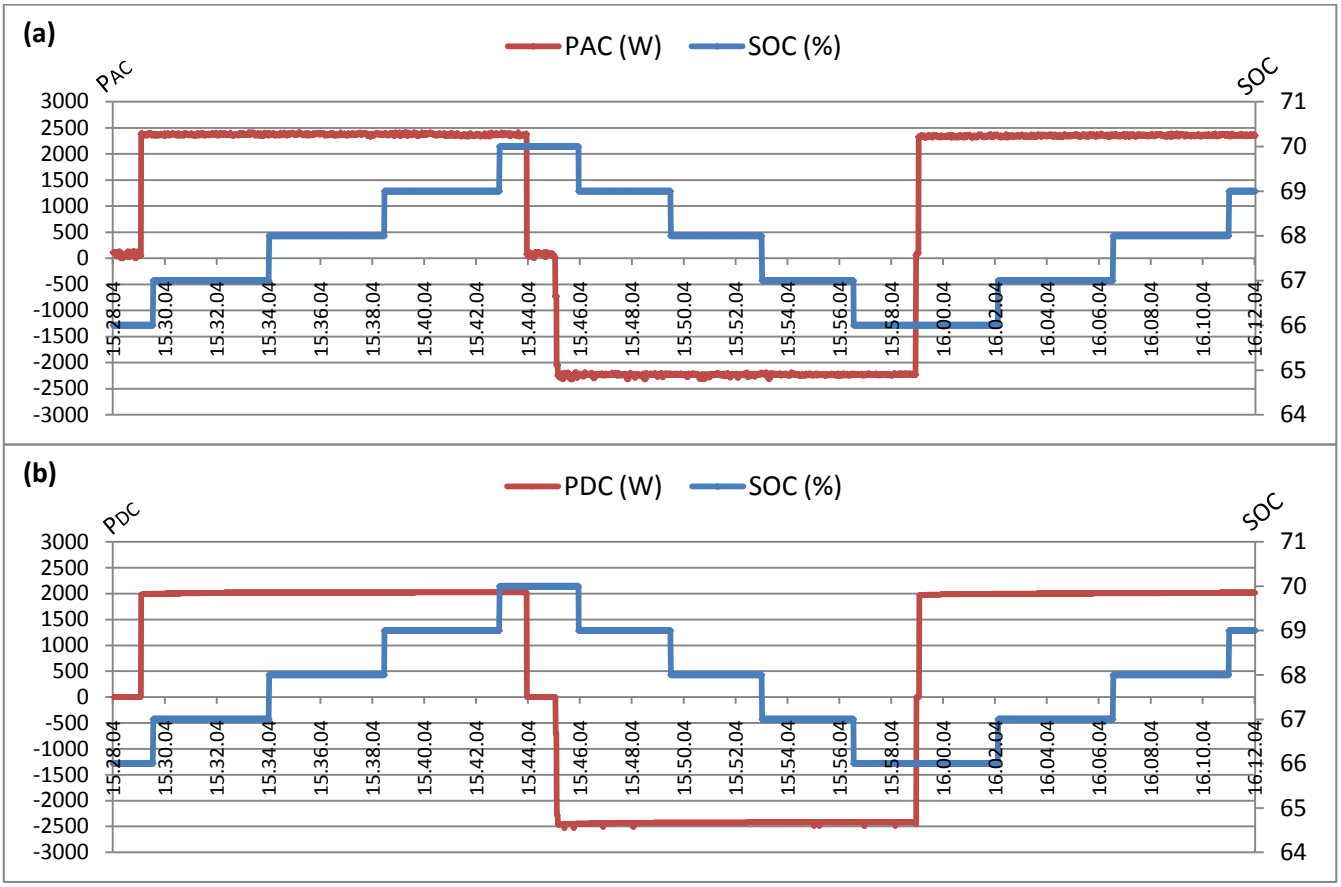

Fig. 8. Tests of monitoring and control requirements during charging and V2G operation. (a) Measurement of P_{AC} and SOC. (b) Calculated P_{DC} based on measurements of I_{DC} and V_{DC} on the battery side and measurement of SOC

In Fig. 8 (b) the calculated power P_{DC} is shown based on the measurements of I_{DC} and V_{DC}. In (3) the formula used to calculate P_{DC} is shown:

$$P_{DC} = V_{DC} \cdot I_{DC} \quad (3)$$

where the current I_{DC} during charging is taken with a positive sign, while with a negative sign during V2G operation.

In (4) and (5) the power P_{DC} is expressed in function of the efficiency η of the charger and the V2G inverter respectively.

$$P_{DC} = \eta_{CH} \cdot P_{AC} \quad (4)$$

$$P_{DC} = \eta_{V2G} \cdot P_{AC} \quad (5)$$

This efficiency is well estimated based on the calculated P_{DC} shown in Fig. 8 (b) and the measured P_{AC}. In particular, during charging, it is estimated an efficiency of about 87%, from grid to battery, while during V2G operation it is observed an efficiency of about 95% from battery to grid. This confirms the features claimed by the manufacturer.

Further analysis on the charging/V2G efficiency is not treated in this paper, since the scope is to define the requirements for EV operation in smart grids.

VI. Conclusions

The requirements needed for electric vehicles interaction in a smart grid scenario have been addressed in this work. The requirements have been defined with respect to the charging and V2G operation mode which an EV could enter during plug-in periods. The study identified that the SOC of the battery and the power exchanged between EVs and the grid are essential monitoring requirements. The activation/deactivation and the power set point have been identified as fundamental control requirements for the EVs charging/V2G operation. The defined requirements have been implemented on a real EV test bed and validation of intelligent EV operations within a VPP framework has been presented. The performed tests, based on the charging/V2G schedule generated by the Edison VPP, have shown that the defined requirements are sufficient to achieve an intelligent coordination of EVs. Experimental tests have shown that 1 second resolution for monitoring and control is possible and that this is enough to ensure an intelligent operation of EVs. The intelligent management of the charging/V2G operation is possible given an open access to BMS data, for monitoring, and to a vehicle computer for control. Estimating power losses and efficiency of the charging/discharging cycles is also possible given the defined requirements. In all, the findings offer to future EV coordinators and grid operators the possibility to increase their interaction for an intelligent deployment of EVs. Also, the results could serve as a stimulus for EV manufacturers to

consider EVs as a more flexible resource, on which the monitoring and control can be externally managed.

REFERENCES

[1] European Commission, "20 20 by 2020 Europe's climate change opportunity", COM (2008) 30 final, Brussels, 2008.

[2] Energinet.dk, "Environmental report 2010", online, 2010

[3] P. Morrison, A. Binder, B. Funieru, C. Sabirin, "Drive train design for medium-sized zero emission electric vehicles", *13th European Conference on Power Electronics and Applications*, 2009.

[4] K. Chen, A. Bouscayrol, A. Berthon, P. Delarue, D. Hissel, and R. Trigui, "Global modeling of different vehicles", *IEEE Vehicular Technology Magazine*, 2009

[5] W. Kempton and J. Tomic, "Vehicle-to-grid power fundamentals: Calculating capacity and net revenue", *J. Power Sources*, vol. 144, no. 1, pp. 268–279, Jun. 2005.

[6] C. Binding, D. Gantenbein, B. Jansen, O. Sundstrom, P. B. Andersen, F. Marra, B. Poulsen and C. Træholt, "Electric Vehicle Fleet Integration in the Danish EDISON Project - A Virtual Power Plant on the Island of Bornholm", *IEEE Power & Energy Society General Meeting*, 2009.

[7] B. Jansen, C. Binding, O. Sundström, D. Gantenbein, "Architecture and Communication of an Electric Vehicle Virtual Power Plant", in *IEEE Proc. First IEEE International Conference on Smart Grid Communications*, 2010

[8] Thunder Sky, LFP Li-ion battery user manual, 2009

[9] J. D. Dogger, B. Roossien, and F. Nieuwenhout, "Characterization of Li-Ion Batteries for Intelligent Management of Distributed Grid-Connected Storage", *IEEE Trans. on Energy Conversion, Vol. 26, No. 1*, 2011

[10] K. Clement-Nyns, E. Haesen and J. Driesen, "The Impact of Charging Plug-In Hybrid Electric Vehicles on a Residential Distribution Grid", *IEEE Transactions on Power Systems*, Vol. 25, No. 1, 2010.

[11] B. G. Kim, F. P. Tredeau and Z. M. Salameh, "Fast Chargeability Lithium Polymer Batteries", in *IEEE Power and Energy Society Conf.*, 2008.

[12] F. Marra, C. Træholt, E. Larsen, Q. Wu, "Average Behavior of Battery-Electric Vehicles for Distributed Energy Studies", *in IEEE Proc. Innovative Smart Grid Technology Europe*, 2010

[13] Nissan Leaf Electric Car, *Charging info*, www.nissanusa.com.

[14] Siemens AG, "Charge CP700A - The charging point with built in safety", online, 2011

[15] J. A. Pecas Lopes, F. J. Soares, P. M. Rocha Almeida, "Integration of Electric Vehicles in the Electric Power System", *in IEEE Proc.*, Vol. 99, No. 1, 2011

[16] A. Bro Pedersen, E. Bragi Hauksson, P. Bach Andersen, B. Poulsen, C. Træholt, and D. Gantenbein "Facilitating a generic communication interface to distributed energy resources", in *IEEE Proc. First IEEE International Conference on Smart Grid Communications*, 2010

Implementation of an Electric Vehicle Test Bed Controlled by a Virtual Power Plant for Contributing to Regulating Power Reserves

F. Marra, *Student Member*, *IEEE*, D. Sacchetti, A. B. Pedersen, P. B. Andersen, C. Træholt, and E. Larsen

***Abstract*-- With the increased focus on Electric Vehicles (EV) research and the potential benefits they bring for smart grid applications, there is a growing need for an evaluation platform connected to the electricity grid. This paper addresses the design of an EV test bed, which using real EV components and communication interfaces, is able to respond in real-time to smart grid control signals. The EV test bed is equipped with a Lithium-ion battery pack, a Battery Management System (BMS), a charger and a Vehicle-to-Grid (V2G) unit for feeding power back to the grid. The designed solution serves as a multifunctional grid-interactive EV, which a Virtual Power Plant (VPP) or a generic EV coordinator could use for testing different control strategies, such as EV contribution to regulating power reserves. The EV coordination is realized using the IEC 61850 modeling standard in the communication. Regulating power requests from the Danish TSO are used as a proof-of-concept, to demonstrate the EV test bed power response. Test results have proven the capability to respond to frequent power control requests and they reveal the potential EV ability for contributing to regulating power reserves.**

***Index Terms*— Electric vehicles, Test Bed, Regulating power, Virtual Power Plant**

I. Introduction

THE Electric Vehicles and Plug-in Hybrid EV (PHEV) are expected to play an important role in the future power system. Within smart grids research, electrical transportation has a complementary role in the overall system management of energy and power [1]; moreover the European target on reducing CO_2 emissions and increasing penetration of renewable energy are among the major drivers for the research [2].

The energy storage capability is the key factor for smart grid applications of EV in power system. When parked and plugged into the grid, EV are expected to either charge intelligently, or discharge feeding power back to the grid [3]. In the latter case, EV would enter a mode known as Vehicle-to-Grid (V2G), permitting the provision of several grid services [4]. In general, if the individual EV can be intelligently managed, a large number of such vehicles can become an asset in the future power system. The charging process could be controlled by modulating the charging power, as well as the discharging process, by enabling the V2G mode when there is a need from the grid [5]. Many projects are addressing the aforementioned EV operation, as coordinated charging using different simulation tools. In [6], the authors analyze, through dynamic simulations, the potential daily profits for EV users, with the provision of regulating power. In [7], the authors studied the benefits offered by EV for facilitating the integration of large scale wind power in Denmark; EV fleets are modeled in a simulation platform as storage units when charging or as small generators during V2G operation. Galus et al. in [8] presented a method for tracking secondary frequency control using groups of PHEV and a simulation platform to simulate an EV aggregator.

The participation of EV in regulating power schemes is possible using an aggregation entity for EV coordination. This is done in the Danish EDISON project [9]-[10], where the contributors proposed a centralized coordination solution for an efficient integration of EV in the power system. The aggregation technology is based on the Virtual Power Plant (VPP) concept [11], where the Edison VPP is the EV coordinator.

Evaluating the contribution of an EV for regulating power reserves in a VPP framework, where a huge amount of communication and hardware interfaces are involved, gives raise to the need of new grid-interactive evaluation platform.

This paper describes the implementation phases of an EV test bed, working under the coordination of a VPP and contributing in regulating power reserves, as secondary frequency control [12]. A real regulating power request from the Danish Transmission System Operator (TSO) is processed by the VPP and sent in form of a charging/discharging power schedule to the EV test bed.

Test results performed using the EV test bed show that an EV is in fact capable of real-time communication with a VPP and can quickly react to contribute to grid power reserves.

II. Electric Vehicles for Smart Grids

The interaction between EV and the electric power system is only possible if the vehicles can connect to the electrical

This work was in part funded through the EDISON project, a research project of the public Danish transmission system operator Energinet.dk's research program FORSKEL, (Project Number 081216).

F. Marra, D. Sacchetti, A. B. Pedersen, P. B. Andersen, C. Træholt, and E. Larsen are with the Centre for Electric Technology, Department of Electrical Engineering, Technical University of Denmark, 2800 Kgs. Lyngby, Denmark (e-mail: fm@elektro.dtu.dk).

grid for charging.

An effective interaction between EV and grid requires the combinations of different factors such as:

- Grid interactive vehicle architectures;
- Controllable charging/discharging operation;

A. Electric vehicle architectures

Among different types of hybrid electric vehicles and pure electric vehicles, a general distinction is based on their ability to plug-in. In this work, non plug-in hybrid vehicles will be disregarded, as an interconnection with the grid is not possible.

This section lists the system architectures capable of charging using the grid [13]. There are mainly two classes of plug-in EV: plug-in hybrid EV (PHEV) and battery-powered EV. An overview on the different architectures is depicted in Fig. 1.

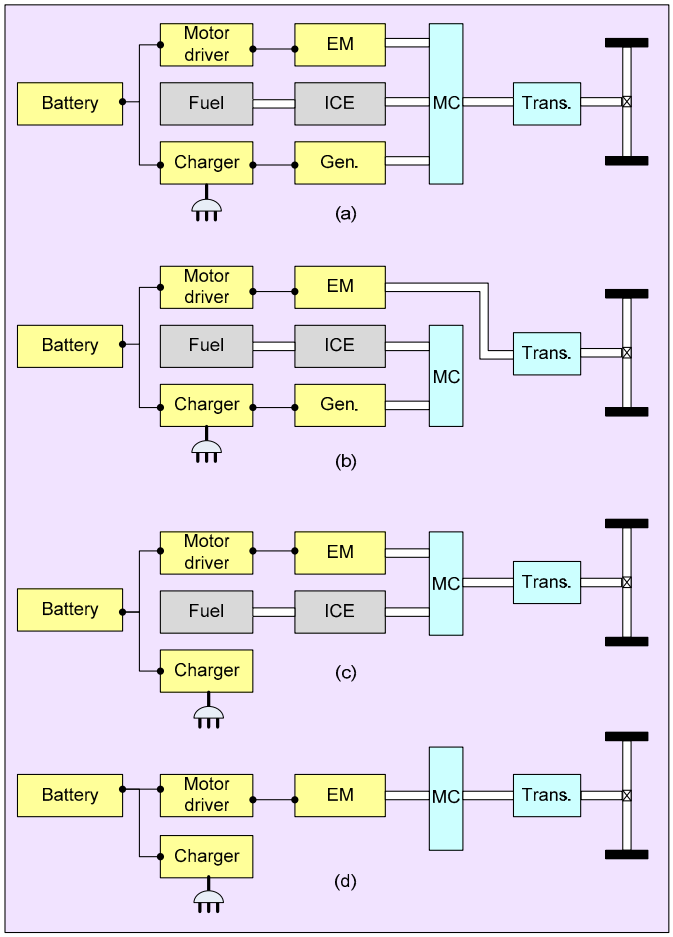

Fig. 1. Plug-in Electric Vehicles system architectures. (a) Series-parallel hybrid EV. (b) Series hybrid EV. (c) Parallel hybrid EV. (d) Battery-powered EV

In the PHEV class, three variants have been developed so far:

- Series-parallel hybrid
- Series hybrid
- Parallel hybrid

The main difference among the topologies is the drive system used and the interconnection of its components, before the power is transferred to the wheels.

In the series-parallel hybrid vehicle, Fig. 1 (a), the system is designed to operate both in a series or parallel configuration. The reconfigurable system is made possible by the use of a planetary gear, which is the mechanical coupling (MC) for the three machines. In the series hybrid vehicle, Fig. 1 (b), the electric traction system and Internal Combustion Engine (ICE) system operate in a series connection. In sequence, the ICE is coupled with a generator (Gen.) which generates the electric power for recharging the battery, the battery then supplies an electric motor driver to transfer power to wheels. In the parallel hybrid vehicle, Fig. 1 (c), the ICE and electric motor (EM) operate in parallel mode, where the ICE supports the electric traction at certain points of the driving pattern, e.g. when higher power is needed to the wheels.

In the battery-powered EV class, Fig. 1 (d), the drive system is realized using only an electric motor and a motor driver. Therefore the only energy source is the battery pack.

In this work a battery-powered EV is the architecture chosen for the EV test bed implementation.

B. Controllable charging/discharging operation

All plug-in EV are able to absorb power from the grid while charging their battery packs. The controlled charging or discharging (V2G) process can be achieved using different infrastructure concepts, such as home charging or public charging stations [14]. According to the IEC 61851 standard [15], the most common power rates for domestic and public charging are depicted in Table I.

TABLE I
CHARGING POWER RATES

AC current	AC voltage	Grid connection	Power
10 A	230 V	single phase	2.3 kW
16 A	230 V	single phase	3.7 kW
32 A	230 V	single phase	7.4 kW
16 A	400 V	three-phase	11 kW
32 A	400 V	three-phase	22 kW

All power rates, regardless of charging or discharging, are characterized by an AC current, usually 16A or 32A, and based on the grid connection type, single-phase or three-phase.

In this work a charging/discharging power rate of ± 2.3 kW is used for the experimental validation.

C. Planned EV test bed operation with Virtual Power Plant

The EV system architecture is planned to respond to different control signals from a centralized EV coordinator.

The control signals for the vehicles can be generated by a VPP and based on different variables such as the power system frequency, the market spot price and others.

In this paper, the centralized control concept for EV fleet management as described by Binding et al. in [10] is used as a study framework. The EV test bed operation is planned within the VPP framework depicted in Fig. 2. Different interfaces have been defined to establish communication between the Edison VPP and other entities in the architecture. While a

generic VPP can aggregate and control various distributed energy resources (DERs), e.g. combined heat and power units (CHPs), PV plants, wind turbines, medium/large consumers, other power units and smart houses, in this paper, only EV are considered.

An interface with the TSO is defined to receive the activation commands for accepted regulating power reserves contracts.

An interface with the Distribution System Operator (DSO) is also defined to collect the grid status for the location of every connected EV. Grid constraints are considered at this interface, to ensure that the charging/discharging operation complies with power quality issues. In addition, the metering information for accounting is also collected via the DSO interface.

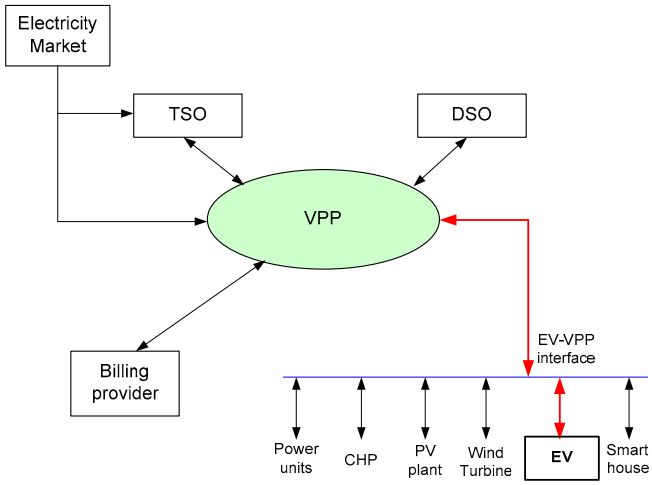

Fig. 2. EV test bed operation in a Virtual Power Plant framework

The transaction interface with a billing provider is used to perform billing to the resources providing regulating services.

In this paper, the EV-VPP interface is implemented to establish communication between the VPP and the EV test bed. The control requests for the EV test bed are generated from the VPP, based on the grid needs of regulating power reserves of the TSO.

III. Test Bed Implementation

Designing an EV test bed for testing the potential EV operation with a VPP was performed in two phases:

- Planning the EV test bed architecture
- Dimensioning the EV components

A. Planning the EV test bed architecture

With reference to the EV architectures described in Section II, a battery-powered EV architecture was the choice for the EV test bed implementation. The main reasons for choosing this architecture is that with a pure battery EV, zero emissions can be achieved during driving [16], while grid interaction is more meaningful, due to a larger storage capacity.

In a battery-EV the following components can be considered:

- a battery pack
- a battery charger
- a BMS
- a three-phase motor driver
- an electric motor

For the scope of the study, the three-phase motor driver and the electric motor are not needed, therefore these two components were not considered in the development.

Since with the architecture of Fig. 1 (d), the V2G operation is not possible, this was enhanced by adding a V2G unit which could operate in a complementary way to the charger. The implemented EV test bed architecture is shown Fig. 3.

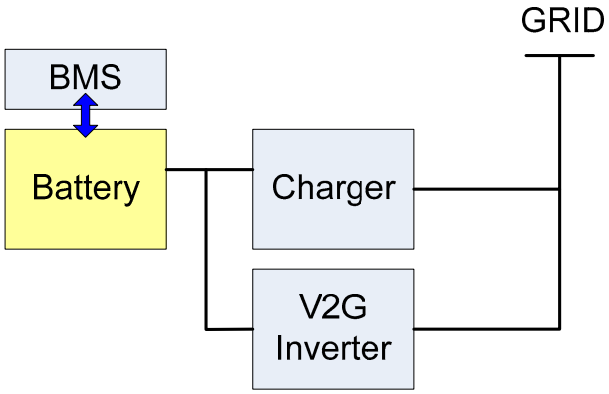

Fig. 3. EV test bed architecture

The battery pack is interfaced to a battery management system (BMS), which monitors its status.

The charger is designed as an AC/DC converter, directly connected to the main grid, by means of a three phase cable connection; while the V2G unit is made of a single phase DC/AC inverter.

It is worth noticing that, since the aim of the EV test bed is to emulate a real EV connected to the grid, all EV components were dimensioned according to realistic EV energy and power levels.

B. EV test bed components

The design of the battery pack took into account the following requirements:

- Common designs of battery-EV [17][18]
- V2G operation requirement

The choice of a battery technology to use for the test bed was based on the analysis of current market trends for EV. Some consulting companies, e.g. Frost & Sullivan [19], foresee more than 70% of EV in 2015 to be powered by lithium-ion (Li-ion) batteries. Compared to other battery technologies, Li-ion batteries offer a greater energy-to-weight ratio, greater power levels and low self-discharge when not in use [16]. For the reasons mentioned, a Li-ion battery was the choice for the EV test bed.

The electrical features of the battery pack were chosen considering common designs of EV battery packs. Generally

battery-EV have battery pack voltages in the range of 300-400V and a battery capacity of at least 10-15 kWh. A battery pack was designed integrating 110 Li-ion series connected battery cells, which leads to a total nominal pack voltage, V_{pack}, of 363 V. Each cell has nominal voltage V_n, of 3.3 V and nominal capacity C_n, of 40 Ah.

Based on the nominal parameters, the following expression is valid for calculating the nominal battery energy:

$$E_n = V_{pack} \cdot C_n = N \cdot V_n \cdot C_n \quad (1)$$

where N is the number of cells.

The requirement of V2G operation, a DC/AC power converter with input DC voltage in the range of 250 – 500 V was used. The rated output power of the V2G inverter is about 4 kW, which leads to a maximum generated AC current of around 16 A. The V2G inverter is also equipped with an internal transformer, which serves as galvanic isolation.

A battery management system (BMS) is linked to the battery pack. The main function of the BMS is to ensure a safe operation of the battery pack during charging or V2G operation. It estimates the SOC information which is used by VPP and monitors the battery voltage, current and temperature.

The charger was designed as a single-phase AC/DC. The output voltage V_{dc} was dimensioned using the empirical formula shown below, according to [20]:

$$V_{dc} = 1.25 \cdot V_{pack} = 453\ V \quad (2)$$

The current I_{dc} on the battery side is dimensioned of 10 A at full load, which leads a charging power of about 4.5 kW.

The implemented test bed with integrated EV components is depicted in Fig. 4.

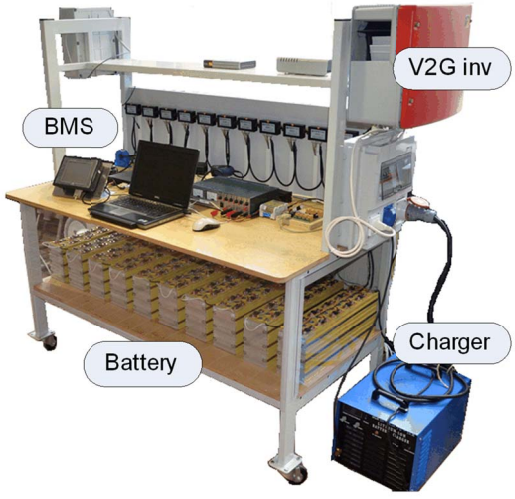

Fig. 4. EV test bed

IV. Communication and Control with VPP

As previously mentioned, the EV test bed was designed to operate as part of a centralized aggregation framework, under the direct control of a VPP, as described in [21]. For the purpose of future research, it will be possible, in any case, to adapt the software system in order to e.g. test decentralized control schemes.

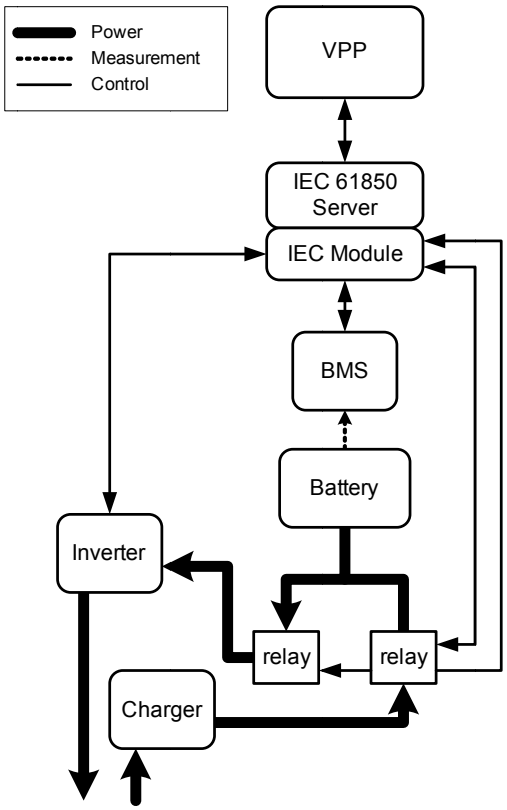

Fig. 5. EV test bed communication and control architecture

To facilitate centralized coordination, the VPP-to-EV interface was implemented in accordance with the communication and control architecture depicted in Fig. 5.

The communication is based on the well-established IEC 61850 standard [22]. As an academic exercise and in the attempt to promote the use of existing web standards in power system communication, the IEC 61850 standard was mapped to HTTP/REST. This work was presented in details in [23].

The VPP used for this paper was designed by Pedersen et al. [23] and has been used for generating and sending power schedules, in response to the requirements for regulating power reserves specified by the TSO.

Though used for an EV test bed in this case, these schedules are simply based on positive/negative power requests with an associated time stamp. For this reason, they are potentially applicable to any type of Distributed Energy Resource (DER) [24].

A. IEC 61850 Server and Module

The server, which was developed in compliance with the IEC 61850 standard, is designed based on a modular plug-in architecture, in order to facilitate an easier adaptation and installation of new devices of virtually any type [23].

A device specific plug-in, or IEC Module, was implemented, in order to enable direct control of the test bed from the VPP, as well as to facilitate the collection of battery status information along with any other measurements.

Because the charger and inverter are two separate pieces of hardware connected to the same battery, an algorithm was written into the plug-in module to guarantee the mutually-exclusive operation of the connecting relays. This prevents the simultaneous operation of both devices.

Another communication link is established between software plug-in and the BMS to extract the state-of-charge (SOC) information from the battery.

B. Charging

As indicated by Fig. 6, there is no direct control link between the IEC Module and the charger; this is because the charger has not communication interface for remote control. For the purpose of this paper, the charger is fixed to a fixed power rate and is coupled or decoupled from the battery by means of a DC relay, which is controlled via RS232, as illustrated in Fig..

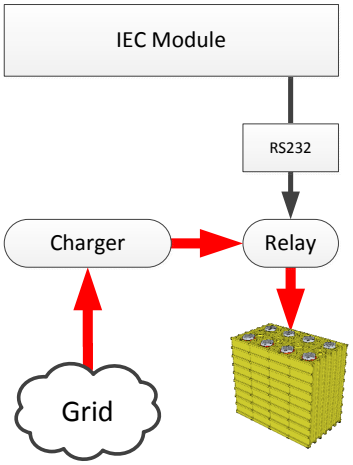

Fig. 6. Charging communication in detail

As previously mentioned, the charger and inverter are both connected to the battery pack using two mutually exclusive relays. In order to ensure that the devices have exclusive "access" to the battery, a simple timing scheme was used in the IEC Module. As depicted in Fig., a time gap was added between two switching events to ensure a safe transition.

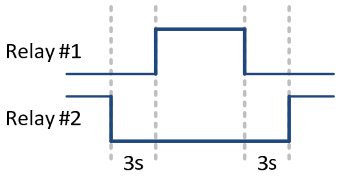

Fig. 7. Relay timing scheme

C. V2G

The coupling of the V2G inverter is achieved by means of an identical DC relay as for the charger. Under V2G operation, the generated power level is controllable and this is managed through an attached communication hub. The same hub implements an HTTP/JSON web interface. A more detailed illustration of the V2G architecture used for the EV test bed is depicted in Fig. 8.

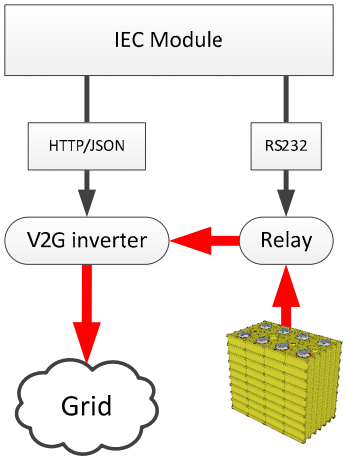

Fig. 8. V2G communication in detail

D. Battery Status Information

The real-time status of the battery is monitored by the BMS. The BMS information is acquired by the IEC Module using RS485 based serial communication link. By means of this link, all battery data can be extracted as a set of values and made available to the VPP via IEC 61850 for detailed monitoring. The set of values includes:

- Battery pack voltage
- Current
- State of charge
- Temperature in different areas of the battery pack
- Remaining energy and single cell voltages

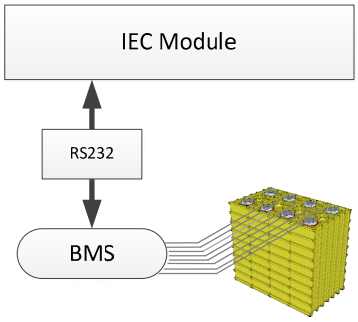

Fig. 9. BMS communication in detail

The BMS comes equipped with an RS232 port for remote monitoring of the battery pack, as well as controlling various limits/alarms. Connected to the BMS are a series of sensors, which connection are depicted as a series of smaller wires in Fig..

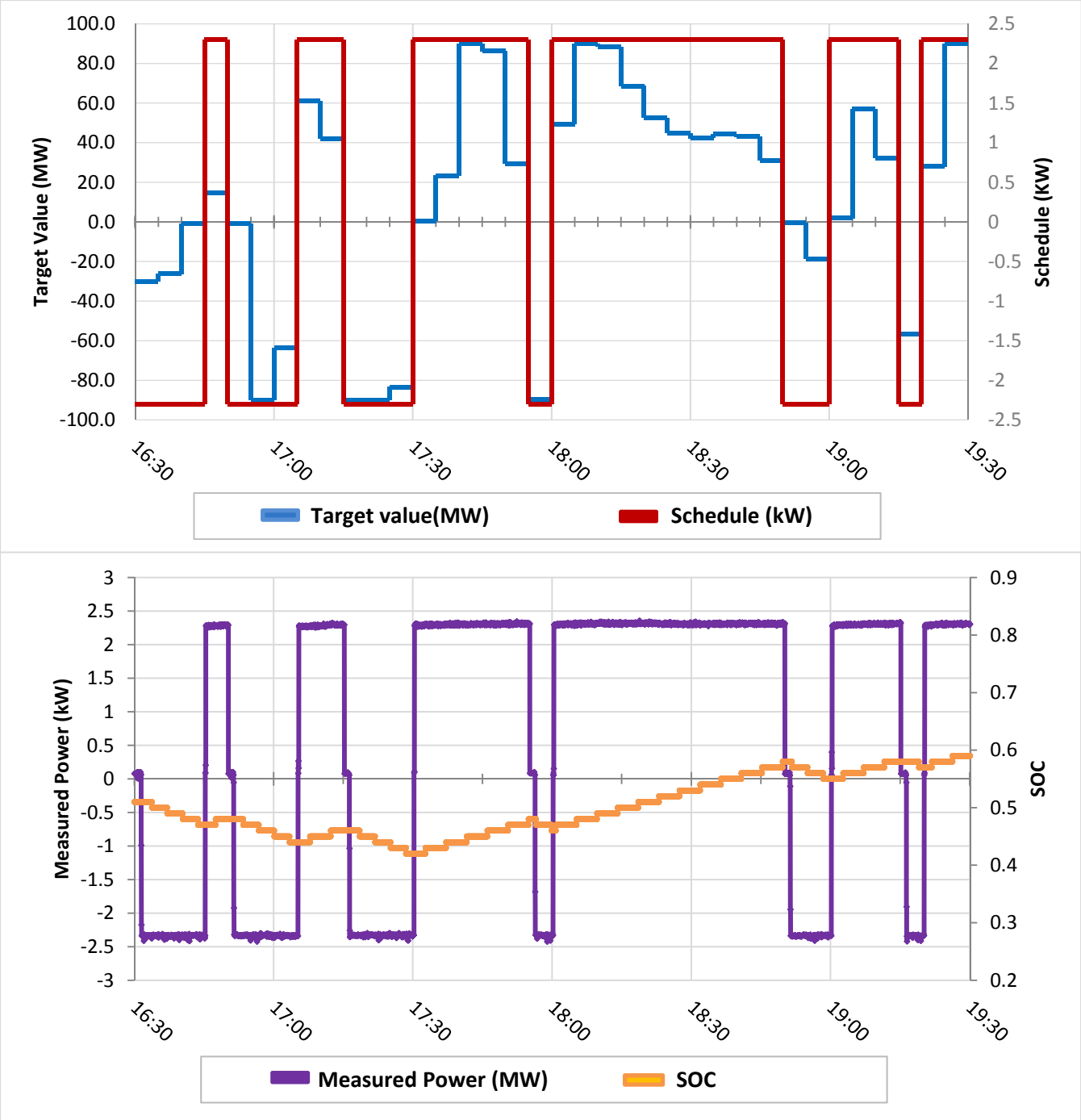

Fig. 10. Test results of EV test bed contribution in regulating power service – Secondary control. (a) Target regulating power of the Danish TSO and VPP generated schedule for the EV test bed and the other EV. (b) Measured power response and battery SOC of EV test bed.

V. Experimental Results

The EV test bed participation in regulating power reserves was tested considering the regulating power required for secondary control, by the Danish TSO, on the 1st of January 2009 [25]. The regulating power profile sent from the TSO to the VPP is given in 5-minutes average MW values as shown in Fig. 10(a). The target regulating power is derived by the sum of all up and down regulation requests sent out by the TSO to an array of providers in the same 5-minutes. The target anyway does not reflect the exact need of the system but rather the value is used to drag the providers in the right direction. Nevertheless, the target value is a very good approximation to the real-time need of regulation reserves.

A new schedule, related to the TSO power target, was generated by the VPP every 5-minutes, and sent to the EV test bed. The regulation was tested in the time interval 16h30 to 19h30. The schedule is shaped as ±2.3 kW power requests with time stamps, indicating the activation/deactivation time of charging and V2G mode, Fig. 10(a). Since each EV has a very small capacity compared to the grid needs, it was assumed that the VPP meets the TSO target by aggregating a number of simulated EV. The EV system response, Fig. 10(b), is taken measuring the electric power flow at the point of

common coupling (PCC) of the EV test bed with the grid. The power was recorded with 1 minute sampling time. Test results are depicted in Fig. 10(b). It is possible to observe that the EV test bed is able to react in real-time to the power schedule sent by the VPP. The measured power profile in Fig. 10(b) validates the effectiveness of the EV architecture proposed in this work. Furthermore, the SOC profile shows the energy variation in the EV test bed battery, during the regulation service. The EV test bed started to contribute to regulating power service with an initial SOC of about 0.5 or 50%.

VI. Conclusions

Testing the capabilities of EV for smart grid applications requires the development of adequate evaluation platforms. In literature it was demonstrated that EV can potentially operate under a number of coordination schemes, including the participation in regulating power reserves. While this was extensively presented by simulation scenarios, in this paper, a real implementation of regulating power reserve performed by a full-scale EV test bed was presented. The test bed was designed to flexibly interact in real-time with an EV coordinator and the electricity grid, under different coordination concepts. To do so, real EV components and communication interfaces were used, that make possible an end-to-end interaction with a VPP. The implementation of an EV test bed from scratch enabled the management of the single components involved in the EV system: charging/discharging units and BMS. With the implemented communication and control architecture it was possible to establish a stable communication between the EV the test bed and the Virtual Power Plant.

The potential offered by EV for regulating power was demonstrated testing the EV test bed hardware and software interfaces. An array of regulating power requests (load frequency control) within a 3-hours time interval, sent by the Danish TSO on the 1st of January 2009, was used as study case. The TSO target values were converted to an EV compatible schedule by the Edison VPP and sent down to the EV test bed among the other simulated EV. Test results revealed the potential capability of EV to respond in real-time to different charging/discharging requests based on different coordination plans. Further investigations will be performed for evaluating the reliability of the communication involved, when several fleets of EV are simultaneously coordinated.

Acknowledgments

The authors would like to thank Sammarco Elettronica, Italy, for the technical support offered in the realization of the Electric Vehicle test bed.

References

[1] J. A. Pecas Lopes, F. Joel Soares, and P. M. Rocha Almeida, "Integration of Electric Vehicles in the Electric Power System", *in Proc. IEEE, Vol. 99*, 2011

[2] European Commission, "20 20 by 2020 Europe's climate change opportunity", COM (2008) 30 final, Brussels, 2008.

[3] A. Brooks, "Integration of electric drive vehicles with the power grid – a new application for vehicle batteries", in *Battery Conference on Applications and Advances. The Seventeenth Annual*, 2002.

[4] W. Kempton and J. Tomic, "Vehicle-to-grid power fundamentals: Calculating capacity and net revenue", *J. Power Sources*, vol. 144, no. 1, pp. 268–279, Jun. 2005.

[5] S. Deilami, A.S. Masoum, P. S. Moses, M. A. S. Masoum, "Real-time coordination of Plug-in Electric Vehicle Charging in Smart Grids to Minimize Power Losses and Improve Voltage Profile", in *IEEE Transactions on Smart Grid*, Vol. 2, no. 3, pp. 456-467, 2011.

[6] N. Rotering, M. Ilic, "Optimal Charge Control of Plug-in Hybrid Electric Vehicles in Deregulated Electricity Markets", in *IEEE Transactions on Power Systems*, Vol. 26, no. 3, pp. 1021-1029, 2011.

[7] J. R. Pillai and B. Bak-Jensen, "Vehicle-to-grid systems for frequency regulation in an Islanded Danish distribution network", in *IEEE Proc. Vehicle Power and Propulsion Conference (VPPC)*, 2010.

[8] M. D. Galus, S. Koch, G. Andersson, "Provision of Load Frequency Control by PHEVs, Controllable Loads, and a Cogeneration Unit", *in IEEE Transactions on Industrial Electronics, Vol. 58*, Nr. 10, 2011.

[9] B. Jansen, C. Binding, O. Sundström, D. Gantenbein, "Architecture and Communication of an Electric Vehicle Virtual Power Plant", in *IEEE Proc. First IEEE International Conference on Smart Grid Communications*, 2010

[10] C. Binding, D. Gantenbein, B. Jansen, O. Sundstrom, P. B. Andersen, F. Marra, B. Poulsen and C. Træholt, "Electric Vehicle Fleet Integration in the Danish EDISON Project - A Virtual Power Plant on the Island of Bornholm", *IEEE Power & Energy Society General Meeting*, 2009.

[11] N. Ruiz, I. Cobelo, J. Oyrzabal, "A Direct Load Control Model for Virtual Power Plant Management", in IEEE Transactions of Power Systems, Vol. 24, No. 2, pp. 959-966, 2009.

[12] J. L. Aguero, M. C. Berequi, F. Issouribehere, "Grid Frequency Control. Secondary frequency control tuning taking into account distributed primary frequency control", in *IEEE Proc. of Power and Energy Society General Meeting*, 2010.

[13] K. Chen, A. Bouscayrol, A. Berthon, P. Delarue, D. Hissel, and R. Trigui, "Global modeling of different vehicles", *IEEE Vehicular Technology Magazine*, 2009

[14] B. Lunz, T. Pollok, A. Schnettler, R. W. De Doncker, D. U. Sauer, "Evaluation of Battery Charging Concepts for Electric Vehicles and Plug-in Hybrid Electric Vehicles", *Advanced Automotive Battery Conference (AABC),* 2009

[15] IEC 61851, Electric vehicle conductive charging system – Electric vehicles requirements for conductive connection of an a.c./d.c. power supply.

[16] P. Morrison, A. Binder, B. Funieru, C. Sabirin, "Drive train design for medium-sized zero emission electric vehicles", *13th European Conference on Power Electronics and Applications*, 2009.

[17] General Motors, "Chevrolet Volt – Quick reference sheet", online

[18] Nissan, "Overview of Nissan Leaf", in *News Releases*, www.nissan-global.com, 2010

[19] Frost & Sullivan, "M5B6-Global Electric Vehicles Lithium-ion Battery Second Life and Recycling Market Analysis", public report, 2010.

[20] Thunder Sky, Li-ion battery user manual

[21] EDISON project, "WP3 report D3.1", www.edison-net.dk

[22] IEC 61850 Part 7-420

[23] A. Bro Pedersen, E. Bragi Hauksson, P. Bach Andersen, B. Poulsen, C. Træholt, and D. Gantenbein "Facilitating a generic communication interface to distributed energy resources", in *IEEE Proc. First IEEE International Conference on Smart Grid Communications*, 2010

[24] A. Timbus, M. Larsson, and C. Yuen, "Active Management of Distributed Energy Resources Using Standardized Communications and Modern Information Technologies", in *IEEE Transactions on Industrial Electronics*, Vol. 56, Nr. 10, pp. 4029-4037, 2009

[25] Energinet.dk, "Load Frequency Control - Secondary Reserve data", January, 2009.

Average Behavior of Battery-Electric Vehicles for Distributed Energy Studies

Francesco Marra, Chresten Træholt, Esben Larsen and Qiuwei Wu
Technical University of Denmark

***Abstract* – The increased focus on electric vehicles (EVs) as distributed energy resources calls for new concepts of aggregated models of batteries. Despite the developed battery models for EV applications, when looking at the scenarios of energy storage, both geographical-temporal aspects and EVs use conditions cannot be neglected for an estimation of the available fleet energy. In this paper we obtained an average behavior of battery-EVs, in relation to a number of variables such as current rates for charging and discharging, temperature, depth-of-discharge and number of cycles. An average approach was applied to calculate the influence of each variable on the battery energy and lifetime. The obtained results show that battery-EVs are non-linear time-variant systems which however can be modeled with good approximation if time, geographical location and battery use conditions are known.**

***Index Terms* – Battery average behavior, distributed energy resources, grid energy storage, plug-in electric vehicles, electric vehicles**

NOMENCLATURE

SOC	State-of-charge: percentage of remaining battery capacity
DOD	Depth-of-discharge: percentage of used battery capacity
SOH	State-of-health: indicator of battery lifetime
HEV	Hybrid electric vehicle are not pluggable into the electricity grid, not grid-interactive
PHEV	Pug-in hybrid electric vehicle are pluggable into the electricity grid, grid-interactive
V2G	Vehicle-to-grid operation: electric vehicles deliver power to the electricity grid

I. INTRODUCTION

The capability of battery-EVs to act as distributed energy storage in the grid is gaining increased attention. Research on smart-grids is addressing the possibility of using these vehicles for power balancing purposes in the power system by remote control of the charge/discharge process [1]. Key challenges for this role are the estimation of the available energy and lifetime of the batteries.

The main factors which characterize a battery-EV are depicted in Fig. 1. Whereas power, safety and cost are classic aspects of a vehicle, the energy and lifetime are more relevant in a distributed energy scenario and thus need to be assessed.

This paper proposes the concept of an average behavior of battery-EVs, in a real-life domain, where external parameters and several use conditions are taken into account. The final goal is the estimation of the available energy and lifetime of a battery-EV.

First, a number of battery models were analyzed to assess different battery performances with respect to different work conditions. The focus of the analysis was dedicated to lithium based batteries, due to their advantages compared with lead-acid and nickel based types, in terms of energy density, power density and lifetime. The analyzed models show the dependency of the battery performances on a number of variables and demonstrate their non-linear time-variant behavior.

As a second step, an assessment on battery-EVs use conditions was performed. The analyzed battery models were combined with probable cases of EVs utilization. Due to the fast charging capability of lithium batteries, the option of charging them at different current rates was considered. Current rates are addressed using the terminology “C rate”, where 1C indicates the nominal current of the battery in Ampere-hours. A trade-off on DOD values was defined in relation to the manufacturer constraints and battery life expectation. The variable of temperature was considered for both ageing assessment and for the evaluation of the available energy at low temperatures.

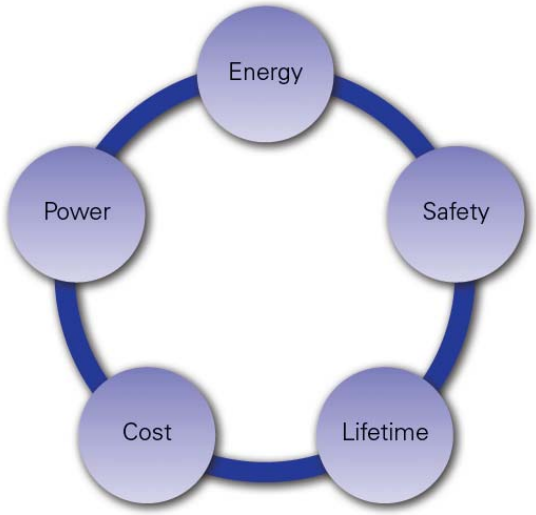

Fig. 1 Factors characterizing a Battery-EV

Finally, an average behavior of a battery-EV was derived using a mathematical average method. This approach wanted to mimics the behavior of EV fleets in localized areas, under a range of work conditions. The developed concept enables the estimation of available energy of an EV fleet, depending on a number of variables such as temperature, current rates, DOD and number of cycles.

II. BACKGROUND

From a fleet aggregator perspective, in a distributed energy scenario, plug-in EVs are considered an energy storage component by means of their battery pack [2]. The batteries are considered to be lithium technology based, since they represent the most promising option for EVs applications, in terms of volumetric and gravimetric energy density [3].
The battery of a generic EV is characterized by a time-variant non-linear behavior of energy and lifetime, which are dependent on a number of variables.

The theoretical energy of a generic battery-EV is described by the following formula:

$$E_n = V_n \cdot C_n = V_n \cdot I_n \cdot h \quad [KWh] \quad (1)$$

The battery pack energy E_n is expressed in KWh and is calculated by multiplying the nominal battery pack voltage V_n with the nominal battery capacity C_n, expressed in Ampere-hours, $I_n \cdot h$.
The battery lifetime is widely considered as the number of complete cycles that brings the battery capacity down to 80% of nominal capacity. The battery lifetime is therefore expressed in number of cycles.
Unfortunately, the real energy and lifetime of a battery are non-linear time-variant, which vary depending on climatic and use conditions. A number of lithium battery models were analyzed, looking at the development of some battery's internal parameters [4]. These works asserted that:

- Low temperature strongly affects the charging/discharging capability and the available energy of a battery
- High temperature accelerates the energy fade and shorten the battery lifetime
- Full DOD accelerates the energy fade and shorten the battery lifetime
- High current rates, for both charging and discharging, accelerate the energy fade and shorten the battery lifetime

Energy fade and lifetime are assessed measuring the variation R/R_{new}, where R is the actual internal resistance of the battery and R_{new} is the initial value of resistance. In [4] it was shown that the increase of the battery internal resistance, known also as ohmic resistance, lowers the battery discharge voltage, shorten the discharge time, increase the internal power losses and have a direct impact on the battery's power characteristics. As a consequence of the above effects, the rise of internal resistance indirectly affects the available energy and lifetime of a battery-EV. The three variables that mainly affect the battery internal resistance are the charge/discharge current rates, the DOD and the temperature. In [4] these variables were addressed to estimate the internal resistance rise over the number of cycles. The study justifies the use of the internal resistance as evaluation index of the battery state of health.

A. Charge/discharge current rates

The dependency of battery behavior on current rates was analyzed in [5]. In Fig. 2, the variation of internal resistance as a function of different current rates is depicted. Discharging an ideal battery, from fully charged state, with 2C rate would take 30 minutes, while discharging it at 5C rate would take 12 minutes. In [5] some tests were conducted with five different current rates and three different temperature values. It was observed that the battery may be fast charged at high current rates if a cooling system keeps the temperature under control. At a temperature of -20°C the 3C fast charging is not possible, while at 0°C the battery may be fast charged if a heating system is provided.

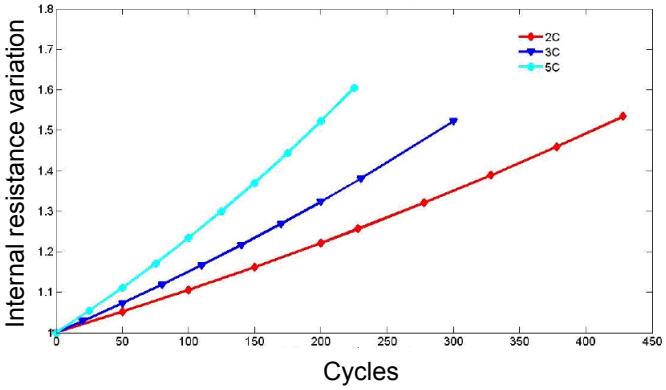

Fig. 2 Internal resistance variation function of current rates [7]

These tests demonstrated that the temperature is an important variable when slow or fast-charging are employed.

B. Depth of discharge (DOD)

The DOD's influence on the battery lifetime was investigated in [6]. The DOD is a fraction of the nominal capacity of the battery. Fig. 3 shows different trends of the internal resistance, function of three different DOD levels.

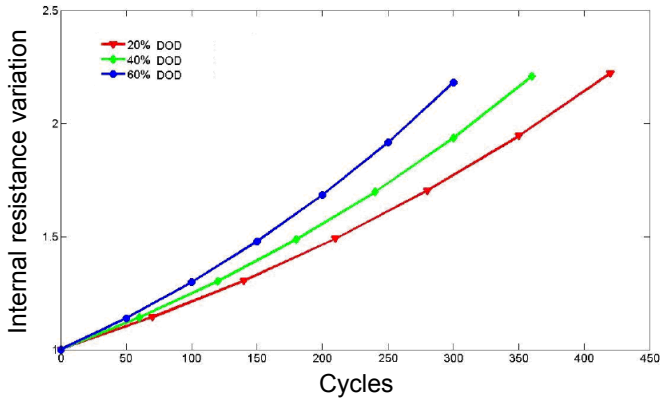

Fig. 3 Internal resistance variation function of DOD [7]

In [6] it was demonstrated that the higher the DOD, the faster battery lifetime decreases.

C. Temperature

In [7] it was shown that a range of temperature conditions at the same current rate, 100% DOD, considerably influences the battery lifetime. In [4], it is possible to compare the internal resistance variation, between two values of temperature: 50°C and 20°C.

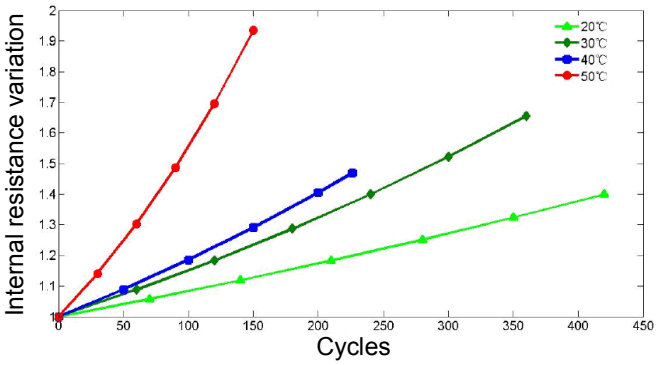

Fig. 4 Internal resistance variation function of temperature [7]

As depicted in Fig. 4, the study conducted under accelerated life tests, shows that the battery lifetime is about 3 times shorter if working at 50°C.

III. Battery-EVs Pre-Assumptions

The possible use conditions of battery-EVs have relevant implications on the battery behavior as described in the previous chapter. Different assumptions on plug-in vehicles utilization were done in order to assess the available energy and expected lifetime of the vehicles. At the scope, PHEVs, pure EVs and HEVs were compared for what concerns battery system design, DOD levels, current rates, temperature performances and number of cycles.

A. Battery system considerations

Since a few years ago, the majority of battery powered vehicles, both hybrid and plug-in were designed using nickel-metal-hydride (NiMH) batteries. The recent progress of lithium batteries has led to levels of energy density and power density which are more preferable than the other battery types. Much effort was dedicated to high power batteries for hybrid-electric vehicles (HEVs), since their main task is to assist the internal combustion engine (ICE), during high power demand operations.

Table 1
Energy and power density compared for HEVs and pure EVs [3]

Battery technology	Application type	Ah	Wh/kg at C/3	W/kg 95% eff.
Lead acid				
Panasonic	HEV	25	26.3	77
Panasonic	EV	60	34.5	47
Ni-MH				
Panasonic	HEV	6.5	46	207
Panasonic	EV	65	68	46
Ovonic	HEV	12	45	195
Ovonic	EV	85	68	40
Li-ion				
Saft	HEV	12	77	256
Saft	EV	41	140	90
Shin-Kobe	HEV	4	56	745
Shin-Kobe	EV	90	105	255

We analyzed a number of sources [3]-[8] that show the different design concepts for battery systems in HEVs and plug-in EVs. As shown in Table 1, it is evident that the batteries for HEVs are quite different from those for EVs in terms of energy and power density. The energy density of EV batteries is significantly higher than that of HEV batteries. This is necessary because the EVs have to comply with the all-electric range, while the stored energy in the HEV units is not a critical requirement [3]. It is also clear from Table1 that the power capability of the batteries designed for HEVs is much higher than those designed for EVs. This requirement follows directly from the lower weight of the HEV batteries and the need to transfer energy in and out of the HEV batteries at high efficiency. For the reasons mentioned above, lithium battery-EVs were assumed for the work.

B. DOD levels for Battery-EVs

We assumed from [3] that the DOD level for HEVs batteries is a very small percentage compared to their effective available energy, Fig. 5. Therefore the HEVs batteries can be used for many years before reaching the end of life condition.

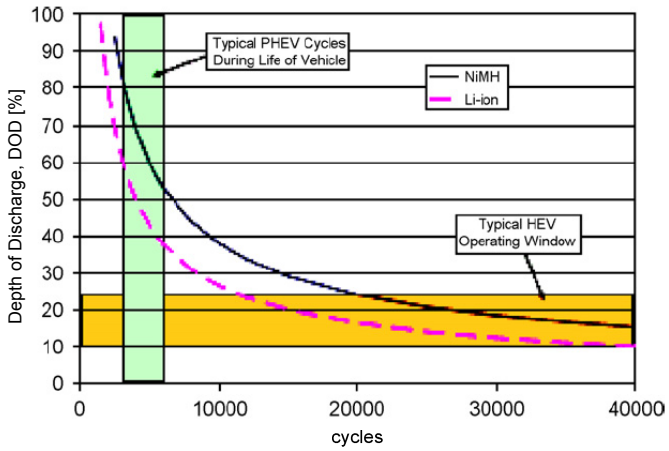

Fig. 5 Lifetime characteristics for different DOD levels [3]

On the other hand, the batteries for plug-in EVs require both high power capability and high energy density. In this case, since the battery is the main energy storage unit, the DOD level needs to be higher than the one of hybrid vehicles, 60 to 80%, in order to guarantee an acceptable vehicle range. Consequently the lifetime is in the range of 4-7 years, depending on the frequency of utilization.
In relation to the available data, the following pre-assumptions were made for the two types of plug-in vehicles, PHEVs and pure EVs:

- a PHEV has a battery energy of 10-12KWh
- a pure EV has a battery energy of 20-50KWh and nominal capacity in the range of 60-150Ah
- the generic battery-EV is equipped with a lithium-based battery, which is the most promising technology for electrical mobility at the moment
- PHEVs batteries are used up to 60% of DOD, while pure EVs are used up to 80% of DOD

C. Current rates for Battery-EVs

A number of charging options were defined in relation to the existing infrastructure and the available power connection points, single-phase or three-phase [9].
We have distinguished among three main use cases for battery-EVs, which are residential charging, public charging and public fast-charging.

Table 2
Charging options

	Charge options	Charging levels
USE CASE 1 Charging at home	1-phase or 3-phase	<16A
USE CASE 2 Charging at Public charging spot	1-phase or 3-phase	16A - 32A
USE CASE 3 Charging at fast-charging public spot	3-phase	>300A

As shown in Table 2, for Use Case 1, a charger of 4KW is assumed; this is the largest charger that can be used for a standard outlet at residential homes without reinforcing the cabling [2]. The current rate resulting for Use Case 1 is derived by the power requirement, considering that the household demand is always a positive amount.

Use Case 2 entails the public charging, where single-phase or three-phase charging spots are available. In this case plug-in EVs can be charged with power and current rates in the range of 16A to 32A.

Use Case 3 entails the option of fast-charging of plug-in EVs. This option can be employed at a 3-phase charging spot only, due to the large amount of power needed. The fast charging option involves a number of aspects that are not only related to electrical infrastructure constraints, but also to physical limitations of EVs batteries. The fast charging case entails current rates of 5C or greater. If we consider that for PHEVs and pure EVs the battery capacity is generally in the range of 60Ah to 150Ah, it is straightforward to derive that the charging current of the fast charging case is always greater than 300A.

D. Temperature performances of Battery-EVs

We analyzed the characteristic curves delivered by some EV battery manufacturer in order to assess the temperature performances of the batteries.

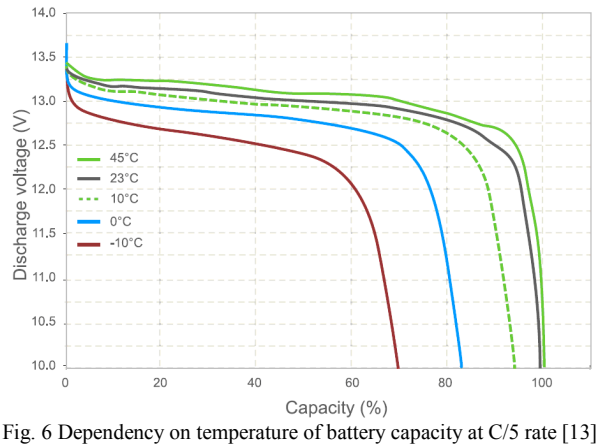

Fig. 6 Dependency on temperature of battery capacity at C/5 rate [13]

It was noted that for all batteries, the temperature considerably affects their behavior in terms of power capability and available energy. For a generic lithium battery the temperature performance can be clearly observed under controlled temperature tests. Figure 6 from [13], shows the behavior of a fully charged EV battery within the temperature range of -10°C to 45°C. The percentage of available energy at -10°C is about 60% of the rated energy, measuring close to the cut-off voltage point of 12V. On the other hand, under warm conditions of 23°C and 45°C the battery is able to completely release its stored energy. The case of 45°C should be anyway avoided since this temperature value negatively affects the battery lifetime, as depicted in Fig. 7.

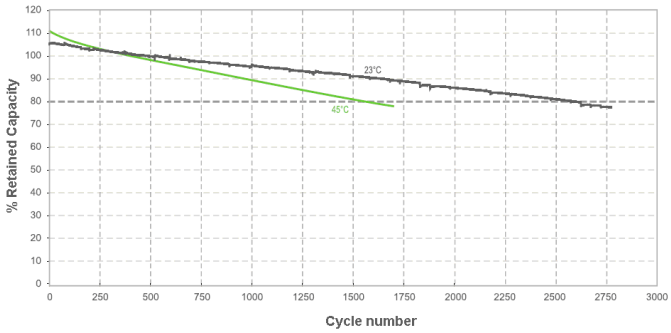

Fig. 7 Lifetime comparison at 23°C and 45°C, C/2 rate [13]

The energy fade at different temperatures, as a function of the number of cycles, is depicted in the graph of Fig. 7 from [13]. It can be easily observed that using the battery at 23°C, with current rate of C/2, the measured lifetime corresponds to about 2600 cycles. While, using the battery at 45°C, with the same current rate, it leads to an overall lifetime of about 1500 cycles.

IV. Average Behavior of Battery-EVs

In this paper, the average behavior of battery-EVs was analytically derived with mathematical average method. The average models were implemented to estimate the available energy and lifetime of the battery, using the analyzed battery models and the vehicle pre-assumptions performed in the previous chapter. The estimation of battery energy and lifetime was related to a number of variables which are temperature, DOD level, current rates and number of cycles. Therefore energy and lifetime can be described by the following functions:

$$L = f(CN, T, DOD, CR) \quad (2)$$

$$E_A = f(CN, T, DOD, CR) \quad (3)$$

The lifetime L in (2) and the available energy E_A in (3) are both function of the following variables:

- Number of cycles, CN. Energy and Lifetime are affected by the number of cycles. This variable counts the number of charge/discharge cycles of a battery-EV. If the vehicle is used in Vehicle-to-Grid mode, the number of cycles CN will increase accordingly.
- Temperature, T. This variable strongly affects the battery-EV performances and lifetime. Low temperature conditions of e.g. -20°C, -10°C are very common at certain latitudes. The available energy is considerably reduced and at the same time the

charging process is not effective as for charging at ambient temperatures, e.g. 20-25°C. At higher temperature, e.g. at 45°C or above, it is demonstrated that the battery lifetime is negatively affected.

- Depth-of-discharge, DOD. The DOD level considerably affects the battery-EV lifetime and energy fade. It was analyzed that using the battery up to 100% DOD instead of 60% of DOD, can result in about 2000 cycles in difference, in terms of lifetime. Therefore battery-EV manufacturers limit the available DOD level, trying to find a good trade-off between vehicle range and battery lifetime.
- Charge/discharge current rates, CR. The current rates during charging/discharging strongly affects the lifetime and the energy fade of the battery. The design of a PHEV or EV is made considering an average current of around C/2 in a normal driving cycle and a peak current in the measure of C to 2C during high speed or accelerations [10]. If the use of the battery-EV is often characterized by high current rates during driving, the battery lifetime decreases. The same consideration is valid in V2G mode, when the battery-EV delivers energy back to the grid. On the other hand, if fast-charging instead of standard charging is applied, the battery lifetime decreases.

A. Average available energy over DOD

The study on the average available energy over DOD was done considering both PHEVs and pure EVs, since these two types of vehicles can be grid interactive and can be employed as distributed energy resources. In this work, battery-EVs were assumed in discharge mode while driving or during V2G operation.

The average available energy was obtained considering the vehicle pre-assumptions made in the previous chapter. The average method conducted to the result depicted in Fig. 8, where two different energy windows are represented for PHEVs and pure EVs respectively:

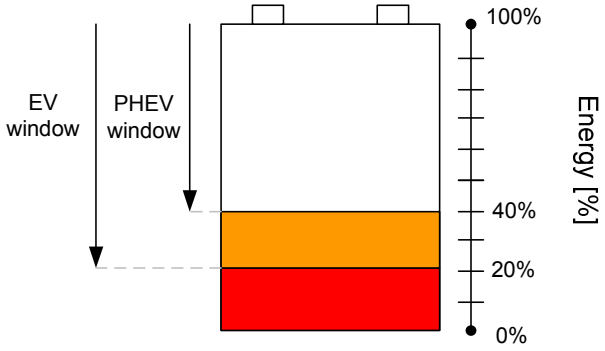

Fig. 8 Available energy window for PHEVs and EVs

From Fig. 8 it follows that for both vehicle types the available energy of the batteries never corresponds to the rated energy of the battery, as formulated in (1).

Lifetime considerations and an assessment on driving pattern performed in [10], leads to consider as available energy window for PHEVs, the 60% of the rated battery capacity. While for pure EVs it is common to use the 80% of DOD. The difference with the PHEVs energy window can be understood considering the different operation of pure EVs than PHEVs. Considering the smaller range of PHEVs in pure electric mode, the frequency of deep discharge cycles would be higher than EVs. To guarantee an acceptable battery lifetime, battery manufacturers identified DOD levels of up to 60% for PHEVs. In pure EVs the battery is used and stressed for the entire driving cycle. For this reason battery manufacturers suggest DOD levels of up to 80%. This information can be managed at fleet operator level, in order to estimate the total available energy from EV fleets.

B. Average available energy over temperature

In Chapter II, we have seen that the available energy of a battery-EV is strongly dependent on temperature conditions. It was shown how the high temperature negatively affects the lifetime of a battery. On the other hand, it was analyzed how the low temperature conditions influence the available energy and the charge/discharge performances of a battery.

In particular, the battery capability to release the stored energy or to accept the incoming power is much reduced at low temperature, even at low C rates.

From a fleet operator point of view, when a large percentage of plug-in EVs are present, the location of such vehicles is important to estimate the available energy as a function of the temperature. An analysis was done using weather forecasts. The average method is valid in a relatively wide geographical area. The definition of a realistic geographical extension is made for two Scandinavian regions, since they are characterized by low average temperatures. Using the temperature forecasts at the time of the work [14], a spring day for Denmark and Norway, we calculated the average temperature, based on the minimum and maximum values.

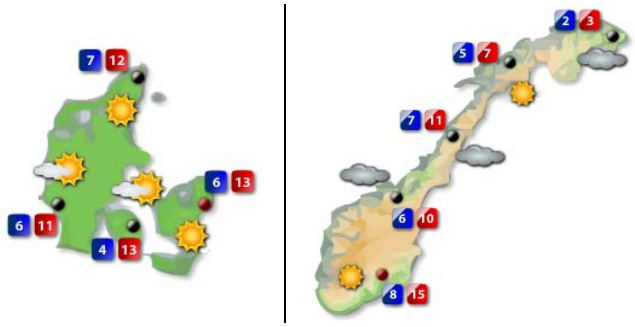

Fig. 9 Temperature values of Scandinavian areas

As depicted in Fig. 9, different locations in Denmark have very similar temperature values. Therefore, an area similar to Denmark's size, 43.000 Km^2, can be described with the same average temperature value. With the same procedure an assessment on the average temperature was made for Norway. The Norwegian case was particularly interesting in this context, since due to its length, an average value of the temperature could not represent the entire country.

An average function was applied for the estimation of the temperature effects on the available energy of a battery-EV. A

number of battery manufacturer's data were compared. The average behavior of a battery-EV over the temperature was calculated considering a temperature range between -20°C and 60°C.

The results depicted in Fig. 10 show that it is reasonable to model the effect of low temperature, at -20 °C, with a reduced capacity of up to 60% of the rated one. This information can be used to estimate the available energy resulting from battery-EVs fleets all around the country. The average method doesn't consider the option of vehicle connection in garages, but it focuses on external location of battery-EVs.

The same assessment was made for high temperature conditions. The same data from the different battery manufacturers were considered. The analysis led to the result that temperatures of 40-45°C are a good working region for the total release of the stored energy, but at the same time the use of batteries at these temperature levels reduces the lifetime.

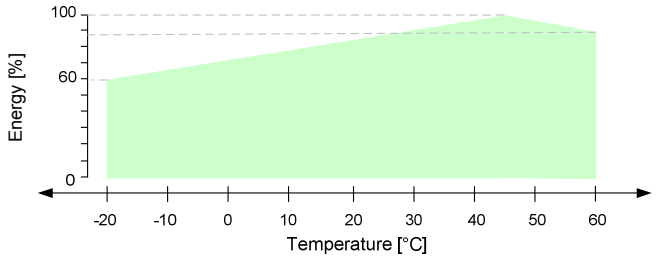

Fig. 10 Average temperature behavior of battery-EVs

At the higher temperature of about 60°C, the available energy is still very high, 10% less of the nominal one, but the battery lifetime is drastically reduced. Ambient temperatures of 20-25°C are indicated by battery manufacturers as optimal working region for battery lifetime. This average method depicts the behavior of a fully charged battery-EV, considering a 100% SOH. The average was calculated considering a number of battery datasheets. As a result, it was possible to model the available energy with a linear trend within the temperature range of -20°C to 60°C. In a scenario of distributed energy resources, under low temperature conditions of e.g. -20°C to -10°C, the energy amount resulting from a fleet of vehicles doesn't correspond to the stored energy in the batteries. Also, this amount of energy cannot be derived anymore by the SOC indicator, since the temperature introduces non-linearity in the system.

C. Average lifetime

We have seen that the lifetime is not a key issue if we look at a daily or weekly time interval. Anyway, when looking at a long-term scale, the lifetime is a key factor for a realistic and correct operation of EV fleets. We have analyzed lifetime characteristics for EV applications from a number of battery manufacturers. For the average lifetime calculation we considered the lifetime curves obtained at discharge conditions of 1C rate and ambient temperature of 20-25°C. This choice comes from two considerations made on EVs driving pattern studies [10]:

- the average current during a driving cycle is considered around 1C, this value takes in account some accelerations that may use 2C rates for about 30 seconds in highway regimes
- the battery pack is supposed to work at the average temperature of 20-25°C, since a cooling system is always provided with the battery system

Based on these considerations, the average method was applied to the battery data reported in Table 5. All data were supplied from different battery manufacturers.

Table 5
Lifetime of different lithium EV batteries

	Battery manufacturers			
	A	B	C	D
Battery type	LFP	LFP	LFP	LiPO
Current rate	1C	1C	1C	1C
DOD	80%	80%	80%	80%
Temp	20-25°C	20-25°C	20-25°C	20-25°C
Lifetime	**1750**	**1600**	**1700**	**1450**

In relation to Table 5, the average behavior of battery-EVs is obtained applying the mathematical average. The resulting average lifetime is depicted in Fig. 10. The vertical line represents the median and it intersects the 80% of retained energy, on the y-axis, after 1631 cycles. The retained energy is assumed 100% at initial conditions.

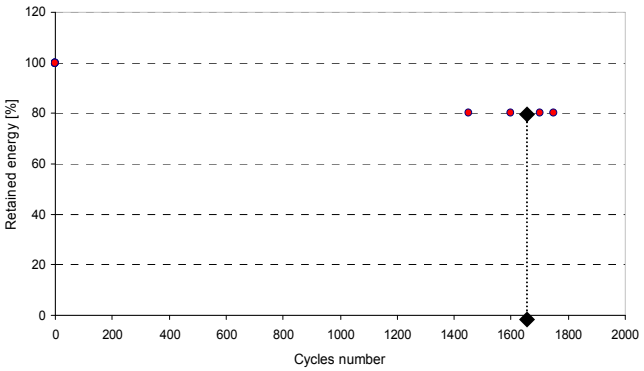

Fig. 10 Average lifetime of battery-EVs

Such number of cycles corresponds to about 4 years considering one charge cycle every day, or about 6-7 years if the charge happens with lower frequency. An assessment could be made to estimate the V2G effect on the lifetime diagram, considering the same variables of temperature, DOD, current rates and number of cycles.

V. CONCLUSIONS

In this paper the average behavior of battery-EVs for distributed energy studies was modeled.

Two battery factors were addressed as key parameters for active grid integration of electric vehicles: the energy and the lifetime. An analysis on battery models, described in other publications was conducted as basis for the work. The available energy and the lifetime were modeled considering

their non-linear and time-variant behavior with respect to a number of variables such as temperature, depth-of-discharge, current rates and number of cycles, using mathematical average method. A definition of EV use cases was given and the possible battery working regions were identified. An average behavior was finally derived using the concept of equations (2) and (3), and calculating the average based on the available data.

The obtained results have shown that the energy and the lifetime of EV batteries vary depending on different work and ambient conditions. To preserve the battery lifetime, the DOD level should not exceed the 80% for pure EVs and 60% for PHEVs. Discharging a battery up to 100% instead of 80% of DOD could result in about 1000 cycles of difference in lifetime. Using the battery at 45-50°C can halve the lifetime. At low temperature, -20°C, the available energy is about 40% less than the rated energy. Charging or discharging the battery at 2C rate instead of 1C or C/2 can halve the lifetime.

A conclusion could be derived saying that a certain percentage of battery-EVs in the grid, in a relatively wide geographical area, can be modeled with good approximation if time, geographical location and battery use conditions are known. When modeling fleets of battery-EVs, neglecting variables such as temperature, DOD, current rates and number of cycles, may result in remarkable errors of available energy.

VI. References

[1] W. Kempton, J. Tomic, S. Letendre, A. Brooks, T. Lipman, "Vehicle-to-Grid Power: Battery, Hybrid, and Fuel Cell Vehicles as Resources for Distributed Electric Power in California", *Online Report, 2001*

[2] K. Clement-Nyns, E. Haesen, and J. Driesen, "The Impact of Charging Plug-In Hybrid Electric Vehicles on a Residential Distribution Grid", *IEEE Transactions on Power Systems, Vol. 25, No. 1, 2010*

[3] S. Amjad, S. Neelakrishnan, and R. Rudramoorthy, "Review of design considerations and technological challenges for successful development and deployment of plug-in hybrid electric vehicles", *Renewable and Sustainable Energy Reviews 14 (2010) 1104–1110*

[4] W. Xuezhe, Z. Bing and X. Wei, "Internal Resistance Identification in Vehicle Power Lithium-ion Battery and Application in Lifetime Evaluation", *IEEE International Conference on Measuring Technology and Mechatronics Automation, 2009*

[5] B. G. Kim, F. P. Tredeau and Z. M. Salameh, "Fast Chargeability Lithium Polymer Batteries", *IEEE Power and Energy Society Conf. 2008*.

[6] T. Guena and P. Leblanc, "How Depth of Discharge Affects the Cycle Life of Lithium-Metal-Polymer Batteries", *IEEE Communication energy conference, INTELEC 2006*

[7] D. Haifeng, W. Xuezhe and S. Zechang, "A New SOH Prediction Concept for the Power Lithium-ion Battery Used on HEVs", *IEEE Vehicle Power and Propulsion Conference, 2009*

[8] A. F. Burke, "Batteries and Ultracapacitors for Electric, Hybrid, and Fuel Cell Vehicles", *Proceedings of the IEEE Vol. 95, No. 4, 2007*

[9] B. Lunz, T. Pollok, A. Schnettler, R. W. De Doncker, and D. U. Sauer, "Evaluation of Battery Charging Concepts for Electric Vehicles and Plug-in Hybrid Electric Vehicles", *Advanced Automotive Battery Conference, 2009*

[10] B. Adornato, R. Patil, Z. Filipi, Z. Baraket and T. Gordon, "Characterizing Naturalistic Driving Patterns for Plug-in Hybrid Electric Vehicle Analysis", *IEEE Vehicle power and propulsion conference, 2009*

[11] F. P. Tredeau and Z. M. Salameh, "Evaluation of Lithium Iron Phosphate Batteries for Electric Vehicles Application", *IEEE Vehicle Power and Propulsion Conference, 2009*

[12] B. G. Kim, F.P. Tredeau and Z. M. Salameh, "Performance Evaluation of Lithium Polymer Batteries for Use in Electric Vehicles", *IEEE Vehicle Power and Propulsion Conference, 2008*

[13] Valence Technology, "Lithium Iron Magnesium Phosphate (LiFeMgPO4) Battery Modules", *online datasheet*

[14] WeatherOnline, http://www.weatheronline.co.uk/

Demand Profile Study of Battery Electric Vehicle under Different Charging Options

Francesco Marra, Guang Ya Yang, Chresten Træholt, Esben Larsen, Claus Nygaard Rasmussen, and Shi You

***Abstract*-- An increased research on electric vehicles (EV) and plug-in hybrid electric vehicles (PHEV) deals with their flexible use in electric power grids. Several research projects on smart grids and electric mobility are now looking into realistic models representing the behavior of an EV during charging, including nonlinearities. In this work, modeling, simulation and testing of the demand profile of a battery-EV are conducted. Realistic work conditions for a lithium-ion EV battery and battery charger are considered as the base for the modeling. Simulation results show that EV charging generates different demand profiles into the grid, depending on the applied charging option. Moreover, a linear region for the control of EV chargers is identified in the range of 20-90% state-of-charge (SOC). Experiments validate the proposed model.**

***Index Terms* - charging, demand profile, electric vehicles, modeling, validation**

I. Introduction

THE electrification of transport sector, by means of battery-EV and PHEV, will most likely contribute to achieve the CO2 target in the coming years [1]. With the expected breakthrough on the market of EV and plug-in hybrid EV (PHEV) there is an increasing need to evaluate their benefits and impacts in the existing electrical systems.

Especially with battery-powered EV, there is the opportunity to achieve zero-emissions during a driving cycle since all energy needed comes from a battery [2]. At the same time, the progressive replacement of conventional vehicles with EV will generate an additional electrical load into the existing distribution grids.

Research on Smart Grids has proposed alternative concepts when dealing with EV, which are seen not as a mere electric load but rather as a flexible resource in the power system [3]. It has been studied in [4] how the charging process of an EV can be intelligently controlled, in order to cope with renewable power fluctuations, electricity price and local grid constraints. Coordinating the charging of a number of EV according to a pre-defined algorithm, would lead to an aggregated load profile which is significantly different from an uncoordinated scenario [5]. From the perspective of a distribution system operator (DSO), the flexibility offered by EV during charging is still seen as a demand profile that needs to be modeled. Modeling the demand of an EV acting as a flexible load in the power system represents an area which was not addressed until few years ago. In [6] the authors proposed a methodology for modeling EV as an additional load in the distribution grid. In the work, it is considered that the charging operation can either take place in uncoordinated manner or it can be intelligently managed during off-peak electricity hours.

Both EV and PHEV battery technologies have received great attention for modeling the charging process. The battery is the most important component of an EV, since it characterizes the vehicle under several points of view: energy and power capacity, range, weight, cost and lifetime. Special attention is given to lithium-ion (Li-ion) battery chemistry and several methods have been used to closely model its behavior. In [7], electrochemical impedance analysis is used to estimate the parameters and derive a model for the battery. It is important to notice that this method is rather complex and deriving an accurate battery model is only possible if special equipment is available. At the same time, this method cannot describe the demand profile of EV charging, as it does not take into account different possible charging options.

In the context of Smart Grids, Virtual Power Plant (VPP) operators and DSO are asking for a simpler, yet comprehensive EV demand model, which is capable of describing in a realistic way the major variables involved during the charging process of an EV [8].

In this paper, modeling of the demand profile of a battery EV is performed, addressing typical aspects of different EV charger options. In the study, the battery modeling methodology proposed by Tremblay et al. in [9] is used. With this method the battery parameters are extracted and the battery manufacturer curves are reproduced without the need of sophisticated tools.

An integrated EV model is proposed, composed of a battery and a charger, where the vehicle State-of-Charge (SOC), the real time charging power, the voltage and current on the battery and grid sides are modeled. The paper is organized as follows: in Section II the methodology used for modeling the EV battery is described. In section III, the proposed EV model is presented.

In section IV, simulations performed in Matlab based on the defined model are presented and discussed. Validation of models is conducted in Section V, using an experimental setup.

Mr. Marra, Mr. Yang, Mr. Træholt, Mr. Larsen, Mr. Nygaard Rasmussen and Mr. You are with the Centre for Electric Technology, Department of Electrical Engineering, Technical University of Denmark, 2800 Kgs. Lyngby, Denmark (e-mail: fm@elektro.dtu.dk).

II. Battery Model

The methodology presented in [9] is used in this work to model a Li-ion EV battery. The choice for such chemistry is related to the recent trends and expectations in the EV sector. According to a market report by Frost & Sullivan [10], more than 70% of EV in 2015 will be powered by Li-ion batteries. Compared to other battery technologies, Li-ion batteries offer a series of advantages: greater energy-to-weight ratio, no memory effect and low-self discharge when not in use [11]. The model of Li-ion battery used in this study is depicted in the scheme of Fig. 1:

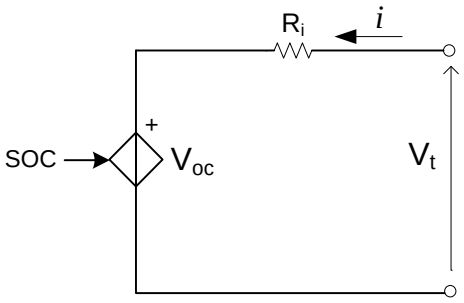

Fig. 1. EV Battery model

The model is composed by a controlled voltage source V_{oc} in series with the equivalent battery cell impedance R_i. The terminal voltage of the battery is indicated with V_t. The only state variable of the model is the SOC and this is defined as follows [12]:

$$SOC = \frac{Q}{Q_{nom}} \qquad (1)$$

where

Q is the actual capacity stored in the battery, Ah

Q_{nom} is the nominal capacity of the battery, Ah

If we neglect the battery efficiency during charging, the SOC variation over the time can be expressed as:

$$\frac{dSOC}{dt} = \frac{i}{Q_{nom}} \qquad (2)$$

where

i is the charging/discharging current

The open circuit voltage of the battery V_{oc} is described by the following formula according to [8]:

$$V_{oc}(Q) = V_0 - \frac{K \cdot Q_{nom}}{Q_{nom} - Q} + A \cdot e^{(-B \cdot Q)} \qquad (3)$$

where

A is the exponential zone amplitude (V)

B is the exponential inverse time constant $(Ah)^{-1}$

V_0 is the battery voltage constant (V)

K is the polarization voltage (V)

It is evident from (3) that the battery voltage is function of the actual stored capacity Q, which is another expression of the SOC level according to (2).

The parameters used to model the Li-ion EV battery are estimated from the discharging curves of a 3.2 V - 40 Ah lithium iron phosphate (LFP) battery cell, following the procedure depicted in the diagram of Fig. 2. The horizontal axis indicates the battery capacity in Ah. The vertical axis indicates the cell voltage. From the curve, it is possible to derive three characteristic points of the battery, which correspond to:

- V_{full} voltage level at fully charged state
- V_{exp} voltage level at end of exponential zone
- V_{nom} voltage level at end of nominal zone

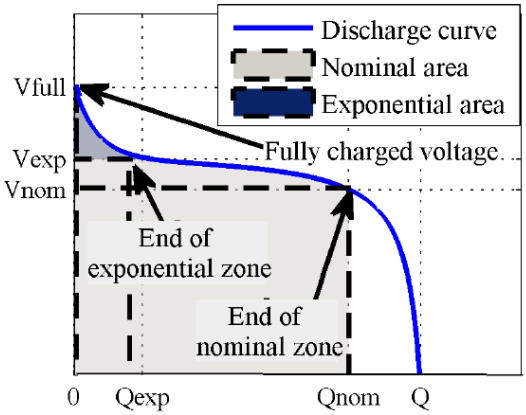

Fig. 2. Procedure for extracting the battery parameters [13]

The estimated parameters for the LFP battery are shown in Table I.

TABLE I
EV Battery Cell Parameters

LFP 40Ah battery				
V_0 (V)	R (Ω)	K (V)	A (V)	B $(Ah)^{-1}$
3.5	0.01	0.025	0.2	0.375

The terminal voltage of the battery cell V_t, is easily derived by adding to the expression of (3), the voltage drop due to the internal impedance R_i:

$$V_t = V_{oc} + R_i \cdot i \qquad (4)$$

The voltage drop is considered positive during charging and negative during discharging. The battery internal impedance is usually provided by the manufacturer on the battery datasheet [14]; however its value was validated to further improve the model. The impedance of the battery cell was measured with *Impedance Spectroscopy* method using the test equipment available at Risø DTU laboratory [15]. The measurements performed determined an internal impedance of about 10 mΩ.

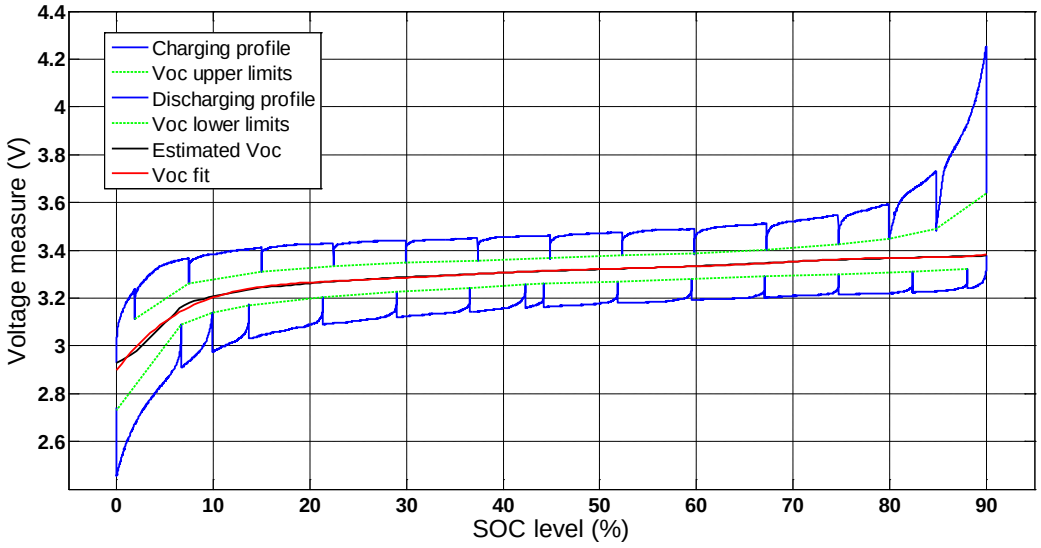

Fig. 3. Validation of voltage profile of a Li-ion EV battery with charge/discharge current of 0.5C

A separate test was conducted with the goal of characterizing the battery cell voltage as a function of the SOC. The test served also to validate the charging/discharging curves given by the manufacturer.

The following steps were followed during the test:

1. Charge with constant current, 0.5C, i.e. 20A, starting from a SOC of 0% (2.5 V), till 90%, (4.25 V).
2. Discharge with constant current, 0.5C, from a SOC of 90% till 0% SOC (2.5 V)

The *Step Current* method, as described in [16], was used to charge/discharge the battery and determine the open circuit voltage V_{oc} profile. In Fig. 3, the measured voltage profiles are shown. During charging, it is noted a rapid increase of voltage within the SOC range of 85 to 90%. Considering that for lifetime reasons a minimum SOC level of 20% is recommended [17], it can be concluded that the SOC window of 20-90% is a suitable energy window to use for EV batteries.

III. Electric Vehicle Charging Model

An EV model was implemented based on the diagram of Fig. 4. The model integrates the battery model described in Section II with an EV charger model. On the grid side, the EV charger is supplied with grid voltage V_c and absorbs the current i_c during charging. On the battery side, V_{pack} and i identify the terminal voltage and the current absorbed by the battery, respectively. The parameters Voc_{eq} and R_{eq} indicate the equivalent voltage and resistance of the EV battery respectively. Based on the validation performed on the single cell, the electrical features of a real EV battery pack were derived and summarized in Table II. Concerning the EV demand study, a battery pack composed of 110 series-connected 3.2 V - 40 Ah LFP cells was considered, which leads to a total battery pack nominal voltage of 352V.

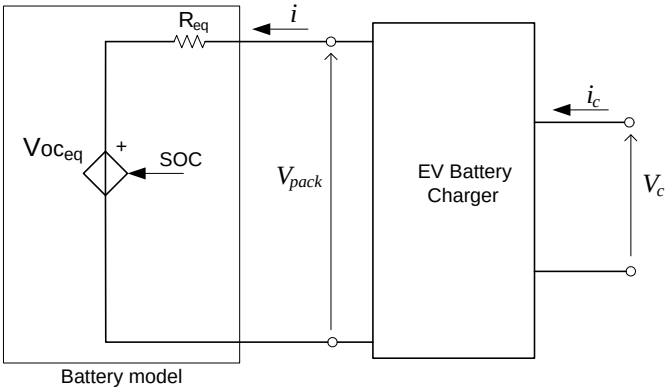

Fig. 4. EV model

TABLE II
EV Battery Pack Parameters

Parameter name	Unit	Value
Nominal EV battery energy, E_{nom}	kWh	14
Nominal EV battery cell voltage, V_{nom}	V	3.2
Nominal EV battery voltage, V_B	V	352
Nominal EV battery capacity, Q_{nom}	Ah	40
Equivalent resistive impedance, R_{eq}	Ω	1.1

The characteristic charging curves of a Li-ion battery are depicted in Fig. 5. On the vertical axis, the charging current level is indicated. On the two secondary axes the battery cell voltage and SOC are indicated. The green, red and blue curves represent the battery voltage, current and SOC respectively. According to most Li-ion battery manufacturers, 0.5C current rate is recommended for charging the battery and this corresponds also to the level stated in the battery datasheet [14]. It is evident that the standard charging algorithm of a Li-ion battery is composed of two distinct operational regions: constant current (CC), until the voltage upper limit is reached; constant voltage (CV), until a SOC level of 100% is reached.

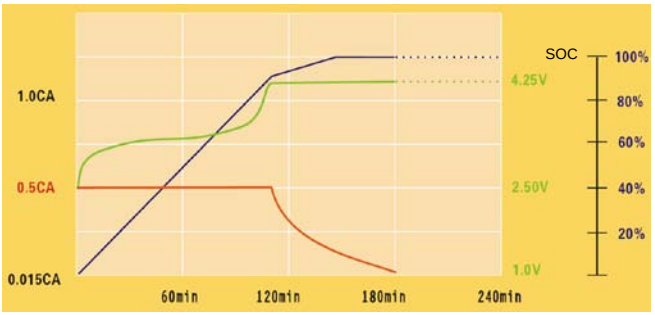

Fig. 5. Typical charging profiles for an EV Li-ion battery [14]

Although the charging curves depicted are obtainable with laboratory equipment, the same profiles are not always valid when charging a real EV battery by means of an EV charger. Different charging strategies can be employed for an EV charger and this will affect the resulting demand profile on the grid side.

In the study, an EV battery charger was modeled as a single-phase AC/DC converter with efficiency η, according to two different charging options.

A. Constant Current – Constant Voltage Option

With Constant Current – Constant Voltage charging option, the charger performs according to the following operations:

- Constant Current (CC) on the battery side, until the maximum cell voltage is reached.
- Constant Voltage (CV) on the battery side, until the battery is fully charged.

In the CC working region, the current i is kept constant during charging until the cut-off voltage level is reached. In general, the power on the grid side P_{ac} and battery side P_{dc} are calculated as:

$$P_{ac} = V_c \cdot i_c \quad (5) \qquad P_{dc} = V_{pack} \cdot i \quad (6)$$

Since V_{pack} is a function of the SOC level of the battery from (3), it leads to P_{ac} also being function of the SOC. Therefore (5) can be rewritten as:

$$P_{ac}(V_{pack}) = V_c \cdot i_c(V_{pack}) \quad (7)$$

Recalling (5) and (6), the expressions of P_{dc} and P_{ac} become:

$$P_{ac}(SOC) = V_c \cdot i_c(SOC) \quad (8)$$

$$P_{dc}(SOC) = V_{pack}(SOC) \cdot i \quad (9)$$

Under the CV working region, the power P_{ac} and the current i_c are not controllable anymore. The only controlled variable is the voltage V_{pack} which is constantly maintained until the SOC level of 100% is reached.

B. Constant Power – Constant Voltage Option

The other charging option available for EV chargers is Constant Power – Constant Voltage. With this option the following functions are implemented:

- Constant Power (CP), P_{ac} = constant, until the maximum cell voltage is reached
- Constant Voltage (CV), V_{pack} = constant, until the SOC level of 100% is reached

The power on the grid side P_{ac} is kept constant during the charging process until the cell voltage threshold is reached. Considering that V_{pack} increases with the SOC according to (3), the current i must be regulated in order to ensure a constant charging power. Moreover, taking into account the efficiency of the charger η, the power on the battery side can be expressed as:

$$P_{dc} = \eta \cdot P_{ac} \quad (10)$$

Considering (8) and (9), i can be calculated as:

$$i(SOC) = \eta \cdot \frac{V_c \cdot i_c}{V_{pack}(\mathrm{SOC})} \quad (11)$$

When the CV mode is entered, the same modeling issues of the previous charging option are valid.

C. Modeling the EV battery SOC

For both charging options, the EV battery SOC is derived from (10), considering the initial SOC condition:

$$SOC(k) = \sum_{k=1}^{N} \frac{dQ(k)}{Q_n} + SOC_i \quad (12)$$

$$dQ(k) = i(k) \cdot T_i \quad (13)$$

$$dSOC(k) = \frac{dQ(k)}{Q_n} \quad (14)$$

where

k	is the simulation's steps number
N	is the number of steps which determines the charging duration
T_i	is the reference time step
i	is the DC current during charging
dQ	is the capacity variation at each time step
$dSOC$	is the SOC variation at each time step
SOC_i	is the initial condition of SOC

In the CV region the capacity variation dQ of the battery becomes nonlinear, as i exponentially decreases over the time. For the same reason, the SOC curve enters the nonlinear region. In more general terms, working in the linear or nonlinear region of an EV battery is meaningful for a number of techno-economic reasons that will be briefly described in the following paragraphs.

EV coordination and EV fleet management

In a Smart Grid scenario, it should be possible to treat EV as a socio-economic solution, which goes beyond the scope of transportation. It is aimed to aggregate and coordinate EV, so they can participate in intelligent charging schemes, e.g. ancillary services [18]. An EV coordinator is able to coordinate EV charging provided that the battery is in the linear SOC region. All other EV charging in the nonlinear

SOC region, i.e. CV region, cannot be included in the coordination scheme.

Battery lifetime and charging efficiency

According to common practice, several EV manufacturers limit the SOC window of a Li-ion battery in the interval [17]:

$$SOC \in [20, 90]\% \qquad (15)$$

The choice for such an interval relates mainly to battery lifetime aspects; charging the upper 10-20% SOC window has shown quicker battery degradation [19]. In [17] it is also recommended to avoid discharging the battery if the SOC is already below 20%. From a charger perspective, the CV region is a low-efficiency working region since the charging power falls far below its nominal power [20].

D. Charging power levels

Due to the electrical characteristics of the low voltage grid where EV are going to be connected, the charging power levels commonly considered are the ones indicated in Table III.

TABLE III
CHARGING POWER LEVELS

AC current	AC voltage	Grid connection	Power
16 A	230 V	single phase	3.7 kW
32 A	230 V	single phase	7.4 kW
16 A	400 V	three-phase	11 kW
32 A	400 V	three-phase	22 kW

The cases are characterized by different charging current i_c as well as by the grid connection type, single-phase or three-phase.

In this paper, the single-phase 3.7 kW charging option is used for simulations and tests, as it is likely to become a common option for home-charging [21]. This corresponds using a 0.25C rate for charging the battery in the CC region.

IV. SIMULATIONS

Simulations were conducted using Matlab to investigate the demand profiles generated by EV charging, according to the two options modelled.

The EV simulation model is made of a single-phase charger, with charging power level of 3.7 kW (c.a. 0.25C). Simulation results are depicted in Fig. 6-9.

In Fig. 6 (a), the power P_{ac} and the SOC profile of the EV under CP-CV charging option are depicted. The time axis is expressed in minutes. The EV starts charging with an initial SOC of 60%. The power is constant over time, until the battery cell voltage reaches 4.0 V; this occurs after about 94 minutes. From this point, the charger enters the CV mode and the charging power decreases as well as the current. In Fig. 6 (b), the charging current i on the battery side and the cell voltage V_t are depicted. In the CP region, it is evident how the current i decreases while the battery voltage increases.

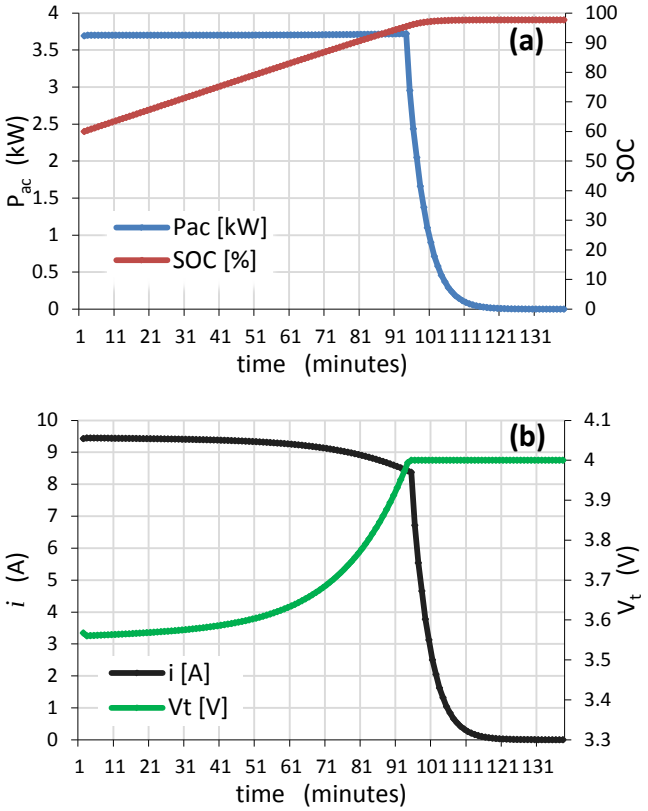

Fig. 6. Simulation of demand profile of EV charger with CP-CV option. (a) P_{ac} and SOC. (b) Current i and battery cell voltage V_t.

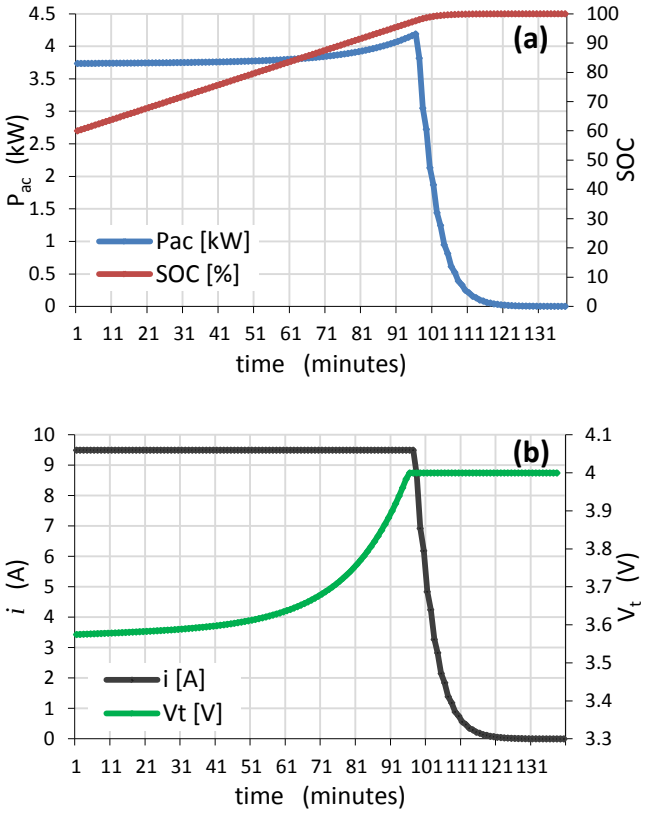

Fig. 7. Simulation of demand profile of EV charger with CC-CV option. (a) P_{ac} and SOC profiles. (b) Current i and battery cell voltage V_t.

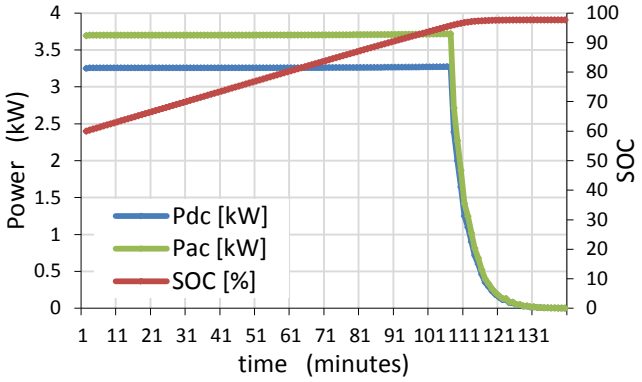

Fig. 8. Simulation of demand profile of EV charging with CP-CV option, charger efficiency η = 0.88, SOC_i = 60%. P_{dc}, P_{ac} and SOC profiles.

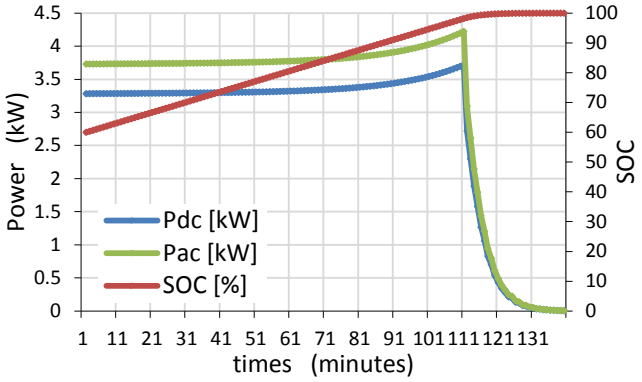

Fig. 9. Simulation of demand profile of EV charging with CC-CV option, charger efficiency η = 0.88, SOC_i = 60%. P_{dc}, P_{ac} and SOC profiles.

In Fig. 7 (a), the charging power P_{ac} and the SOC profile are depicted according to CC-CV charging option. As for the previous case, the EV starts charging with an initial SOC of 60%. It is possible to note that P_{ac} profile is not constant over the time, but it increases until the battery cell voltage reaches the maximum, i.e. after 96 minutes. From this point, the charger enters the CV mode and the charging power decreases accordingly. In Fig. 7 (b), the charging current i and the cell voltage V_t are depicted. It is evident that the current i is constant during the CC operation, while the battery terminal voltage continues to increase. Considering same initial charging power of 3.7 kW, charging a battery with a CC-CV charger takes few minutes less than with a CP-CV charger. Furthermore, both charging strategies depict a linear SOC profile until about 95%.

Simulations were performed again, modelling this time a charger efficiency η of 0.88. While the demand profiles remain similar in shape, the charging time needed is considerably longer than in the previous cases. In Fig. 8, the demand profiles of an EV charger with CP-CC option are depicted. In Fig. 9, the demand profiles of the EV charging with CC-CV option are depicted. Due to the charger efficiency, the battery charging process takes about 13 minutes longer than in the previous simulations.

V. Model Validation

The developed EV charging model was validated with an experimental setup made of real EV components. An EV battery pack with parameters as indicated in Table II was used in the tests. This is connected to an EV battery charger with parameters are shown in Table IV.

TABLE IV
EV Battery Charger Parameters

Parameter name	Unit	Value
Power range, P	kW	0 - 5.5
Voltage range, V_{pack}	V	60 - 452
Charging current, i	A	0 - 12
Power factor, PF	-	0.93
Efficiency, η	-	0.88

The charging process was initiated with an initial SOC of about 60%, as for the simulations. The EV charger has an adjustable power level and this was set to 3.7 kW, according to the first option in Table III. A power meter with 1-minute resolution was used to measure the active power absorbed by the charger. The charging process was remotely controlled by means of a software application which activates a circuit breaker between the charger and the grid. Test results are shown in Fig. 10. After about 95 minutes, the charging process was stopped as the cut-off voltage of 4V per battery cell was reached, that corresponds to a SOC of about 90%. From the measurements performed, looking at the charging power profile P_{ac}, it is possible to recognize a charger using CC option, with similar profile as the one obtained in simulation, Fig. 7 (a) and Fig. 9. The power absorbed by the charger increases steadily, similarly as the EV battery voltage. A power increase of 11.4% was observed at the end of the CC region, with respect to the initial power of 3.7 kW.

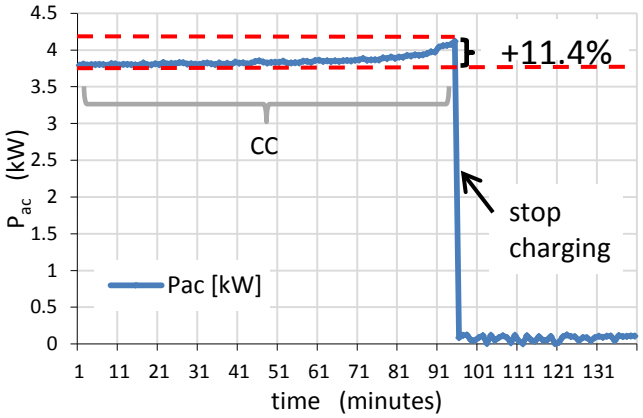

Fig. 10. Charging test of EV battery using a charger with CC-CV option

VI. Conclusions

In this paper, the EV demand profile during a charging process was studied. The work presented a simple yet effective strategy for modelling the charging of an EV considering a validated Li-ion battery model. Simulation results have shown that the demand profile due to EV charging can have different characteristics based on the two charging options implemented by the charger. In particular, a CP-CV charger ensures that the power level set for charging is never exceeded. On the contrary, a CC-CV charger has shown up to 11.4% additional load when the CV working region of

the battery is approached. This might raise new concerns for grid constraints in residential areas.

Simulations were performed first without modelling the efficiency of the charger. Then an efficiency of 0.88 was considered in the EV charging model. In this case, the demand profiles change. Assuming the same initial SOC, the charging time resulted 14% longer than without modelling the efficiency. The demand profile of an EV charger with CC-CV charging option was validated using a full-scale EV setup, made of an EV battery pack and a battery charger.

A preferable SOC usage window was identified for an EV battery. Experimental charging/discharging tests performed on a single LFP battery cell have shown a relatively flat voltage profile up to about 80% SOC, while an exponential voltage increase from 80 to 90%. Based on the findings of simulations and tests, it was determined that both charging current and power are controllable till a SOC level of about 90%.

The model developed has proven reliability and can potentially be used by DSOs and EV coordinators such as Virtual Power Plant operators, in order to estimate the demand of an EV fleet or a single EV. Furthermore, the developed EV model can be used as input for dynamic modelling of EV in power system analysis.

VII. References

[1] European Commission, “20 20 by 2020 Europe's climate change opportunity”, COM (2008) 30 final, Brussels, 2008.

[2] K. Chen, A. Bouscayrol, A. Berthon, P. Delarue, D. Hissel, and R. Trigui, “Global modeling of different vehicles”, *IEEE Vehicular Technology Magazine*, 2009.

[3] J. A. P. Lopes, F. J. Soares, P. M. R. Almeida, “Integration of Electric Vehicles in the Electric Power System”, *in Proceedings of the IEEE*, vol. 99, no. 1, pp. 168-183, 2011.

[4] O. Sundström and C. Binding, “Planning Electric-Drive Vehicle Charging under Constrained Grid Conditions”, in *2010 International Conference on Power System Technology (POWERCON)*, 2010.

[5] K. Clement-Nyns, E. Haesen and J. Driesen, “The Impact of Charging Plug-In Hybrid Electric Vehicles on a Residential Distribution Grid”, *IEEE Transactions on Power Systems*, vol. 25, no. 1, pp. 371-380, 2010.

[6] K. Qian, C. Zhou, M. Allan, Y. Yuan, “Modeling of Load Demand Due to EV Battery Charging in Distribution Systems”, *IEEE Transactions on Power System*, vol. 26, pp. 802-810, 2011.

[7] K. X. Zhang, and T. Jow, “Electrochemical impedance study on the low temperature of li-ion batteries, *“Electrochimica Acta”*, vol. 49, no. 7, pp. 1057–1061, 2004.

[8] EDISON project, “WP3 report D3.1”, www.edison-net.dk.

[9] O. Tremblay, L.A. Dessaint, A. Dekkiche, “A Generic Battery Model for the Dynamic Simulation of Hybrid Electric Vehicles”, *IEEE Vehicle Power and Propulsion Conf*erence, 2007.

[10] Frost & Sullivan, public report “M5B6-Global Electric Vehicles Lithium-ion Battery Second Life and Recycling Market Analysis”, online, 2010.

[11] S. Amjad, S. Neelakrishnan, and R. Rudramoorthy, “Review of design considerations and technological challenges for successful development and deployment of plug-in hybrid electric vehicles”, *Renewable and Sustainable Energy Reviews 14*, pp. 1104–1110, 2010.

[12] H. He, R. Xiong, X. Zhang, F. Sun and J. Fan, “State-of-Charge Estimation of the Lithium-Ion Battery Using an Adaptive Extended Kalman Filter Based on an Improved”, in *IEEE Transaction on Vehicular Technology*, vol. 60, n. 4, pp. 1461-1469, 2011.

[13] O. Tremblay and L. Dessaint, “Experimental Validation of a Battery Dynamic Model for EV Applications”, in *World Electric Vehicle Journal*, Vol. 3, AVERE, 2009.

[14] Thunder Sky, LFP Battery User Manual, 2010.

[15] S. H. Jensen, A. Hauch, P. Vang Hendriksen, M. Mogensen, N. Bonanos, and T. Jacobsen, "A Method to Separate Process Conributions in impedance Spectra by Variation of Test Conditions", in *Journal of the Electrochemical Society*, vol. 154, no. 12, pp. 1325-1330, 2007.

[16] Min Chen and G.A. Rincon-Mora, "Accurate electrical battery model capable of predicting runtime and I-V performance", in *IEEE Transactions on Energy Conversion*, vol. 21, no. 2, pp. 504-511, 2006.

[17] F. Marra, C. Træholt, E. Larsen and Q. Wu, “Average Behavior of Battery-Electric Vehicles for Distributed Energy Studies”, *IEEE Innovative Smart Grid Technology Conference*, 2010.

[18] M. D. Galus, S. Koch, G. Andersson, “Provision of Load Frequency Control by PHEVs, Controllable Loads, and a Cogeneration Unit”, *in IEEE Transactions on Industrial Electronics*, vol. 58, no. 10, pp. 4568-4582, 2011.

[19] Nissan Leaf Electric Car, *Charging info*, www.nissanusa.com.

[20] E. M. Marwell, E. P. Finger and E. Sands "Lead Acid Traction Batteries", in *Library of Congress Catalog* card 81-65733; ISBN: 0-939488-00-0S, Curtis Instruments, 1981.

[21] IEC 61850 Part 7-420.

Energy Storage Options for Voltage Support in Low-Voltage Grids with High Penetration of Photovoltaic

Francesco Marra, Y. Tarek Fawzy, Thorsten Bülo and Boštjan Blažič

***Abstract*— The generation of power by photovoltaic (PV) systems is constantly increasing in low-voltage (LV) distribution grids, in line with the European environmental targets. To cope with the effects on grid voltage profiles during high generation and low demand periods, new solutions need to be established. In the long term, these solutions should also aim to allow further more PV installed capacity, while meeting the power quality requirements. In this paper, different concepts of energy storage are proposed to ensure the voltage quality requirements in a LV grid with high PV penetration. The proposed storage concepts can cooperate with reactive power methods and can be used to avoid grid reinforcement and active power curtailment. For the study, a residential LV grid with high share of PV generation is used. Simulation results show substantial benefits for the LV feeders operation, as well as an increased potential for local consumption.**

***Index Terms*— Active distribution grids, energy storage, low voltage grids, reactive power control, voltage rise mitigation**

I. Introduction

THE renewable energy sector has experienced a large growth in the last decade. The need of fulfilling the European environmental targets [1] aiming for an increased sustainability have led to important advances in solar technologies. Lately, these advances are also pushed by the research on smart grids on active distribution networks [2].

Especially LV grids have seen in the last few years an exponential increase of PV installations at the residential level. Increasing the PV penetration is a fundamental target which however poses new challenges for the operation of distribution grids [3]-[4]. One of the issues to cope with is the grid voltage variation along a LV feeder, due to high generation and low demand periods [5]. Historically, LV grids have been planned to deliver unidirectional power to the loads. With distributed generation such as PV, the situation of power flow inversion is more likely to happen [6]. This can lead to overvoltage problems at the PV generator point of connection (PCC) that in extreme cases requires the curtailment of active power [7]. The European power quality standard EN 50160 states that during each period of one week, 95% of the 10-minutes average voltage values shall be within the range of U_n +/- 10%, where U_n is the nominal voltage [8]. Central coordination and local voltage support approaches have been described by Carvalho *et Al.* in [9] to deal with voltage variations. The first one can provide voltage support, using a communication infrastructure for the real time monitoring and the coordination of individual PV generators. An example is the use of controllable tap-changer 10/0.4 kV transformers to adjust the voltage setting as required; however, this adjustment changes the operational condition of all LV feeders supplied by the same transformer. Also, the voltage adjustment is only possible if the grid is equipped with such transformers, which is rather uncommon in the real case.

Local methods based on reactive power for voltage control have been the most used so far, as they are implemented on each PV inverter that can work independently [10]-[11].

Reactive power methods do not necessarily require a supervisory control and communication, as the single PV inverters are able to adapt in real time to the actual local voltage situation [12], however, the amount of reactive power needed for voltage support will considerably rise up with the PV penetration, thus the rethinking of solutions including storage for voltage support is necessary [13].

Storage solutions can play an important role in relation to the national electricity tariff systems of the different European countries [14]. Considering the case of Germany, the "self-consumption" tariff (EEG) is already applied from 2009 to the residential PV sector [15]. Though the self-consumption act is planned to be amended, a general incentive for private consumption will persist [16].

The need of storage for grid support will lead to a higher synergy between PV power and electricity consumers, giving the opportunity of self-consumption.

In this paper, different storage concepts for mitigating voltage variations in LV grid feeders with high PV penetration are proposed. The investigations are performed with a simulation study using the model of a highly PV-penetrated LV grid, which is a demonstration site within the Meta PV project [12]. The model comprises existing PV systems and additional storage systems.

II. System Model

The fundamental building blocks of a PV system are: the PV array, composed of single PV cells made of semiconducting materials and a PV inverter that converts the power from the PV array into grid-compatible electric

The authors acknowledge the co-funding of the European Commission in the 7th Framework Programme (FP7) through grant agreement No. TREN/FP7EN/239511/METAPV.

Mr. F. Marra, Mr. Y. T. Fawzy, and Mr. T. Bülo are with the Department of Technology Development, SMA Solar Technology AG, Sonnenallee 1, 34266 Niestetal, Germany (e-mail: fm@elektro.dtu.dk).

Mr. Blažič is with the Department of Electrical Engineering, University of Ljubljana, Slovenia.

power. To cope with the excess of PV power generation and low load in LV feeders, in this paper, the standard PV system is enhanced with storage system concepts. One concept is that a storage system can provide voltage support for the whole feeder from a strategically defined location; a second concept relies instead on a number of storage systems to achieve the same target, for example, one storage system on location with PV.

A. LV Grid Analysis

During high generation and low demand conditions, the active power injected in a feeder can cause voltage rise above the allowed limits, according to [9] and this can be expressed by (2) and (3):

$$\Delta U = \left(R \cdot P + X \cdot Q\right) / V_G \quad (2)$$

$$P = P_{PV} - P_L \quad (3)$$

where R and X are the cable resistance and reactance at a certain distance from the transformer, P and Q the active and reactive power exchanged at the PCC, V_G the base grid voltage. Voltage sensitivity analysis can be used for estimating the voltage variation due to active power injection at a certain location. A voltage sensitivity matrix for a grid feeder can be derived for active and reactive power by solving nonlinear load flow equations using the Newton–Raphson algorithm [11]. The same matrix can be used to identify critical locations in relation to load/generation conditions. The most remote node in the feeder, presents the highest sensitivity value, thus it is the most critical location for active power injection in relation to voltage variation.

For mitigating voltage rise problems in a LV grid feeder with PV, various reactive power methods have been already implemented at each PV inverter interface and have been introduced in large scale field tests. The following are the main ones [10]:

a) *fixed cos φ* (power factor)
b) *cos φ(P_{PV})*: power factor as a function of the active power (P_{PV}) fed into the grid
c) *fixed Q* (reactive power)
d) *Q(U)*: reactive power as a function of the voltage at the PCC.

The effectiveness of such methods has been proven and different performances in relation to grid losses and components loading are observable [10]. One of the limitations is that many existing PV installations are not capable of reactive power consumption. The additional utilization of storage systems is an effective approach to reduce voltage rise problems.

In this paper, storage solutions for voltage support and their possible combination with reactive power are being investigated with respect to their effectiveness and their operational requirements.

B. Energy Storage Systems

Lately, a wide range of energy storage technologies have been investigated by several researches to cope with the intermittency of renewable energy resources (RES). These include electrochemical batteries with various chemistries, supercapacitors, compressed air energy storage, flywheels and others [18]. In this paper, battery-based energy storage systems are assumed for providing voltage support in LV grids. The performance comparison of different battery chemistries, such as energy-to-weight ratio, self-discharge rate and charge/discharge efficiency are out of the scope of the present work, therefore they are not treated.

The charge and discharge equations of a battery system are shown in (4) and (5) [17], where P_d is the discharging power of the battery and P_c is the charging power; E is the energy stored in the battery at time t; Δt is the duration time of each interval. The two coefficients η_d and η_c are the discharge and charge efficiencies respectively.

$$E(t+\Delta t) = E(t) - \Delta t \cdot P_d / \eta_d \quad (4)$$

$$E(t+\Delta t) = E(t) + \Delta t \cdot P_c \cdot \eta_c \quad (5)$$

The operation of the battery system should also take into account power and energy constraints.

The power limits of a battery system can be described by (6) and (7):

$$0 \le P_d(t) \le P_d^{\max} \quad (6)$$

$$0 \le P_c(t) \le P_c^{\max} \quad (7)$$

The same power limits are important for sizing the power converters of the battery system. The storage power ramp rates are therefore generically described by (6) and (7). In this paper, the symbol P_s is used to represent the power flow, including the two phases of charge and discharge.

The energy limits of a battery system can be described by (8):

$$E_{\min} \le E(t) \le E_{\max} \quad (8)$$

where E_{min} and E_{max} are the minimum and maximum energy levels stored in the battery respectively. The energy limits, or state of charge limits (SOC), can be set according to the storage application and to the battery technology, however, in this paper, we will refer to (8) as the usable energy window of the storage system, regardless of the optimal energy management of a particular type of battery.

III. Problem Formulation

Considering (2), the idea is to introduce in the expression the component P_s which represents the storage power by the energy storage system. Therefore, it is possible to rewrite (2) into (9) where the nodal exchanged power P^* is, this time, the combination of the load power P_L, the generated power P_{PV} and storage power P_s, as indicated in (10):

$$\Delta U = \left(R \cdot P^* + X \cdot Q\right) / V_G \quad (9)$$

$$P^* = P_{PV} - P_L - P_S \quad (10)$$

With the main target of investigating on storage solutions, emphasis is given to the active power component P^* rather than Q in (9). Furthermore, the cooperation of storage and reactive power methods is also investigated, assuming different scenarios for reactive power.

In a LV feeder with high penetration of PV, the integration of storage for voltage support can be performed from a single location, or by multiple storage systems at different locations. The first strategy proposed in this paper

identifies a centralized storage concept, while the second strategy defines a distributed storage concept.

Considering the voltage limit V_{max} in a LV feeder, a storage system should be activated in order not to reach the limit in any of the feeder's nodes.

A. Solution Algorithm

Considering the different locations on which the storage system can be integrated and the voltage sensitivity matrix in Table IV, it is possible to calculate the storage power that lowers the nodal voltages below the limit. The main problem is to identify the minimum storage power P_s that meets the voltage target, according to centralized and distributed concepts. This can be implemented with the storage participation in different locations in the grid, or with multiple storage participation. Fig. 1 shows the algorithm proposed in this paper.

The proposed solution is a linear problem. This algorithm is implemented in Matlab and results are checked with PowerFactory load flow simulations. The algorithm can be summarized as follows:

1) Enter the LV grid model under study, with worst case load/generation conditions on each node
2) Run the load flow grid simulation
3) Identify the critical node/s where the voltage is above V_{max}
4) Add a combination of storage in the LV feeder
5) Solve the objective function for P_s which is to find the minimum power that keeps the critical voltage below V_{max}
6) If $V > V_{max}$ update P_s using $P_s = P_s + \Delta P_s$ and go back to step 5
7) Go back to step 4, set another storage configuration, repeat step 5 and 6.

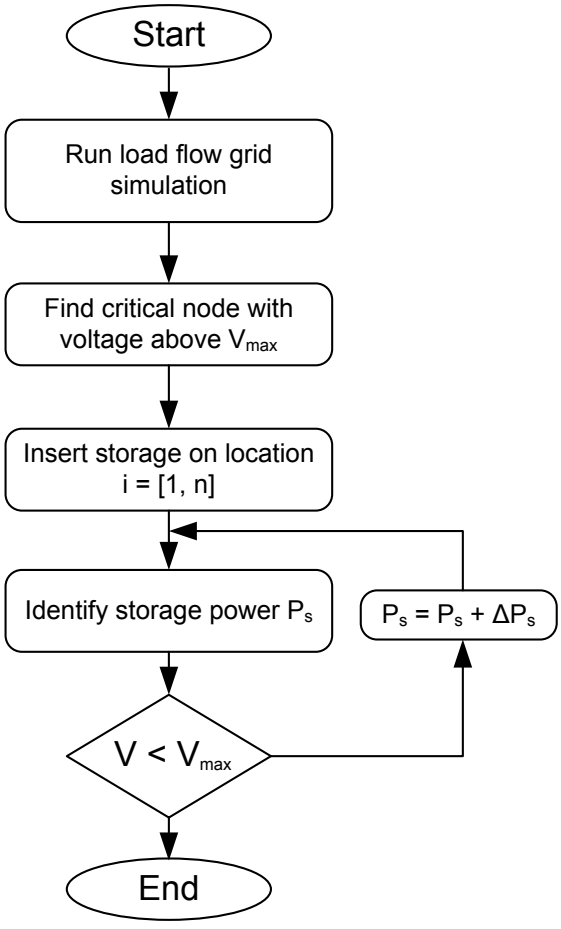

Fig. 1. Proposed method for storage planning

The step 7 is repeated until all possible combinations of storage locations are covered, including the cases of multiple storages at the different nodes.

IV. Case Study

The algorithm implementation and performance assessment is performed for a LV grid with high PV penetration, Fig. 7, with main parameters in Table I. The PV penetration per feeder, which is defined as the ratio of PV installed capacity over the feeder capacity, is indicated in Table II.

TABLE I
LV Grid Parameters

Grid type	Urban
Transformer	630 kVA
Feeders nr.	9
Feeder capacity (average)	195 kVA
Cables R/X (average)	4.6
Number of households	271
PV installed capacity (kW)	143.23 kW
Grid topology	Radial

TABLE II
Feeders Characteristics

Feeder	No. of households	No. of PV sources	PV power/kW	PV penetr. %
2	2	0	0	0
3	41	2	10.38	5.3
4	36	2	8.80	4.5
5	19	0	0	0
6	18	3	11.10	5.7
9	48	9	39.67	20.3
10	15	2	8.80	4.5
11	33	9	42.60	21.8
12	52	5	21.88	11.22

A. Identification of Critical Node

From the voltage sensitivity analysis performed on the grid, node 7 in the feeder LS11 of Fig. 2 is found the most critical location in the grid. The voltage sensitivity to active power matrix for feeder LS11 is shown in Table III.

TABLE III
Voltage Sensitivity Matrix

dV/dP p.u./MW	1	2	3	4	5	6	7
1	0.37	0.36	0.37	0.35	0.35	0.34	0.34
2	0.37	0.72	0.36	0.71	0.71	0.69	0.72
3	0.36	0.36	0.76	0.35	0.35	0.34	0.35
4	0.36	0.72	0.36	0.91	0.91	0.88	0.88
5	0.36	0.72	0.36	0.89	1.35	0.71	0.69
6	0.36	0.71	0.36	0.91	0.89	0.98	0.98
7	0.36	0.71	0.35	0.89	0.68	0.88	1.51

Using 6-days measurements-based load/generation profiles, representing the worst case scenario of high generation and low load conditions, gives the voltage profiles of Fig. 3. The voltages on the nodes with PV, 2, 4, 5

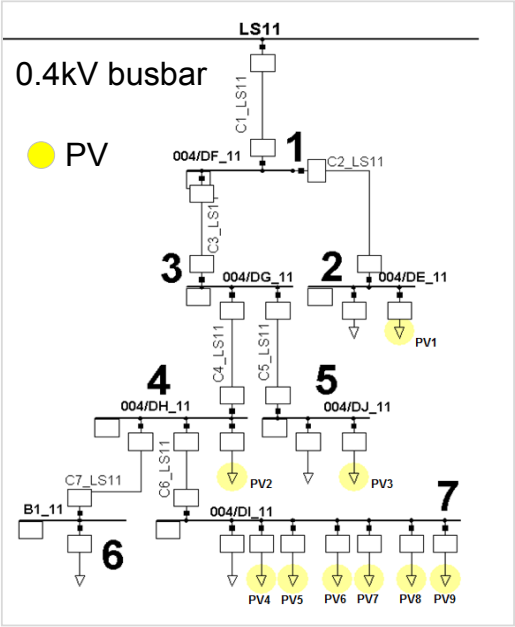

Fig. 2. Single line diagram of feeder 11

and 7, are displayed respectively, emphasizing voltage rise and unbalance problems.

To evaluate the storage requirements for voltage rise mitigation in the feeder, under the described scenario, the two concepts of centralized and distributed storage are investigated.

B. Centralized Storage

The first concept addressed is centralized storage (CS); this is implemented by placing a single storage unit on a feeder node. With this concept, only one storage device is present in the feeder, providing the voltage support function required.

The control of the storage under the CS concept is according to $P_s = f(U)$, where U is the most critical nodal voltage in the feeder. In this case study, three different scenarios are investigated for the CS concept: CS1, storage on node 2; CS2, storage on node 4; CS3, storage on node 7.

The proposed algorithm in Fig. 1 is used to estimate the power requirement for the different options.

C. Distributed storage

The second investigated concept is the distributed multiple storage concept (DS). With this concept, a storage device is integrated at each PV location in the feeder. In relation to the algorithm of Fig. 1, the DS concept corresponds to the combination of storage power P_{Si} by all nodes with PV that leads to a voltage below V_{max} in the whole feeder. The control of the storage devices under the DS concept is done according to $P_{Si} = f(P_{PV})$. Assuming the case of all PV inverters with same nominal power and same solar radiation, the storage contribution P_{Si} from each storage device would be also the same for all. The DS scenario proposed prioritizes the equal participation from all PV power producers.

D. Combined Storage and Reactive Power

From the two main storage concepts, three variants are studied that consider the reactive power combination with the energy storage systems. The investigated combined storage and reactive power options are as follows:

- CS3 concept with all PV inverters working with fixed PF = 0.95 (*CS3 – distr. Q*)
- CS3 concept with reactive power capability, all PV inverters with PF = 1 (*CS3 with Q*)
- DS concept with all PV inverters working with PF = 0.95, (*DS with Q*)

The power factor PF is defined as [13]:

$$PF = \frac{P}{S} = \cos\varphi \qquad (11)$$

where P is the real power flow (in watts), S is the apparent power flow (in volt-amperes, VA) and φ is the angle difference between the voltage and current waveforms on a given phase. The power factor is continuously variable between 0 and 1 and in this case study it indicates a component that consumes reactive power (in VAr).

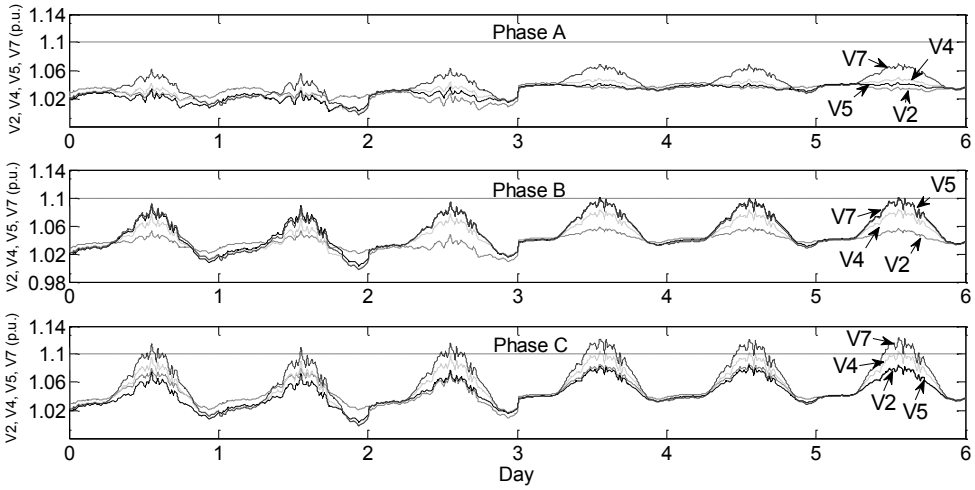

Fig. 3. Phase voltages on feeder 11 with PV without voltage support

V. Simulation Results

Dynamic grid simulations are performed for the LV feeder with the different storage options. The results for the 6th day are summarized in Table IV. During the 6th day, a worst case scenario occurs in relation to low load and high generation conditions. In Fig. 4, the storage power for CS1, CS2, CS3 and DS are depicted for the 6-days interval. It is evident that placing a CS on node 7, CS3, leads to a minimum aggregated power and energy requirement, while a minimum device power and energy level is obtainable with the DS concept.

The results of combined storage and reactive power options are depicted for the 6th day in Table V. The comparison with the "only" storage options is given in Fig. 5 and Fig. 6, where the CS3 and DS results are depicted as a reference. With all PV inverters consuming reactive power, the storage power and energy levels are significantly reduced in both concepts of DS and CS. In Fig. 5 and 6, this is particularly evident for the options named "DS with Q" and "CS3 – distr. Q".

TABLE IV
SUMMARY OF STORAGE RESULTS

Storage option	Total Ps (kW)	Ps/device (kW)	Total E (kWh)	E/device (kWh)
CS1	11.1	11.1	30.2	30.2
CS2	4.75	4.75	12	12
CS3	3	3	7	7
DS	4.2	0.9	10.2	2.5

TABLE V
COMBINED STORAGE AND REACTIVE POWER RESULTS

Storage option	Total Ps (kW)	Ps/device (kW)	Total E (kWh)	E/device (kWh)
DS with Q	4.5	0.5	2.7	0.3
CS3 distr. Q	1.9	1.9	1.0	1.0
CS3 with Q	2.8	2.8	4.1	4.1

With a CS option providing a fixed amount of reactive power, "CS with Q", the storage power and energy are decreased accordingly. For this case study, Q is chosen of 1 kVAr, which is the level or reactive power obtainable with a PF of 0.95 and active power P_S of 3 kW (which is the CS3 power requirement).

The energy levels of the storage devices under the different concepts can be put in relation to local consumption. In particular, under the DS concept, local consumption is possible in such a way that the energy stored for voltage support can be used by PV system owners to supply any domestic appliances, during off-generation hours. On this point, there is space for further investigations.

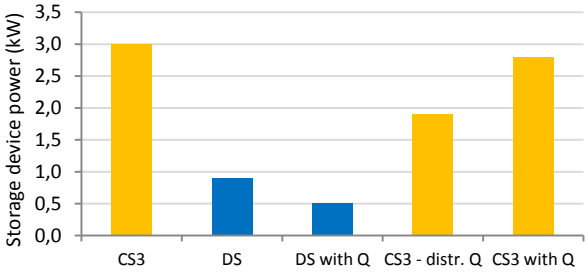

Fig. 5. Storage device power for all options

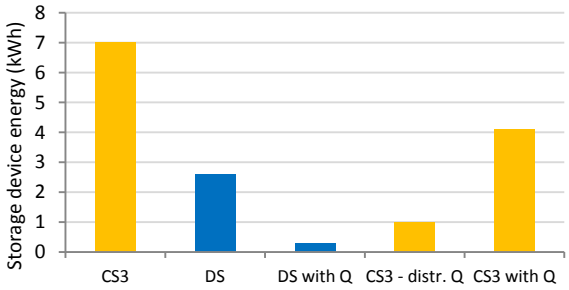

Fig. 6. Storage device energy for all options

VI. Conclusions

In this paper, different storage planning options for LV grids with high share of PV have been proposed.

Distributed storage solutions at each PV location have shown that a relatively small power and energy are needed to provide voltage support, securing voltage quality according to standard EN 50160.

The identification of the best location under the centralized storage concept is solved with an iterative method, based on voltage sensitivity analysis. A CS option at the end of the feeder is found as the option with minimum power/energy requirement for voltage support.

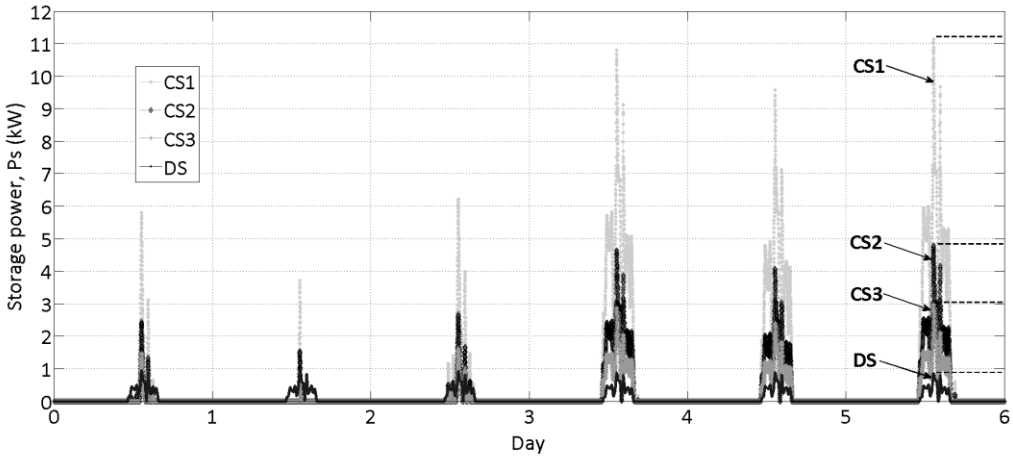

Fig. 4. Storage device power for the *CS* and *DS*

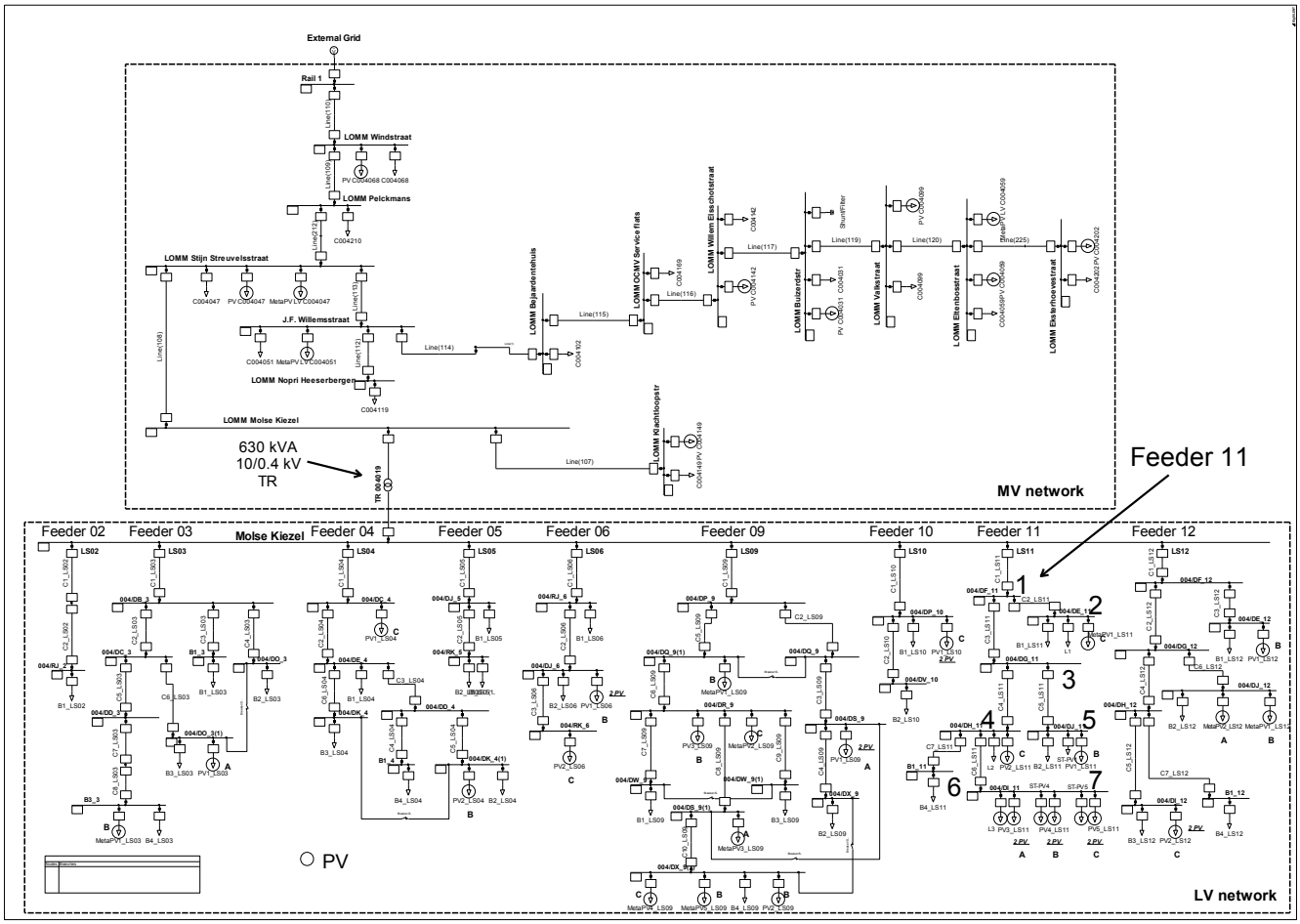

Fig. 7. Single-line diagram of the LV Belgian grid

To minimize storage power and energy for CS and DS, all storage options can cooperate with reactive power methods at the PV interface. Having all PV inverters operating at the constant power factor of 0.95 has shown to significantly lower the required storage power and energy levels.

The storage solutions proposed can potentially relieve the DSOs from voltage quality concerns due to high PV generation and low demand periods. Furthermore, the deployment of such storage solutions would limit the practice of power curtailment, thus allowing an increased PV penetration. The discharging phase of the storages, which is not treated in this work, offers the opportunity of self-consumption in the centralized and distributed concept.

VII. References

[1] European Commission, "20 20 by 2020 Europe's climate change opportunity", COM (2008) 30 final, Brussels, 2008.

[2] V. F. Martins, and C. L. T. Borges, "Active Distribution Network Integrated Planning Incorporating Distributed Generation and Load Response Uncertainties", *IEEE Trans. Power Syst.*, vol. 26, no. 4, pp. 2164-2172, 2011.

[3] H. A. Gil, G. Joos, "Models for Quantifying the Economic Benefits of Distributed Generation", *IEEE Trans. Power Syst.*, vol. 23, no. 2, pp. 327-335, 2008.

[4] S. Paudyal, C. A. Cañizares, and K. Bhattacharya, "Optimal Operation of Distribution Feeders in Smart Grids", *IEEE Trans. Ind. Electron.*, vol. 58, no. 10, pp. 4495-5503, 2011.

[5] X. Liu, A. Aichhorn, L. Liu, H. Li, "Coordinated Control of Distributed Energy Storage System With Tap Changer Transformers for Voltage Rise Mitigation Under High Photovoltaic Penetration", *IEEE Trans. Smart Grid*, vol. 3, no. 2, pp. 897-906, 2012.

[6] M. Delfanti, M. Merlo, M. Pozzi, V. Olivieri, and M. Gallanti, "Power flows in the Italian distribution electric system with Dispersed Generation", in *Proc. 2009 20th Int. Conf. and Exhib. on Electricity Distribution - Part 1, CIRED 2009*, 2009.

[7] N. Etherden, and M. H. J. Bollen, "Increasing the Hosting capacity of Distribution Networks by Curtailment of Renewable Energy Sources", in *Proc. 2011 IEEE PowerTech*, Trondheim, 2011.

[8] Standard EN 50160, "Voltage Characteristics of electricity supplied by public distribution networks", Cenelec 2010.

[9] P. Carvalho, P. Correia, and L. Ferreira, "Distributed Reactive Power Generation Control for Voltage rise Mitigation in Distribution Networks", *IEEE Trans. Power Syst.*, vol. 23, no. 2, pp. 766-772, 2008.

[10] Y. T. Fawzy, D. Premm, B. Bletterie, and A. Gorsek, "Active contribution of PV inverters to voltage control – from a smart grid vision to full-scale implementation", *J. of Elektrotechnik & Informationstechnik*, vol. 128, no. 4, pp.110-115, 2011.

[11] E. Demirok, P. Casado Gonzalez, K. H. B. Frederiksen, D. Sera, P. Rodriguez, and R. Teodorescu, "Local Reactive Power Control Methods for Overvoltage Prevention of Distributed Solar Inverters in Low-Voltage Grids", *IEEE J. of Photovoltaics*, vol. 1, no. 2, pp. 174-182, 2011.

[12] B. Blazic, I. Papic, B. Uljanic, B. Bletterie, C. Dierckxsens, K. De Brabandere, W. Deprez, Y. T. Fawzy, "Integration of Photovoltaic Systems with Voltage Control Capabilities into LV networks", in *Proc. 2011 1st Int. Workshop of Solar Power into Power Syst.*, 2011.

[13] C. A. Hill, M. C. Such, D. Chen, J. Gonzales, W. M. Grady, "Battery Energy Storage for Enabling Integration of Distributed Solar Power Generation", *IEEE Trans. Smart Grid*, vol. 3, no. 2, pp. 850-857, 2012.

[14] M. Ragwitz, A. Held, E. Stricker, A. Krechting, G. Resch, C. Panzer, "Recent experiences with feed-in tariff systems in the EU - A research paper for the International Feed-in Cooperation" [online]. Available: www.feed-in-cooperation.org

[15] M. Braun, K. Budenbender, M. Perrin, H. Collin, Z. Feng, and D. Magnor, "Photovoltaic Self-Consumption in Germany – Using Lithium-Ion Storage to Increase Self-Consumed Photovoltaic Energy", in *Proc. 2009 24th Europ. Photov. Solar Energy Conf.*, 2009.

[16] Renewable Energy Sources Act (EEG), "Tariffs, degression and sample calculations pursuant to the new Renewable Energy Sources Act" [online]. Available: www.bmu.de

[17] Y. Riffonneau, S. Bacha, F. Barruel, and S. Ploix, “Optimal Power Flow Management for Grid Connected PV Systems With Batteries”, *IEEE Trans. on Sust. Energy*, vol. 2, no. 3, pp. 309-320, 2011.
[18] J. P. Barton, and D. G. Infield, “Energy storage and its use with intermittent renewable energy”, *IEEE Trans. on Energy Conversion*, vol. 19, no. 2, pp. 441-448, 2004.

VIII. BIOGRAPHIES

Francesco Marra (Student member, IEEE) received the B.Sc. and mechatronic engineering degree from Polytechnic of Turin, Italy, in 2006 and 2008, respectively. He is currently within the Electrical Engineering department of the Technical University of Denmark, where he is pursuing the Ph.D. degree. Previously, he has been within SMA Solar Technology working on PV integration and energy storage. His fields of interest include grid integration of renewable energy and control systems.

Yehia Tarek Fawzy received his B.Sc. in 2005 in Power Engineering at the University of Ain Shams, Cairo, Egypt. Afterwards, he received his M. Eng. in control and mechatronics at the university of Paderborn, Germany in 2008. Since then he is working for SMA Solar Technology AG as a systems engineer. His activities are focused to development and evaluation of control concepts for grid integration of PV systems. His research interests include analysis, modelling and optimization of PV system behaviour in terms of network stability and power quality.

Thorsten Bülo (Member, IEEE) received the B.Sc., M.Sc. and Ph.D. degrees, all in electrical engineering, from the University of Kassel, Germany in 2002, 2004 and 2010, respectively. He is currently manager of the team Grid Integration of the SMA Solar Technology AG in Niestetal, Germany.

Boštjan Blažič received the B.Sc., M.Sc. and Ph.D. degrees, all in electrical engineering, from the University of Ljubljana, Slovenia, in 2000, 2003 and 2005, respectively. He is presently an assistant professor at the Faculty of Electrical Engineering, Ljubljana. His research interests encompass power quality, distributed generation, mathematical analysis and control of power converters.

www.elektro.dtu.dk/cee

Department of Electrical Engineering
Center for Electric Power and Energy (CEE)
Technical University of Denmark
Elektrovej 325
DK-2800 Kgs. Lyngby
Denmark
Tel: (+45) 45 25 35 00
Fax: (+45) 45 88 61 11
E-mail: cee@elektro.dtu.dk